PhD THESIS

Urban Mobility Network Design:

Functional Analysis and Modeling for a Concentric City

Author:

Marcos Medina-Tapia

PhD Supervisor:

Prof. Francesc Robusté

2021

Urban mobility network design:

Functional Analysis and Modeling for a Concentric City

Author:

Marcos Medina-Tapia

PhD Supervisor:

Prof. Francesc Robusté

PhD Program in Transportation Engineering and Infrastructures
Department of Civil and Environmental Engineering
Civil Engineering School of Barcelona
Technical University of Catalonia – UPC BarcelonaTech

Barcelona, March 2021

To Alina, Franco, and Camila

Acknowledgments

The dissertation would not have been possible without the support of the University of Santiago of Chile (USACH) and Chile's CONICYT PFCHA/BCH 72160291 Scholarship Program. In Barcelona, the author acknowledges the support received by Abertis Chair (Cátedra Abertis) and BIT-Barcelona Innovative Transportation Research Group at BarcelonaTech, providing the necessary resources for the research work.

A mi familia, Alina, Franco y Camila, por emprender juntos esta aventura, que sin duda fue lo mejor de todo, viviendo momentos inolvidables. Por cierto, agradecer la paciencia tenida durante todos estos años.

A mis padres, Cristina y Jorge, que siempre me han apoyado, comprendido e incentivado a crecer día a día. También quiero agradecer a mi familia en general, hermanos, Sra. Nana, cuñados, cuñadas y sobrin@s.

A Francesc Robusté, mi director de tesis, que ha sido un gran profesor incentivándome al máximo, entregándome su experiencia para hacer un buen trabajo, pero sobre todo agradezco su calidad humana, ya que siempre estuvo preocupado de mi estancia y la de mi familia.

A la *familia* del BIT. A mis compañeros de doctorado que fueron un gran apoyo durante mi permanencia. Quiero agradecer sinceramente a mis amig@s del "B1-006", se extraña las "sesiones amistosas" previas a presentar en un congreso: Marcel Sala, Marga Martínez, César Trapote, Enrique Jiménez y Hugo Badía. También, quiero agradecer a todos los profesores de la UPC, especialmente a Miquel Estrada y Francesc Soriguera, con los que compartí gratos momentos. Tampoco quiero olvidar a destacados profesores que conocí durante mi estancia, como Jaume Barceló, Manel Grifoll, Mateu Turró, Lidia Montero, Magín Campos. También un recuerdo a los chic@s con los cuales compartí distintos momentos en la universidad: Estefanía, Masoud, Bruno, Elisa. Muchas gracias Silvia Aranda.

A Sandra González, quien siempre tuvo gran disposición y paciencia hacia mí, sin duda, admirable.

A todos los profesores del Foro de Ingeniería del Transporte (FIT), con los cuales compartí jornadas y veladas muy interesantes de los Congresos de Ingeniería del Transporte y de los Campus FIT, de los cuales participé, particularmente, quiero recordar el gran evento en la Sede de la UPM en

Cercedilla. En este sentido quiero recordar a los profesores Andrés Monzón, Luigi dell'Olio, Alfredo García, José Luis Moura, Ángel Ibeas, Marga Novales.

A todos los profesores del Departamento de Ingeniería Geográfica de la USACH, quienes me brindaron su apoyo en este proceso.

Personalmente podría agregar un anejo a la tesis hablando de las personas que conocí y que me ayudaron durante esos 4 años: en la UPC, en el barrio, en el colegio de mis hij@s, en el hoquei, etc. Por ello, quiero agradecer a todas las personas que hicieron posible que mi estadía, en Barcelona, haya sido inolvidable. Especialmente, porque sentí, desde el primer día en BCN, una preocupación por mí y mi familia: *moltes gràcies a tots i totes*.

Abstract

Urban mobility efficiency requires a simultaneous interaction of urban structure and transportation systems. Urban activities define urban development. Traffic is a result of the interaction between the urban activity system that generates the mobility demand, and the transportation networks supply.

Continuous population growth in cities, urban sprawl and time lag regarding the equilibrium supply-demand may create excessive traffic congestion and, thus, inefficiency. The international trend recuperating public space for citizens (tactical city planning) and the trigger of Covid19 pandemics puts pressure on the "right" supply and layout of transportation networks of a city.

This research focuses on how to adapt infrastructure and land uses to meet the mobility needs in a city. We seek a balanced design among transportation networks, population distribution, land use, and infrastructure. A macroscopic approach identifies the infrastructure requirements to reach an appropriate level of service for urban mobility.

A Continuous Approximation formulation for a concentric city includes the key performance conditions of public and private transportation infrastructure. The analytical models use variables defined as densities, and solve the optimization problem minimizing the total costs. We apply the four-step Urban Transportation Planning process as defined in the Chicago Area Transportation Study: trip generation and attraction, spatial distribution, modal split and traffic assignment using the incremental method.

We focus on the role of heterogeneously distributed demand, and design effects on urban structure based on functionality, and we test several policies. Multi-center cities can reduce the total costs between 2.6% and 11.6%, which is relevant as a planning measure. Autonomous vehicles could have a neutral effect on the reduction in travel costs. When we apply the models to Santiago (Chile), the system optimization advises to increment the subway services and lines.

The model provides robust approaches to elaborate spatial planning instruments and policies, which is a promising contribution to City Planning science.

Keywords: *Urban mobility. Network design. Public Transportation. Traffic. Private Transportation. Continuous approximation. Concentric city. Urban subcenters. Autonomous vehicles. Santiago, Chile.*

Francesc Robusté
Professor of Transportation, PhD

Resumen

La eficiencia de la movilidad urbana requiere una interacción simultánea de la estructura urbana y los sistemas de transporte. Las actividades urbanas definen el desarrollo urbano. El tráfico es el resultado de la interacción entre el sistema de actividad urbana que genera la demanda de movilidad y la oferta de las redes de transporte.

El crecimiento continuo de la población en las ciudades, la expansión urbana y el desfase en el equilibrio entre la oferta y la demanda pueden crear una congestión excesiva del tráfico y, por lo tanto, ineficiencia. La tendencia internacional a recuperar el espacio público para los ciudadanos (urbanismo táctico) y el detonante de la pandemia de Covid19 tensiona la oferta y el diseño "adecuados" de las redes de transporte de una ciudad.

Esta investigación se centra en cómo adaptar la infraestructura y los usos del suelo para satisfacer las necesidades de movilidad en una ciudad. Buscamos un diseño equilibrado entre redes de transporte, distribución de la población, uso del suelo e infraestructura. Un enfoque macroscópico identifica los requisitos de infraestructura para alcanzar un nivel de servicio apropiado para la movilidad urbana.

Una formulación de Aproximaciones Continuas para una ciudad concéntrica incluye las condiciones clave de desempeño de la infraestructura de transporte público y privado. Los modelos analíticos utilizan variables definidas como densidades y resuelven el problema de optimización minimizando los costes totales. Aplicamos el proceso de Planificación del Transporte Urbano de cuatro pasos clásico: generación y atracción de viajes, distribución espacial, reparto modal y asignación de tráfico utilizando el método incremental.

Nos enfocamos en el papel de la demanda distribuida heterogéneamente y los efectos del diseño en la estructura urbana basados en la funcionalidad, y probamos varias políticas. Las ciudades multi-céntricas pueden reducir los costes totales entre un 2,6% y un 11,6%, lo que es relevante como medida de planificación. Los vehículos autónomos podrían tener un efecto neutral en la reducción de los costes de viaje. Cuando aplicamos los modelos a Santiago (Chile), la optimización del sistema aconseja incrementar los servicios y líneas de metro.

El modelo proporciona enfoques sólidos para elaborar instrumentos y políticas de planificación espacial, lo que es una contribución prometedora para la ciencia de la planificación urbana.

Palabras clave: *Movilidad urbana. Diseño de red. Transporte público. Tráfico. Transporte privado. Aproximaciones continuas. Ciudad concéntrica. Subcentros urbanos. Vehículos autónomos. Santiago, Chile*.

Francesc Robusté
Profesor de Transporte, PhD

Publications and Conferences

The dissertation has already been published in three indexed papers, WOS and Scopus:

Medina-Tapia, M., & Robusté, F. (2018). **Exploring paradigm shift impacts in urban mobility: Autonomous Vehicles and Smart Cities**. *Transportation Research Procedia*, 33, 203–210. doi: 10.1016/j.trpro.2018.10.093

Medina-Tapia, M., & Robusté, F. (2019). **Implementation of connected and autonomous vehicles in cities could have neutral effects on the total travel time costs: modeling and analysis for a circular city**. *Sustainability*, 11(2), 482. doi: 10.3390/su11020482

Medina-Tapia, M., Robusté, F., & Estrada, M. (2020). **Modeling public transportation networks for a circular city: the role of urban subcenters and mobility density**. *Transportation Research Procedia*, 47, 353–360. doi: 10.1016/j.trpro.2020.03.109

Moreover, two papers are written and will be submitted to a journal for publication:

Medina-Tapia, M., Robusté, F., & Estrada, M. (2021). **Adaptive transit network design for spatially heterogeneous demand**.

Medina-Tapia, M., Robusté, F., & Estrada, M. (2021). **Spatial analysis of public transportation infrastructure in Santiago, Chile**.

Finally, results of the dissertation have been presented in congress and seminars:

2016: XII Spanish Transportation Engineering Congress, Valencia, Spain. **Relocalización de paradas de transporte público para ser incorporado dentro planes de contingencia como resultado de la construcción de obras de mejoramiento vial**.

2017: II Scientific Campus of the Transportation Engineering Forum, Universidad Politécnica de Madrid, España. **Planificación y diseño de un área urbana: implicaciones para una smart city**.

2018: XIII Spanish Transportation Engineering Congress, Gijón, Spain. **Exploring paradigm shift impacts in urban mobility: autonomous vehicles and smart cities**.

2018: XX Pan-American Conference on Traffic, Transportation Engineering and Logistics, Universidad Nacional, Medellín, Colombia. **Impact assessment of autonomous vehicle implementation on urban road networks**.

2019: III Scientific Campus of the Transportation Engineering Forum, Universidad Politécnica de Madrid, España. **Diseño óptimo de redes de transporte público que se adaptan a condiciones locales y no-homogéneas en una ciudad circular**.

2019: 14th Edition of the CIMNE Coffee Talks. Barcelona. **Ingeniería de transporte y planificación urbana: Diseño de redes de transporte público en una ciudad concéntrica**.

2019: 22nd Euro Working Group on Transportation Meeting, Technical University of Catalonia, Barcelona. **Modeling public transportation networks for a circular city: the role of urban subcenters and mobility density**.

Contents

List of Tables

Appendices

List of Figures

Appendices

1. Introduction and objectives

A city is a part of a territory that concentrates population and contains commercial areas, services, and even industries. A city is not a static system where its inhabitants need to travel from one point to another for many purposes: work, education, and others. Moreover, people need to move goods between two points because of the needs of a city's manufacturing activities. Therefore, a city is a complex system containing residential and non-residential elements heterogeneously distributed over the territory.

The development of cities involves the interaction of urban elements where transportation plays an essential role. In this interaction, transportation needs infrastructure for its operation, in which attributes define this infrastructure such as location, design, materiality, capacity, and others.

The interaction between transportation and infrastructure determines a transportation system. According to Vuchic (2007), transportation systems

generate effects on a city's form and urban structure. The former considers the size, geometric shape, and primary structural network. The latter includes population densities and the distribution of land use. In this sense, the operation of both urban mobility and transportation impacts the urban space used by cars, transit, logistics vehicles, and other modes (motorized, non-motorized, and active mobility).

Historical, social, and geographical conditions define the physical characteristics of a city. The physical layout of a city may come from planning, natural development for a long time, or a mixed process of both. For adequate functional planning of a city, planners should consider both the transportation system operation and infrastructure to enhance people's mobility and freight.

The above components—urban form and structure—are critical elements for the impact analysis of transportation and urban mobility on an urban system and vice versa.

In the next point, this chapter exposes the problem statement and justification of the research based on those components. After this, the following point presents the objectives of this dissertation. Finally, the current chapter gives a road map of the whole document.

1.1. Transportation and its effects on a city

In an integrated urbanism-mobility approach, one of the classical key references is given by Colin Buchanan in his book *Traffic in Towns* (1963), whose assertions are still in force.

According to Buchanan (1963), the increase in cars is

> *"…an extraordinary problem because nothing less is involved than a threat to the whole familiar physical form of towns…"* (p. 7)
>
> *"…traffic congestion has already placed in jeopardy the well-being of many of the inhabitants and the efficiency of many of the activities."* (p. 7)
>
> *"The conflict between towns and traffic obviously stems from the physical structure of towns…this soon became apparent after the invention of the motor vehicle because it soon exerted a strong influence towards changing the form of towns…"* (p. 29)

Moreover, this problem will not disappear because

> *"…the future of the motor vehicle, or of some equivalent machine, is assured."* (p. 25)
>
> *"…the population appears as intent upon owning cars as the manufacturers are upon meeting the demand."* (p. 28)

Buchanan poses a balance between the organization of a city and the transportation mode used by its inhabitants. Thus, this situation implies

> *"…a problem of design, of the actual layout and form of buildings and access way, and the manner of distribution of traffic from one part of a town to another. It is a basic problem, as relevant to a small isolated town"… "as to the constituent towns of the largest conurbation."* (p. 31)
>
> *"…new settlements could well take on new forms based on transport systems."* (p. 30)

The author wrote the above almost six decades ago, but these assertions and their consequences are still valid currently. It may cause effects on an urban system, deteriorating both mobility and urban development. This consequence may equivalently impact a public transportation system.

Under this research framework, the problem statement and its discussion focus on three aspects: transportation problems, consequences on urban systems, and management strategies and planning instruments to improve transportation. These factors justify the current dissertation, and thereby the research thesis.

1.1.1. Transportation problems

Traffic congestion and transit

Congestion is a condition reached when a new vehicle enters into the traffic flow, increasing the travel time for other vehicles (Bull & Thomson, 2002). Congestion costs can increase more rapidly than traffic growth.

Congestion, delays in trips, and other causes may frustrate commuters. However, two situations may partially cause those frustrations: the increase in the number of vehicles and the design, structure, and capacity offered by cities. The congestion may affect the main characteristic offered by cars: the

ability to provide a door-to-door service. It may deteriorate citizens' work performance who use a car, even more for people who use it as a work tool. This externality can even affect the economic efficiency of a country.

Regarding the increase in traffic, the number of private vehicles depends on the increase in salaries, but also this increase depends on other factors, for example, the price of cars, insurance, parking, garage availability, level of frustration due to traffic, other cheaper modes of transportation, and changes in travel habits or patterns. Regarding freight vehicles, the increase in vehicles will depend on the utility of this transportation mode for companies.

The excessive growth of cars generates a decline in the transit of the *spiral* type. This process is known as the "vicious circle of public transportation" (see, for example, Ortúzar & Willumsen, 2011).

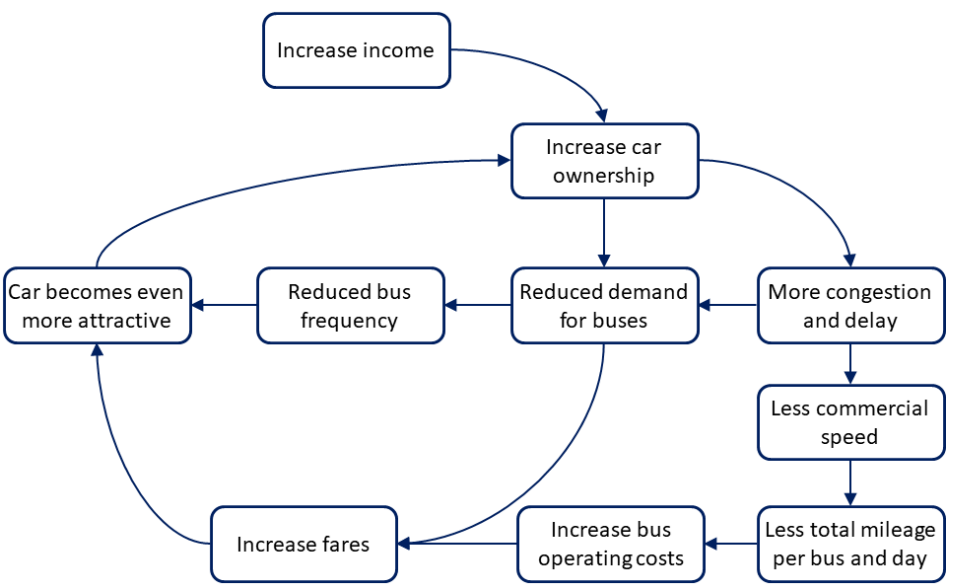

Figure 1.1. Car-and-transit vicious circle.

Source: Adapted from Ortúzar and Willumsen (2011).

According to the vicious circle (Figure 1.1), economic growth encourages people to buy more cars. Therefore, new car owners will leave the transit system and use their cars. Transit operators will increase fares, reduce frequencies (level of service), or both. The transit is thereby less attractive yet than before. After a few years, the city will face increasing congestion, delays in transit vehicles, an increment in operating costs, and new fares for transit users. Finally, the traffic system will be more attractive, and other people will prefer buying new cars.

This consequence is only possible to reverse with the implementation of measures (management or planning) to encourage the use of transit and, in parallel, discourages the use of cars. Moreover, cities must accommodate traffic and transit, minimizing system costs and without deteriorating the environment.

Quality and level of service

In a decision-making process of transit services, a potential user will consider at least one or a combination of the following attributes of a public transportation system: reliability, waiting time, security concerning walking, waiting, and riding, trip comfortability, trip cost, number of transfers, and travel time considering all stages of a trip.

The design of transit networks should consider the above operating factors. It is worth mentioning that decisions in the urban planning process usually do not consider those factors. Some factors are more accessible to incorporate into urban planning than others. This dissertation includes most of those factors but not considers specific operating variables, i.e., security and comfortability.

The "quality of service reflects the passenger's perception of transit performance" (TCQSM, TRB, 2013). Two factors classify the quality of transit services: transit availability and transit comfort and convenience. The former determines whether a transit system is a feasible option for a trip; the latter measures passengers' comfort and convenience for a transit system. Transit comfort and convenience only have relevance whether a transit service is available. Thus, public transportation will only be an option for a trip, whether the transit satisfies the following four factors of availability:

- *Spatial availability*: A passenger can access a transit service, i.e., the service is available near the origin and destination,
- *Temporal availability*: A passenger has an available service when he/she begins his/her trip, including the return trip,
- *Capacity availability*: A passenger has sufficient space at a stop/station, on a vehicle, and in facilities of a transit system, and
- *Information availability*: A passenger can obtain data about how to use a transit system.

This dissertation studies the design of transit networks, considering the first three factors assuming a passenger has information availability of a transit

system. This research will incorporate these factors through decision variables or constraints of the problem.

In traffic (HCM, TRB, 2010), there are two criteria for characterizing traffic flow conditions: quality and level of service. The former requires quantitative measures, in which demand is one of the leading indicators to measure traffic: vehicles arriving, traffic flow, discharging, and others. On the contrary, the level of service of a road (LOS) is a qualitative measure that describes the operational conditions. Six states define a level of service, i.e., speed, travel time, traffic interruptions, freedom to maneuver, comfort, and convenience. Letters A to F characterize the level of traffic, i.e., LOS A represents the best-operating conditions, and LOS F represents the worst conditions (TRB, 2010). Thus, urban planning must incorporate some traffic conditions to transit systems, particularly the components that affect road network design, i.e., average flows, capacity, structure shape, spatial location, and others.

1.1.2. Consequences on urban systems

Cities have been spreading out for decades. In transportation, several reasons support this assertion, e.g., cars provide freedom of movement in a city. A road network is a connex graph—there is at least one path between two points—in which a rational driver will choose the shortest path (minimum travel time in a congested system). That freedom and the increase of speed have boosted that drivers increase the traveled distance during their travels, e.g., longer commuting. The extensive use of automobiles affects the urban form, causing urban sprawl (*urban dispersion*), among other consequences. Figure 1.2 shows the vicious circle of consequences that generate congestion in a city.

Congestion generates impacts on the environment and, at the same time, people's pressures to increase road capacity. Thus, cities invest in infrastructure to reduce travel times, e.g., the construction of freeways. The new capacity often generates a reduction of friction to mobility, and new users change their modal choice to private transportation.

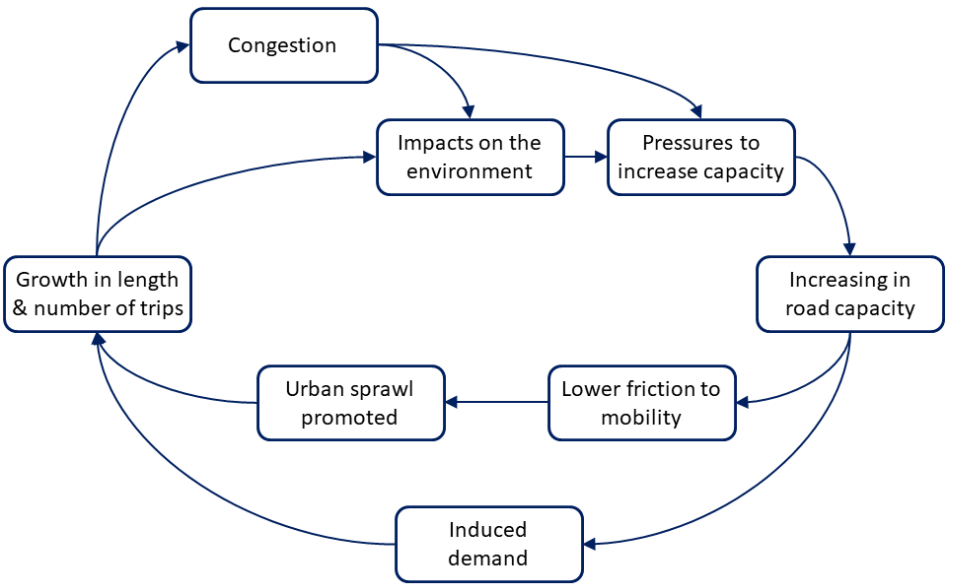

Figure 1.2. The vicious circle of congestion.

Source: Adapted from Rodrigue et al. (2017).

This new scenario and other components promote urban sprawl in cities. Drivers also have some limitations; one of them is parking. Due to the scarcity of urban land, parking in central areas is more expensive than in the periphery. This factor only thereby comes to justify that cities had spread out in the last decades.

The answer is neither clear nor unequivocal between concentrated urban areas (high density) and scattered (low density). The dispersion can quickly become sprawl whether automobiles are the center of mobility in a city. New urbanizations—new cities or extensions of existing areas—must adopt new forms based on transit services. The infrastructure could adapt it, or it could maintain a balance between both components.

The increment in population, the number of cars, and the urban sprawl cause congestion. This consequence has limited the benefits of investments made for the reduction of travel times.

1.1.3. Management and planning

The solution depends on the type of problem, the budget, and the period of implementation: short-term and long-term planning.

TSM/TDM

Some strategies allow solving conflicts between transportation and urban problems, i.e., TSM/TDM strategies.

- *Transportation systems management* (TSM): Strategies of relatively low cost developed during the '70s for improving a transportation system. TSM actions can influence supply and demand for encouraging the efficiency, safety, capacity, or LOS of a transportation system without increasing the infrastructure size or other expensive large-scale actions (Schoon, 1996). Some strategies aim for traffic signal improvements, intersection improvements, intelligent transportation systems, and others.
- *Transportation demand management* (TDM): Strategies that increase the productivity and efficiency of a transportation system, modifying demand behavior (Ferguson, 2018). TDM strategies encourage the increment of car occupancy, modal change to transit, and reducing congestion, e.g., moving car trips outside of rush hour, carpooling, non-motorized travel, parking management, financial incentives, and others.

Both types of strategies have implementations in the short or medium term. In both previous cases, the objective of these strategies is to optimize the use of existing infrastructure, these even require certain minimum infrastructure conditions, so there will be positive effects on transportation.

Spatial planning instruments

The development of spatial planning instruments (SPI) materializes urban planning in cities. These instruments are norms, plans, or even strategies that encourage positive transformation actions on a territory. The actions work over public and private entities, and these have a medium-to-long-term goal. The Chilean regulations identify three types of instruments: normative, indicative, and exceptional protection zones, e.g., urban development plan, urban regulatory plan, the master plan of transportation, and others (Precht, Reyes, & Salamanca, 2016).

In urban planning, UN countries agreed on the "New Urban Agenda" (NUA) at the Habitat III conference (2016). NUA will serve as a guide for urbanization from 2016 to 2036. Therefore, UN countries committed to

> *"…promoting the development of urban spatial frameworks, including urban planning and design instruments that support sustainable*

> *management and use of natural resources and land, appropriate compactness and density, polycentrism, and mixed uses…"* (Chapter 51)
>
> *"…adopting a smart-city approach that makes use of opportunities from digitalization, clean energy, and technologies, as well as innovative transport technologies…"* (Chapter 66)
>
> *"…promote integrated urban and territorial planning…based on several principles of equitable, efficient and sustainable use of land and natural resources, compactness, polycentrism, appropriate density and connectivity, and multiple uses of space, as well as mixed social and economic uses in built-up areas, in order to prevent urban sprawl, reduce mobility challenges and needs and service delivery costs…"* (Chapter 98)

The present dissertation takes into account these principles of urban planning for the development of modeling of transportation systems.

1.2. Justification of the research

A standard question emerges for old or new cities, for concentrated or dispersed cities, or any other type of city:

> How is it possible to adapt the infrastructure and all land uses—residential and non-residential—to meet the needs of people who want to travel for any purpose and mode?

The previous question promotes a balanced network design between the distribution of population and land uses and its infrastructure.

In the highlighted book called *Urban Networks-Network Urbanism* (2008), Gabriel Dupuy criticizes the role of traditional urbanism in current cities. The author promotes an integral city-mobility approach. This new interdisciplinary approach focuses its theory on articulating urban space through the concept of network, i.e., networks generate their spatial organization, and these continually evolve.

This new approach has a direct connection between urbanism and network operability. The transportation system and the urban system must have a connected operation because both depend on the other. Thus, a planner should take a similar role as a network operator to solve an urban problem correctly. Therefore, traffic and transit are an essential part of an urban planning problem.

The above means that spatial components in transportation components are essential, and urban planning requires planning instruments for its implementation over a region. The planning instruments can be normative, indicative, or investment portfolios. The elaboration of these instruments needs studies to define the quantity and type of infrastructure for a town. Since these plans are long-term, the design of the infrastructure network is a crucial factor. Hence, these new methodologies allow contributing to engineering and urban planning.

Urban planning must consider that a city needs minimum physical conditions to be satisfied in order to maintain an adequate level of urban mobility and transportation by considering heterogeneous demand. Conditions include, e.g., urban size, location, and size of the central business district (CBD), the proportion of public space destined for transportation relative to the built space, the spatial distribution of land uses, and population density, among others. If a city does not meet these minimum physical conditions, the transportation supply must adapt to the demand or vice versa. Thus, TSM and TDM strategies could guarantee an adequate level of urban mobility. However, all TSM and TDM management strategies also require minimal infrastructure conditions for their success.

Policies and strategies may be favorable and improve urban mobility as long as the network design and infrastructure supply enable it. In this way, in the design and infrastructure supply, the decision variables of a transportation problem can simultaneously restrict a transportation system's ability to achieve efficiency in urban mobility.

1.3. Thesis objectives

Spatial planning instruments require several studies to determine the infrastructure needs considering the demand of a city. This research aims to develop a macroscopic method to identify the infrastructure needs that sustain an adequate level of service for urban mobility and transportation. The proposed methodology based its formulation on analytical models to deduce the critical components of a network structure. These key components must ensure the critical conditions of the private and public transportation infrastructure.

Therefore, the dissertation focuses its investigation on urban design based on functionality, the role of demand, and the effects of design on the urban

structure. In this case, the demand spatially varies over a city in volume, extension, and spatial heterogeneity. In the framework of a non-homogeneous demand pattern, the networks should adapt to different scenarios of distribution of demand. Thus, these network-adapted configurations have to be in balance with the agency's costs.

The research has four specific goals based on the main objective. Therefore, the investigation also requires:

- Develop an **analytical model** that replicates the system operation for **public and private urban transportation** in a radio-centric city with radial and circular routes/roads. The model must identify the optimal configuration of infrastructure in a city by considering a non-homogeneous demand pattern and balancing users and agency costs. This model allows identifying the critical variables of a transportation system for efficient mobility.
- Determine **optimal characteristics for an adequate design of urban networks** considering the urban form and structure. The methodology focuses on a concentric city considering the functionality in designing a primary transportation network regarding urban form. The analysis focuses on urban density, transportation systems, a central business district, and subcenters regarding urban structure.
- Apply the methodology to **two policies considering different levels of analysis**. The analysis focuses on subcenter analysis and the implementation of autonomous vehicles. Mainly, the selected policies respond to two types of transportation: traffic and transit. Moreover, the policies have effects on transportation, urban planning, and the interaction of both.
- Evaluate the theoretical analysis proposed in the previous points and **apply it to a radio-centric city** such as Santiago, Chile.

1.4. Dissertation outline

The thesis document continues with five chapters: state of the art, modeling, analysis of infrastructure and urban mobility, applications, and conclusions. Finally, the document ends with a list of references and appendices.

The next chapter presents state of the art, which contains a revision of previous investigations about four topics: urban form, urban structure, the design of transportation networks, and a method of modeling. Finally, the chapter ends with a summary of the analyzed contents.

The third chapter includes the modeling of urban mobility and network design. This chapter has five parts: demand modeling, development of the

modeling of a transit and traffic system, methodologies for the discretization of solutions, and finally, the global summary of this chapter.

In the fourth chapter, the research applies theoretical models in standard cases in order to analyze the infrastructure and urban mobility and the physical conditions for adequate mobility.

The chapter of application in some policies presents the results obtained from theoretical models applied in two policies: implementation or urban subcenters and analysis of autonomous-vehicles effects.

The sixth chapter presents the application to a real case for Santiago (Chile).

Finally, the research document presents conclusions and future research on this subject.

2. State of the Art

In the literature, scholars have a widespread agreement on the mutual influence between land use and mobility. Acheampong and Silva (2015) thereby identified several studies in which urban structural variables statistically influence mobility behavior.

Regarding this point, Vukan Vuchic (2007) acknowledges that transportation systems have affected urban systems.

> "*A review of historic developments will show how long-distance transportation had a major role in determining the locations of cities; how their size has been influenced by both long-distance as well as local, intraurban travel and transportation systems; and how the latter has affected the urban form (shape of urban area and its basic transportation network) and urban structure (distribution of land uses and population densities).*" (p. 1)

Similarly, Rodrigue et al. (2017) also identify both components (Figure 2.1). The spatial imprint of a transportation system and its physical infrastructures define an urban form. The connections between the urban form and their interactions among people, freight, and information define an urban spatial structure. From this, scholars may evaluate how a specific urban structure can change or adapt to a specific transportation system and vice versa.

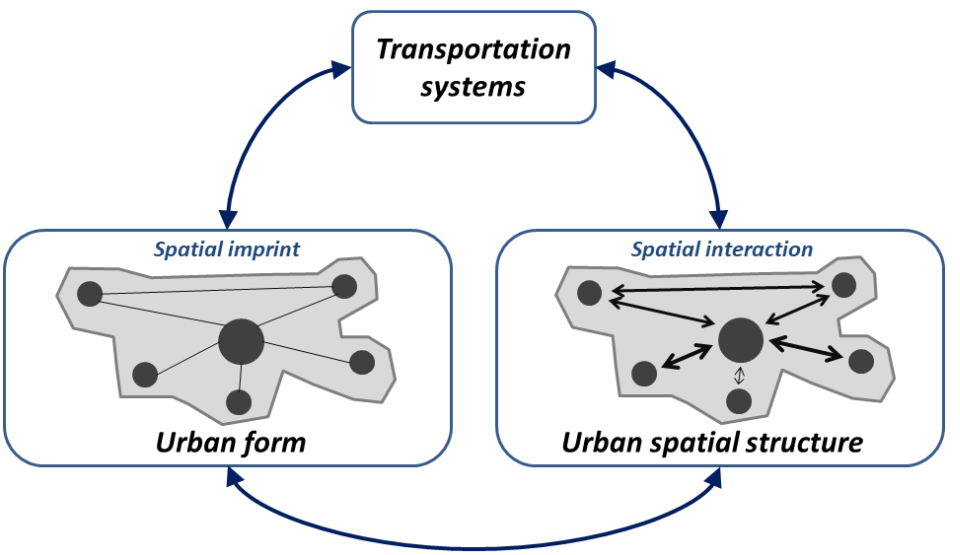

Figure 2.1. Influence of transportation systems on urban components.

Source: Adapted from Rodrigue et al. (2017).

It is worth mentioning that an urban transportation system has four primary sub-systems: transit, traffic, logistics systems, and personal mobility. The latter has had remarkable growth during the last decade. The present dissertation only models the two first transportation sub-systems.

The previous definitions structure the present chapter. It has five parts: analysis of urban form (2.1) and urban spatial structure (2.2), the design of transportation networks (2.3), a description of modeling methods (2.4), and, finally, the summary of this chapter (2.5).

2.1. Urban form: shape and transportation networks

According to Vuchic (2007) and Rodrigue et al. (2017), two components define an urban form: the urban shape and essential transportation networks.

2.1.1. Urban shape

The first cities did not have any planning or, in some cases, a few rules defined a minimal layout in ancient cities, which had an orientation to walking mainly. Therefore, cities were compact with activities agglomerated in mixed uses. Many modern cities inherited this morphology in which walking and cycling join a high percentage of the modal partition, e.g., European cities and Eastern Asian cities. Australian, Canadian, and American cities have encouraged the use of private transportation. On the other hand, Latin American cities were their origins defining a grid center, but those grew expansively without strengthened planning (Rodrigue et al., 2017).

Transportation and its evolution have generated changes in the shape of cities. Technological changes in public and private transportation have allowed users to move away from historical city centers. In terms of infrastructure, agencies began to build radial and ring/circular roads, which promoted the development of suburbs. Simultaneously, new clusters that group activities defined a polycentric structure; thus, commuters did not only travel to the CBD. Also, distribution centers appeared in the suburbs to generate new connections for a city, a region, and the world (Rodrigue et al., 2017).

Transportation modes in a city simultaneously define the urban and network shape. Snellen et al. (2002) identified six basic shapes basing on previous investigations (Figure 2.2).

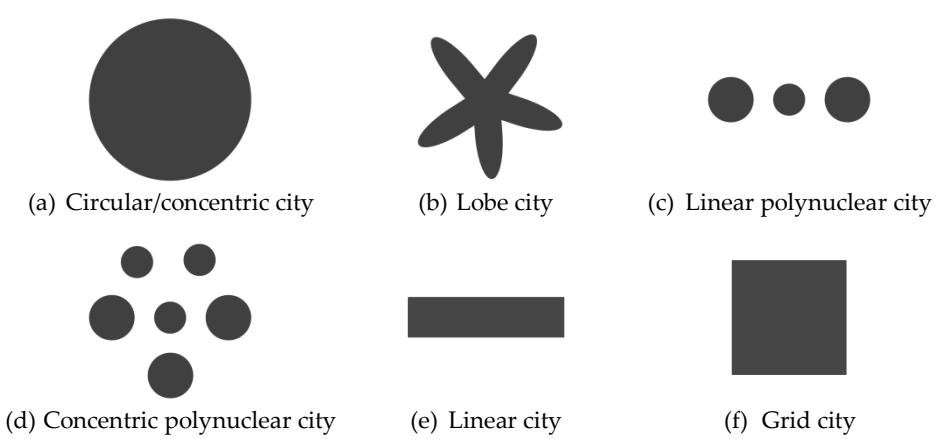

Figure 2.2. Morphological urban shapes.

Source: Snellen et al. (2002).

A circular or concentric city (Figure 2.2(a)) may grow from a small historical center to outer along radial roads, which connect the city to other cities. When a city grows, new dwellings and activities use the space between those radial roads. Often, these cities combine radial, ring roads, and even grid networks in the city center. Many cities have a radio-centric structure, e.g., Moscow, Milan, Canberra, Chengdu, and Santiago of Chile (Medina-Tapia & Robusté, 2019b). Otherwise, some cities have similar forms, e.g., semicircular cities have a center very close to the coastal edge.

A lobe city (Figure 2.2(b)) may have a similar origin to the previous case, but some areas between radial roads do not have any buildings (e.g., Eindhoven). A linear polynuclear city or concentric polynuclear city (Figure 2.2(c) and (d)) comes from small settlements in a natural or planned way (e.g., Almere). A linear city may be an extreme version of a grid city (Figure 2.2(e)). A grid city (Figure 2.2(f)) may have a square or rectangular shape (e.g., Haarlem). These cities have their origin in planning, promoting a high mobility role (Snellen et al., 2002).

In the literature, many academic publications analyze the optimum size of cities and CBDs. It is worth mentioning the works of Mills and de Ferranti (1971), Solow and Vickrey (1971), Solow (1973), and Sheshinski (1973).

2.1.2. Basic transportation networks

Nodes and linkages functionally articulate a network. Nodes represent physical elements (e.g., intersections, stations, airports) or sets of economic activities (e.g., residential neighborhoods, financial centers, commercial zones) depending on the hierarchy and the scale of analysis (macro, meso, or microscopic). A link can represent from streets to railways depending on modes, hierarchy, and the analysis scale in which linkages contain the flow between two nodes (Rodrigue et al., 2017).

For road networks, Snellen et al. (2002) defined five basic types (Figure 2.3(a)-(e)). The former is the central element of a linear or grid city. The radial network allows direct access to the city center, although this network type also has congestion problems. The ring network may concentrate traffic to reduce it on nearby roads, i.e., many city centers have a ring road around it. Roman cities implemented grid street patterns from the first centuries. This pattern may optimize the accessibility of a city. The standard and shifted grids provide many route options to disperse traffic on many streets, although it presents many intersections in a road system.

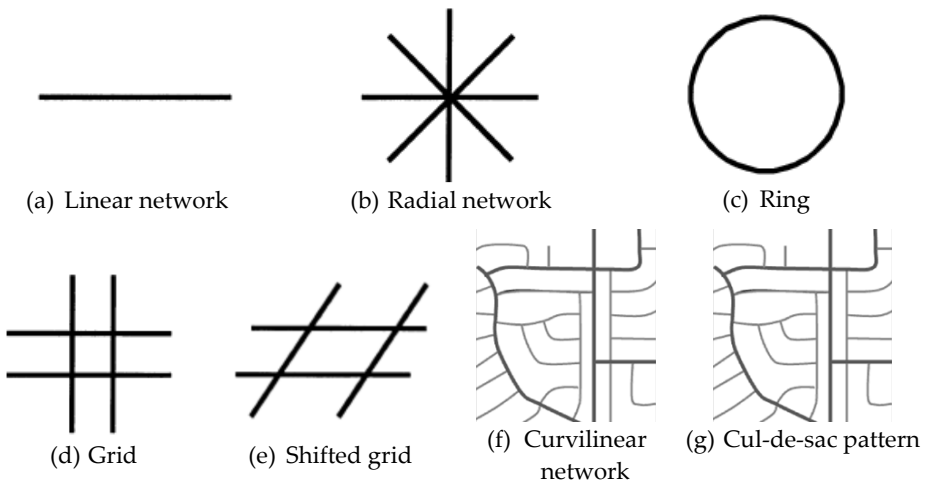

Figure 2.3. Types of elementary transportation networks.

Source: Adapted from Snellen et al. (2002) and Rodrigue et al. (2017).

Later, Marshall et al. (2010) proposed three types of street networks (Figure 2.3(d), (f), and (g)): grid, curvilinear, and cul-de-sac street pattern. Private transportation promoted trips in cars. Therefore, some cities changed their network from a grid to a curvilinear pattern. Curvilinear patterns reduce connectivity and population density. Cul-de-sac pattern aisles a set of connected streets, in which some of those have a connection to the main road. This pattern is typical in a peripheral zone for reducing non-local travels, but it increases the number of trips and car consumption.

On the other hand, public transportation networks mix infrastructure and operation. Thompson (1977) compared four types of transit networks: radial, ubiquitous, grid, and timed transfer. In the first, a route connects each origin-destination zone to the city center. In the second, there is a direct route between each origin-destination pair, and it is "*the highest degree of a direct trip-based system*" (Badia, 2016, p. 7). In the third, a route connects each origin-destination pair. Finally, a timed transfer system connects the origin-destination pair through several transfer points. The two last represent transfer-based schemes. Recently, Badia (2016) reviewed outstanding bibliographical references on public transportation networks identifying seven transit network shapes: linear, parallel lines, hub-and-spoke, radial, ring-radial, grid, and hybrid.

Therefore, for this dissertation, elementary public transportation networks present three main categories: linear, radial, and grids.

First, a linear network is the most basic network and has three sub-classes: corridor-route, route-and-feeder, and parallel-line schemes (Table 2.1). In the former sub-class, authors determine the optimal stop spacing on a transit corridor (e.g., Saka, 2001). Medina et al. (2013) simultaneously determine the stop density (spacing) and frequency on a corridor. In the second sub-class, other authors simultaneously optimize a route and its feeder routes. For example, Wirasinghe (1980) optimizes a rail route and a feeder system on a rectangular grid. Kuah and Perl (1988) optimize feeder bus routes and bus-stop spacing on a corridor. In the latter class, papers model parallel lines of a transit system. Byrne (1976) models a transit system in a rectangular city where the commercial speed is not the same for all the lines. Thus, users do not choose the closest route if that route is slower than other routes.

Table 2.1. Papers based on linear corridors.

Corridor route	Route and feeder	Parallel lines
Saka (2001)	Wirasinghe (1980)	Byrne and Vuchic (1972)
Medina et al. (Medina-Tapia et al., 2013)	Kuah and Perl (1988)	Byrne (1976)

Source: Based on Badia (2016).

Second, a circular-radial street pattern has works grouped in three categories: radial, ring-radial, and hybrid radial networks (Table 2.2).

Table 2.2. Papers based on radial networks.

Radial	Ring-radial		Hybrid radial
Byrne (1975)	Chen et al. (2015)	Vaughan (1986)	Badia et al. (2014)
Tirachini et al. (2010)		Nourbakhsh (2014)	

Source: Based on Badia (2016).

Radial networks are a type of direct trip-based structure (Byrne, 1975; Tirachini et al., 2010). In this way, Byrne (1975) optimized the combination between route location and headway on a radial transit system. Tirachini et al. (2010) compared transit technologies (bus, tramway, and metro) considering a circular city's radial scheme and CBD. For several scenarios, the results show that bus rapid transit (BRT) is the best alternative.

Considering ring-radial networks, Chen et al. (2015) proposed two models; one of them considers a ring-radial structure with a city center that has

double coverage, but the periphery only has radial routes. In this system, users can travel on radial services without any transfers (direct trip-based system). On the other hand, some authors analyze transfer-based systems. Vaughan (1986) design a ring-radial network considering a many-to-many demand through a continuous function for representing the commuting trip demand. More recently, Nourbakhsh (2014) proposed several procedures for designing transit networks taking into account low and heterogeneous spatial demand.

Some hybrid networks consider a radial structure. Badia et al. (2014) analyze a scheme in which a radial/circular system operates in a central area, and a hub-and-spoke system serves to the periphery (transfer-based system).

Table 2.3. Papers based on grid networks.

Radial	Grid		Hybrid grid
Badia et al. (2016)	Holroyd (1967)	Chen et al. (2015)	Daganzo (2010)
	Aldaihani et al. (2004)	Badia et al. (2016)	Badia et al. (2016)

Source: Based on Badia (2016).

Third, grid networks have three types of transit schemes: radial, grid, and hybrid structures. Some of them are direct trip-based or transfer-based systems (Table 2.3).

Daganzo (2010) proposed a model that combines a grid and the hub-and-spoke structure (hybrid grid) on a square region with a homogeneous demand. The objective function has two components: agency and user costs. It has three decision variables: central grid size, stop or route spacing, and headway. After modeling, user costs dominate over operational costs. The results point that if the infrastructure is expensive, a hub-and-spoke structure is more attractive considering bus-stop spacing; thus, the distance between routes must keep a critical threshold. Moreover, BRT is an adequate system in cities with medium to high density.

Recently, Badia et al. (2016) analyze four types of grid structure: radial, direct trip-based, transfer-based, and hybrid structures. The results show that a radial network is more suitable in concentrated cities, the direct trip-based system is more attractive in cities with intermediate degrees of dispersion, and a transfer-based structure is the best option if activities are decentralized.

Also, other authors analyze grid networks. Aldaihani et al. (2004) proposed a model to design a hierarchical transit system, which combines fixed routes and on-demand services on a grid network.

2.2. Urban spatial structure: land-use and population densities

Urban areas contain the majority of social and economic activities. If trips to those activities are obligatory, the number of trips will be predictable. Other trips are not mandatory, in which the production depends on regular personal activities or special needs. Moreover, production activities related to manufacturing and distribution (i.e., freight transportation) also produce many city travels. Therefore, transportation and land use have an interrelation due to the type, location, and interaction of urban activities.

The use of urban land is highly heterogeneous, and a transportation system partially configures this heterogeneity. Central areas of a city have high levels of spatial clusterings, such as retail, while peripheral areas have lower levels of clustering corresponding to residential and storage zones.

2.2.1. Land-use concentration and urban densities

Transportation and land use have a reciprocal relation, and their imbalances generate mutual effects as well. Therefore, the effects of this imperfect distribution of land use on a territory will affect the efficiency of transportation systems in an urban system.

Concentration of activities

Four categories of urban spatial structures define the distribution of activities in a city, depending on centralization and clustering (Rodrigue et al., 2017).

- *Centralization*: It is a spatial configuration of activities regarding an entire urban area. A centralized city has many of its activities in the city center, while a decentralized city does not.
- *Clustering*: It is a spatial configuration regarding a specific part of an urban area. Around a specific point concentrates a group of activities (cluster), e.g., a smaller town that the expansion of a metropolis absorbed.

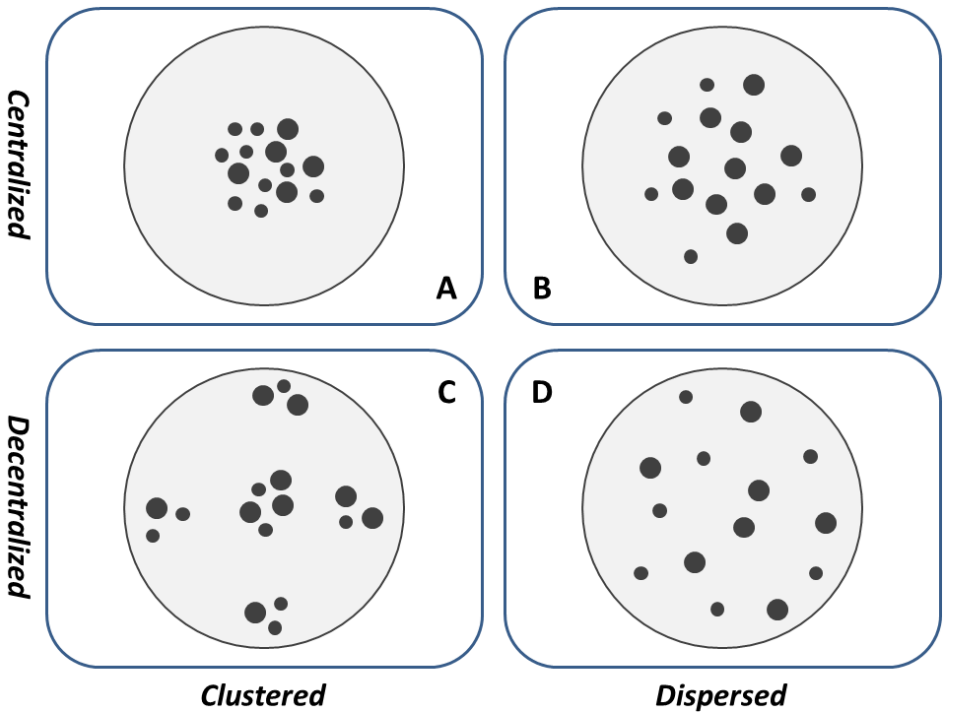

Figure 2.4. Urban spatial structures considering the level of centralization and clustering.

Source: Rodrigue et al. (2017).

Figure 2.4 represents the classification of urban structures, considering the level of centralization and clustering. Case A is a centralized and grouped scheme that concentrates activities close to each other in a city's central area. Case C is a relevant scenario in which territories have decentralized activities but maintaining a high level of grouping (a multicentric or polycentric city).

Dispersion of cities

Many cities currently suffer a dispersed growth called urban sprawl. In some cases, the consequences are fast and uncontrolled. Cities are thus growing horizontally—expansive growth—in which the increase of cars plays a decisive role in this process. On the other hand, the decentralization of activities occurs because travel time remains stable, even if travel distance increases by car or transit due to new technological development in transportation.

From these concepts, three types of urban development are therefore identified regarding concentrated cities or disperse cities: compact city,

polycentric development, and dispersed development (Wegener & Fürst, 2004).

- *Compact city*: This type of city involves the intensive use of land, which has a monocentric urban structure and minimizes the expansion of urbanized areas, thereby protecting the environment and rural areas.
- *Polycentric development*: This urban strategy implies a development with a high density around employment and business centers in the suburbs. The "decentralized concentration" is because large compact cities are not efficient due to high-energy consumption, high congestion levels, and a critical accumulation of environmental pollution in the city.
- *Urban sprawl*: Many people prefer to live in single-family homes and do not like mobility restrictions. Considering this, people inhabit houses beyond the outer edge of a city, and the city grows scattered. This type of urban development can be planned or spontaneous, but the latter is a common consequence of unsatisfactory urban planning.

The above is a classification of cities, but also those are strategies or policies defined in an urban plan. Regarding the dispersion of cities, many factors generate the development of suburbs: low cost of land, availability of large areas to urbanize, the environment, safety, and the benefits of cars and services oriented to cars (e.g., strip centers and malls). With the expansion of urban areas, the agencies build ring roads around major cities. Moreover, many cities develop multi-centers creating peri-urban areas outside of the urban nucleus and even suburbs.

Portugal et al. (1996), based on Smeed (1968), stresses that a continuous extension of the infrastructure supply is irrational in a congested network. Moreover, the authors emphasize that road space should consider the land as a scarce resource, in which a city must orient the public space to public transportation, gradually restricting private transportation and promoting intermodality through a park-and-ride strategy.

Urban density

Population density is one of the factors that define the urban structure of a city, existing an indirect connection with the building height. Unfortunately, few works have addressed the analysis of population density and height of buildings, and some have an engineering approach. Solow (1972) developed an equilibrium model between residential density and the income for a monocentric city considering transportation costs. Brueckner et al. (2015) analyze the effect of height restrictions on the value of land-use.

2.2.2. Transportation and land-use interaction

The relation between transportation and land-use has many theoretical approaches: location and distance influence the organization of spatial elements and their activities. Rodrigue et al. (2017) present a preliminary classification of models considering transportation, population, and land uses.

- *Early models*: This category includes classic models, e.g., Von Thunen's model of land use proposed in the 19th century. The model has its basis on a central place and its concentric impacts on land use of the surrounding land. Subsequently, Weber proposed an industrial location model at the beginning of the 20th century. His model minimizes total transportation costs to access raw materials and transfer production to the market.
- *Concentric urban land uses*: Burgess proposed one of the first models of this type in 1925. This model was an adaptation of Von Thunen's model. The objective was to model social classes, but the model also considered both transportation and mobility. One of the conclusions was regarding the cost of daily trips. If improvements reduce travel costs, then more people can live further away, promoting urban expansion.
- *Polycentric and zonal land uses*: Sector and multiple nuclei of land-use models allow analyzing this type of urban form, e.g., the influence of transportation corridors (Hoyt, 1939) and multiple nuclei under urban growth (Harris and Ullman, 1945).
- *Hybrid land uses*: These models include concentric, sectorial, and nuclei behavior to explain the use of urban land, e.g., Isard (1955) analyzes the concentric effect of CBDs and subcenters and the radial effect of roads.
- *Land use market*: These models seek to explain land use as a market in which activities compete for land use in a location. Transportation and accessibility are explanatory factors of land rent.

Spatial equilibrium models have abundant literature, as Wegener and Fürst (2004) notes in their paper of state of the art about land-use and transportation interaction (LUTI). After that, Acheampong and Silva (2015) provide an overview of some 60 years of research in the field of LUTI modeling. The authors emphasize that this type of modeling has challenges for its improvement. New technologies—e.g., GIS, microsimulation, and others—have enhanced this research field, although models must understand the uncertainty propagation over time. Investigations should deepen the models of demand for trips based on activities and practical models. It is relevant for integrating the environment and the forecast of urban policies on climate change and energy shortages. Finally, methodologies need to measure accessibility.

For example, Wong (1998) developed a user-balancing model with traffic allocation for dense transportation networks and variable demand. Van Zuylen and Taale (2004) solved the traffic assignment problem for ring roads through game theory with two levels and three players with complete information. The authors also analyze different scenarios such as non-cooperation, cooperation between authorities, and optimization of the system, minimizing a function of the total cost with the cooperation among social actors.

2.3. Design of transportation networks

Dupuy (2008) points out that the analysis of the city-mobility approach should consider three dimensions:

- *Topological dimension*: This dimension encourages urban opening and decentralization, e.g., a ubiquitous network ensures the maximum connection in a city independent of location, barriers, or limits.
- *Kinetic dimension*: This considers the speed of movements in a network.
- *Adaptive dimension*: The ability to adapt networks to needs demanded. This dimension ensures the permanence and long duration of the infrastructures.

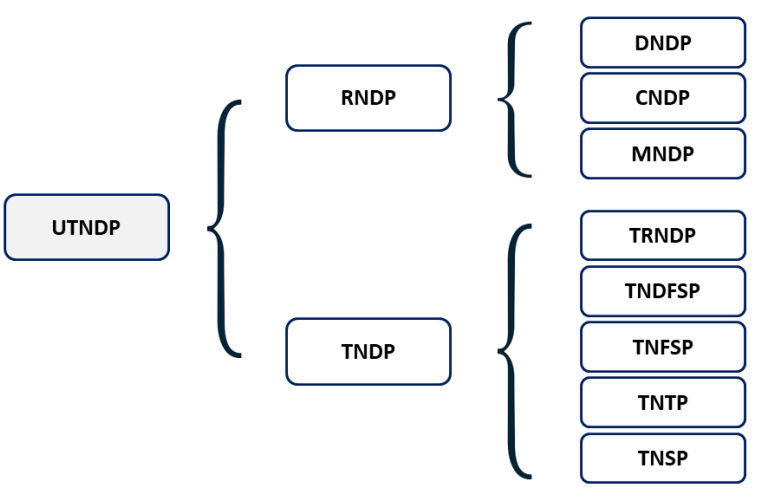

Figure 2.5. Classification of transportation network design problems.

Source: Based on Farahani et al. (2013).

The planning process is fundamental for the appropriate functioning of a transportation system. One of the first early stages of planning is the strategic design for any transportation structure. The urban transportation network

design problem (UTNDP) solves an entire hierarchy of decision-making processes in transportation planning (Figure 2.5) in which the decisions may be strategic, tactical, and operational (Magnanti & Wong, 1984). UTNDP includes two sub-problems: the road network design problem (RNDP) and the transit network design problem (TNDP) (Farahani et al., 2013).

In the literature (Farahani et al., 2013), RNDP has three types of problems based on the addressed decisions:

- Discrete network design problems (DNDP) focused on discrete design decisions,
- Continuous network design problems (CNDP) focused on continuous design decisions, and
- Mixed network design problems (MNDP) combine continuous and discrete decisions.

Discrete models are appropriate for current networks, although these require efficient algorithms to solve large problems. On the contrary, continuous models are useful for finding fundamental relations among variables (Miyagawa, 2018).

Depending on the type of decisions (Farahani et al., 2013), TNDP contains five sub-problems:

- Transit route network design problems (TRNDP) solve the design of transit routes,
- Transit network design and frequency setting problems (TNDFSP) determine the design of transit routes and frequency of each bus route (R. Smith, 2014),
- Transit network frequencies setting problems (TNFSP) solve the frequency setting for route system,
- Transit network timetabling problems (TNTP) solve the timetable problem considering frequencies and routes given, and
- Transit network scheduling problems (TNSP) solve the frequency and timetable decisions considering a route structure.

This dissertation aims to determine spatial and temporary variables for road and transit design considering strategic planning decisions. Therefore, the traffic problem is a continuous network design problem (CNDP); and the transit problem is a transit network design and frequency-setting problem (TNDFSP), which simultaneously determines routes and preliminary frequencies. Discrete and analytical models can solve a TNDFSP (Ibarra-

Rojas, Delgado, Giesen, & Muñoz, 2015), although parsimonious models contain interesting characteristics for strategic decisions.

The parsimonious models are analytical models that rely on a few parameters and assumptions to study macroscopic transportation systems (Daganzo, Gayah, & Gonzales, 2012). For example, in transit design, a diverse list of parsimonious models exists in the literature: Chang and Schonfeld (1991), Daganzo (2010), Estrada et al. (2011), Badia et al. (2014, 2016), and others.

2.3.1. Transit system

In this research line, a diverse and extensive list of works analytically analyzes the operation of public transportation systems. The investigations have their basis on the classic articles of Vuchic and Newell (1968), Wirasinghe and Ghoneim (1981), Chua (1984), Jara-Díaz and Basso (2003), Jara-Díaz and Gschwender (2003a), Fielbaum (2019), and others. Additionally, several works on networks use a structure of polar coordinates developed by Haight (1964) and Smeed (1965, 1968).

Vaughan's paper (1986) analyzes the behavior of a ring-radial network considering a many-to-many demand. A continuous function represents the commuting trip demand. The buses travel at a constant speed, and the model imposes a fleet-size constraint.

Daganzo (2010) analyzes characteristics of shape and operation in order to provide a high level of competitiveness for a public transportation network. The author models a square region with a uniform density, which combines a grid with a hub-and-spoke pattern.

Badia et al. (2014) present an extension of the hybrid model formulated by Daganzo (2010). The modeling considers a ring-radial pattern in the central area and hub-and-spoke in the periphery. The model minimizes a cost function with four decision variables: CBD size, headway, the spacing between routes, and stops. In this line, other works are possible to mention, e.g., Foletta et al. (2010), Estrada et al. (2011), and Roca-Riu (2012).

Chen et al. (2015) propose an analysis of urban networks using two continuous approximations (CA) models, which minimize a cost function. The first case analyzes a city with a ring-radial structure, and the second case considers a grid structure for a transit system. Those models allow

determining the optimal size of a CBD, the city border, time headway, and spacing of transit routes.

More recently, Smith (2014) evaluates the impact of spatially heterogeneous demand over a hybrid transit system considering a transit network design with elastic demand. Ouyang et al. (2014) formulated a method based on continuum approximations, which designs bus networks for an urban grid system with non-homogeneous demand. The model achieves improvements of 8% in numerical examples considering demand spatially varies over a city. Moreover, Nourbakhsh (2014) proposed network design methods to improve transit systems, considering low and heterogeneous spatial demand.

Unfortunately, these papers do not consider that time headways must vary considering local conditions within a city. Moreover, no works have expressed an analytical formulation representing the optimal transit infrastructure needs and adapting to spatially heterogeneous and non-symmetric demand over a town. Finally, the discretization method is relevant if variables of a network spatially vary over a city depending on attributes of transit technologies needed: speeds and operating attributes, the capacity of vehicles and operation, frequencies, costs of capital, operation, and infrastructure of a transit system.

2.3.2. Traffic system

Traffic congestion is one of the most significant problems for cities, as Colin Buchanan asserted in the '60s (Buchanan, 1963). Several strategies have an application to smooth out congestion, most of them under the umbrella of transportation demand management (TDM).

In previous papers (Farahani et al., 2013), three main decisions analyze, considering a continuous network design problem (CNDP) as a sub-problem of the road network design problem (RNDP): determining road tolls, scheduling traffic light, and street capacity expansion. The first group includes works such as Yang (1997). The second group includes works such as Chiou (2008) and Ziyou and Yifan (2002). The third group contains the majority of works about road network design problems (Farahani et al., 2013), e.g., Mathew and Shrama (2009), Wang and Lo (2010), and González and Robusté (2011).

In this research line, González and Robusté (2011) proposed a mobility management tool to determine the percentage of road space necessary for a

public transportation system concerning private transportation considering congestion externalities.

Furthermore, other authors analyze other decisions. An important decision is to define the hierarchy of a road network (Li, Chen, Wang, Lam, & Wong, 2013; Miyagawa, 2018).

Li et al. (2013) proposed a system equilibrium model to optimize a primary road network density. The model applied to a two-dimensional monocentric city considers four agent types: local authorities, housing agencies, households, and workers. The optimization model determines the density of main roads maximizing the social welfare of the system.

Miyagawa (2018) proposed an analytical model to determine the optimal spacing between roads considering a hierarchical grid road network with two types of roads: minor and major roads. The travel time has two components: free travel time and the delay at road intersections. Moreover, the model is useful for designing hierarchical road networks. This model optimizes the average travel time and analyzes trade-offs between the travel time on types of roads. According to its results, several variables affect the optimal road pattern, e.g., the road length, the intersection delay, the travel speed, and the city size. Moreover, the model analyzes the effects on the accessibility to primary roads and intersections. Finally, the author applied the model to Tokyo city.

The article writes by Tsekeris and Geroliminis (2013) uses the "macroscopic fundamental diagram" (MFD) to analyze the relation between traffic and land use applied to a concentric city.

Finally, a few contributions analyze the traffic network design considering spatially, non-homogeneous demand using the continuous approximation method. This dissertation concentrates its work on these contributions.

2.4. Methods of modeling

Daganzo, Gayah, and Gonzales (2012) analyze parsimonious models and their importance, considering these formulations rely on a few assumptions and have few degrees of freedom or input parameters.

Ibarra-Rojas et al. (2015) describe a list of transportation problems considering their scale, i.e., strategic, tactical, and operational planning

decisions. According to strategic decisions in network design, discrete and continuous methods can solve transportation problems, although this assertion extends the analysis to any strategic planning decision.

2.4.1. Parsimonious models

Classical models play an essential role in the research and technical development of transport systems in many cities. The next list presents a summary from the discussion of attributes of these models made by Daganzo et al. (2012):

- The amount of data increases with the size of a system.
- The included information is ultimately unknowable (e.g., detailed time-dependent origin-destination data of trips).
- It requires computers and sophisticated numerical methods.
- The models are less transparent and difficult to verify. For this, accessing the machine code is necessary.
- Detailed models might give the user a false sense of precision.
- It is difficult to separate noise in the output from the meaningful relations that are of interest.
- The models are most useful for evaluating specific policies or small solution spaces.

Parsimonious models are analytically tractable (it is easy to work), physically realistic (it is consistent with real-world behavior), and conceptually insightful (it reveals fundamental properties of the analyzed system). Therefore, the model is an effective parsimonious model. Useful parsimonious models are appropriate to describe the "aggregate behavior of large systems with many agents" (Daganzo et al., 2012) and can be obtained in two ways: analytical formulation and experimentation.

The main advantage is that parsimonious models change complicated models with integer variables and uncertainty into much easier models with continuous variables and differentiable functions. Effective parsimonious models have five benefits: fewer data needs, reduced computational complexity, improved system representation, transparency, and insightfulness. The last one may help to identify simple and effective policies. Several examples use these models in transportation, at least in eight sub-areas: regional and urban economics, traffic flow, queuing theory, city planning, network dynamics, public transportation, logistics, and infrastructure management.

According to Daganzo et al. (2012), it is necessary to advance numerical solutions, and advanced numeric techniques may refine preliminary results of transportation strategies through empirical experiments and other techniques.

2.4.2. Continuous approximation method

The continuous approximation method (CA) solves the problem on a local cost basis using variables that are densities (Daganzo, 2005). Gordon Newell proposed the CA method, according to Daganzo (2005). Newell formulated a continuous model that obtains the optimal bus schedule of departures from a bus depot, in which the demand function is considered continuous (1971).

If there is no perfect information, such as passenger arrivals, traffic conditions, and others, it is possible to model with smooth and continuous functions because the information is not accurate (Newell, 1973). These are common conditions in the design of networks. The CA method assumes the following conditions: the input data varies slowly over the domain; the total cost is the aggregation of small sub-region costs, and their constraints depend on the characteristics of these sub-regions (Daganzo, 2005).

The CA method solves a total cost function, which depends on local attributes. It substitutes the optimization of discrete variables for continuous density variables. The method works well when the function does not change rapidly (Daganzo, 2005).

The cost functions are continuous, including a local cost ($tc(r,\theta)$) for each city point (r,θ) in polar coordinates. The total cost (TC) comes from integrating a local cost function on the circular city region of a radius R (Equation 2.1).

$$TC = \int_0^{2\pi} \int_0^R tc(r,\theta)\, dr\, r\, d\theta \qquad (2.1)$$

The optimization of an urban system comes from first-order optimization conditions from the above local cost function concerning a decision variable ($s(r)$), which depends on local attributes (r). These optimized analytical formulations allow getting the optimal value on all city points (Equation 2.2).

$$\frac{\partial\, ct(r,\theta)}{\partial\, s(r)} = 0 \;\Rightarrow\; s(r)^* \qquad (2.2)$$

The method has applications in a wide range of transportation and logistics investigations, e.g., Clarens and Hurdle (1975), Daganzo and Pilachowski (2011), Medina et al. (2013), Pulido et al. (2015), and others.

Clarens and Hurdle (1975) optimize the bus operation in which passengers travel from one terminal to a set of destinations (one-to-many). This work considers that demand varies according to time. The paper uses an analytical model that minimizes the total cost using the continuous approximation method to obtain the optimal headway.

Daganzo and Pilachowski (2011) optimize the bus bunching process based on a system in which buses cooperate with information for buses that come behind. The authors propose a continuous model because it allows identifying "control laws" and quantify their performance.

Medina et al. (2013) optimize both the bus stops location and bus operations simultaneously, considering their quantity and location are significant to transit operational efficiency. The proposed model uses a continuous and multiperiod approximation of a demand corridor, allowing for the determination of the density of stops, which minimizes the sum of operator costs and total costs to passengers.

Pulido et al. (2015) locate warehouses to design physical distribution strategies for a delivery system with time windows. That continuous approximation model includes a cost function with four variables: warehouse density, number of consolidated orders per route, routing zone size, and order consolidation time.

After considering the above, the continuous approximation (henceforth CA) method may be one of the best tools to optimize the macroscopic network design.

2.4.3. Discretization

A few works propose a method that allows the discretization of results from the application of the CA method, e.g., Ouyang and Daganzo (2006), Medina (2011), and Medina-Tapia et al. (2013).

Ouyang and Daganzo (2006) proposed an algorithm for discretizing location issues and other logistic problems. The disk model is the basis of the proposed algorithm, in which each facility location has a disk around it. If

one disc overlaps over another, then the solution is infeasible. In this case, the disc must slide to the opposite side. Finally, a feasible solution has a non-overlapping pattern of a disc. In the paper, the authors compare the results between discrete and continuous modeling. The algorithm finds discrete locations with a similar cost regarding traditional modeling.

Medina (2011) and Medina-Tapia et al. (2013) optimize both the bus stops locations and bus operations simultaneously. The bus stop locations come from a continuous density function later discretized using a method based on Ouyang and Daganzo (2006). The algorithm begins with a feasible solution regarding the number of stops to be located in which an initial solution can have equidistant locations among them. The stops change their positions in a bus corridor, moving away or approaching each other in order to find the equivalent areas. The algorithm stops when the solution finally achieves a given tolerance.

2.5. Summary

- Each city is different from another regarding its origin, functionality, modes of transportation, and urban development levels. However, it is possible to identify attributes considering form and spatial structure.
- Basic schemes of transit networks have different roles in a city, i.e., access to the center, connect contiguous zones, disperse traffic on several streets, traffic calming in residential zones, and others.
- Public transportation networks combine the infrastructure and operation of a system: spacing, headway, direct-trip, transfer-trip based, and others, including the demand and its distribution.
- Transportation and land-use have a two-directional relation in which the structure of land use and population densities are decision variables of the network design problem. At the same time, infrastructure projects may generate positive changes in land use.
- Transportation network design depends on two components: the level of service and urban structure.
- A wide variety of research includes studies on UTNDP, considering the design of traffic networks (RNDP) and public transportation (TNDP). Nevertheless, a few investigations consider analyzing the effects of non-homogeneous demand over a city.
- The parsimonious models are analytically tractable. Several authors have used them to analyze large systems in transportation. Those models can be physically realistic and widely accurate but will not substitute detailed models.

- One of the techniques that allow working up parsimonious models is the CA method. This model is useful for strategic analysis in the transportation system and the challenges of urban planning. The CA method is an adequate tool to define an objective image, one of the first urban planning stages.

3. Modeling urban mobility and network design

The chapter aims to propose a mathematical methodology for modeling urban mobility and designing transportation networks: transit and traffic systems. This chapter has five sections. First, the next section will present the approach to model the demand. Second, the modeling of a generic transit system has five sub-sections: the preliminary concepts, the assignment of trips, the presentation of cost functions, the problem formulation, and the method for optimizing systems. Third, this section contains the traffic system modeling considering similar aspects in comparison to transit network design. Fourth, two methods for the discretization convert the continuous results, presenting their advantages and disadvantages. Finally, the chapter finishes highlighting the main assertions presented in this section.

3.1. Demand modeling

In the literature of transportation network design, three approaches facilitate demand modeling at each transportation stage. First, the demand is spatially homogeneous over a town (e.g., S. Chang & Schonfeld, 1991; Daganzo, 2010). Figure 3.1(a) represents a spatially homogeneous demand at d_0. Second, the demand is variable and symmetric, where the maximum value linearly or exponentially decreases from the center to the suburbs (e.g., Byrne, 1975). The case of Figure 3.1(b) shows a maximum demand is in the center of a city (d_0), and decreases linearly towards the periphery with slope m. Obviously, given d_0 and m, the demand distribution only makes sense for distances $x \leq d_0/m$ from the CBD, in which, it is valid noting that $x_{max} = d_0/m$. Third, Figure 3.1(c) also represents symmetric demand, but it decreases exponentially (negative exponential) towards the periphery.

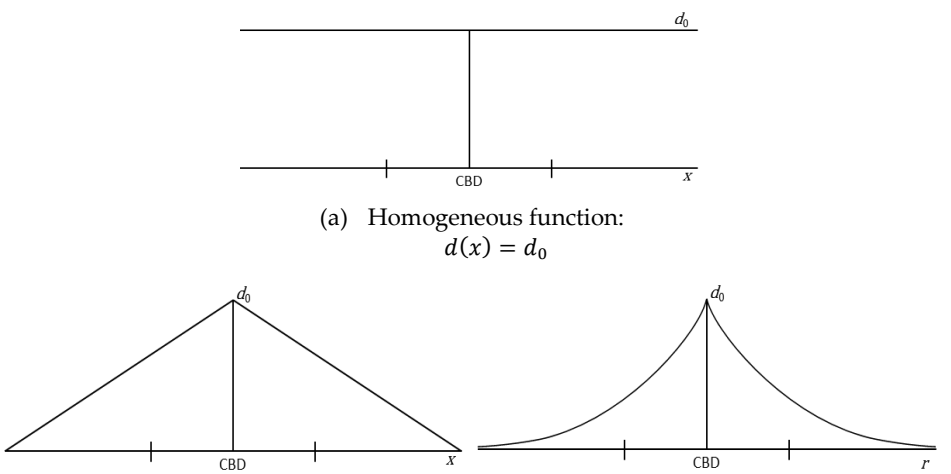

(a) Homogeneous function: $d(x) = d_0$

(b) Linear function: $d(x) = -mx + d_0$

(c) Exponential symmetric function: $d(r) = d_0 \cdot e^{-\lambda r}$

Figure 3.1. Traditional spatial distributions of demand.

It is worth mentioning that these last two formulations represent that demand varies spatially, in which demand is symmetric for both cases. A case more realistic than the previous scenarios, the demand has a variable behavior but not symmetric. In this dissertation, the demand is spatially continuous, two-dimensional, and non-homogeneous.

3.1.1. Trip generation and attraction

The dissertation will analyze several cases from a city in which demand distribution is homogeneous to the last case in which the network design considers heterogeneous demand. The importance has its basis on the latter may reduce the total system cost compared to the analysis of homogeneous transit-route grids, as Ouyang et al. (2014) stated.

Thus, Figure 3.2 shows two examples of a concentric city that presents two different densities for generated and attracted trips. Figure 3.2(a) and (b) represent the trips generated and attracted of a monocentric city in which the CBD mainly attracts trips from other areas of the city and generates fewer trips than the periphery. On the other hand, Figure 3.2(c) and (d) represent trips of an asymmetrically concentrated city, in which there is an attractive area for trips from the center to the eastern sector of the city.

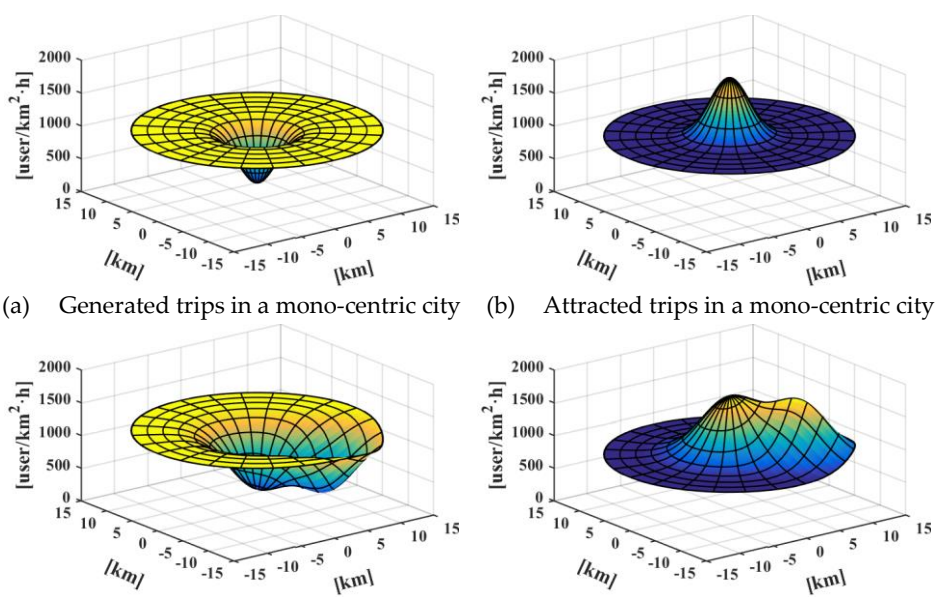

(a) Generated trips in a mono-centric city (b) Attracted trips in a mono-centric city

(c) Generated trips in an asymmetrically concentrated city (d) Attracted trips in an asymmetrically concentrated city

Figure 3.2. Examples of heterogeneous demand distributions.

3.1.2. Trip distribution

The demand distribution function $D(r_f, \theta_f, r_t, \theta_t)$ in [user/km⁴·h] (Vaughan, 1986) represents the spatial density in polar coordinates of passengers per hour who begin a trip from an area $dr_f\ r_f\ d\theta_f$ in [km²] about an origin point

(r_f, θ_f) to an area $dr_t\ r_t\ d\theta_t$ in [km²] about a destination point (r_t, θ_t) (Figure 3.3).

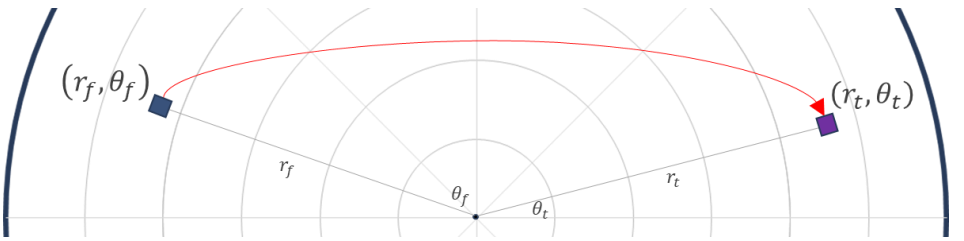

Figure 3.3. Scheme of a density of users that travels between two points.

Source: Medina-Tapia & Robusté (Medina-Tapia & Robusté, 2019b).

The above function may be calculated through any method of interpolation from an origin-destination survey using, e.g., bicubic spline interpolation. From this function, Δ is the total trip demand, in [user/h], of a concentric city of radius R (Equation 3.1).

$$\Delta = \int_0^{2\pi} \int_0^{R} \int_0^{2\pi} \int_0^{R} D(r_f, \theta_f, r_t, \theta_t)\ r_t\ dr_t\ d\theta_t\ \ r_f\ dr_f\ d\theta_f \tag{3.1}$$

Moreover, the above function also allows obtaining the function of generated demand $\lambda(r, \theta)$ at a point (r, θ) in [user/km²·h] (Equation 3.2), and attracted demand $\rho(r, \theta)$ at a point (r, θ) in [user/km²·h] (Equation 3.3).

$$\lambda(r, \theta) = \int_0^{2\pi} \int_0^{R} D(r, \theta, r_t, \theta_t)\ r_t\ dr_t\ d\theta_t \tag{3.2}$$

$$\rho(r, \theta) = \int_0^{2\pi} \int_0^{R} D(r_f, \theta_f, r, \theta)\ r_f\ dr_f\ d\theta_f \tag{3.3}$$

3.2. Modeling a transit system

The transit design of a concentric city allows obtaining independent results of a particular network. However, its conclusions apply to many cities with a radio-centric structure (e.g., Paris, Milan, Moscow, Canberra, Chengdu, Santiago of Chile, and others). The CA method and only relevant inputs of the problem allow obtaining an analytical result that identifies relevant factors and gets numerical results in reasonable computational times. This subchapter has a basis on a paper (Medina-Tapia, Robusté, & Estrada, 2021) detailed in Appendix D.

3.2.1. Preliminary concepts

The region of analysis is a concentric city of radius R [km], including ring and radial routes. Moreover, the modeling considers the rush hour of the city (P_m) as the period of analysis because the peak period defines the required infrastructure.

Users have a non-homogeneous continuous distribution over the city. Thus, each point (r, θ), which is in polar coordinates, has a different density value $D(r_f, \theta_f, r_t, \theta_t)$ in [user/km^4·h], representing the trip density distribution from a point (r_f, θ_f) to (r_t, θ_t), e.g., from an infinitesimal orange area to a black area in Figure 3.4. This function defines the generated and attracted analytical demand function: $\lambda(r, \theta)$ and $\rho(r, \theta)$ expressed in Equations 3.2 and 3.3. These conditions are essential because the demand has an imperfect distribution over a city, a condition typical of all cities, mainly in developing countries. Thus, the approach allows correctly characterizing the demand to obtain an adapted transit scheme.

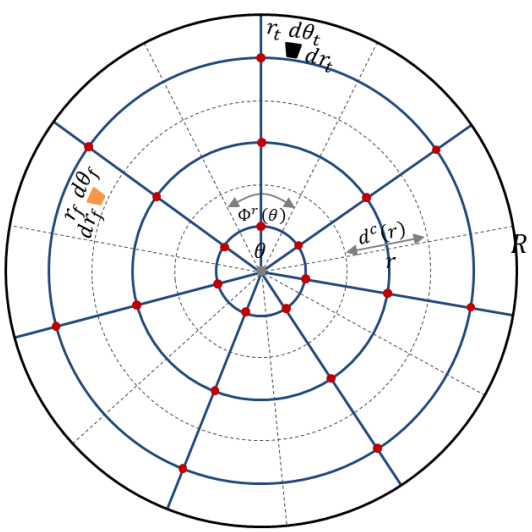

Figure 3.4. Transit structure: ring and radial services (blue lines) and transfer points (red points).

The model assumes that passengers can travel on two types of transit routes: ring and radial routes ($L = \{c, r\}$) in four directions.

- *Ring routes*: users can travel clockwise or anticlockwise direction ($c = \{c_c: clockwise, c_a: anticlockwise\}$).
- *Radial routes*: users can go to the center or come out from this ($r = \{r_i: inside, r_o: outside\}$).

Parameters

The transit network design models a system during the peak period (rush hour, i.e., P_m) in which it lasts T hours (Appendix A). The model analyzes three types of modes (HRT, LRT, and BRT) in which the system has identical vehicles for all routes. Each type has different attributes and unitary cost values. The operation of transit services has the following attributes:

- *Cruising speed (v^t),*
- *Time lost by braking and acceleration (τ),*
- *Stoping time per station/stop (τ' and τ''),*
- *Time lost by crossing an intersection (τ'''),*
- *Positioning time at terminals of a route (t^f), and*
- *The number of work shifts on a vehicle (η^d).*

The user-related parameters include the perception of time and average access values:

- *Perception of time by users (α, β , γ, and δ),*
- *Average access speed ($v^a(r)$) including walking speed (v^w), and*
- *Average distance to transfer between two stations (χ^T).*

The list of unitary cost parameters considers users, capital, operation, and infrastructure cost:

- *Travel time value by average user (μ),*
- *Unitary cost per vehicle (φ^k),*
- *Driver's wage per hour (φ^g),*
- *Operating cost per kilometer traveled at a cruising speed (φ^o), and*
- *Linear (φ^p) and nodal (φ^s) infrastructure cost.*

Infrastructure also depends on the types of services, which also influence their attributes and unitary costs.

- *Linear infrastructure* has railways for HRTs and LRTs, and roads for BRTs.
- *Nodal infrastructure* is at intersections of two railways/roads with stations for HRTs and LRTs and stops for BRTs.

The system has constraints for network design and transit operations.

- *Vehicle capacity constraint*: Capacity depending on the type of vehicle (K^v),
- *Spatial constraint*: The model through constraints ensures that vehicles reach the cruising speed between stops/station (K^d), and

- *Headway constraint*: The model avoids frequencies that could be dangerous for the operation of a system, especially for railway services (K^h).

Finally, the detailed explanation of previous parameters is in Appendix A, including the definition and their units.

Assumptions

The following points present the assumptions of this work.

- The passenger arrival rate at each point is deterministic and high. Therefore, the model considers a transit operation by frequency.
- Passengers board/alight a vehicle of a service that has fixed and known transit stations. Hence, the model does not consider user reassignment on the network.
- Users can take one or two services performing up to one transfer between routes.
- The users' cost is independent of age, socioeconomic level, time of the day (period), or other conditions.
- The drivers' salary is steady. In other words, wages do not depend on the number of passengers transported.
- The unitary cost of operations is the same when a vehicle travels at cruising speed, a car accelerates and brakes at a station, and users board and alight at a station.

3.2.2. Trip assignment

Considering a static assignment problem, passengers take the shortest distance route using a ring, a radial route, or both types of routes. Therefore, the demand will consider three mobility patterns:

- If the destination is on the same side of the city between $\theta - 2$ and $\theta + 2$ angles, and the trip destination is closer to the central city point than the trip origin. Users will initially use a radial route and a ring route secondly.
- If the destination is in the same city side, and the origin is closer to the concentric city center than the trip destination. The users should firstly use a ring route and secondly a radial route.
- If the destination is on the opposite city side, these trips are between $\theta + 2$ and $\theta - 2 + 2\pi$ angles. It is worth noting that these angles have two radians concerning the radial axis of a point (r, θ) in a concentric city.

Based on the demand distribution function, four density functions represent the demand for each stage of a trip: access, waiting, in-vehicle travel, and transfer function.

- $f^A(r,\theta)$ is the density of users who board and alight from a transit vehicle [user/km²·h],
- $f_l^W(r,\theta)$ is the density of users who wait for a transit vehicle with direction $l \in L = \{c, r\}$ [user/km²·h],
- $f_l^V(r,\theta)$ is the density of users who travel on a transit vehicle with direction $l \in L = \{c_c, c_a, r_i, r_o\}$ [user/km·h], and
- $f_l^T(r,\theta)$ is the density of users who transfer between two vehicles of transit with direction $l \in L = \{c, r\}$ [user/km²·h].

These density functions will be able to calculate how many people access, wait, travel, and transfer at each point of a city considering different components of the generalized cost of a system. Appendix B presents the all-or-nothing assignment problem applied to a continuous space for transit systems.

3.2.3. Cost functions

The model formulation contains two components: user (T_T^u in [user·h/P_m]) and agency (C_T^a in [\$/P_m]) costs as Equation 3.4 shows it in which the travel time value (μ in [\$/user·h]) multiplies the user cost function (Jara-Díaz, 1982a, 1982b; Jara-Díaz & Cortés, 1996; Jara-Díaz & Gschwender, 2003b, 2009).

$$TC_T = \mu \cdot T_T^u + C_T^a \tag{3.4}$$

Variables

The network design of transit embraces two types of sub-problems: fixed and flexible spatial transit systems. In the former, the ring and radial services just run on a radius given or an angle given, respectively. In the latter, services can overlap their routes to save costs on infrastructure. The first case has four variables: two spatial variables and two temporary variables. The second case has three variables in which one unique headway defines the transit operation (Table 3.1).

Table 3.1. Decision variables to model each sub-problem of a transit system.

Variable	Route	Fixed-spatial transit system	Flexible-spatial transit system
Spatial variables	Ring routes	$d^c(r)$	$d^c(r,\theta)$
	Radial routes	$\Phi^r(\theta)$	$\Phi^r(r,\theta)$
Temporary variables	Ring routes	$h^c(r)$	H
	Radial routes	$h^r(\theta)$	

User costs

The total time of users ([user·h/P_m]) contains four functions (Equation 3.5): access (T_A), waiting (T_W), trip (T_V), and transfer time (T_T).

$$T_T^u = T_A + T_W + T_V + T_T \quad \text{(a)}$$

where

$$T_A = \int_0^{2\pi}\int_0^R f^A(r,\theta)\cdot T\cdot t^A(r,\theta)\ r\,dr\,d\theta \quad \text{(b)}$$

$$T_W = \int_0^{2\pi}\int_0^R \sum_{l\in L} f_l^W(r,\theta)\cdot T\cdot t_l^W(r,\theta)\ r\,dr\,d\theta \quad \text{(c)} \qquad (3.5)$$

$$T_V = \int_0^{2\pi}\int_0^R \sum_{l\in L} f_l^V(r,\theta)\cdot T\cdot t_l^V(r,\theta)\ r\,dr\,d\theta \quad \text{(d)}$$

$$T_T = \int_0^{2\pi}\int_0^R \sum_{l\in L} f_l^T(r,\theta)\cdot T\cdot t_l^T(r,\theta)\ r\,dr\,d\theta \quad \text{(e)}$$

The time functions represent the total time for each trip stage of a transit system. The calculation of these functions comes from the integration of the local time function over the circular region (Equation 3.5):

- *Access time*: Passengers lose time to get to the closest station or to the destination from the origin. First, the demand in rush hour ($f^A(r,\theta)\cdot T$ in [user/km^2·P_m]) is the density of users that board and alight at a station/stop during the rush hour. Second, the average accessibility time per user ($t^A(r,\theta)$ in [h]) depends on the time perception and the average access time.
- *Waiting time*: The passenger density that boards a vehicle is $f_l^W(r,\theta)\cdot T$ in direction $l\in L=\{c,r\}$ during rush hour ([user/km^2· P_m]). The average waiting time per passenger at a station is $t_l^W(r,\theta)$ in [h]. It depends on the time perception factor and time headway of a service.

- *In-vehicle travel time*: The total travel time depends on two components: the user load density in rush hour ($f_l^V(r,\theta)\cdot T$ in direction $l \in L = \{c_c, c_a, r_i, r_o\}$ in [user/km·P_m]), and the travel time per kilometer ([h/km]).
- *Transfer time*: Two factors comprise this local time: the user density that transfers at a point (r,θ) to direction $l \in L = \{c, r\}$ ($f_l^T(r,\theta)\cdot T$ in [user/km²]), and the average transfer time function ([h]). The latter depends on the time headway waiting for a service and the average time walking between arriving and boarding stops.

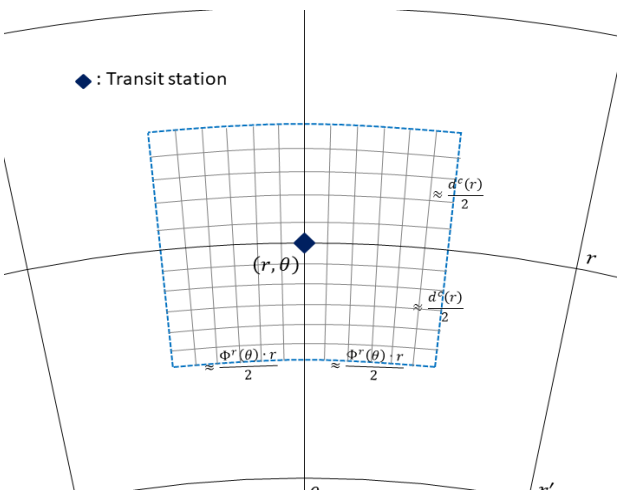

Figure 3.5. Access coverage to a station at a city point.

The formulations of local time functions per passenger or kilometer for the previous functions are in Table 3.2, and their explanations are the following.

- *Average access time per passenger* ($t^A(r,\theta)$): The access time is half of the maximum walking distance ($d^c(\cdot) + \Phi^r(\cdot)\cdot r/4$), as shown in Figure 3.5, multiplied by the access speed $v^a(r)$ (e.g., Kuah & Perl, 1988; Wirasinghe & Ghoneim, 1981).
- *Average waiting time per passenger* ($t_l^W(r,\theta)$, $l \in \{c, r\}$): The waiting time per passenger depends on the time perception factor (β) (TRB, 2013). The model assumes that the headways are deterministic and perfectly regular, i.e., 1/2 headway (e.g., Larson & Odoni, 2007; Medina-Tapia et al., 2013).
- *In-vehicle travel time per kilometer* ($t_l^V(r,\theta)$, $l \in \{c_c, c_a, r_i, r_o\}$): It depends on three components. First, traveling on the vehicle affects the users' time perception (γ). The second component is the travel time density based on the cruising speed of vehicles ($1/v^t$). Third, the time density generated by losing time at stops/stations considering acceleration and braking operations (τ), passengers that board and alight at stops/stations ($\tau' + \tau''$), and crossing an intersection (τ'''). Thus, $\tau^s = \tau + \tau' + \tau'' + \tau'''$ in [h/station] (Jara-Díaz & Tirachini, 2013).

- *Transfer time per passenger* ($t_l^T(r,\theta)$, $l \in \{c,r\}$): The average transfer time that is multiplied by a perception of the time (δ) (TRB, 2013) incurred by a passenger ($\xi^T/v^w + h^c(r)/2$ for ring services or $\xi^T/v^w + h^r(\theta)/2$ for radial services).

Table 3.2. Time functions of passengers.

Stage	Route	Fixed-spatial transit system	Flexible-spatial transit system
Access time $t^A(r,\theta)$		$\alpha \cdot \frac{d^c(r) + \Phi^r(\theta) \cdot r}{4 \cdot v^a(r)}$	$\alpha \cdot \frac{d^c(r,\theta) + \Phi^r(r,\theta) \cdot r}{4 \cdot v^a(r)}$
Waiting time $t_l^W(r,\theta)$	Ring routes	$\beta \cdot \frac{h^c(r)}{2}$	$\beta \cdot \frac{H}{2}$
	Radial routes	$\beta \cdot \frac{h^r(\theta)}{2}$	
IVT time $t_l^V(r,\theta)$	Ring routes	$\gamma \cdot \left(\frac{1}{v^t} + \frac{\tau^s}{\Phi^r(\theta) \cdot r}\right)$	$\gamma \cdot \left(\frac{1}{v^t} + \frac{\tau^s}{\Phi^r(r,\theta) \cdot r}\right)$
	Radial routes	$\gamma \cdot \left(\frac{1}{v^t} + \frac{\tau^s}{d^c(r)}\right)$	$\gamma \cdot \left(\frac{1}{v^t} + \frac{\tau^s}{d^c(r,\theta)}\right)$
Travel time $t_l^T(r,\theta)$	Ring routes	$\delta \cdot \left(\frac{\xi^T}{v^w} + \frac{h^c(r)}{2}\right)$	$\delta \cdot \left(\frac{\xi^T}{v^w} + \frac{H}{2}\right)$
	Radial routes	$\delta \cdot \left(\frac{\xi^T}{v^w} + \frac{h^r(\theta)}{2}\right)$	

Agency costs

The agency's operating costs are proportional to the fleet size (F in [veh]).

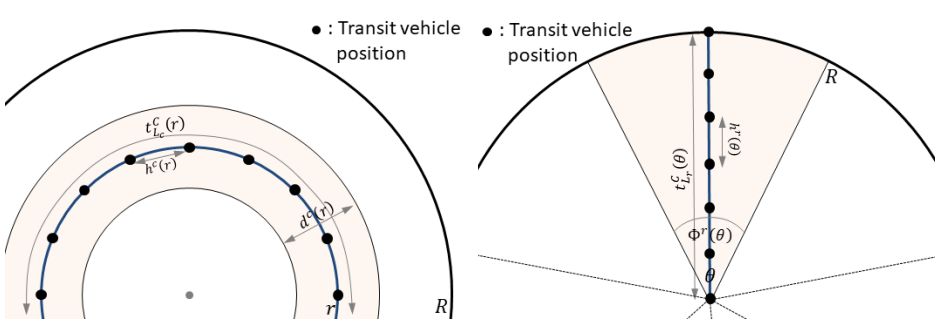

(a) Ring routes (b) Radial routes

Figure 3.6. Representation of elements to calculate the fleet size.

The fleet is the sum of vehicles that travel on rings and radial routes ($F = F_c + F_r$ in [veh]). The fleet size of a service on a corridor is the ratio between the cycle time and headway (Jara-Díaz, Fielbaum, & Gschwender, 2017). Figure 3.6 shows vehicles as black dots obtained from the ratio. In Equation 3.6, the number of vehicles on rings or radial routes depends on the density of routes, i.e., the inverse of the distance between routes. Moreover, $t_l^C(\cdot)$ is the cycle time of a vehicle on a corridor line of type $l = \{c, r\}$ [h/route].

$$F_l = \begin{cases} \int_0^R \frac{t_c^C(r)}{h^c(r)} \cdot \frac{1}{d^c(r)}\ dr & l = c \\ \int_0^{2\pi} \frac{t_r^C(\theta)}{h^r(\theta)} \cdot \frac{1}{\Phi^r(\theta)}\ d\theta & l = r \end{cases} \quad \text{(a)}$$

where

$$t_l^C(\cdot) = \begin{cases} t_c^C(r) = 2 \cdot \int_0^{2\pi} \frac{1}{v^t} + \frac{t^f}{2\pi r} + \frac{\tau^s}{\Phi^r(\theta) \cdot r}\ r\ d\theta & l = c \\ t_r^C(\theta) = 2 \cdot \int_0^{R} \frac{1}{v^t} + \frac{t^f}{R} + \frac{\tau^s}{d^c(r)}\ dr & l = r \end{cases} \quad \text{(b)} \quad (3.6)$$

The cycle time depends on the travel time density based on three elements: cruising speed ($1/v^t$), the time lost at terminals ($\frac{t^f}{2\pi r}$ or $\frac{t^f}{R}$), the time density generated by acceleration and braking operations ($\frac{\tau}{\Phi^r(\theta)\cdot r}$ or $\frac{\tau}{d^c(r)}$), the dwell time density by passengers that board and alight at stops/stations ($\frac{\tau'+\tau''}{\Phi^r(\theta)\cdot r}$ or $\frac{\tau'+\tau''}{d^c(r)}$), and the time lost at an intersection ($\frac{\tau'''}{\Phi^r(\theta)\cdot r}$ or $\frac{\tau'''}{d^c(r)}$). Thus, $\tau^s = \tau + \tau' + \tau'' + \tau'''$ in [h/station].

In Equations 3.7, the agency cost has three components (C_T^a in [\$/P_m]): capital (C_K), operational (C_O), and infrastructure cost (C_I). The last two costs have sub-components. The operational cost ($C_O = C_G + C_V$) includes the on-vehicle crew cost (C_G), and in-operation vehicle cost (C_V). The infrastructure cost ($C_I = C_P + C_S$) includes the linear (C_P) and nodal infrastructure (C_S).

- *Capital cost* in Equation 3.7(a): The cost ($C_K = \sum_{l \in L} F_l \cdot \varphi^k$ in [\$/P_m]) depends on the fleet in direction $l \in \{c, r\}$ (F_l in [veh]) and the cost per vehicle (φ^k in [\$/veh·P_m]).
- *Operational cost* in Equation 3.7(c-e): First, the total salary ($C_G = F \cdot \eta^d \cdot T \cdot \varphi^g$ in [\$]) is in proportion to three components: the fleet (F_l, $l \in \{c, r\}$), the number of work shifts on a vehicle (η^d), and the salary in the rush hour ($T \cdot \varphi^g$). Second, the total operating cost (C_V in [\$]) comprises of two components: the number of vehicles that run on a corridor ($2 \cdot T/h^c(r)$ or $2 \cdot T/h^r(\theta)$ respectively), the operation cost per unit of distance traveled on

a cruising speed (φ^o) considering the width of a transit corridor $d^c(r)$ or $\Phi^r(\theta)$.

$$C_T^a = C_K + C_O + C_I \quad \text{(a)}$$

where

$$C_K = \sum_{l \in L} F_l \cdot \varphi^k \quad \text{(b)}$$

$$C_O = C_G + C_V \quad \text{(c)}$$

$$C_G = \sum_{l \in L} F_l \cdot \eta^d \cdot T \cdot \varphi^g \quad \text{(d)}$$

$$C_V = \int_0^{2\pi} \int_0^R \left(\frac{2 \cdot T \cdot \varphi^o}{h^c(r) \cdot d^c(r)} + \frac{2 \cdot T \cdot \varphi^o}{h^r(\theta) \cdot \Phi^r(\theta) \cdot r} \right) \cdot r \; dr \; d\theta \quad \text{(e)} \qquad (3.7)$$

$$C_I = C_P + C_S \quad \text{(f)}$$

$$C_P = 2 \cdot \int_0^{2\pi} \int_0^R \frac{1}{d^c(r)} \cdot \varphi^p + \frac{1}{\Phi^r(\theta) \cdot r} \cdot \varphi^p \; r \; dr \; d\theta \quad \text{(g)}$$

$$C_S = 4 \cdot \int_0^{2\pi} \int_0^R \frac{1}{\Phi^r(\theta)} \cdot \frac{1}{d^c(r)} \cdot \varphi^s \; dr \; d\theta \quad \text{(h)}$$

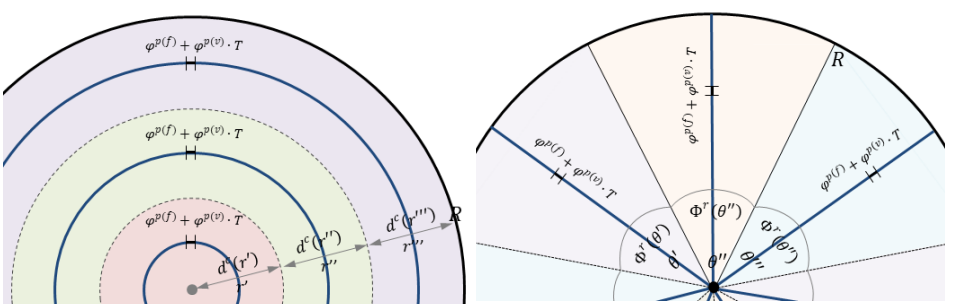

(a) Ring services (b) Radial services

Figure 3.7. Scheme of transit corridors for the linear infrastructure cost function.

- *Infrastructure cost* in Equation 3.7(f-h): The linear infrastructure cost (C_P) depends on the number of routes and its length of rings and radial routes ($\frac{1}{d^c(r)}$ or $\frac{1}{\Phi^r(\theta) \cdot r}$ in [km·route] in direction $l \in \{c, r\}$), and the unitary cost (φ^p in [$/km·route·$P_m$]). The unitary cost per km in the rush hour has a fixed component and another variable part ($\varphi^p = \varphi^{p(f)} + \varphi^{p(v)} \cdot T$ in [$/km·route·$P_m$], Figure 3.7(g)). The nodal infrastructure (C_S) depends on the number of intersections $\frac{1}{\Phi^r(\theta)} \cdot \frac{1}{d^c(r)}$ and the unitary cost φ^s in [$/station·route·$P_m$] (Figure 3.7(h)), considering each intersection has four stations or stops (Figure 3.8).

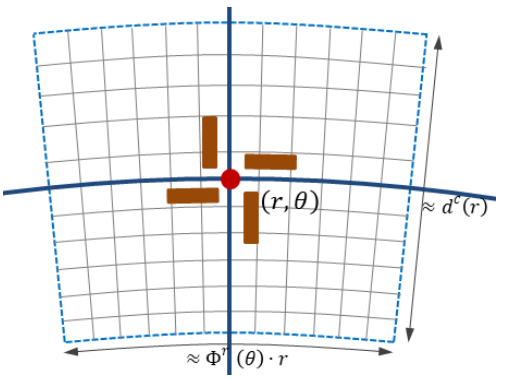

Figure 3.8. Scheme of a transit intersection for the nodal infrastructure cost function.

3.2.4. Problem formulation and optimization

The transit network design and frequency setting problem (TNDFSP) minimizes the total cost, taking into account a heterogeneous demand distribution.

Problem formulations

The mathematical problem is a nonlinear system with inequality constraints, replacing the user and agency sub-cost functions on the objective function (Equation 3.8(a) and 3.9(a), respectively). The formulation of the total cost of a transit system ($TC_T = \mu \cdot T_T^u + C_T^a$) in monetary units ([\$/P_m] contains two components: the user cost component (T_T^u in [user·h/P_m]), which is multiplied by the travel time value (μ in [\$/user·h]), and the second component of agency costs (C_T^a in [\$/P_m]).

- *Fixed spatial transit system*: First, the problem has four decision variables ($d^c(r), \Phi^r(\theta), h^c(r), h^r(\theta)$) according to the spatial and temporal deployment of resources. In this problem, the fixed variables do not change along a corridor. Second, the problem has three sets of constraints. The first of these (Equations 3.8(b) and (c)) ensures that occupancy does not exceed the capacity of each vehicle (K^v in [user/veh]). Second, the minimum distance between stations ensures that transit vehicles reach the cruising speed before arriving at the next station and can correctly brake (Equations 3.8(d) and (e)). In the case of radial routes (Equation 3.8(e)), $K^{d(r)} = K^{d(c)}/r_{min}$, where r_{min} is a minimum radius in which this constraint applies in [km/route] or [rad/route], respectively. Finally, the operator requires a minimum

separation (time) between consecutive vehicles (TRB, 2013). Equations 3.8(f) and (g) ensure that the optimum frequency is feasible (K^h in [h/veh]).

$$Min\ TC_T = \mu \cdot (T_A + T_W + T_V + T_T) + (C_K + C_V + C_I) \quad \text{(a)}$$

s.t.

$$\max_{\theta, l \in \{c_c, c_a\}} \left(f_l^V(r,\theta) \cdot d^c(r) \cdot h^c(r) \right) \leq K^v \quad \forall\, r \quad \text{(b)}$$

$$\max_{r, l \in \{r_i, r_o\}} \left(f_l^V(r,\theta) \cdot \Phi^r(\theta) \cdot \frac{R+r}{2} \cdot h^r(\theta) \right) \leq K^v \quad \forall\, \theta \quad \text{(c)} \qquad (3.8)$$

$$d^c(r) \geq K^{d(c)} \quad \forall\, r \quad \text{(d)}$$

$$\Phi^r(\theta) \geq K^{d(r)} \quad \forall\, \theta \quad \text{(e)}$$

$$h^c(r) \geq K^h \quad \forall\, r \quad \text{(f)}$$

$$h^r(\theta) \geq K^h \quad \forall\, \theta \quad \text{(g)}$$

- *Flexible spatial transit system*: First, the problem has three decision variables ($d^c(r,\theta), \Phi^r(r,\theta), H$), which is flexible due to the spatial variables that could change along a corridor route. Second, the problem has three sets of constraints. The first set (Equations 3.9(b) and (c)) ensures that the demand does not exceed the capacity of a vehicle (K^v in [user/veh]). The second set (Equations 3.9(d) and (e)) makes sure a minimum distance between stations to reach the cruising speed before arriving at the next station braking correctly (K^d in [km/route] or [rad/route], respectively). The third constraint (Equation 3.9(f)) makes sure that the optimum headway has a minimum separation between vehicles in time units (K^h in [h/veh]) (TRB, 2013).

$$Min\ TC_T = \mu \cdot (T_A + T_W + T_V + T_T) + (C_K + C_V + C_I) \quad \text{(a)}$$

s.t.

$$\max_{(r,\theta), l \in \{c_c, c_a\}} \left(f_l^V(r,\theta) \cdot d^c(r,\theta) \cdot H \right) \leq K^v \quad \text{(b)}$$

$$\max_{(r,\theta), l \in \{r_i, r_o\}} \left(f_l^V(r,\theta) \cdot \Phi^r(r,\theta) \cdot \frac{R+r}{2} \cdot H \right) \leq K^v \quad \text{(c)} \qquad (3.9)$$

$$d^c(r,\theta) \geq K^{d(c)} \quad \forall\, (r,\theta) \quad \text{(d)}$$

$$\Phi^r(r,\theta) \geq K^{d(r)} \quad \forall\, (r,\theta) \quad \text{(e)}$$

$$H \geq K^h \quad \text{(f)}$$

Table 3.3. Optimal analytical functions of a spatially fixed transit system.

Optimal analytical functions

$$\boldsymbol{d^c(r)} = \sqrt{\frac{\int_0^{2\pi}\left(\mu\cdot\gamma\cdot\frac{1}{2}\cdot\left(\frac{R}{r}+1\right)\cdot f_r^V(r,\theta)\cdot T\cdot\tau^s + 2\cdot\left(\left(\frac{1}{v^t}+\frac{t^f}{2\pi r}+\frac{\tau^s}{\boldsymbol{\Phi^r(\theta)}\cdot r}\right)\cdot\frac{\varphi^v}{\boldsymbol{h^c(r)}}+\frac{\tau^s\cdot\varphi^v}{\boldsymbol{\Phi^r(\theta)}\cdot r\cdot\boldsymbol{h^r(\theta)}}+\frac{T\cdot\varphi^o}{\boldsymbol{h^c(r)}}+\varphi^p+\frac{2\cdot\varphi^s}{\boldsymbol{\Phi^r(\theta)}\cdot r}\right)\right)\cdot r\, d\theta}{\mu\cdot\int_0^{2\pi}\frac{\alpha\cdot f^A(r,\theta)\cdot T}{4\cdot v^a(r)}\, r\, d\theta + \boldsymbol{\lambda_1^c(r)}\cdot\max_{\theta,l\in\{c_c,c_a\}}\left(f_l^V(r,\theta)\right)\cdot\boldsymbol{h^c(r)}-\boldsymbol{\lambda_2^c(r)}}}$$

$$\boldsymbol{\Phi^r(\theta)} = \sqrt{\frac{\int_0^{R}\left(\mu\cdot\gamma\cdot f_c^V(r,\theta)\cdot T\cdot\tau^s + 2\cdot\left(\left(\frac{1}{v^t}+\frac{t^f}{R}+\frac{\tau^s}{\boldsymbol{d^c(r)}}\right)\cdot\frac{\varphi^v}{\boldsymbol{h^r(\theta)}}+\frac{\tau^s\cdot\varphi^v}{\boldsymbol{d^c(r)}\cdot\boldsymbol{h^c(r)}}+\frac{T\cdot\varphi^o}{\boldsymbol{h^r(\theta)}}+\varphi^p+\frac{2\cdot\varphi^s}{\boldsymbol{d^c(r)}}\right)\right)\, dr}{\mu\cdot\int_0^{R}\frac{\alpha\cdot f^A(r,\theta)\cdot T\cdot r}{4\cdot v^a(r)}\cdot r\ dr + \boldsymbol{\lambda_1^r(\theta)}\cdot\max_{r,l\in\{r_i,r_o\}}\left(f_l^V(r,\theta)\cdot\frac{R+r}{2}\right)\cdot\boldsymbol{h^r(\theta)}-\boldsymbol{\lambda_2^r(\theta)}}}$$

$$\boldsymbol{h^c(r)} = \sqrt{\frac{2\cdot\int_0^{2\pi}\left(\left(\frac{1}{v^t}+\frac{t^f}{2\pi r}+\frac{\tau^s}{\boldsymbol{\Phi^r(\theta)}\cdot r}\right)\cdot\varphi^v+T\cdot\varphi^o\right)\cdot\frac{1}{\boldsymbol{d^c(r)}}\ r\, d\theta}{\mu\cdot\int_0^{2\pi}\left(\frac{\beta}{2}\cdot f_c^W(r,\theta)\cdot T+\frac{\delta}{4}\cdot\left(\frac{R}{r}+1\right)\cdot f_c^T(r,\theta)\cdot T\right)\cdot r\, d\theta + \boldsymbol{\lambda_1^c(r)}\cdot\max_{\theta,l\in\{c_c,c_a\}}\left(f_l^V(r,\theta)\right)\cdot\boldsymbol{d^c(r)}-\boldsymbol{\lambda_3^c(r)}}}$$

$$\boldsymbol{h^r(\theta)} = \sqrt{\frac{2\cdot\int_0^{R}\left(\left(\frac{1}{v^t}+\frac{t^f}{R}+\frac{\tau^s}{\boldsymbol{d^c(r)}}\right)\cdot\varphi^v+T\cdot\varphi^o\right)\cdot\frac{1}{\boldsymbol{\Phi^r(\theta)}}\ dr}{\mu\cdot\int_0^{R}\left(\frac{\beta}{2}\cdot f_r^W(r,\theta)\cdot T+\frac{\delta}{4}\cdot\left(\frac{R}{r}+1\right)\cdot f_r^T(r,\theta)\cdot T\right)\cdot r\, dr + \boldsymbol{\lambda_1^r(\theta)}\cdot\max_{r,l\in\{r_i,r_o\}}\left(f_l^V(r,\theta)\cdot\frac{R+r}{2}\right)\cdot\boldsymbol{\Phi^r(\theta)}-\boldsymbol{\lambda_3^r(\theta)}}}$$

Table 3.4. Optimal analytical functions of a spatially flexible transit system.

Optimal analytical functions

$$\boldsymbol{d^c(r,\theta)} = \sqrt{\frac{\mu\cdot\gamma\cdot\frac{1}{2}\cdot\left(\frac{R}{r}+1\right)\cdot f_r^V(r,\theta)\cdot T\cdot\tau^s + 2\cdot\left(\left(\frac{1}{v^t}+\frac{t^f}{2\pi r}+\frac{\tau^s}{\boldsymbol{\Phi^r(r,\theta)}\cdot r}\right)\cdot\frac{\varphi^v}{\boldsymbol{H}}+\frac{\tau^s\cdot\varphi^v}{\boldsymbol{\Phi^r(r,\theta)}\cdot r\cdot\boldsymbol{H}}+\frac{T\cdot\varphi^o}{\boldsymbol{H}}+\varphi^p+\frac{2\cdot\varphi^s}{\boldsymbol{\Phi^r(r,\theta)}\cdot r}\right)}{\mu\cdot\frac{\alpha\cdot f^A(r,\theta)\cdot T}{4\cdot v^a(r)}+\boldsymbol{\lambda_1^c(r,\theta)}\cdot\max_{l\in\{c_c,c_a\}}\left(f_l^V(r,\theta)\right)\cdot\boldsymbol{H}-\boldsymbol{\lambda_2^c(r,\theta)}}}$$

$$\boldsymbol{\Phi^r(r,\theta)} = \sqrt{\frac{\mu\cdot\gamma\cdot f_c^V(r,\theta)\cdot T\cdot\tau^s + 2\cdot\left(\left(\frac{1}{v^t}+\frac{t^f}{R}+\frac{\tau^s}{\boldsymbol{d^c(r,\theta)}}\right)\cdot\frac{\varphi^v}{\boldsymbol{H}}+\frac{\tau^s\cdot\varphi^v}{\boldsymbol{d^c(r,\theta)}\cdot\boldsymbol{H}}+\frac{T\cdot\varphi^o}{\boldsymbol{H}}+\varphi^p+\frac{2\cdot\varphi^s}{\boldsymbol{d^c(r,\theta)}}\right)}{\mu\cdot\frac{\alpha\cdot f^A(r,\theta)\cdot T\cdot r}{4\cdot v^a(r)}\cdot r+\boldsymbol{\lambda_1^r(r,\theta)}\cdot\max_{l\in\{r_i,r_o\}}\left(f_l^V(r,\theta)\cdot\frac{R+r}{2}\cdot\boldsymbol{H}\right)-\boldsymbol{\lambda_2^r(r,\theta)}}}$$

$$\boldsymbol{H} = \sqrt{\frac{2\cdot\int_0^{2\pi}\int_0^R\left(\left(\left(\frac{1}{v^t}+\frac{t^f}{2\pi r}+\frac{\tau^s}{\boldsymbol{\Phi^r(r,\theta)}\cdot r}\right)\cdot\varphi^v+T\cdot\varphi^o\right)\cdot\frac{1}{\boldsymbol{d^c(r,\theta)}}+\left(\frac{1}{v^t}+\frac{t^f}{R}+\frac{\tau^s}{\boldsymbol{d^c(r,\theta)}}\right)\cdot\varphi^v+T\cdot\varphi^o\right)\cdot\frac{1}{\boldsymbol{\Phi^r(r,\theta)}\cdot r}\ r\,dr\,d\theta}{\begin{array}{l}\mu\cdot\int_0^{2\pi}\int_0^R\left(\frac{\beta}{2}\cdot\left(f_c^W(r,\theta)\cdot T+f_r^W(r,\theta)\cdot T\right)+\frac{\delta}{4}\cdot\left(\frac{R}{r}+1\right)\cdot\left(f_c^T(r,\theta)\cdot T+f_r^T(r,\theta)\cdot T\right)\right)\ r\,dr\,d\theta+\cdots\\ \ldots+\boldsymbol{\lambda_1^c(r,\theta)}\cdot\max_{(r,\theta),l\in\{c_c,c_a\}}\left(f_l^V(r,\theta)\cdot\boldsymbol{d^c(r,\theta)}\right)+\boldsymbol{\lambda_1^r(r,\theta)}\cdot\max_{(r,\theta),l\in\{r_i,r_o\}}\left(f_l^V(r,\theta)\cdot\boldsymbol{\Phi^r(r,\theta)}\cdot\frac{R+r}{2}\right)-\boldsymbol{\lambda_3}\end{array}}}$$

Method for solving the problem

The Karush-Kuhn-Tucker (KKT) conditions allow finding the necessary conditions to solve a nonlinear system. The first-order optimization conditions enable obtaining optimized analytical functions, and it will permit getting the optimal value at overall city points. The necessary conditions are not sufficient for optimality, but all local minimum satisfies them. Therefore, a convexity analysis of the problem is required to find the optimal solution.

$$\begin{aligned}
&\frac{\partial\, tc(r,\theta)}{\partial\, x_i^{\circ}(\cdot)} + \sum_{j=1}^{n_c} \lambda_j^c(r) \cdot \frac{\partial\, c_j^c(r,\theta)}{\partial\, x_i^{\circ}(\cdot)} + \sum_{j=1}^{n_c} \lambda_j^r(\theta) \cdot \frac{\partial\, c_j^r(r,\theta)}{\partial\, x_i^{\circ}(\cdot)} = 0 \quad \forall\, i = 1, \dots, n_v && \text{(a)} \\
&c_j^{\circ}(r,\theta) - K_j \le 0 \quad \forall\, j = 1, \dots, n_c && \text{(b)} \\
&\lambda_j^{\circ}(\cdot) \cdot \left(c_j^{\circ}(r,\theta) - K_j\right) = 0 \quad \forall\, j = 1, \dots, n_c && \text{(c)} \\
&\lambda_j^{\circ}(\cdot) \ge 0 \quad \forall\, j = 1, \dots, n_c && \text{(d)} \\
&x_i^{\circ}(\cdot) > K^{min} \quad \forall\, i = 1, \dots, n_v && \text{(e)}
\end{aligned} \tag{3.10}$$

where

- *Fixed spatial transit system*:

$$\begin{aligned}
n_v = 4, n_c = 6, \\
x_i^{\circ}(\cdot) = \{d^c(r), \Phi^r(\theta), h^c(r), h^r(\theta)\} \\
\lambda_j^{\circ}(\cdot) = \{\lambda_1^c(r), \lambda_2^c(r), \lambda_3^c(r), \lambda_1^r(\theta), \lambda_2^r(\theta), \lambda_3^r(\theta)\}
\end{aligned}$$

- *Flexible spatial transit system*:

$$\begin{aligned}
n_v = 3, n_c = 5, \\
x_i^{\circ}(\cdot) = \{d^c(r,\theta), \Phi^r(r,\theta), H\} \\
\lambda_j^{\circ}(\cdot) = \{\lambda_1^c(r,\theta), \lambda_2^c(r,\theta), \lambda_1^r(r,\theta), \lambda_2^r(r,\theta), \lambda_3\}
\end{aligned}$$

Using the CA method, the $tc(r,\theta)$ is a local cost function at a point (r,θ). Equations 3.10 shows the set of KKT conditions considering the number of variables n_v and constraints n_c. The stationarity conditions (Equation 3.10(a)) come from the local cost function considering multipliers ($\lambda_j^{\circ}(\cdot)$) and constraints for rings ($c_j^c(r,\theta)$) and radial ($c_j^r(r,\theta)$) routes. The second condition (Equation 3.10(b)) embraces the constraints (c_j°). The third condition (Equation 3.10(c)) is a complementary slackness expression. If an inequality becomes an equality equation (tight), its slack is zero, and its multiplier takes any non-negative value (Equation 3.10(d)). Finally, each decision variable (x_i°) must be higher than a K^{min} (K^v, K^h, $K^{d(c)}$,$K^{d(r)}$, respectively; Equation 3.10(e)).

Optimal analytical solutions

The model allows obtaining the optimal analytical functions for each decision variable through the formulation of Equation 3.10(a): the distance between

routes and the headway between vehicles on each type of route (Table 3.3 and Table 3.4), respectively.

- *Optimal distance function between ring routes in* [km/route]: From stationarity conditions, the isolation of the decision variable ($d^c(\cdot)$) allows obtaining a square root of an analytical ratio. The numerator of this ratio is a cost function obtained from two components. The first component is the cost due to users on radial routes that arrive at a station. The second component is the operation and infrastructure cost on a ring route at r. The denominator represents the cost per area due to access to a station and two more components from the constraints: user density per kilometer on a vehicle multiplied by a Lagrange multiplier ($\lambda_1^c(\cdot)$), and a second Lagrange multiplier ($\lambda_2^c(\cdot)$).
- *Optimal distance function between radial routes in* [rad/route]: The analytical structure of the optimal angle between radial routes ($\Phi^r(\cdot)$) is similar to the previous function. Moreover, two factors include the denominator containing the multipliers $\lambda_1^r(\cdot)$ and $\lambda_2^r(\cdot)$.
- *Optimal headway function on routes in* [h/veh]: The optimal headway has the same structure for ring and radial routes. In the case of a flexible spatial transit, the numerator and denominator include the cost of both types of routes.

It is worth mentioning that the equations of Table 3.3 and Table 3.4 have two new parameters. First, the time lost at a station ($\tau^s = \tau + \tau' + \tau'' + \tau'''$ in [h/station]). Second, the equations have grouped the cost per vehicle and the salary cost per vehicle in rush hour ($\varphi^v = \varphi^k + \eta^d \cdot T \cdot \varphi^g$ in [\$/veh·P_m]). The optimal analytical functions ($d^c(\cdot), \Phi^r(\cdot), h^c(\cdot), h^r(\cdot), H$) depend on the result of the other type of route and headways.

3.2.5. Methodology for obtaining continuous solutions

Inequality systems

The optimal functions $d^c(r)$ and $h^c(r)$ (Equations in Table 3.3) have a common factor $\lambda_1^c(r) \cdot \max_{\theta, l \in L_c} \left(f_l^V(r, \theta) \right)$. This factor allows equating the two expressions obtained from Equation 3.11(a). Thus, KKT conditions (Equation 3.10) allow formulating an equation system to solve the problem of ring services in the set of Equations 3.11, where Equations 3.11(b) are the constraints, Equations 3.11(c) are the complementary slackness, and Equations 3.11(d) is the integrality of multipliers.

$$
\begin{aligned}
&\boldsymbol{d^c(r)^2}\cdot\int_0^{2\pi}\frac{\mu\cdot\alpha\cdot f^A(r,\theta)\cdot T}{4\cdot v^a(r)}\cdot r\,d\theta\\
&-\boldsymbol{d^c(r)}\cdot\boldsymbol{h^c(r)}\cdot\int_0^{2\pi}\mu\cdot\left(\frac{\beta}{2}\cdot f_{L_c}^W(r,\theta)\cdot T+\frac{\delta}{4}\cdot\left(\frac{R}{r}+1\right)\cdot f_{L_c}^T(r,\theta)\cdot T\right)\cdot r\,d\theta+\boldsymbol{d^c(r)}\cdot\left(\boldsymbol{\lambda_3^c(r)}-\boldsymbol{\lambda_2^c(r)}\right) \quad \text{(a)}\\
&-\int_0^{2\pi}\left(\frac{1}{2}\cdot\mu\cdot\gamma\cdot f_{L_r}^V(r,\theta)\cdot\left(\frac{R}{r}+1\right)\cdot T\cdot\tau^s+\frac{2\cdot\tau^s\cdot\varphi^v}{\Phi^r(\theta)\cdot r\cdot h^r(\theta)}+2\cdot\varphi^p+\frac{4\cdot\varphi^s}{\Phi^r(\theta)\cdot r}\right)\cdot r\,d\theta=0\quad\forall\,r
\end{aligned}
$$

$$
\begin{aligned}
&\max_{\theta,l\in L_c}\left(f_l^V(r,\theta)\cdot\boldsymbol{d^c(r)}\cdot\boldsymbol{h^c(r)}\right)\le K^v\quad\forall\,r\\
&\boldsymbol{d^c(r)}\ge K^d\quad\forall\,r\\
&\boldsymbol{h^c(r)}\ge K^h\quad\forall\,r
\end{aligned}
\qquad \text{(b)}
$$

$$
\begin{aligned}
&\boldsymbol{\lambda_1^c(r)}\cdot\left(\max_{\theta,l\in L_c}\left(f_l^V(r,\theta)\cdot\boldsymbol{d^c(r)}\cdot\boldsymbol{h^c(r)}\right)-K^v\right)=0\quad\forall\,r\\
&\boldsymbol{\lambda_2^c(r)}\cdot\left(-d^c(r)+K^{d(c)}\right)=0\quad\forall\,r\\
&\boldsymbol{\lambda_3^c(r)}\cdot\left(-h^c(r)+K^h\right)=0\quad\forall\,r
\end{aligned}
\qquad \text{(c)}
$$

$$
\begin{aligned}
&\boldsymbol{\lambda_1^c(r)}\ge 0\quad\forall\,r\\
&\boldsymbol{\lambda_2^c(r)}\ge 0\quad\forall\,r\\
&\boldsymbol{\lambda_3^c(r)}\ge 0\quad\forall\,r
\end{aligned}
\qquad \text{(d)} \qquad (3.11)
$$

For the radial routes case, analytical development is similar to the ring case to obtain an analytical equation system to solve the radial service problem (Equations 3.12). The meaning of the equations is similar to the previous case: the set of Equations 3.12(b) is the constraints, the set of Equations 3.12(c) contains the complementary slackness conditions, and the set of Equations 3.12(d) represents the integrality of multipliers.

$$
\begin{aligned}
&\boldsymbol{\Phi^r(\theta)^2}\cdot\int_0^{R}\frac{\mu\cdot\alpha\cdot f^A(r,\theta)\cdot T\cdot r}{4\cdot v^a(r)}\cdot r\;dr\\
&-\boldsymbol{\Phi^r(\theta)}\cdot\boldsymbol{h^r(\theta)}\cdot\int_0^{R}\mu\cdot\left(\frac{\beta}{2}\cdot f_{L_r}^W(r,\theta)\cdot T+\frac{\delta}{4}\cdot\left(\frac{R}{r}+1\right)\cdot f_{L_r}^T(r,\theta)\cdot T\right)\cdot r\;dr+\boldsymbol{\Phi^r(\theta)}\cdot\left(\boldsymbol{\lambda_3^r(r)}-\boldsymbol{\lambda_2^r(r)}\right) \quad \text{(a)}\\
&-\int_0^{R}\left(\mu\cdot\gamma\cdot f_{L_c}^V(r,\theta)\cdot T\cdot\tau^s+\frac{2\cdot\tau^s\cdot\varphi^v}{h^c(r)\cdot d^c(r)}+2\cdot\varphi^p+\frac{4\cdot\varphi^s}{d^c(r)}\right)dr=0\quad\forall\,\theta
\end{aligned}
$$

$$
\begin{aligned}
&\max_{r,l\in L_r}\left(f_l^V(r,\theta)\cdot\boldsymbol{\Phi^r(\theta)}\cdot\frac{R+r}{2}\cdot\boldsymbol{h^r(\theta)}\right)\le K^v\quad\forall\,\theta\\
&\boldsymbol{\Phi^r(\theta)}\ge K^{d(r)}\quad\forall\,\theta\\
&\boldsymbol{h^r(\theta)}\ge K^h\quad\forall\,\theta
\end{aligned}
\qquad \text{(b)}
$$

$$
\begin{aligned}
&\boldsymbol{\lambda_1^r(\theta)}\cdot\left(\max_{r,l\in L_r}\left(f_l^V(r,\theta)\cdot\boldsymbol{\Phi^r(\theta)}\cdot\frac{R+r}{2}\cdot\boldsymbol{h^r(\theta)}\right)-K^v\right)=0\quad\forall\,\theta\\
&\boldsymbol{\lambda_2^r(r)}\cdot\left(-\boldsymbol{\Phi^r(\theta)}+K^{d(r)}\right)=0\quad\forall\,r\\
&\boldsymbol{\lambda_3^r(r)}\cdot\left(-\boldsymbol{h^r(\theta)}+K^h\right)=0\quad\forall\,r
\end{aligned}
\qquad \text{(c)}
$$

$$
\begin{aligned}
&\boldsymbol{\lambda_1^r(\theta)}\ge 0\quad\forall\,\theta\\
&\boldsymbol{\lambda_2^r(\theta)}\ge 0\quad\forall\,\theta\\
&\boldsymbol{\lambda_3^r(\theta)}\ge 0\quad\forall\,\theta
\end{aligned}
\qquad \text{(d)} \qquad (3.12)
$$

Method of two phases

Each set of Equations 3.11 and 3.12 contains a system with inequalities that allow obtaining the optimal solution. In consequence, this dissertation proposes an algorithm based on the CA method (Figure 3.9). The algorithm

consists of iterating the analytical expressions of ring and radial corridors until reaching convergence.

The method has two phases. The first stage consists of the initialization of variables in which a feasible solution uses the minimum value of each variable, respectively: $\{K^d, K^h\}$. Moreover, the algorithm creates a variable that stores the number of iterations (i). The second stage is an iterative process in which the model calculates the four decision variables. The process will iterate while the solutions are feasible, and the error is higher than the tolerance for each variable. The first sub-problem calculates the two variables $(d^{c(i)}(r), h^{c(i)}(r))$ for a set of ring corridor routes ($r \in [0 \dots R]$) if there are feasible solutions and first-order optimization conditions are satisfied. In the case of radial services $(\Phi^{r(i)}(\theta), h^{r(i)}(\theta))$, the process is identical. The variable will increase by one unit. After that, the algorithm analyses the convexity of the problem. The algorithm will stop when the error is less than the tolerance.

Algorithm: Solution of the continuous transit problem

Initialize $d^{c(0)}(r) = K^{d(c)}$; $\Phi^{r(0)}(\theta) = K^{d(r)}$; $h^{c(0)}(r) = K^h$; $h^{r(0)}(\theta) = K^h$
i := 1
while (abs($d^{c(i)}(r) - d^{c(i-1)}(r)$) > tolerance or abs($\Phi^{r(i)}(\theta) - \Phi^{r(i-1)}(\theta)$) > tolerance or
abs($h^{c(i)}(r) - h^{c(i-1)}(r)$) > tolerance or abs($h^{r(i)}(\theta) - h^{r(i-1)}(\theta)$) > tolerance)

for each $r \in [0 \dots R]$ **do**
$\{d^{c(i)}(r), h^{c(i)}(r)\} \leftarrow$ *SystemOfEquations*($\{\Phi^{r(i-1)}(\theta), h^{r(i-1)}(\theta)\}$)
end for

for each $\theta \in [0 \dots 2\pi]$ **do**
$\{\Phi^{r(i)}(\theta), h^{r(i)}(\theta)\} \leftarrow$ *SystemOfEquations*($\{d^{c(i-1)}(r), h^{c(i-1)}(r)\}$)
end for

i := i + 1
end while

Figure 3.9. The algorithm based on successive approximations numerically solves the transit problem through two phases.

3.3. Modeling a traffic system

3.3.1. Preliminary concepts

Consider a concentric city that has a radius of R [km] whose demand is spatially continuous. The circular city has major rings and radial roads. Thus,

the model assumes that users can take two types of roads represented by black lines in Figure 3.10: rings and radial roads ($W = \{c, r\}$) considering four directions. Each road serves an area called a *road corridor*. Corridors contain origins and destinations of private trips, e.g., the infinitesimal orange area and the blue area in Figure 3.10, respectively. The drivers use rings or radial roads turning at an intersection (green points):

- *On ring roads*: users can travel clockwise or anticlockwise direction ($c = \{c_c: clockwise, c_a: anticlockwise\}$).
- *On radial roads*: users can travel to the center or come out from this ($r = \{r_i: inside, r_o: outside\}$).

The modeling considers the four-stage of the transportation model. The modeling of demand maintains a similar scheme to the transit case. The generated demand $\lambda(r, \theta)$ at a point (r, θ)—in polar coordinates—is a density function in [user/km²·h] (Equation 3.2, p. 38), and the attracted analytical demand function—in polar coordinates—is $\rho(r, \theta)$ (Equation 3.3, p. 38).

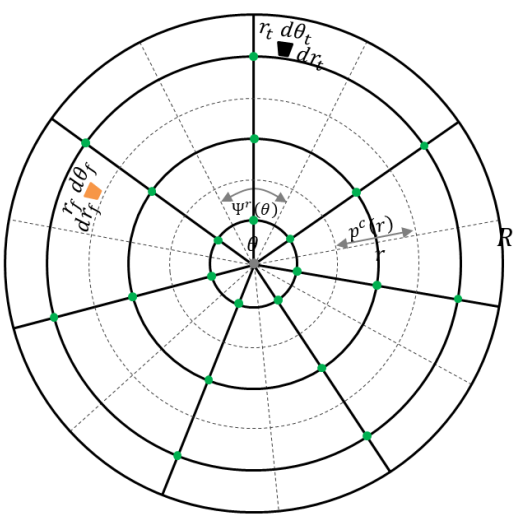

Figure 3.10. Road structure: rings, radial roads, and intersections.

The model embraces at least one vehicle type, but it could include other additional types of vehicles. For example, in Medina and Robusté (2019b), the analysis of impacts of connected and autonomous vehicles (CAVs) considering two types of vehicles ($V = \{mv: MV;\ av: AV\}$) including dedicated lanes for CAVs allowing the formation of platoons. The third section of Chapter 5 explains the results in detail. Appendix E explains this subchapter.

Parameters

The period of the analysis is also the rush hour (P_m) because the peak period defines the needs of infrastructure required. The peak period lasts T hours. Appendix A contains lists of all parameters used by the model.

The first group of parameters includes parameters that define the attributes and behavior of car users:

- *Users per car*: the average number of users in a car (η_u),
- *Car speeds*: speed to access main roads (v_v^F), speed to local roads (v_v^A), free-flow speed (v_v^{ff}), cruising speed (v_v^p), and
- *Parking behavior*: the average distance looking for a parking spot before destination (d_p), and the average walking speed after parking (v^a).

In a second set, the operating parameters define attributes of roads and parking:

- *Accessing penalization*: average penalization time for accessing the nearest primary road from origin ($t_v^{F\prime}$), and accessing the local roads from primary roads ($t_v^{A\prime}$),
- *Road parameters*: the parameters of BPR volume-delay function (a and b), the capacity road per lane (k_v), the number of lanes on roads (η^l), the average time crossing an intersection (τ_v^i), and
- *Parking parameters*: it includes the average density of parking vacant spaces (λ_P).

Third, the list of unitary cost parameters considers users, capital, operation, and infrastructure cost:

- *Travel time value by average user (μ)*,
- *Unitary cost per vehicle and distance unit (φ_v^t)*,
- *Parking fee (φ^f)*, and
- *Linear infrastructure cost (φ_v^p)*.

Assumptions

The following points summarize the model assumptions.

- The private transportation demand is known, deterministic, and the function varies concerning its position.
- Car users take the cheapest route (minimum generalized cost) to the destination, and they can use ring streets, radial streets, or both of them.

- The travel time value is the same for all users.
- The road capacity is proportional to the number of lanes.
- Neither a driver can stop and wait for a vacant parking space nor return upstream when looking for a parking spot (Arnott & Rowse, 1999).
- Vehicles park on service streets; therefore, they do not cause a reduction in road capacity. The model does not consider the parking capacity.
- The model does not include urban freight distribution and public transportation costs.

3.3.2. Trip assignment

The modeling assumes a static traffic assignment problem in a continuous space implementing an incremental assignment method, which gives a correct strategic planning approach.

The method divides the distribution matrix at M_n factors ($\sum_n M_n = 1$, where n is the number of iterations). Thenceforth, this way iteratively assigns to the network each part of the fractioned matrix.

Thus, at step 0, the method uses the all-or-nothing method. For this step, there are three cases (Medina-Tapia & Robusté, 2018a).

- *Radial-circular trip*: Users can take a radial road first and then take a circular road,
- *Ring-radial trip*: The users take a ring road and, after that, a radial road, or
- *Radial-radial trip*: The users take a radial road from the origin to the city center and, subsequently, they take a road of radial type to the destination.

In the following steps, the assignment considers the travel time calculated from accumulated flows. In order to finish the algorithm, the method must sequentially assign all fractions to the network. The assignment results are the density functions of demand (third section of Appendix B, p. 180).

The model has three types of demand density functions obtained from the assignment method.

- $f^F_{w,v}(r,\theta)$ is the density of vehicles of type $v \in V$ that access from the origin to the closest circular or radial primary road $w \in W$ [veh/km²·h],
- $f^R_{w,v}(r,\theta)$ is the density of vehicles flow of type $v \in V$ that travel on a circular or radial primary road $w \in W$ considering its direction [veh/km·h], and
- $f^A_{w,v}(r,\theta)$ is the density of vehicles of type $v \in V$ that arrive from a circular or radial primary road to the destination $w \in W$ [veh/km²·h].

3.3.3. Cost functions

The total cost function (TC_C in [\$/P_m]) has two elements during the peak hour P_m (Equation 3.13): the total cost of users (C_C^u in [\$/P_m]) and the agency cost (C_C^a in [\$/P_m]).

$$TC_C = C_C^u + C_C^a \tag{3.13}$$

Variables

The two decision variables of the model are the distance between rings and radials roads. Table 3.5 explains both continuous spatial variables represented in Figure 3.10.

Table 3.5. Decision variables to model a traffic system.

Decision variables	
$p^c(r)$	distance function between ring roads at the radius r km [km/road]; and
$\Psi^r(\theta)$	angle function between radial roads at an angle θ [radian/road] where $p^r(r,\theta) = \Psi^r(\theta) \cdot r$ is the distance between radial roads at a city point (r,θ) [km/road].

User costs

The total user cost function (C_C^u in [\$/P_m] where P_m represents the rush hour in a city) contains three components (Equation 3.14): the accessibility cost to the closest primary road (C_F), the cost spent during a regular car trip (C_R), and the arriving cost at the destination (C_A).

The cost functions represent the total cost for each stage of a trip in a car. As in the case of public transportation, these functions come from the integration of the local cost function over the circular region of a city (Equation 3.14):

- *Access cost to main roads*: The local access cost function has two components: the demand density in rush hour ($f_{w,v}^F(r,\theta) \cdot T/\eta_u$ in [veh/km²·P_m]), and the average access cost per vehicle ($c_{w,v}^F(r,\theta)$) in [\$/veh]). The access cost to the main road is the integration of the local access cost over the city region considering the types of vehicles $v \in V$ (C_F in [\$/P_m]).
- *Regular trip cost*: Similar to the previous case, the total trip cost (C_R in [\$/P_m]) is thereby the integration of a local cost function over the circular region. The elements of the local cost function are the demand density in rush hour ($f_{w,v}^R(r,\theta) \cdot T/\eta_u$ in [veh/km·P_m]) and the local generalized travel cost on all roads ($c_{w,v}^R(r,\theta)$ in [\$/km·veh]).

- *Arriving cost to trip destinations*: The total arriving cost (C_A in [\$/P_m]) is also the integration of the local cost composed of the demand function in the rush period ($f^A_{w,v}(r,\theta)\cdot T/\eta_u$ in [veh/P_m]), and the expected walking cost and parking fee ($c^A_{w,v}(r,\theta)$ in [\$/veh]).

$$C^u_C = C_F + C_R + C_A$$

where

$$C_F = \int_0^{2\pi}\int_0^{R}\sum_{w\in W}\sum_{v\in V}\frac{1}{\eta_u}\cdot f^F_{w,v}(r,\theta)\cdot T\cdot c^F_{w,v}(r,\theta)\ \ r\,dr\,d\theta$$

$$C_R = \int_0^{2\pi}\int_0^{R}\frac{1}{\eta_u}\cdot\sum_{v\in V} f^R_{c,v}(r,\theta)\cdot T\cdot c^R_{c,v}(r)+\frac{1}{2}\cdot\left(\frac{R}{r}+1\right)\cdot f^R_{r,v}(r,\theta)\cdot T\cdot c^R_{r,v}(r,\theta)\ \ r\,dr\,d\theta \quad (3.14)$$

$$C_A = \int_0^{2\pi}\int_0^{R}\sum_{w\in W}\sum_{v\in V}\frac{1}{\eta_u}\cdot f^A_{w,v}(r)\cdot T\cdot c^A_{w,v}(r)\ \ r\,dr\,d\theta$$

Equations in Table 3.6 show the average local destination cost ([\$/veh]) for each road type.

- *Average access cost* ($c^F_{w,v}(r,\theta)$ in [\$/veh], $w\in\{c,r\}$): The average access cost for accessing has two components. First, cars travel a quarter of the distance between the origin and the closest primary road. The average travel cost is the multiplication of this distance and the generalized cost κ^F_v ($\kappa^F_v = \mu_v\cdot\eta_u/v^F_v + \varphi^t_v$ in [\$/km·veh]). Second, the users incur a penalty time for accessing the closest primary road. This penalty time is a cost using a unitary cost factor $\kappa^{F\prime}_v$ ($\kappa^{F\prime}_v = \mu_v\cdot\eta_u + v^F_v\cdot\varphi^t_v$ in [\$/h·veh]).
- *Generalized travel cost* ($c^R_{w,v}(r,\theta)$ in [\$/km·veh], $w\in\{c,r\}$): For a regular trip, the generalized travel cost function has three components. The first component represents congestion effects using a Bureau of Public Roads (BPR) function. The free-flow travel cost per kilometer is the inverse of free-flow speed multiplied by the value of travel time ($\mu_v\cdot\eta_u/v^{ff}_v$). The congestion level depends on the traffic flow ($F^R_{W_c,v}(r,\theta) = f^R_{W_c,v}(r,\theta)\cdot p^c(r)/\eta_u$ and $F^R_{W_r,v}(r,\theta) = f^R_{W_r,v}(r,\theta)\cdot(R+r)/2\cdot\Psi^r(\theta)/\eta_u$) and the capacity of a road ($K^R_{w,v}(r,\theta)$) where vehicles can travel to one of the two available directions: $c\in\{c_c: clockwise, c_a: anticlockwise\}$ for rings, and $r\in\{r_i: inside, r_o: outside\}$ for radial roads. Second, the unitary cost of a regulated crossroad by traffic lights is the ratio between the cost spent by crossing a road ($\mu_v\cdot\eta_u\cdot\tau^i_v$) and the distance between roads ($r\cdot\Psi^r(\theta)$ or $p^c(r)$). Finally, the last component is the operational cost of a vehicle per traveled kilometer (φ^t_v).
- *Average destination cost* ($c^A_{w,v}(r,\theta)$ in [\$/veh], $w\in\{c,r\}$): After a user parked his car, he will pay the parking fee and walk to the final destination. The average destination cost has five elements. First, users incur a cost for accessing local roads ($t^{A\prime}_v\cdot\kappa^{A\prime}_v$ where $\kappa^{A\prime}_v = \mu_v\cdot\eta_u + v^F_v\cdot\varphi^t_v$ in [\$/h·veh]). Second, the driving cost on local streets before a user starts to look for a vacant parking spot. This sub-cost is composed of the average distance (e.g., $(p^c(r)-d_p)/4$) and

the generalized cost ($\kappa_v^A = \mu_v \cdot \eta_u / v_v^A + \varphi_v^t$). Third, the cost incurred by users, which are looking for a parking space, is the multiplication of the average distance between vacant spots ($1/\lambda_P$) and the generalized cost ($\kappa_v^P = \mu_v \cdot \eta_u / v_v^P + \varphi_v^t$). Fourth, walking to the destination is the distance between a user parked and the final destination. According to Arnott and Rowse (1999), the expected walking distance after parking the vehicle has two cases. If a driver finds a vacant space before his destination ($x < d$) then this driver will walk $d - x$ km. In another case, the driver will walk $x - d$ km to the destination. Therefore, the user walking cost is the multiplication of the expected walking distance and the generalized cost ($\kappa_v^A = \mu_v \cdot \eta_u / v^a$). Fifth, the cost finally includes a car-parking fee (φ^f).

Table 3.6. Cost functions of users.

Stage	Route	Unitary cost functions
Access cost $c_{w,v}^F(r,\theta)$	Ring routes	$\frac{p^c(r)}{4} \cdot \kappa_v^F + t_v^{F\prime} \cdot \kappa_v^{F\prime}$
	Radial routes	$\frac{r \cdot \Psi^r(\theta)}{4} \cdot \kappa_v^F + t_v^{F\prime} \cdot \kappa_v^{F\prime}$
Travel cost $c_{w,v}^R(r,\theta)$	Ring routes	$\frac{\mu_v}{v_v^{ff}} \cdot \left(1 + a \cdot \left(\frac{F_{w,v}^R(r,\theta)}{K_{w,v}^R(r,\theta)}\right)^b\right) + \frac{\mu_v \cdot \eta_u \cdot \tau_v^i}{r \cdot \Psi^r(\theta)} + \varphi_v^t$
	Radial routes	$\frac{\mu_v}{v_v^{ff}} \cdot \left(1 + a \cdot \left(\frac{F_{w,v}^R(r,\theta)}{K_{w,v}^R(r,\theta)}\right)^b\right) + \frac{\mu_v \cdot \eta_u \cdot \tau_v^i}{p^c(r)} + \varphi_v^t$
Destination cost $c_{w,v}^A(r,\theta)$	Ring routes	$t_v^{A\prime} \cdot \kappa_v^{A\prime} + \left(\frac{p^c(r) - d_p}{4}\right) \cdot \kappa_v^A + \frac{\kappa_v^P}{\lambda_P} + \left(\frac{2 \cdot e^{-\lambda_P \cdot d_p}}{\lambda_P} + d_p - \frac{1}{\lambda_P}\right) \cdot \kappa_v^A + \varphi^f$
	Radial routes	$t_v^{A\prime} \cdot \kappa_v^{A\prime} + \left(\frac{r \cdot \Psi^r(\theta) - d_p}{4}\right) \cdot \kappa_v^A + \frac{\kappa_v^P}{\lambda_P} + \left(\frac{2 \cdot e^{-\lambda_P \cdot d_p}}{\lambda_P} + d_p - \frac{1}{\lambda_P}\right) \cdot \kappa_v^A + \varphi^f$

Agency costs

In the agency cost (C_I in [\$/P_m], Equation 3.15), the local cost function ([\$/km^2]) is the multiplication of the cost per linear kilometer and the road density ($1/p^c(r)$ or $1/r \cdot \Psi^r(\theta)$). The unitary cost contains two parts: a fixed and a variable element, i.e., $\varphi_v^p = \varphi_v^{p(f)} + \varphi_v^{p(v)} \cdot T$.

$$C_I = 2 \cdot \int_0^{2\pi} \int_0^R \sum_{v \in V} \frac{\varphi_v^p}{p^c(r)} + \frac{\varphi_v^p}{r \cdot \Psi^r(\theta)} \; r \, dr \, d\theta \qquad (3.15)$$

3.3.4. Problem formulation and optimization

The formulated model has its basis on the CA method in which its objective function represents the total system cost for a continuous network design problem (CNDP). Thus, the model solves a system optimum (SO) using an incremental traffic assignment in a continuous space. The CA method solves a function of costs, which each point (r, θ) in polar coordinates (r is the radius and θ is the angle in radians) depends on local cost attributes.

Problem formulations

The total cost function (TC_C in [\$/P_m]) results from the integration of the local cost function of a differential region in polar coordinates ($r\, dr\, d\theta$) over the circular region ($0 \le r \le R$, $0 \le \theta \le 2\pi$). The total cost function ($TC_C = C_C^u + C_C^a$ in Equation 3.16(a)) has two components: the total cost of users (C_C^u in [\$/P_m]) and the agency cost (C_C^a in [\$/P_m]).

$$Min\ TC_C = (C_F + C_R + C_A) + C_I \qquad \text{(a)}$$

s.t.

$$\max_{\theta, w \in W_c} \left(\frac{\frac{1}{\eta_u} \cdot f_{w,v}^R(r,\theta) \cdot p^c(r)}{K_{w,v}^R(r,\theta)} \right) \le 0.9 \qquad \forall\, r \qquad \text{(b)}$$

$$\max_{r, w \in W_r} \left(\frac{\frac{1}{\eta_u} \cdot f_{w,v}^R(r,\theta) \cdot \Psi^r(\theta) \cdot \frac{R+r}{2}}{K_{w,v}^R(r,\theta)} \right) \le 0.9 \qquad \forall\, \theta \qquad \text{(c)} \qquad (3.16)$$

$$p^c(r) \ge K^{d(c)} \qquad \forall\, r \qquad \text{(d)}$$

$$\Psi^r(\theta) \ge K^{d(r)} \qquad \forall\, \theta \qquad \text{(e)}$$

The model also considers that the congestion must not overtake 90 percent of the road capacity for any direction of a road (Equations 3.16(b) and (c)). Finally, the distance between roads must be greater than $K^{d(d)}$ (Equation 3.16(d)). For radial routes (Equation 3.16(e)), $K^{d(r)} = K^{d(c)}/r_{min}$, where r_{min} is a minimum radius in which the model apply the constraint from this point.

Method for solving the problem

The nonlinear system has two decision variables ($x_i^\circ(\cdot) = \{p^c(r), \Psi^r(\theta)\}$, $n_v = 2$), and four constraints ($n_c = 4$). The set of Equations 3.17 shows the KKT conditions in which Equation 3.17(a) is the first condition for each decision variable. The second condition contains the constraints c_j° (Equation 3.17(b)).

The third condition set is the complementary slackness (Equation 3.17(c)); if an inequality constraint is active, its slack is zero, and its multiplier ($\lambda_j^\circ(\cdot)$) takes any non-negative value (Equation 3.17(a)). The multipliers ($\lambda_j^\circ(\cdot)$) are non-negative (Equation 3.17(d)). The decision variables must be not less than K^{min} (Equation 3.17(e)). In Equation 3.17, the expression contains an equation system with inequalities. This system of equations allows obtaining the optimal solution through the method of successive approximations.

$$
\begin{aligned}
&\frac{\partial\, tc(r,\theta)}{\partial\, x_i^\circ(\cdot)} + \sum_{j=1}^{n_c} \lambda_j^c(r) \cdot \frac{\partial\, c_j^c(r,\theta)}{\partial\, x_i^\circ(\cdot)} + \sum_{j=1}^{n_c} \lambda_j^r(\theta) \cdot \frac{\partial\, c_j^r(r,\theta)}{\partial\, x_i^\circ(\cdot)} = 0 \quad \forall\, i = 1, \dots, n_v && \text{(a)} \\
&c_j^\circ(r,\theta) - K_j \le 0 \quad \forall\, j = 1, \dots, n_c && \text{(b)} \\
&\lambda_j^\circ(\cdot) \cdot \left(c_j^\circ(r,\theta) - K_j\right) = 0 \quad \forall\, j = 1, \dots, n_c && \text{(c)} \\
&\lambda_j^\circ(\cdot) \ge 0 \quad \forall\, j = 1, \dots, n_c && \text{(d)} \\
&x_i^\circ(\cdot) > K^{min} \quad \forall\, i = 1, \dots, n_v && \text{(e)}
\end{aligned}
\qquad (3.17)
$$

where $n_v = 2, n_c = 4$,
$x_i^\circ(\cdot) = \{p^c(r), \Psi^r(\theta)\}$
$\lambda_j^\circ(\cdot) = \{\lambda_1^c(r), \lambda_2^c(r), \lambda_1^r(\theta), \lambda_2^r(\theta)\}$

Optimal analytical solutions

The conditions obtained from the KKT method are first-order optimization functions. Table 3.7 presents the analytical functions to get optimal values on all city road corridors: $p^c(r)$ and $\Psi^r(\theta)$. These analytical functions are necessary conditions for the optimal solution. Although these necessary conditions are not sufficient for optimality, all local minimum satisfies it. To find the optimal solution is required to analyze the convexity of the problem. In this case, the local function by a road corridor (ring or radial road) is convex for non-negative solutions in the first and fourth quadrants of a plot.

Optimal analytical expressions of $p^c(r)$ and $\Psi^r(\theta)$ depend on b value. The analysis supposes that if $a = 2$ and $b = 3$, the function is a quartic function, which is also a convex function. Specifically, the function is a compound quadratic polynomial introducing a change of variable $u = {d_c}^2$, converting it to a quadratic function. The solution has one solution and three non-valid ones (negative and complex roots).

Table 3.7. Optimal analytical functions of a traffic system.

Optimal analytical functions
$$p^c(r)^{b+1} \cdot \int_0^{2\pi} \sum_{d \in D} \sum_{w \in W} \sum_{v \in V} \frac{1}{\eta_u} \cdot f^R_{c,d,v}(r,\theta) \cdot T \cdot \frac{\mu_v \cdot a \cdot b}{v^{ff}_{w,v}} \cdot \left(\frac{\frac{1}{\eta_u} \cdot f^R_{c,d,v}(r,\theta)}{K^R_{c,w,v}(r,\theta)} \right)^b \; r \, d\theta$$ $$+ p^c(r)^2 \cdot \int_0^{2\pi} \sum_{v \in V} \frac{1}{4} \cdot \left(\frac{1}{\eta_u} \cdot f^F_{c,v}(r,\theta) \cdot T + \frac{1}{\eta_u} \cdot f^A_{c,v}(r,\theta) \cdot T \right) \cdot \Psi^F_v \; r \, d\theta$$ $$- \left(\int_0^{2\pi} \sum_{d \in D} \sum_{w \in W} \sum_{v \in V} \frac{1}{\eta_u} \cdot f^R_{r,v}(r,\theta) \cdot T \cdot \mu_v \cdot \tau^i_{w,v} \; r \, d\theta + \int_0^{2\pi} \sum_{w \in W} \sum_{v \in V} \left(\varphi^{h(f)}_{w,v} + \varphi^{h(v)}_{w,v} \cdot T \right) \; r \, d\theta \right) + \lambda_c(r) \cdot \max_\theta \left(\frac{\frac{1}{\eta_u} \cdot f^R_{c,v}(r,\theta)}{K^R_{c,w,v}(r,\theta)} \right) = 0$$
$$\Psi^r(\theta)^{b+1} \cdot \int_0^{R} \sum_{w \in W} \sum_{v \in V} \frac{1}{\eta_u} \cdot f^R_{r,v}(r,\theta) \cdot T \cdot \frac{\mu_v \cdot a \cdot b}{v^c_{w,v}} \cdot \left(\frac{\frac{1}{\eta_u} \cdot f^R_{r,v}(r,\theta) \cdot r}{K^V_{r,w,v}(r,\theta)} \right)^b \; dr$$ $$+ \Psi^r(\theta)^2 \cdot \int_0^{R} \sum_{v \in V} \frac{1}{4} \cdot \left(\frac{1}{\eta_u} \cdot f^F_{r,v}(r,\theta) + \frac{1}{\eta_u} \cdot f^A_{r,v}(r,\theta) \right) \cdot T \cdot \Psi^F_v \cdot r \; dr$$ $$- \left(\int_0^{R} \sum_{w \in W} \sum_{v \in V} \frac{1}{\eta_u} \cdot f^R_{c,v}(r,\theta) \cdot T \cdot \mu_v \cdot \tau^i_{w,v} \cdot \frac{1}{r} \; dr + \int_0^{R} \sum_{w \in W} \sum_{v \in V} \left(\varphi^{h(f)}_{w} + \varphi^{h(v)}_{w} \cdot T \right) \cdot \frac{1}{r} \; dr \right) + \lambda_r(\theta) \cdot \max_r \left(\frac{\frac{1}{\eta_u} \cdot f^R_{r,v}(r,\theta)}{K^V_{r,w,v}(r,\theta)} \right) = 0$$

3.3.5. Methodology for obtaining continuous solutions

Inequality systems

Equations 3.17(a) of the variables $p^c(r)$ (Equation 3.18) and $\Psi^r(\theta)$ (Equation 3.19) have three components. The first element shows the total cost density of vehicles multiplied by a factor of congestion density. Second, it expresses the total cost of two components: the sub-cost will represent the driver cost crossing an intersection by a radial road and the cost of constructing and maintaining a road. Third, the total cost density of drivers that leave their origin and arrive at a destination point.

$$
\begin{aligned}
&\boldsymbol{p^c(r)^{b-1}} \cdot \int_0^{2\pi} \sum_{d\in D}\sum_{v\in V} f^R_{c,d,v}(r,\theta)\cdot T \cdot \frac{\mu_v \cdot a \cdot b}{v^{ff}_{w,v}} \cdot \left(\frac{f^R_{c,d,v}(r,\theta)}{K^R_{c,w,v}(r,\theta)}\right)^b \; r\, d\theta \\
&- \boldsymbol{p^c(r)^{-2}} \cdot \int_0^{2\pi} \sum_{d\in D}\sum_{v\in V} f^R_{r,d,v}(r,\theta)\cdot T \cdot \mu_v \cdot \tau^i_{w,v} + \sum_{v\in V}\left(\varphi^{h(f)}_{w,v} + \varphi^{h(v)}_{w,v}\cdot T\right) \; r\, d\theta \qquad \text{(a)} \\
&+ \int_0^{2\pi} \sum_{v\in V} \frac{1}{4}\cdot\left(f^F_{c,v}(r,\theta)\cdot T + f^A_{c,v}(r,\theta)\cdot T\right)\cdot \Psi^F_v \; r\, d\theta + \boldsymbol{\lambda^c_1(r)} \cdot \max_{(r,\theta,d,v)}\left(\sum_{v\in V}\frac{f^R_{c,d,v}(r,\theta)}{K^R_{w.v}(r,\theta)}\right) = 0 \qquad \forall\, r \\
&\max_{\theta,w\in W_c}\left(\frac{\frac{1}{\eta_u}\cdot f^R_{w,v}(r,\theta)\cdot p^c(r)}{K^R_{w,v}(r,\theta)}\right) \le 0.9 \qquad \forall\, r \qquad \text{(b)} \\
&p^c(r) \ge K^{d(c)} \quad \forall\, r \\
&\boldsymbol{\lambda^c_1(r)} \cdot \left(\max_{\theta,w\in W_c}\left(\frac{\frac{1}{\eta_u}\cdot f^R_{w,v}(r,\theta)\cdot p^c(r)}{K^R_{w,v}(r,\theta)}\right) - 0.9\right) = 0 \qquad \forall\, r \qquad \text{(c)} \\
&\boldsymbol{\lambda^c_2(r)} \cdot \left(-p^c(r) + K^{d(c)}\right) = 0 \quad \forall\, r \\
&\boldsymbol{\lambda^c_1(r)} \ge 0 \quad \forall\, r \\
&\boldsymbol{\lambda^c_2(r)} \ge 0 \quad \forall\, r \qquad \text{(d)}
\end{aligned}
\tag{3.18}
$$

$$
\begin{aligned}
&\boldsymbol{\Psi^r(\theta)^{b-1}} \cdot \int_0^{R} \sum_{d\in D}\sum_{v\in V} f^R_{r,d,v}(r,\theta)\cdot T \cdot \frac{\mu_v \cdot a \cdot b}{v^{ff}_{w,v}} \cdot \left(\frac{f^R_{r,d,v}(r,\theta)\cdot r}{K^R_{r,w,v}(r,\theta)}\right)^b \; dr \\
&- \boldsymbol{\Psi^r(\theta)^{-2}} \cdot \int_0^{R} \sum_{d\in D}\sum_{v\in V} f^R_{c,d,v}(r,\theta)\cdot T \cdot \mu_v \cdot \tau^i_{w,v}\cdot\frac{1}{r} + \sum_{v\in V}\left(\varphi^{h(f)}_{w} + \varphi^{h(v)}_{w}\cdot T\right)\cdot\frac{1}{r} \; dr \qquad \text{(a)} \\
&+ \int_0^{R} \sum_{v\in V} \frac{1}{4}\cdot\left(f^F_{r,v}(r,\theta) + f^A_{r,v}(r,\theta)\right)\cdot T\cdot \Psi^F_v \cdot r \; dr + \lambda_r(\theta)\cdot \max_{(r,\theta,d,v)}\left(\sum_{v\in V}\frac{f^R_{r,d,v}(r,\theta)\cdot r}{K^R_{w.v}(r,\theta)}\right) = 0 \quad \forall\, \theta \\
&\max_{r,w\in W_r}\left(\frac{\frac{1}{\eta_u}\cdot f^R_{w,v}(r,\theta)\cdot \Psi^r(\theta)\cdot\frac{R+r}{2}}{K^R_{w,v}(r,\theta)}\right) \le 0.9 \quad \forall\, \theta \qquad \text{(b)} \\
&\Psi^r(\theta) \ge K^{d(r)} \quad \forall\, \theta \\
&\boldsymbol{\lambda^r_1(\theta)} \cdot \left(\max_{r,w\in W_r}\left(\frac{\frac{1}{\eta_u}\cdot f^R_{w,v}(r,\theta)\cdot \Psi^r(\theta)\cdot\frac{R+r}{2}}{K^R_{w,v}(r,\theta)}\right) - 0.9\right) = 0 \quad \forall\, \theta \qquad \text{(c)} \\
&\boldsymbol{\lambda^r_2(r)} \cdot \left(-\Psi^r(\theta) + K^{d(r)}\right) = 0 \quad \forall\, \theta \\
&\boldsymbol{\lambda^r_1(\theta)} \ge 0 \quad \forall\, \theta \\
&\boldsymbol{\lambda^r_2(\theta)} \ge 0 \quad \forall\, \theta \qquad \text{(d)}
\end{aligned}
\tag{3.19}
$$

Method of two phases

The solution to the system of inequalities gives the optimal solution. Similar to the previous case, the iterative algorithm (Figure 3.11) gives solutions when reaching convergence.

This method has two phases. The first stage consists of the initialization of variables in which a feasible solution uses the minimum value of each variable, respectively: $\{K^d, K^h\}$. Moreover, the algorithm creates a variable that stores the number of iterations (i). The second stage is an iterative process in which the model calculates the two decision variables. The process will iterate while the solutions are feasible, and the error is higher than the tolerance for each variable. The first sub-problem calculates the two variables ($p^{c(i)}(r)$) for a set of ring corridor routes ($r \in [0 \ldots R]$) if there are feasible solutions and first-order optimization conditions are satisfied. In the case of radial services, the process is identical. After that, the variable will increase by one unit. The convexity of the problem is analyzed. The algorithm will stop when the error is less than the tolerance. Finally, the algorithm will find the optimal solution.

Algorithm: Solution of the continuous traffic problem

Initialize $p^{c(0)}(r) = K^{d(c)}$; $\Psi^{r(0)}(\theta) = K^{d(r)}$
for 1... n
    m $\leftarrow M_n$
    $D^{\circ} \leftarrow D(r_f, \theta_f, r_t, \theta_t)$×m

    i := 1
    while (abs($p^{c(i)}(r) - p^{c(i-1)}(r)$) > tolerance or
            abs($\Psi^{r(i)}(\theta) - \Psi^{r(i-1)}(\theta)$) > tolerance)
        for each $r \in [0 \ldots R]$ **do**
            $p^{c(i)}(r) \leftarrow$ *SystemOfEquations*($\Psi^{r(i-1)}(\theta)$)
        end for

        for each $\theta \in [0 \ldots 2\pi]$ **do**
            $\Psi^{r(i)}(\theta) \leftarrow$ *SystemOfEquations*($p^{c(i-1)}(r)$)
        end for

        i := i + 1
    end while
end for

Figure 3.11. The algorithm based on successive approximations numerically solves the traffic problem through two phases.

3.4. Discretization of continuous functions

The discretization of continuum results from the model allows the location of corridors or routes and the transit service frequency.

3.4.1. Method for the system of inequalities

The method uses the inverse of optimal continuous functions (density functions of circular or radial corridor routes) to calculate the area below the function's curve. The discretization of continuum results from the model allows the corridor location, routes, and the transit service frequency. The method proposed by Medina-Tapia et al. (2013) has its basis on the disk model (Ouyang & Daganzo, 2006).

The second algorithm searches similar areas, i.e., the integral of an area gives a unitary value or close to one. Figure 3.13 shows a density function ($\delta(x)$ is a blue line) that represent the inverse of the distance between circular routes ($1/d^c(r)$), or the angle between radial routes ($1/\Phi^r(\theta)$). The x-axis represents the distance of a corridor route in kilometers or radians. Moreover, the gray zones symbolize the area below the density curve between the two following thresholds. A blue point represents the position of the route at the point $x_{2\cdot i}$, in which each zone Z_i is defined between $x_{2\cdot i-1}$ and $x_{2\cdot i+1}$ (red points). Therefore, the position of $x_{2\cdot i-1}$, $x_{2\cdot i}$ and $x_{2\cdot i+1}$ is obtained from a system of inequalities for rings (Equation 3.20) and radial routes (Equation 3.21).

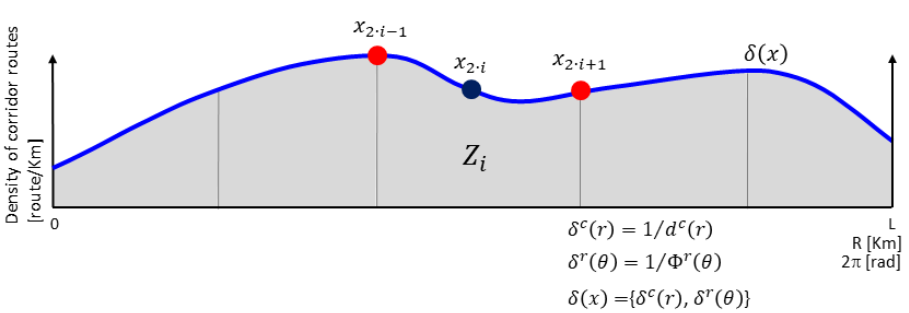

Figure 3.12. Discretization using the method of inequalities system.

In the first stage of the discretization of a continuous density function ($\delta(x)$), the algorithm calculates the number of zones from the total area under the density function. Second, each zone takes equidistant borders as a feasible initial solution. Third, the set of inequalities for circular (Equation 3.20) and radial (Equation 3.21) routes allow determining a discrete solution. The

inequalities (a) and (b) have a slack or tolerance (ξ), and inequality (c) is strict. The solution is not unique.

$$\int_{x_{2\cdot i-1}}^{x_{2\cdot i}} \delta^c(r)\, dr \le \frac{1}{2}\cdot(1+\xi) \quad \forall\, Z_i \qquad \text{(a)}$$
$$\int_{x_{2\cdot i}}^{x_{2\cdot i+1}} \delta^c(r)\, dr \le \frac{1}{2}\cdot(1+\xi) \quad \forall\, Z_i \qquad \text{(b)} \qquad (3.20)$$
$$\int_{x_{2\cdot i-1}}^{x_{2\cdot i+1}} \max_{\theta, l\in L_c}\left(f_l^V(r,\theta)\cdot h^c(x_{2\cdot i})\right) dr \le K^v \quad \forall\, Z_i \qquad \text{(c)}$$

$$\int_{x_{2\cdot i-1}}^{x_{2\cdot i}} \delta^r(\theta)\, d\theta \le \frac{1}{2}\cdot(1+\xi) \quad \forall\, Z_i \qquad \text{(a)}$$
$$\int_{x_{2\cdot i}}^{x_{2\cdot i+1}} \delta^r(\theta)\, d\theta \le \frac{1}{2}\cdot(1+\xi) \quad \forall\, Z_i \qquad \text{(b)} \qquad (3.21)$$
$$\int_{x_{2\cdot i-1}}^{x_{2\cdot i+1}} \max_{r, l\in L_r}\left(f_l^V(r,\theta)\cdot\frac{R+r}{2}\cdot h^c(x_{2\cdot i})\right) d\theta \le K^v \quad \forall\, Z_i \qquad \text{(c)}$$

3.4.2. Method of equivalent areas

The algorithm bases its process on Ouyang and Daganzo's disk model (2006), Medina (2011), and Medina-Tapia et al. (2013). The method also uses the inverse of optimal continuous functions (density functions of circular or radial corridor routes). The second algorithm finds equivalent areas with unitary value or close to one.

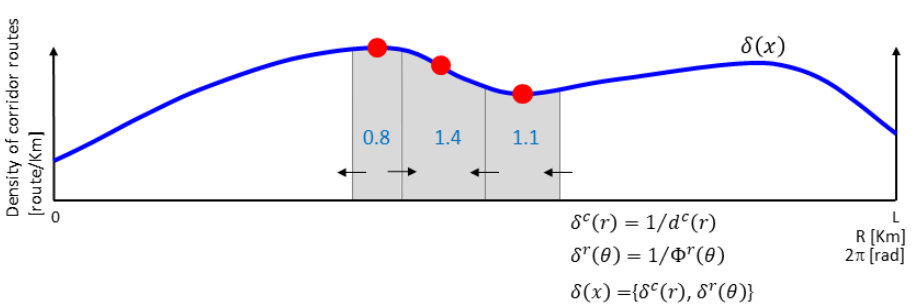

Figure 3.13. Graphic representation of the method of equivalent areas.

Figure 3.13 shows a density function ($\delta(x)$) that could represent the distance between circular corridor routes ($d^c(r)$) or the angle between radial corridor routes ($\Phi^r(\theta)$). The x-axis represents the distance of a corridor line in kilometers or radians. Moreover, the three gray zones in the plot symbolize the area below the density curve. In some cases, the area is higher than one. In other cases, the opposite situation happens. This process requires moving

the border of a corridor until reaching the equilibrium between all areas. Within an area, between two borders of a corridor, a corridor route is located. The specific location will be at a point between two borders in which the area on each side of a corridor's location has the same value (0.5).

Algorithm: Discretization of a continuous function $\delta(x)$

Initialize
    total_area := $\int_0^L \delta(x)\, dx$
    N_r := round(total_area)
    zona_list = *ZoneCreate*(N_r)
for each zona ∈ zona_list **do**
    border(zona)^{left} := **if** zona = 1 **then** 0 **else** *border*(zona-1)^{right} **end if**
    border(zona)^{right} := **if** zona = N_r **then** L **else** *border*(zona)^{left} + L/N_r **end if**
end for

i := 1
while each *AreaCalculate*(zone ∈ zone_list) ≠ (total_area/N_r + tolerance)
    for each zona ∈ zona_list **do**
        if *AreaCalculate*(zona) > 1 **then**
            border(zona)^{left} := *border*(zona)^{left} +Δ, if zona ≠ 1
            border(zona)^{right} := *border*(zona)^{right} –Δ, if zona ≠ N_r
        elseif *AreaCalculate*(zona) < 1 **then**
            border(zona)^{left} := *border*(zona)^{left} –Δ, if zona ≠ 1
            border(zona)^{right} := *border*(zona)^{right} +Δ, if zona ≠ N_r
        end if
    end for

    i := i + 1
end while

Figure 3.14. Algorithm of the method of equivalent areas to discretize a continuous density function.

The algorithm in Figure 3.14 discretizes a continuous density function ($\delta(x)$) that can be the distance between circular corridor routes ($d^c(r)$) or the angle between radial corridor routes ($\Phi^r(\theta)$). In the first stage, the algorithm calculates the total area under the density function and initializes the zone number using a rounding function. After that, it creates a variable that stores the created zones (zona_list). Each zone takes equidistant borders as a feasible initial solution. In the second stage, the algorithm iterates to reach the solution. Borders of a zone move away or approach each other. If the area is higher than one, then the borders approach a distance Δ each border. If the area is less than one, then the borders move away from each other (Δ). Finally, the algorithm will stop when the areas are equivalent, and these are close to total_area/N_r plus a tolerance value.

3.5. Summary

- The dissertation proposes models for concentric cities in which several cities have an equivalent urban network in form and structure defined by ring and radial routes/roads.
- The non-homogeneous demand modeling used in this dissertation stands out over traditional distributions approaching the real distribution of demand for generic analyzes that become independent of a city's particular network.
- The proposed model for designing transportation networks can adapt to non-homogeneously distributed demands, considering local demand conditions.
- Modeling a transit system considers the essential stages of a trip. Moreover, the agency's costs also include relevant aspects such as capital, operation, and infrastructure. A relevant contribution is including the latter in the model considering modal infrastructure costs (stations/stops) and linear corridors (routes/roads).
- Regarding traffic systems, it highlights the modeling of users' and agency costs. Notably, it highlights the congestion modeling using a flow-delay function.
- Another contribution of this work is to obtain continuous outcomes through an algorithm. This method speeds up the computation time compared to optimization methods, including those implemented in any software.
- The discretization of continuous outcomes over the city is yet another significant contribution to this research. The proposal has a basis on two methods: the former aims the optimization, and the latter generates a heuristic that obtains results in reduced times.

4. Infrastructure and urban mobility

The chapter analyses the design of a strategic transportation network applying the proposed methodology in a concentric city. The first part focuses on population density, formulating standard demand scenarios: homogeneous, heterogeneous, mono-centric, and multi-subcenters cities. Secondly, the dissertation evaluates the optimal characteristics for an adequate design of urban networks (or their trade-offs) considering two types of networks: transit and traffic systems. It is worth noting that the analysis concentrates on the transportation functionality interaction with elements of urban structure as primary transportation systems, central business district, and subcenters.

4.1. Scenarios of demand

The four proposed scenarios (Figure 4.1) have their basis on proposed mathematical expressions formulated by Ouyang et al. (2014): homogeneous city, heterogeneous city, mono-centric city, and multi-subcenters city. Appendix C details the formulations and parameter values used in each urban scenario.

- First, in a homogeneous city, each point of a city has a stable trip generation and attraction density ($\lambda(r,\theta)$ and $\rho(r,\theta)$ in Equations 3.2 and 3.3, respectively). In this case, the rate is 1,000 [user/km²·h].
- Second, the heterogeneous city is the opposite case to a homogeneous city in which each point on a city has distinct densities of generation and attraction of trips. This scenario came from a random selection concerning the total number of generated/attracted trips.
- Third, the mono-centric city contains a central business district (CBD) that generates and attracts more trips than the rest of the city.
- Finally, the case of the multi-subcenters city contains four subcenters. The role of urban subcenters is to "bring economic activities (e.g., services, employment) closer to people who live in peripheral urban spaces" (Medina-Tapia, Robusté, & Estrada, 2020).

Figure 4.1 shows the distribution of generation and attraction of trips for each urban scenario. The x-axis and y-axis represent the extension of a city expressed in [km]. The model analyzes a city 30 kilometers in diameter; the city center is the point $(0,0)$. The z-axis represents the demand density in [user/km²·h]. It is worth mentioning that the homogenous city is a baseline of this investigation, comparing it with the non-homogeneous demand scenarios. All scenarios have an equivalent number of generated and attracted trips (Δ in Equation 3.1). However, the distribution of rates changes throughout the city, keeping an average rate of 1,000 [user/km²·h].

Additionally, the analysis embraces the gradualness of implementing the scenarios starting from the baseline, increasing the size of the CBD or subcenters, respectively. Figure 4.2 shows the gradual implementation of a CBD from an area representing 5% of total trips to 25% of those. Similarly, Figure 4.3 also shows a gradual implementation of multi-subcenters from 5% to 25% of total trips as a scenario that includes an urban planning strategy. It is worth noting that the scenario homogeneous (Figure 4.1(a) and (b)) is before the two gradual processes of implementations: a CBD and multi-subcenters presented in Figure 4.2 and Figure 4.3.

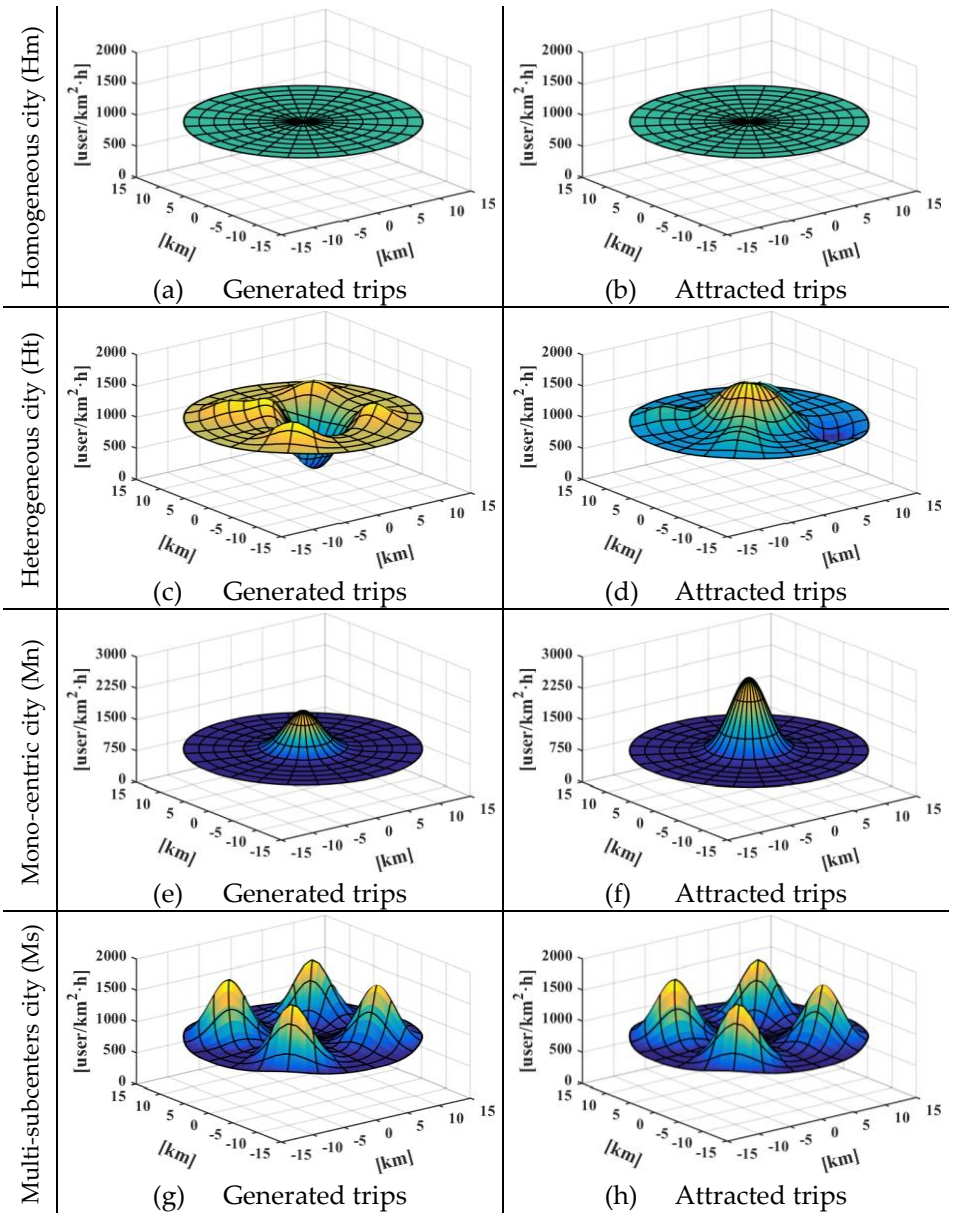

Figure 4.1. Urban scenarios analyzed with 1,000 [user/km²·h].

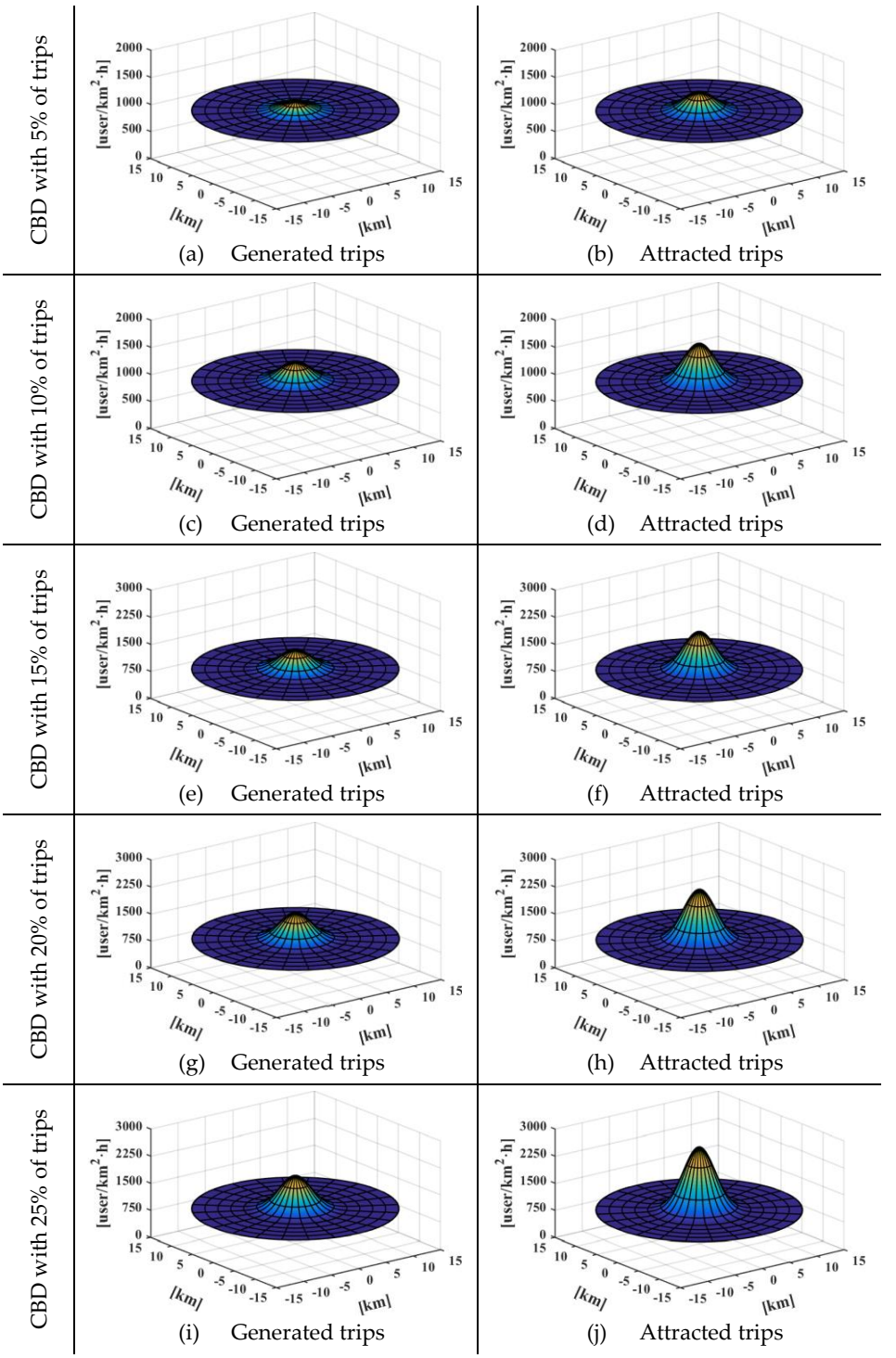

Figure 4.2. Scenarios of mono-centric cities, including a CBD calculated with an average density of 1,000 [user/km²·h].

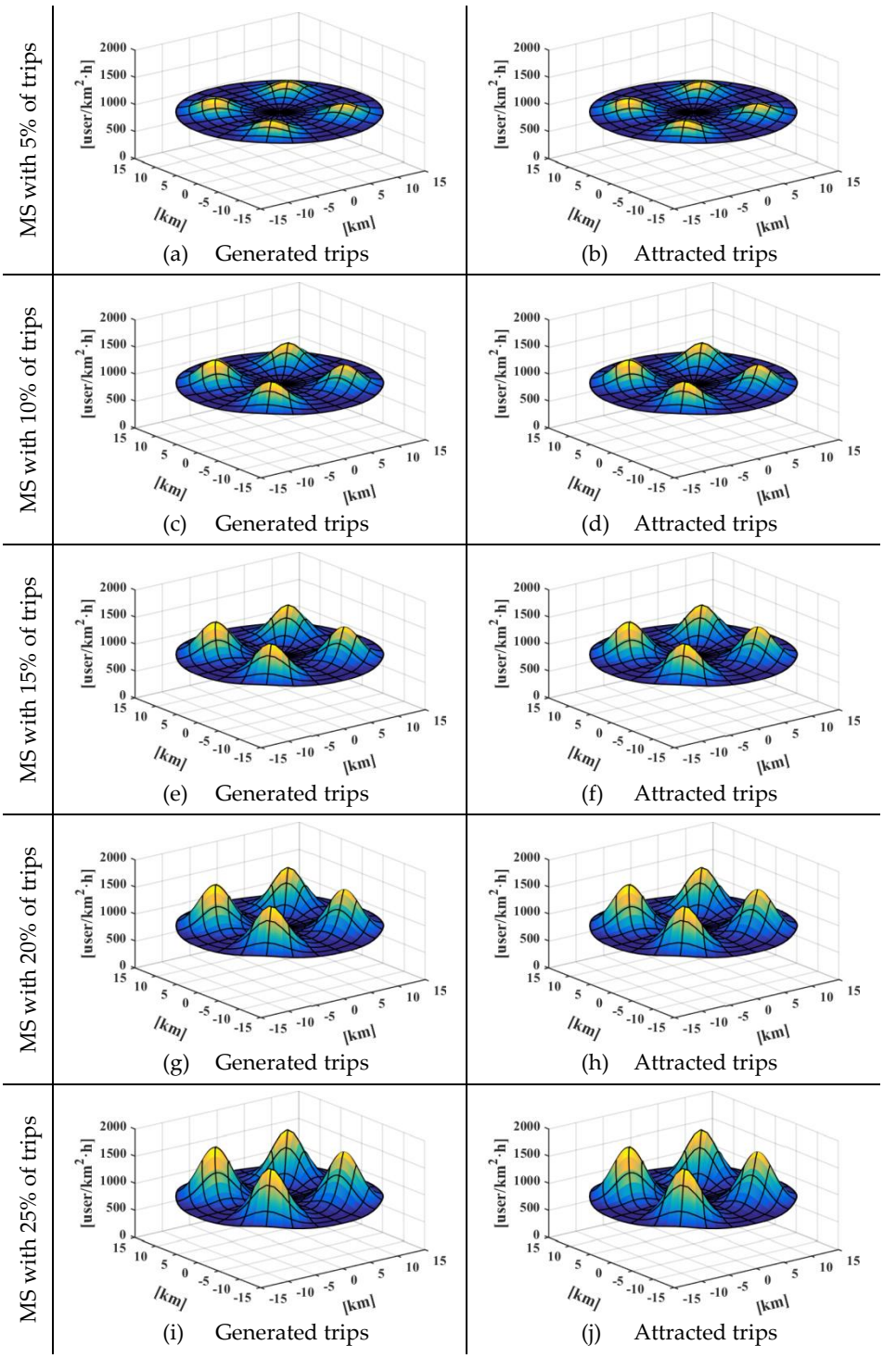

Figure 4.3. Scenarios of multi-subcenters cities (MS) calculated with an average density of 1,000 [user/km²·h].

4.2. Transit network design

The modeling analyzes a circular city that has a radius of R km in which the rush hour P_m lasts T hours. A trip on transit has four stages: access, waiting, in-vehicle travel, and transfer. This subchapter has a basis on a paper (Medina-Tapia et al., 2021), and Appendix D explains it.

4.2.1. Demand density functions and parameters

Each stage of a trip has a demand formulation expressed as a density function. It is worth remembering the modeling assumes that users choose the shortest route between the origin and destination (Section 3.2.2). Equation 4.1 contains demand density functions.

$$f^A(r,\theta) = \int_0^{2\pi}\int_0^R D(r,\theta,r_t,\theta_t)\, r_t\, dr_t\, d\theta_t + \int_0^{2\pi}\int_0^R D(r_f,\theta_f,r,\theta)\, r_f\, dr_f\, d\theta_f$$

$$f_c^W(r,\theta) = \int_{\theta-2}^{\theta+2}\int_r^R D(r,\theta,r_t,\theta_t)\, r_t\, dr_t\, d\theta_t$$

$$f_r^W(r,\theta) = \int_{\theta-2}^{\theta+2}\int_0^r D(r,\theta,r_t,\theta_t)\, r_t\, dr_t\, d\theta_t + \int_{\theta+2}^{\theta-2+2\pi}\int_0^R D(r,\theta,r_t,\theta_t)\, r_t\, dr_t\, d\theta_t$$

$$\begin{aligned} f_c^V(r,\theta) = {} & \int_{\theta}^{\theta+2}\int_r^R \left\{ \int_{\theta_t-2}^{\theta} D(r,\theta_f,r_t,\theta_t)\, r\, d\theta_f \right\} r_t\, dr_t\, d\theta_t + \int_{\theta}^{\theta+2} \left\{ \int_{\theta_t-2}^{\theta}\int_r^R D(r_f,\theta_f,r,\theta_t)\, r_f\, dr_f\, d\theta_f \right\} r\, d\theta_t \\ & + \int_{\theta-2}^{\theta}\int_r^R \left\{ \int_{\theta}^{\theta_t+2} D(r,\theta_f,r_t,\theta_t)\, r\, d\theta_f \right\} r_t\, dr_t\, d\theta_t + \int_{\theta-2}^{\theta} \left\{ \int_{\theta}^{\theta_t+2}\int_r^R D(r_f,\theta_f,r,\theta_t)\, r_f\, dr_f\, d\theta_f \right\} r\, d\theta_t \end{aligned} \quad (4.1)$$

$$\begin{aligned} f_r^V(r,\theta) = {} & \int_{\theta-2}^{\theta+2}\int_0^r \left\{ \int_r^R D(r_f,\theta,r_t,\theta_t)\, dr_f \right\} r_t\, dr_t\, d\theta_t + \int_{\theta+2}^{\theta-2+2\pi}\int_0^R \left\{ \int_r^R D(r_f,\theta,r_t,\theta_t)\, dr_f \right\} r_t\, dr_t\, d\theta_t \\ & + \int_r^R \left\{ \int_{\theta-2}^{\theta+2}\int_0^r D(r_f,\theta_f,r_t,\theta)\, r_f\, dr_f\, d\theta_f \right\} dr_t + \int_r^R \left\{ \int_{\theta+2}^{\theta-2+2\pi}\int_0^R D(r_f,\theta_f,r_t,\theta)\, r_f\, dr_f\, d\theta_f \right\} dr_t \end{aligned}$$

$$f_c^T(r,\theta) = \int_r^R\int_{\theta-2}^{\theta+2} D(r_f,\theta,r,\theta_t)\, r_t\, d\theta_t\, dr_f$$

$$f_r^T(r,\theta) = \int_{\theta-2}^{\theta+2}\int_r^R D(r,\theta_f,r_t,\theta)\, r_f\, dr_t\, d\theta_f$$

These density functions allow calculating how many people access, wait, travel, and transfer at each city point. Appendix B presents the all-or-nothing assignment problem applied to a continuous space for transit systems. This

appendix contains a methodology presenting the formulations of demand density functions.

Homogeneous demand function

Demand depends on both the width of transit corridors and demand density functions. This section analyzes an urban scenario in which the demand is homogenous over a city, i.e., each point of the city generates/attracts the same density of trips. Figure 4.4 shows the density functions for a spatially homogeneous city of 1,000 [user/km²·h] of generated trips obtained from Equations 4.1 and explained in Appendix B.

- In the first stage of a trip, the access density function in [user/km²·h] comes from the formulation presented in Equation 4.1 ($f^A(r,\theta)$). Figure 4.4(a) shows a homogeneous surface at 2,000 [user/km²·h], which depends on generated and attracted trips (boarding and alighting of users) considering both types of corridor routes.
- In the second stage of a trip, users wait for a ring or radial service. Equation 4.1 ($f_c^W(r,\theta)$ and $f_r^W(r,\theta)$) present the formulations to obtain the demand density of passengers in [user/km²·h]. In Figure 4.4(b), the density $f_c^W(r,\theta)$ increases closer to the city center because the probability of starting a trip closes from the center and finish it to the outside is higher around the center than in the city periphery. The opposite happens in radial transit, where the probability is higher in the periphery than in the city center ($f_r^W(r,\theta)$, Figure 4.4(c)).
- The third stage is the in-vehicle density surface in [user/km·h] considering the width (km) of a transit corridor of an in-vehicle trip at each city point ($f_c^V(r,\theta)$ and $f_r^V(r,\theta)$, Equation 4.1). The concentration of ring density is on an intermediate ring between the center and outer ring ($f_c^V(r,\theta)$, Figure 4.4(d)) because the intermediate ring has more likely to receive more trips in a scenario with homogeneous demand. Furthermore, radial trips increase in points close to the city center because it joins trips from the same city side and the opposite side ($f_r^V(r,\theta)$, Figure 4.4(e)).
- In the last stage, the transfer density function ($f_c^T(r,\theta)$ and $f_r^T(r,\theta)$, Equation 4.1) represents the density of users in [user/km²·h] who transfer between two types of routes. The surface is similar in both types of services considering a homogeneous demand (Figure 4.4(f) and (g)) because the density functions are equivalent if a user transfers from a ring to a radial service or vice versa.

Therefore, the exhibits in Figure 4.4 show that if the generated and attracted demand rate is a fixed value, the demand at each stage of a trip is not constant.

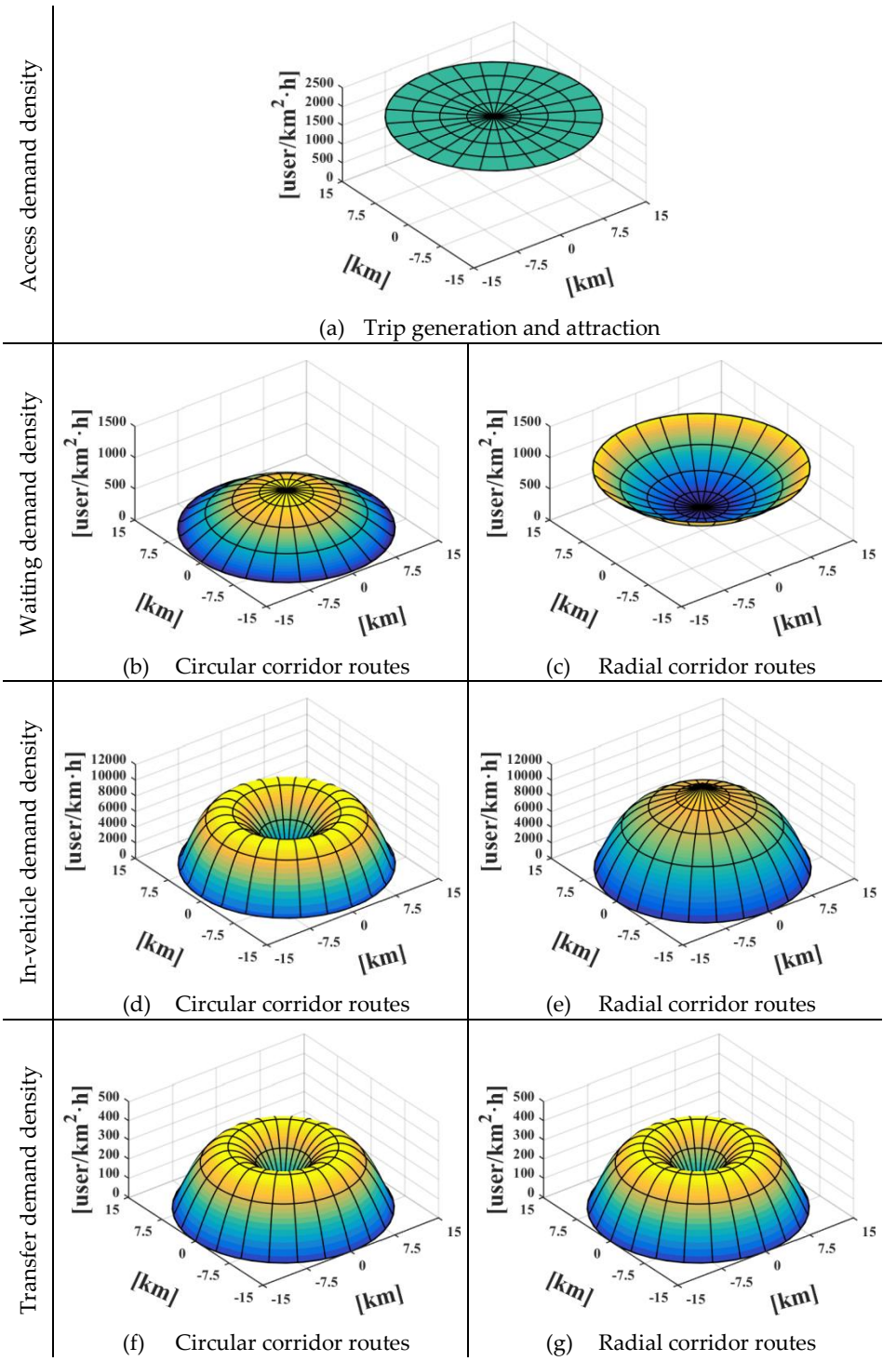

(a) Trip generation and attraction

(b) Circular corridor routes

(c) Radial corridor routes

(d) Circular corridor routes

(e) Radial corridor routes

(f) Circular corridor routes

(g) Radial corridor routes

Figure 4.4. Demand density functions obtained from a homogeneous demand city considering 1,000 [user/km²·h] and using a transit network.

Non-homogeneous demand functions

The non-homogeneous demand density functions come from the three scenarios presented in Section 4.1 (p. 72). The demand varies over the city: heterogeneous, mono-centric, and multi-subcenters cities, considering an average density rate of 1,000 [user/km^2·h] for a transit network.

- *Heterogeneous city scenario*: The trip density of generation and attraction randomly varies at each city point. Figure 4.5 shows demand density functions for each stage of a trip in this urban case. The demand densities have a similar macro-structure compared to the homogeneous case, although local conditions change at each city point of the urban region, and the magnitude of in-vehicle densities are more significant for this case (Figure 4.5(d) and (e)).
- *Mono-centric city scenario*: The case has a central business district (CBD), which concentrates more trips than the rest of the city. Figure 4.6 shows demand density functions for each stage of a trip in which the center of the city concentrates the access density of trips (Figure 4.6(a)). The center concentrates the waiting demand for circular services, while the outer of the city concentrates this demand for radial services (Figure 4.6(b) and (c)). Secondly, the intermediate ring zone concentrates in-vehicle trips of circular services (Figure 4.6(d)), while the radial density increases to the city center, but the density is more significant (Figure 4.6(e)) than the case of a homogeneous city (Figure 4.4(e), p. 78). Finally, the transfer density functions rise at the city center (Figure 4.6(f) and (g)), although it is slightly higher in the case of circular services.
- *Multi-subcenters city scenario*: The urban case has four subcenters in which trip densities around subcenters are more significant than the rest of the city points. Figure 4.7 shows demand density functions for each stage of a trip. For this reason, the subcenters concentrate the access densities (Figure 4.7(a)). The waiting density for circular services increases closer to the city center, but the maximum concentration is in subcenters and their vicinity (Figure 4.7(b)). The opposite happens in radial services, where the periphery has high levels of density, but the maximum values are also near the subcenters (Figure 4.7(c)). The concentration of in-vehicle trip densities on ring services are on the intermediate zone (Figure 4.7(d)). On the other hand, in-vehicle trip densities on radial services have a significant concentration on radial services where lie the subcenters (Figure 4.7(e)). The transfer demand densities are significant near the subcenters for circular and radial services (Figure 4.7(f) and (g)).

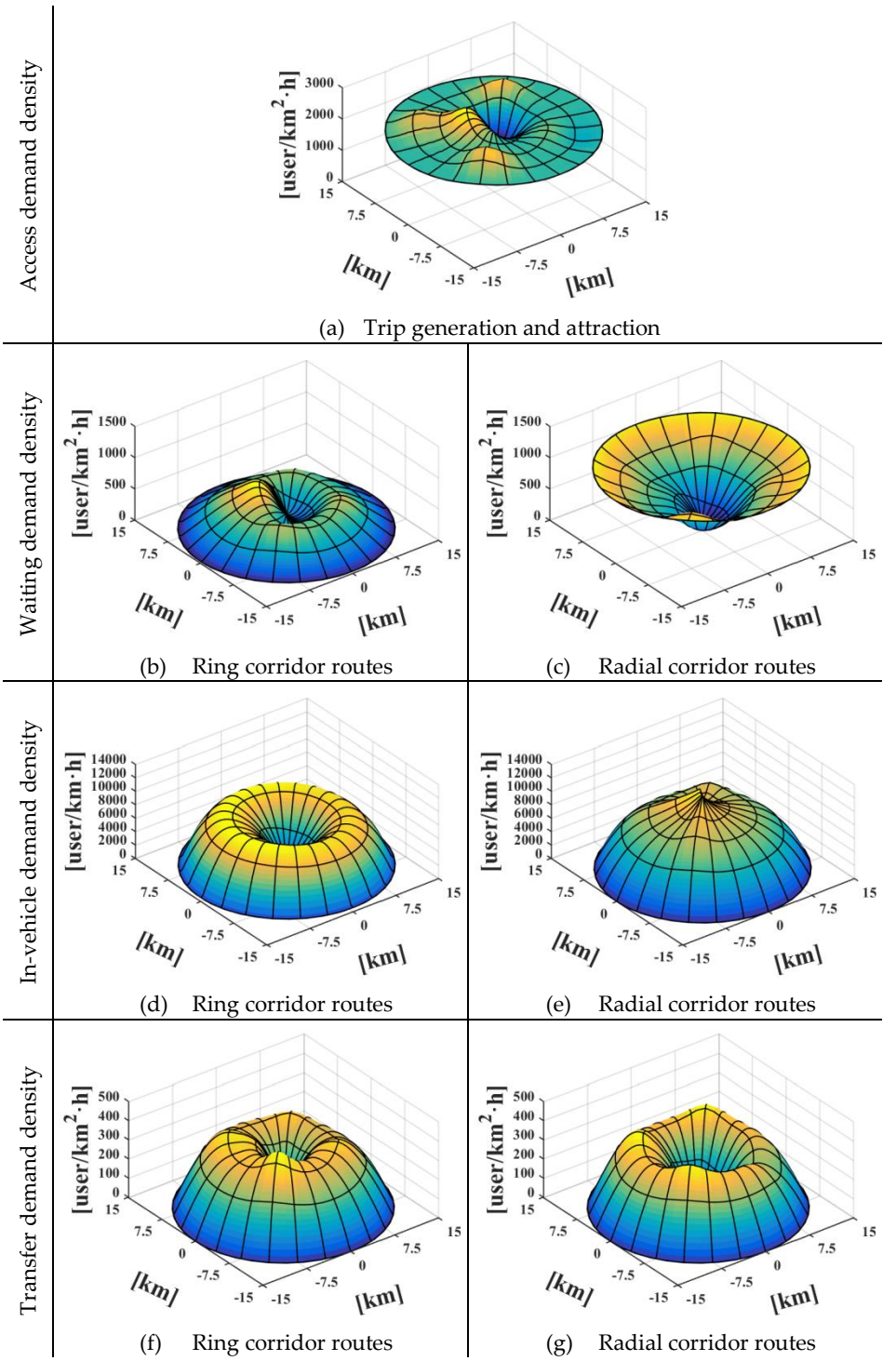

Figure 4.5. Demand density functions obtained from a heterogeneous demand city considering 1,000 [user/km²·h] and using a transit network.

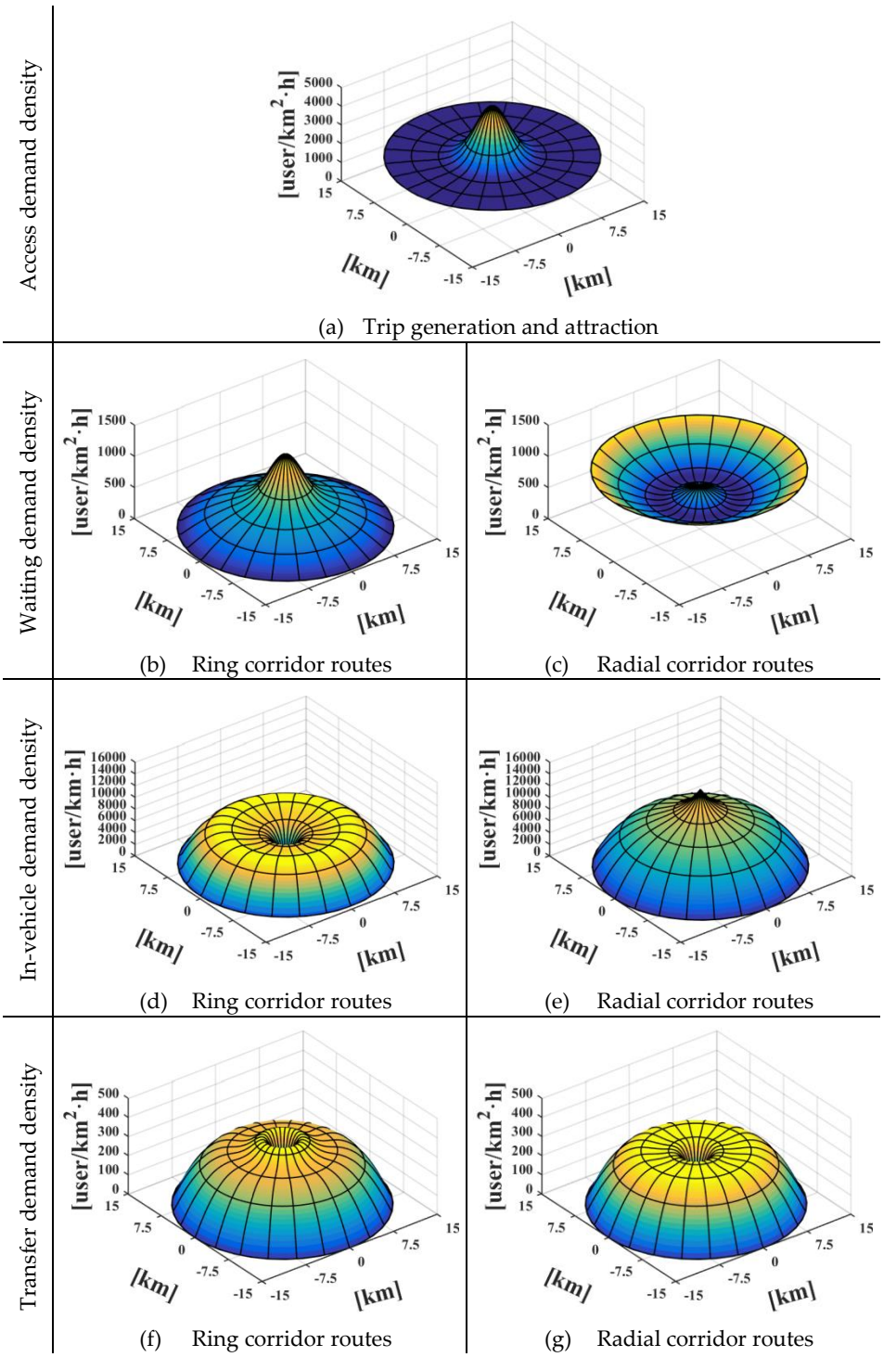

Figure 4.6. Demand density functions obtained from a mono-centric city considering 1,000 [user/km²·h] and using a transit network.

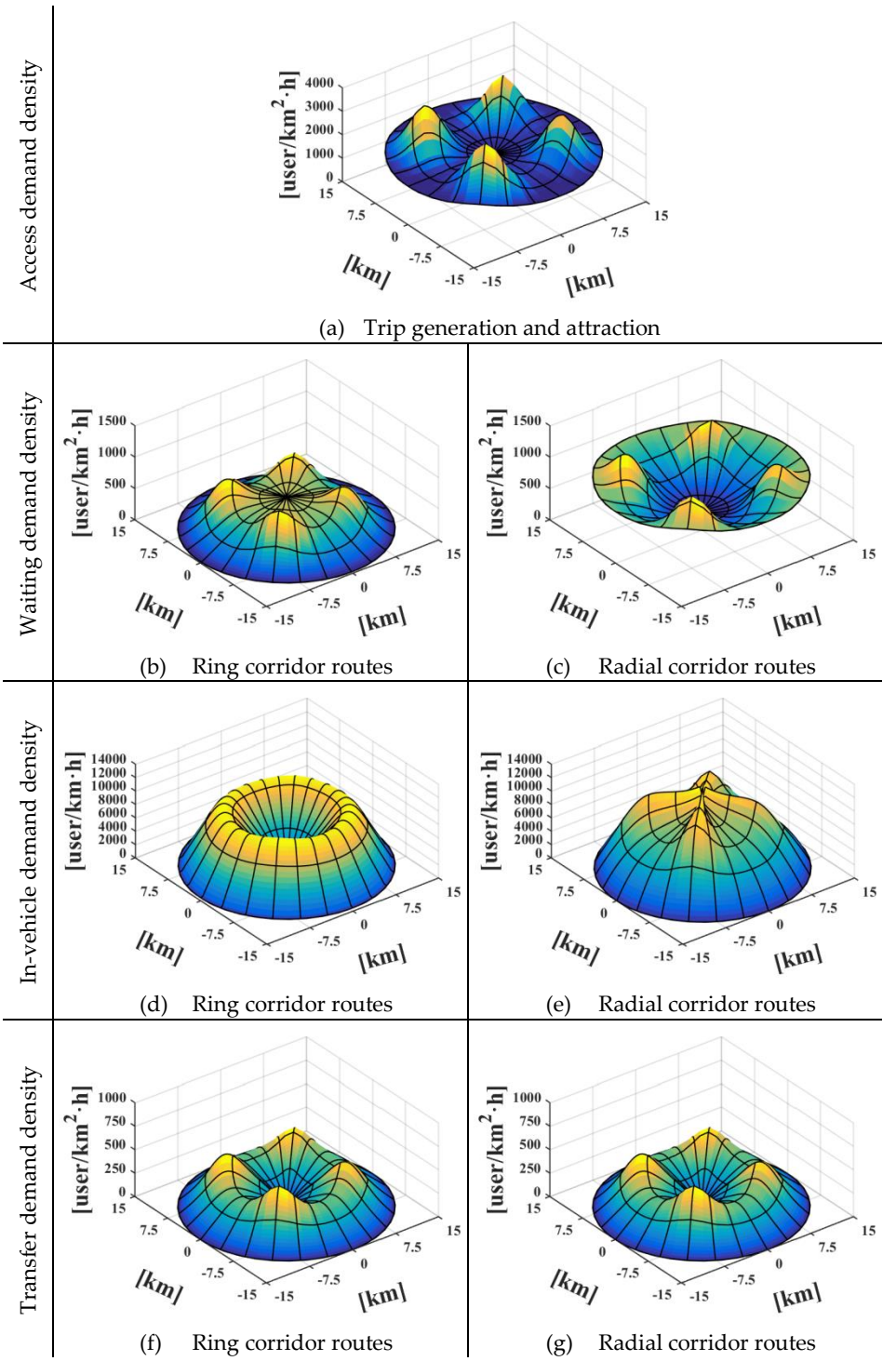

Figure 4.7. Demand density functions obtained from a multi-subcenters city considering 1,000 [user/km²·h] using a transit network.

Parameters

The modeling analyzes a concentric city with a radius of 15 km (R), considering the rush hour lasts 1.5 hours (T). Table 4.1 presents the list of transit operation parameters for each modal case. It is worth noting each stage of a trip depends on the time perception factor: α, β, γ, and δ (TRB, 2013).

Table 4.1. Parameters to model each transit modal scenario.

Parameter		HRT	LRT	BRT
T	[h]		1.5	
α	[dimensionless]		2.2	
β	[dimensionless]		2.1	
γ	[dimensionless]		1.0	
δ	[dimensionless]		2.5	
$v^a(r)$	[km/h]		$v^a(r) = 3.0 + 1.4\bar{6} \cdot r$	
v^t	[km/h]	80	60	50
v^w	[km/h]		3.0	
τ	[h/station]	0.0053 (19.2 [s/station])	0.0034 (12.2 [s/station])	0.0026 (9.3 [s/station])
τ'	[h/station]	0.0014 (5 [s/station])	0.0014 (5 [s/station])	0.0028 (10 [s/station])
τ''	[h/station]	0.0097 (35 [s/station])	0.0083 (30 [s/station])	0.0069 (25 [s/station])
τ'''	[h/station]	0 (0 [s/station])	0.0167 (60 [s/station])	0.0167 (60 [s/station])
τ^s	[h/station]	0.0117 (42.1 [s/station])	0.0333 (119.7 [s/station])	0.0488 (175.62 [s/station])
t^f	[h]	0.1 (6 [min])	0.1 (6 [min])	0.0667 (4 [min])
χ^T	[km]	0.04	0.08	0.08
η^d	[shift/veh]	1	1	1

Considering the accessibility, the model assumes that speed linearly increases from the city center to the periphery. At the city center, the speed will be 3.0 [km/h], which is about 83 [cm/s]. At the outer line, the speed will be 25 [km/h] because the user could take a feeder bus or another vehicle. Therefore, the access speed function is $v^a(r) = 3.0 + 22/15 \cdot r$.

Concerning operation parameters, the cruising speed (v^t) depends on the type of vehicles, whose values come from TRB (2013). At a station, τ is the average time lost by deceleration and acceleration is based on TRB (2013). The average fixed dead time and the minimum stopping time at a station use standard values.

Table 4.2. Time lost by deceleration and acceleration (TRB, 2013).

Parameter		HRT	LRT	BRT
a^a	[m/s²]	1.3	1.0	0.8
a^d	[m/s²]	1.3	1.3	1.0
τ	[h/station]	0.0053 (19.2 [s])	0.0034 (12.2 [s])	0.0026 (9.3 [s])

According to transit infrastructure costs, the fixed costs come from the Australian technical report ATC (2006) for linear and nodal infrastructures. The analysis assumes the variable costs are 1% of the fixed costs.

Table 4.3. Transit infrastructure unitary costs for modeling based on ATC (2006).

Unitary cost		HRT	LRT	BRT
$\varphi^{p(f)}$	[$/km·route·$P_m$]	245.1	169.6	141.3
$\varphi^{p(v)}$	[$/km·route·h]		$\varphi^{p(f)} \cdot 1\%$	
$\varphi^{s(f)}$	[$/station·route·$P_m$]	169.9	8.3	1.6
$\varphi^{s(v)}$	[$/station·route·h]		$\varphi^{s(f)} \cdot 1\%$	

The next table presents the list of unitary cost parameters used for modeling. The value of travel time takes an expected value, while the rest of the parameters rely on ATC (2006).

Table 4.4. Unitary costs to model a transit system based on ATC (2006).

Unitary cost		HRT	LRT	BRT
μ	[$/user·h]		10	
φ^k	[$/veh·$P_m$]	135.6	83.8	38.5
φ^g	[$/shift·h]	27	25	23
φ^o	[$/veh·km·route]	3.7	2.6	1.6
φ^p	[$/km·route·$P_m$]	248.8	172.1	143.4
φ^s	[$/station·route·$P_m$]	172.4	8.4	1.6

The model's constraints require a threshold in each modal scenario. The thresholds K^v and K^h come from ATC (2006), but K^d was calculated using the acceleration and deceleration to reach the cruising speed.

Table 4.5. Restriction thresholds for modeling based on ATC (2006).

Unitary cost		HRT	LRT	BRT
K^v	[user/veh]	750	190	101
K^d	[km/route]	0.481	0.171	0.079
K^h	[h/veh]	0.0342 (123 [seg])	0.0328 (118 [seg])	0.0167 (60 [seg])

Finally, in these applied cases, the modeling assumes that long-term urban changes would not affect the structure of unitary costs.

4.2.2. Spatially homogeneous demand case

Feasible and optimal solutions

For a homogeneous demand city, Figure 4.8 shows the feasible regions defined by the constraints of the model for the radius 7.5 [km], and the exhibit (b) shows it for the angle π [rad], for each transit technology: HRT (green area), LRT (blue area), and BRT (red area).

- First, rings and radial routes have equivalent minimum constraints shown in Equations 3.8(d-g) (p. 49). Second, occupancy is not stable at each city point due to demand density traveling on a vehicle varies over the city. If demand density changes, an iso-capacity curve will also change at a different radius.
- Demand density for radial routes is higher than for ring routes, shown in Section 4.2.1. Therefore, the iso-capacity curve is more restrictive in radial routes than in rings in which the latter is more significant for the three technologies. Even the case of Figure 4.8(a) has overlapping areas among transit technologies, but the technologies cannot cover all solution space in the case Figure 4.8(b).

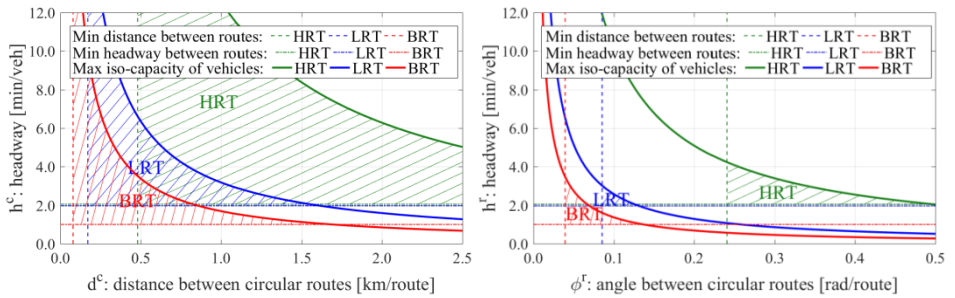

(a) Feasible region for a ring at a radius 7.5 [km]

(b) Feasible region for a radial at an angle π [rad]

Figure 4.8. Feasible region for a homogeneous city (1,000 [user/km²·h]) considering three transit technologies.

Figure 4.9 shows optimal solutions describing a curve for each technological type. Using the spatial, temporary, and capacity constraints (Section 3.2.4, p. 48), the exhibits present iso-capacity curves at different radius due to the variation of demand density. Figure 4.9(a) shows the curve of optimal solutions for rings considering several radii. The generation and attraction rates are constant throughout the city. Nevertheless, demand densities vary regarding radii (Figure 4.4); then, solutions for ring routes vary according to the radius (Figure 4.9(a)). On the other hand, Figure 4.9(b) shows the optimal solutions for a radial route at the angle π considering the solution does not change for any angle.

- For ring routes (Figure 4.9(a)), feasible regions are more significant at the city extremes than in the intermediate zone, being the most demanded. The temporary constraints are active from the city center to 11 or 12 km of radius. In the outskirts, spatial distributions are more significant for HRT, LRT, and BRT—in this order—than at the city center, considering even less frequency (headways rise to the periphery).
- For radial routes (Figure 4.9(b)), optimal solutions are stable for all angles, opposite to ring routes. HRT systems activate both minimum spatial and temporary constraints. Whereas the solutions of LRTs and BRTs active the maximum occupancy and minimum headway constraints.
- Two exceptional cases in Figure 4.9(a) show the effects of the active capacity constraints for LRT and BRT. For an LRT (Figure 4.9(c)), the temporary and capacity constraints are active within 5 and 12 km due to the high density at the intermediate zone, increasing ring route densities in this zone. For a BRT (Figure 4.9(d)), both constraints are also active between 5 and 12 km. After that, only the iso-capacity constraint is active around 12.5 km of radius.

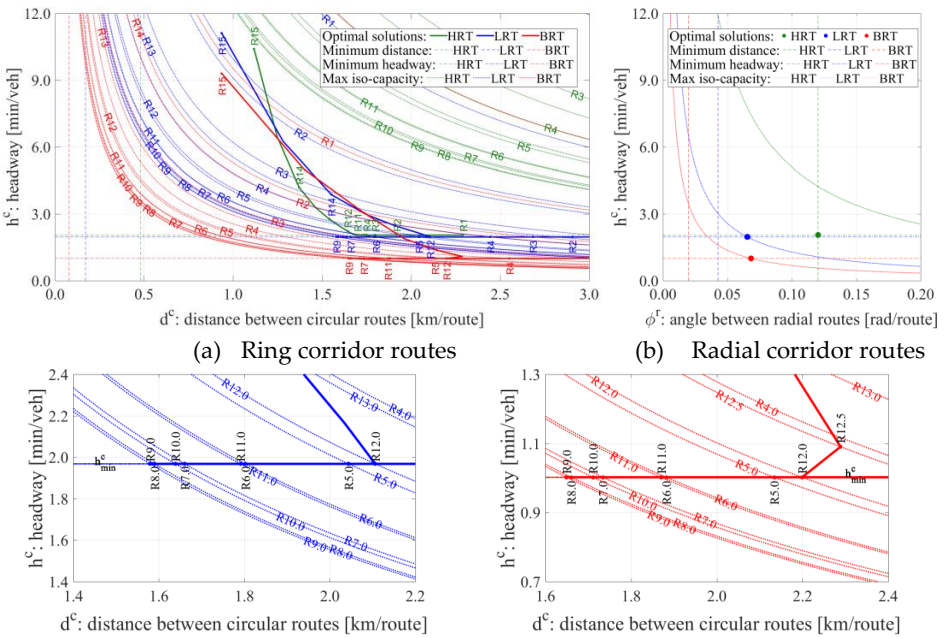

(a) Ring corridor routes (b) Radial corridor routes

(c) Case LRT (d) Case BRT

Figure 4.9. Optimal solutions calculate for a homogeneous city with a generation rate of 1,000 [user/km²·h].

Note: RX contours in the previous exhibits represent the optimal solution for a concentric city whose radius is equivalent to R=X km.

Consequently, the density of rings and headways will increase its value if the radius increases toward the city outer. Therefore, a concentric city must bolster transit rings in the periphery.

Figure 4.10 shows feasible regions from 500 to 3,500 [user/km²·h] obtained from the network design problem, considering the constraints for each transit technology: HRT, LRT, and BRT.

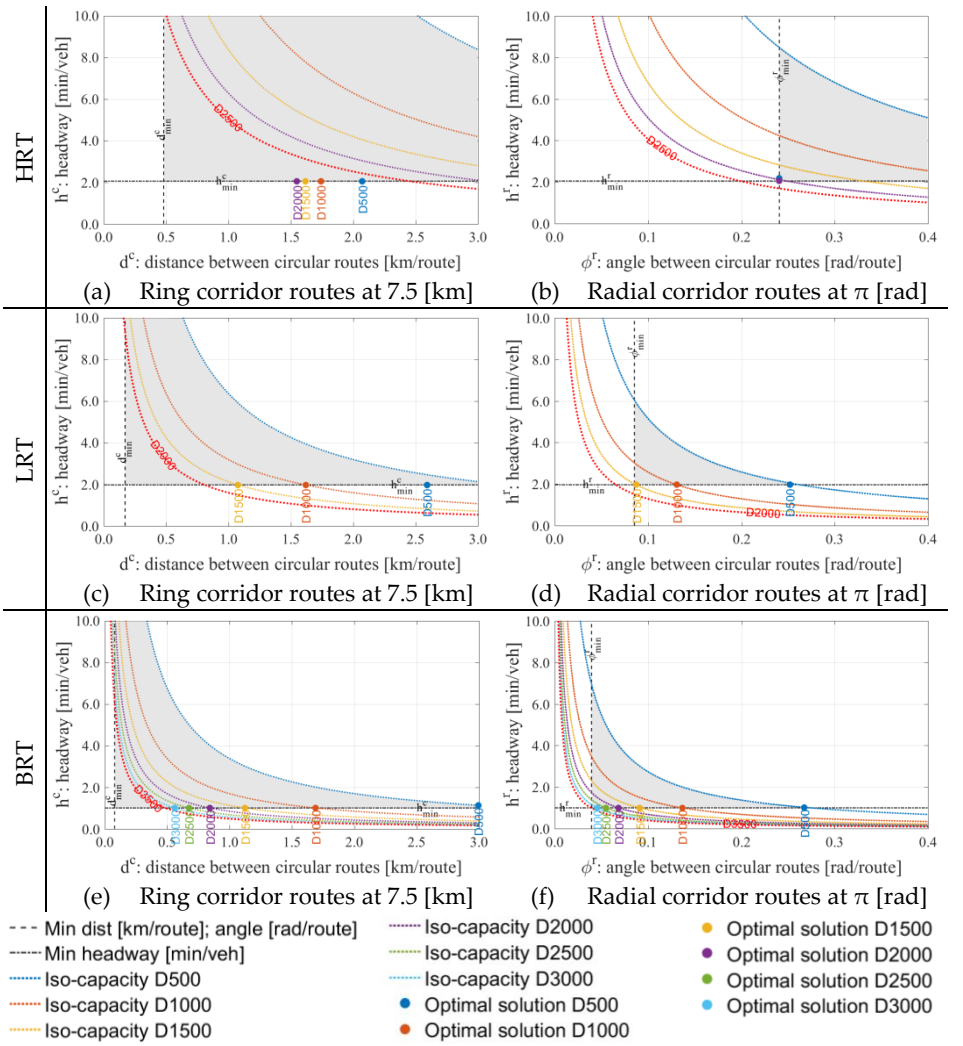

Figure 4.10. Feasible regions from the set of constraints and optimal solutions considering transit technologies.

Note: DX contours represent the demand density that equivalent to D=X [user/km²·h].

Three types of lines form feasible regions in Figure 4.10: dotted lines represent iso-capacity curves obtained from vehicle capacity constraints (Equations 3.8(b) and (c), p. 49), dashed lines represent spatial constraints (Equations 3.8(d) and (e), p. 49), and dash-dot lines represent minimum time headways (Equations 3.8(f) and (g), p. 49). It is worth noting that the iso-capacity curves in which the capacity constraint is active. Thus, the dotted lines depend on demand, i.e., if the demand increases, the feasible region decreases in size.

- For ring routes, if demand increases, the implementation of BRTs reaches the optimum with high frequencies, and corridors are close to each other.

However, an HRT system has an implementation with less frequency, and the distance is higher from each other than BRT and LRT systems if the capacity reaches road saturation.

- For radial routes, the user demand is higher, so optimal solutions have more differences than in the previous case. The constraints are active in almost all cases, so the temporary and capacity constraints are active over 1,000 [user/km^2·h] for LRT and BRT systems. In HRT systems, temporary and spatial constraints are active over 1,000 [user/km^2·h].
- Red dotted lines represent iso-capacity constraints when these lines are smaller than the minimum distance and headway: the system will be unfeasible, at least one of the two route types, frequently radial routes. Thus, the maximum feasible demand is 2,000 [user/km^2·h] for HRTs, 1,500 [user/km^2·h] for LRTs, and 3,000 [user/km^2·h] for BRTs. The analysis gives a paradox for a homogeneous distribution scheme in which the bus at a BRT has less individual capacity but offers greater capacity for the system.

Considering the above, the minimum distance between vehicles for HRT systems is significant in the network design; on the contrary, this restriction prevents it from reaching higher demand levels. On the other hand, adding oversized vehicles in a transit system (higher capacity of buses or tramways) will be able to feasible areas more significant for BRTs and LRTs.

In Figure 4.11, lines represent the density of corridors considering different levels of demand for a circular city with a homogeneous trip distribution and, points represent the discrete location obtained from the algorithm presented in Section 3.4 (p. 67). Moreover, levels of demand progressively increase, resizing the feasible space for solutions explained previously.

- Figure 4.11(a) shows that optimal density curves are continuous without breaks because the constraints are no active, as shown in Figure 4.10(a). Figure 4.11(b) shows the same density for cities over D1000 [user/km^2·h], although the occupancy also increases, reducing the available capacity of each subway car.
- Figure 4.11(c) and (e) show the activation of temporary and capacity constraints around the intermediate ring zone. Thus, LRT's and BRT's ring density of D1000 [user/km^2·h] show the consequences explained previously.
- In radial densities, route density increases rapidly if the city's homogeneous demand also increases.

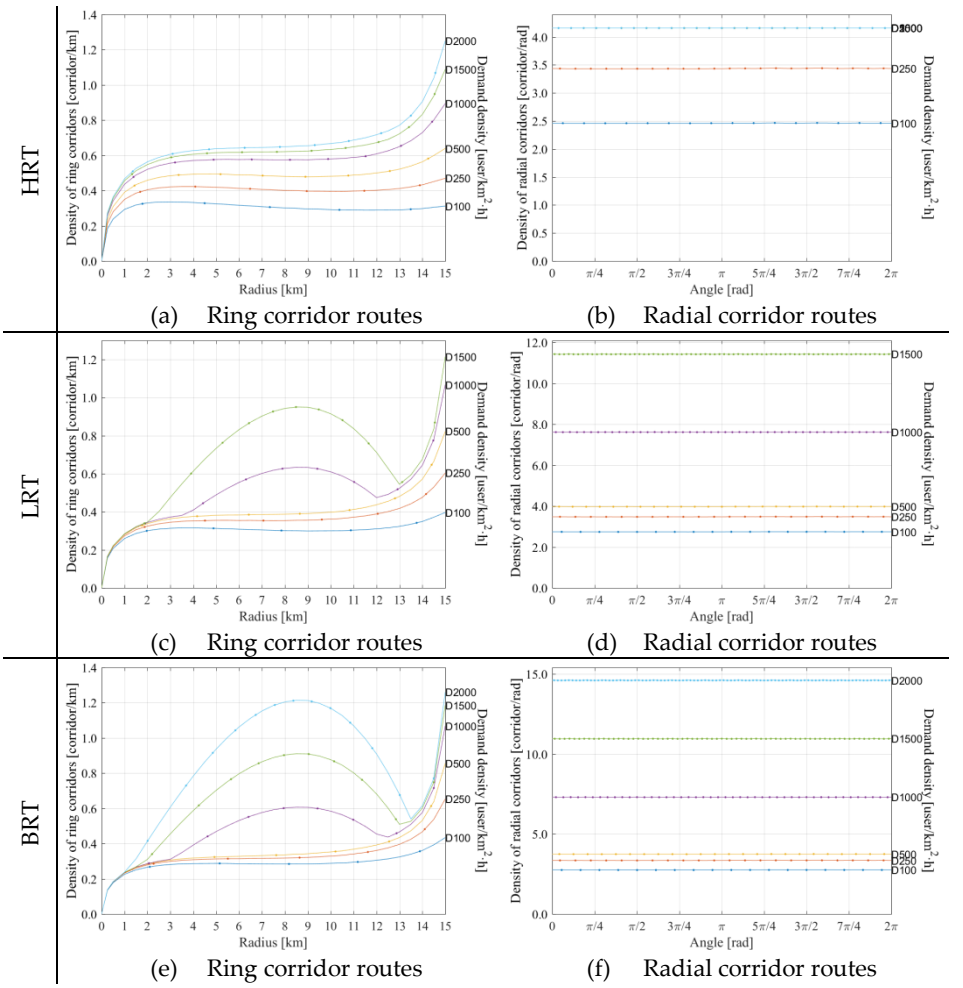

Figure 4.11. Optimal transit structures regarding demand scenarios.
Note: DX texts represent the demand density that is equivalent to D=X [user/km²·h].

Effects of transit operation on infrastructure

The exhibits of Figure 4.12 allow analyzing the system costs considering the three transit technologies.

- Figure 4.12(a) shows the behavior of the total, user, and agency costs regarding levels of demand increasing progressively and considering the system feasibility. HRT has a lower total cost than other technologies.
- Figure 4.12(b) represents the average cost by a user in which the green curve (HRT) decreases concerning the demand. The BRT system reaches the minimal values at approximately 500 [user/km²·h]; after that, the average cost increase, showing the lowest economic efficiency.

- Figure 4.12(c) represents the agency cost divided by users; it could represent a transit fare. BRT is more attractive for low and super-high demand levels if this type is unique feasible. LRT is less expensive if the density is less than 1,000 [user/km²·h]. Finally, HRT is the most expensive in low demand levels. However, this is the best technology between 1,000 and 2,000 [user/km²·h].

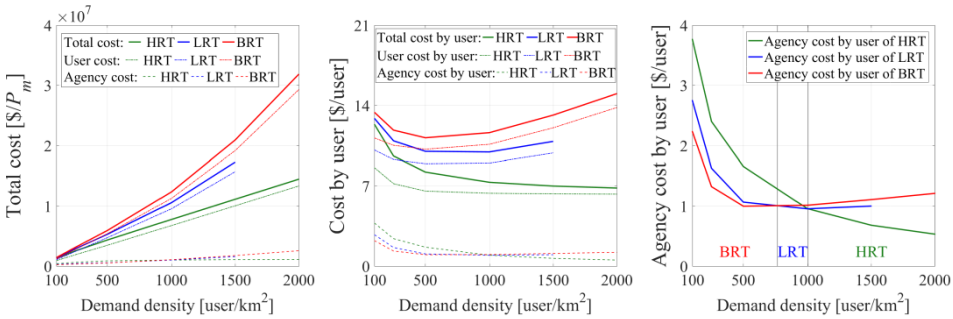

(a) Total cost (b) Total cost by user (c) Agency cost by user

Figure 4.12. Transit system cost considering progressive homogeneous demand scenarios.

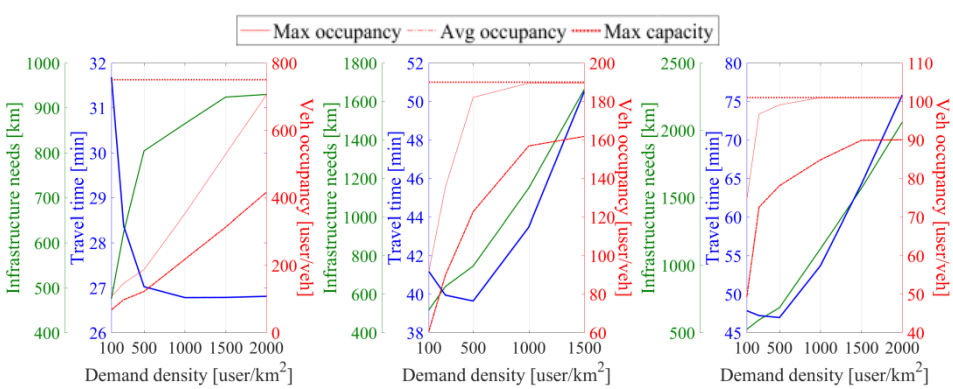

(a) HRT (b) LRT (c) BRT

Figure 4.13. Transit occupation and travel time according to progressive homogeneous demand scenarios.

Figure 4.13 shows some demand effects on transit operation (Figure 4.13(a) HRT, (b) LRT, and (c) BRT) and infrastructure considering different demand levels. The color of lines represents each label on the y-axis.

- The transit occupancy increases if demand densities also increase. However, only the HRT system does not reach the maximum capacity.
- LRT and BRT systems reach the saturation quickly if demand exceeds 1,000 [user/km²·h].
- The travel time decreases whether the demand increases in the case of HRT because the infrastructure increases as well. For LRT and BRT systems, the

travel time decreases to reach a minimal value (500 [user/km²·h]); after that, the systems are inefficient.

4.2.3. Non-homogeneous demand systems

The dissertation analyzes four scenarios of demand distribution for a city that generates 1,000 [user/km²·h] presented in Section 4.1 (Hm, Ht, Mn, and Ms).

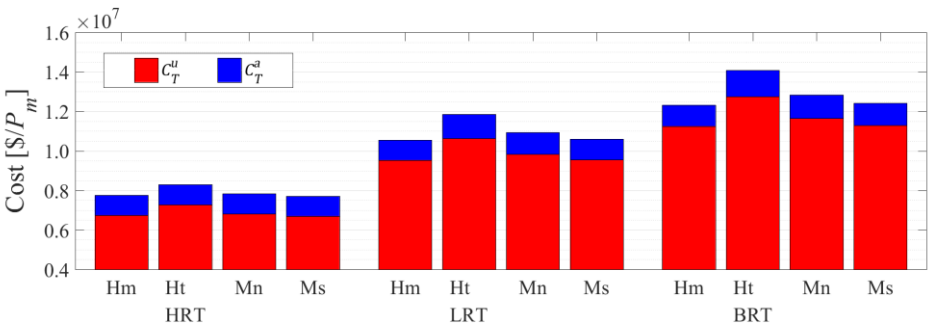

Figure 4.14. Costs of transit technologies considering four urban scenarios of a city with 1,000 [user/km²·h].

Figure 4.14 compares the total cost for each urban scenario and transit technology in which the following points are the main outcomes:

- The implementation of HRT systems presents the least cost of all types of cities. A homogeneous city (Hm) is the best urban alternative for almost all types of technologies. This result seems to be logical due to Hm reduces the saturation and costs due to the concentration of users at any city point.
- An Mn city generates a reduction of costs from 5.5% for HRTs to 8.6% for BRTs regarding a Ht city. However, Ms cities reduce the costs from 6.9% for HRTs to 11.6% for BRTs regarding a Ht city. The muti-subcenters city for HRTs provides the best reduction of costs, around 45.1% regarding the worst-case (a BRT for a Ht city).
- The previous conclusion contrasts against the Ht case that has the highest total costs. The best alternative is implementing subcenters (Ms) because the latter has an equivalent total cost to a homogeneous city.

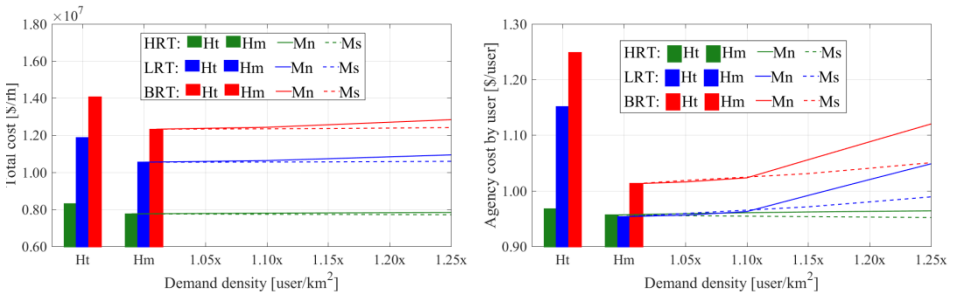

(a) Total cost (b) Agency cost by user

Figure 4.15. Transit costs according to urban scenarios and transit mode systems.

The results shows the importance of CBD and subcenters depends on the size of these. Figure 4.15 compares the four urban scenarios presented in Section 4.1 (Ht, Hm, Mn, and Ms) in which the two latter progressively increase the demand from 5% (1.05x) to 25% (1.25x) of the total number of trips.

- *Total cost* (Figure 4.15(a)): The total cost of a monocentric city increases if the size of the CBD also increases considering the total number of trips; and otherwise, the total cost of a multi-subcenters city decreases if the subcenters size increases. Even the cost is less than at a homogeneously distributed city, reducing 0.6% for an HRT system.
- *Agency cost by users* (Figure 4.15(b)): This analysis makes sure a system economically sustainable. First, a Hm city reduces costs for all technologies in comparison to a Ht case. Second, the implementation of small subcenters (less than 25% of total trips) generates similar levels of costs in comparison to the homogeneous case. Even in HRTs, the subcenters structure improves the system better than the homogeneous case, reducing the cost by 0.5% concerning the most idealized case.

If multi-subcenters grow up due to the generation/attraction of trips, the cost reduces regarding a monocentric demand structure. Therefore, a decentralized city is more effective than policies that seek the concentration of equipment and services at specific points in a city.

Effects on urban structure and frequency

Each scenario of demand (Hm, Ht, Mn, and Ms) requires a specific structure of transit. Figure 4.16 shows the optimal solutions according to both the transit technologies and the urban scenarios.

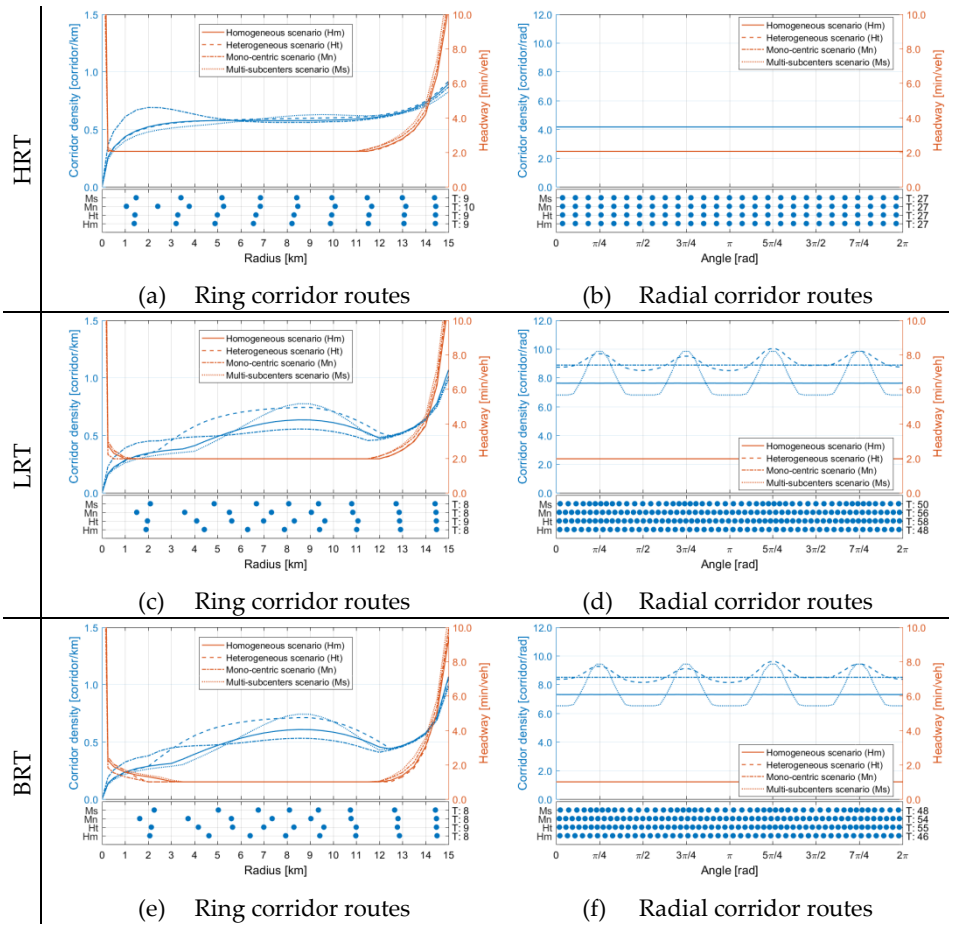

Figure 4.16. Optimal solutions for transit technologies according to urban scenarios.

Each exhibit in Figure 4.16 has two elements: the above exhibit contains the continuous optimal solutions, and the below exhibit contains discrete solutions: transit route locations. In the above exhibit, blue lines represent the optimal density of rings in [corridor/km] and radial routes in [corridor/rad]; orange lines represent the optimal headways along a transit corridor. In the bottom exhibit, blue points represent the discrete location of corridors using the discretization process (Section 3.4), including the corridor number next to the right axis.

- For HRTs, ring routes in Figure 4.16(a) for a homogeneous demand city (solid lines) has a homogeneous distribution of corridors at the intermediate zone (about 0.5 [corridor/km]). However, the density decreases to the city center tending to zero and increases towards the periphery (about 0.8 [corridor/km], almost double than the intermediate zone). The headway reaches the minimum headway (2.05 [min/veh]) and rapidly rises towards

the city center and the periphery. In an Mn scenario (dash-dot lines), the central area concentrates ring routes requiring one more ring and reducing the density to the city outer. Ms reaches as ring corridors as the Hm scenario for all technologies. For radial routes, Figure 4.16(b) shows a uniform distribution for all urban cases. The radial density reaches the minimum distance between routes (4.158 [corridor/rad]) and the minimum headway (2.052 [min/veh]) without saving infrastructure (all scenarios have the same number of radials).

- For LRTs, the saturation of the vehicle capacity causes an alteration of the ring density in the intermediate zone of the city (Figure 4.16(c)). The Mn case is the least affected scenario because it reduces the demand in this area, increasing the demand towards the city center: the Hm case has as rings as the Mn and Ms. However, the Ht case requires one more ring regarding other urban scenarios. In radial routes (Figure 4.16(d)), Hm and Mn have a uniform distribution of route densities. On the other hand, Ms has a better distribution of the demand and allows grouping the infrastructure offer making it more efficient.
- For BRTs, in Figure 4.16(e) and (f), the system has similar route densities for rings compared to the LRT system, but radials are less than the previous case. Moreover, the headways are smaller than the headways of LRTs.

Analysis of transit occupation and travel time

Figure 4.17 shows the location of transit corridors considering a multi-subcenters demand structure. The discretization algorithm presented in Section 3.4 (p. 67) gives the transit route location. Moreover, the transit network links contain the saturation level using a color ramp from 0 to 1. In saturation, the occupancy reaches the maximum capacity.

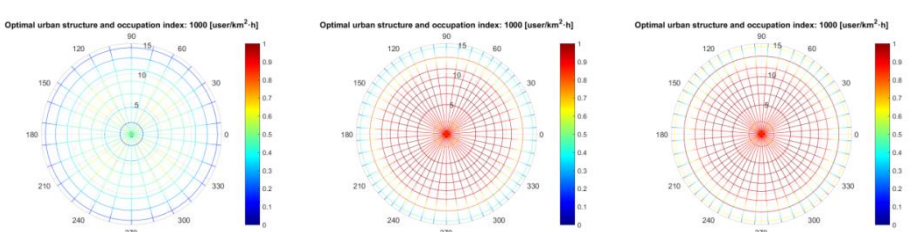

(a) HRT (b) LRT (c) BRT

Figure 4.17. Saturation levels of transit corridors for a multi-subcenters city case.

In Figure 4.18, the bars show the percentage of trips classified in time intervals. Each interval of the color ramp represents trips lasting 15 minutes.

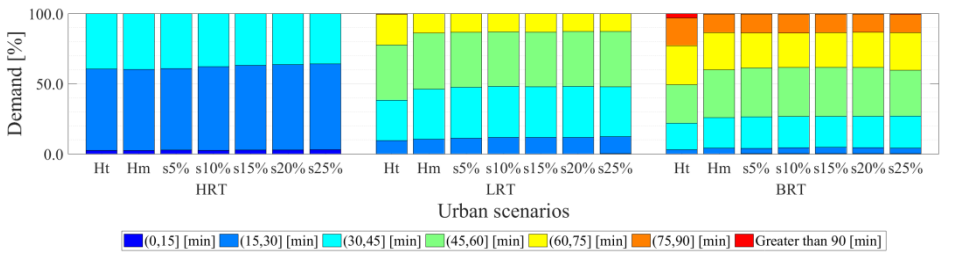

Figure 4.18. Costs among transit technologies in a city with 1,000 [user/km²·h].

The bars in Figure 4.18 compare the travel time among urban scenarios for three transit technologies: Ht, Hm, and the progressive increment of Ms from 5% to 25% of trips with respect to the total number of these.

- HRT is the only system with trips lasting less than 15 minutes, while the most extended trips last less than 45 minutes.
- LRT increases the travel time compared to HRTs in which longer trips take between 75 and 90 minutes for the Ht scenario, although the implementation of subcenters reduces them even more.
- BRT has the worst performance considering travel time because the maximum travel time exceeds 90 minutes. However, a homogeneous distribution also reduces the duration of trips. However, the implementation of subcenters improves travel times.

The improvements due to the implementation of subcenters are observable for all technologies, even in HRTs. However, this problem is most significant in a BRT system, considering the analyzed urban strategies do not eliminate times higher than 90 min.

4.2.4. Sensitivity analysis

One of the main parameters is the travel time value per average user (μ). For this reason, the section analyzes the effects of the value of time on the optimal solutions for rings and radial routes and the effects on the total cost of the systems considering the three analyzed technologies: HRT, LRT, and BRT.

The next two figures (Figure 4.19 and Figure 4.20) show how the variability of three different scenarios of values of time ($\mu \in \{1,5,10\}$ [$/user·h]) for optimal solutions of rings and radial routes of a homogeneous concentric city of 1,000 [user/km²·h], considering HRT, LRT, and BRT technologies.

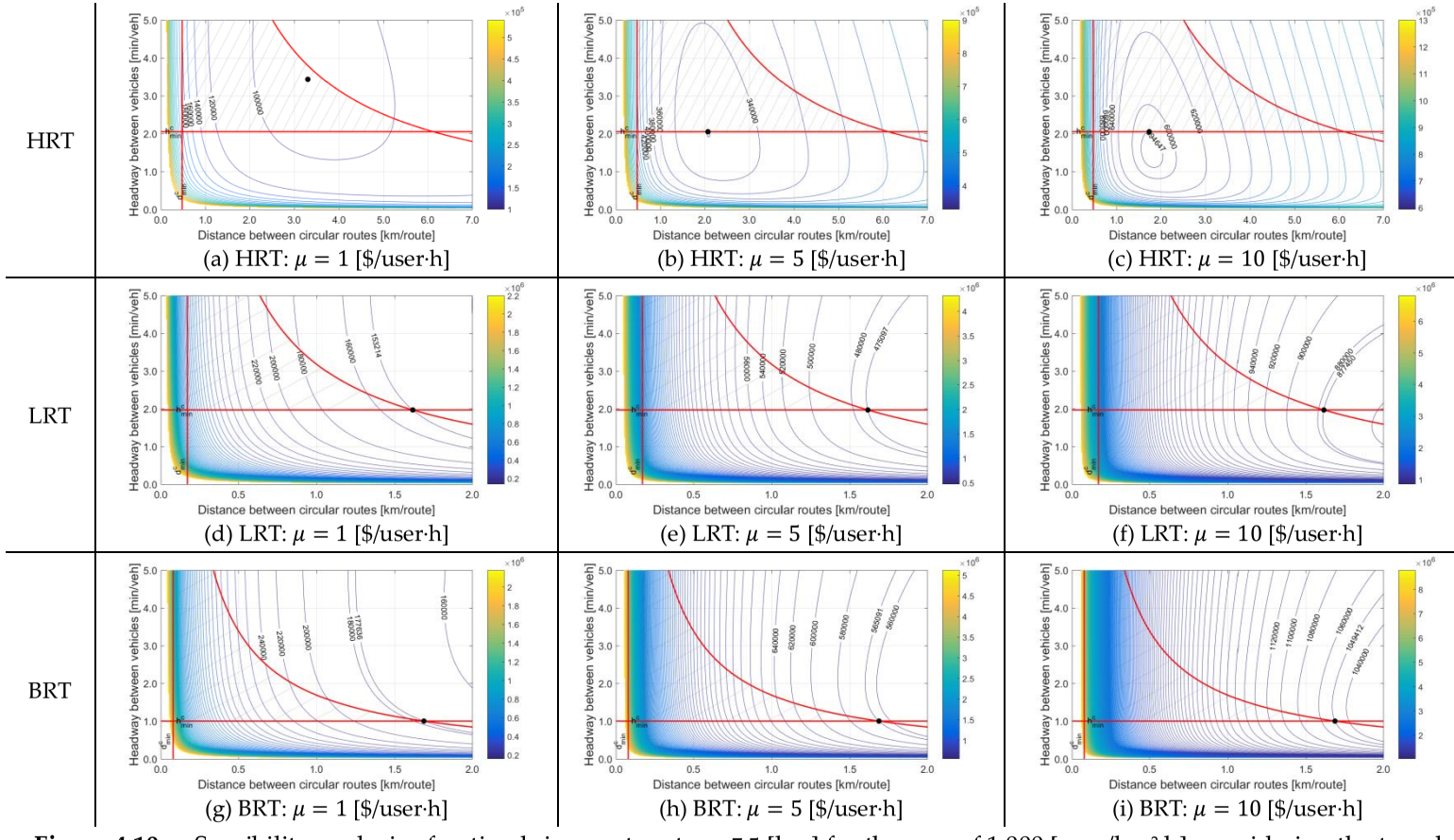

Figure 4.19. Sensibility analysis of optimal ring routes at $r = 7.5$ [km] for the case of 1,000 [user/km²·h], considering the travel time value and technologies.

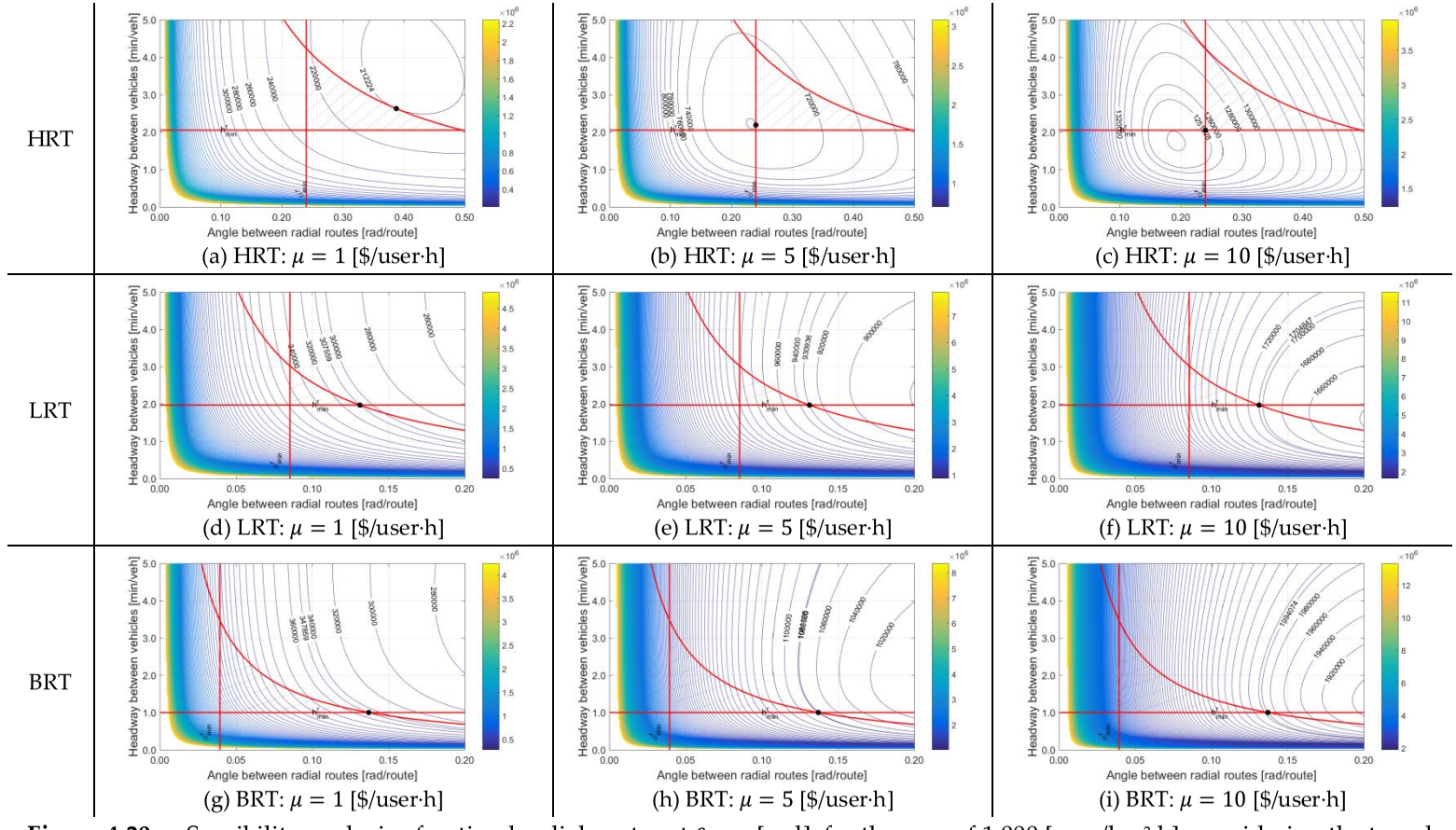

Figure 4.20. Sensibility analysis of optimal radial routes at $\theta = \pi$ [rad] for the case of 1,000 [user/km²·h], considering the travel time value and technologies.

Each x-axis of each inhibit of Figure 4.19 is the distance between rings, i.e., the spatial decision variable of the problem ($d^c(r = 7.5)$ in [km/route]), for the radius 7.5 [km] of the circular city. Similarly, each x-axis in Figure 4.20 is the angle between radial routes ($\Phi^r(\theta = \pi)$ in [rad/route]) at an angle of π [rad]). Each y-axis of inhibits is the headway between vehicles, i.e., the headway between vehicles ($h^c(r = 7.5)$ for rings and $h^r(\theta = \pi)$ for radial routes in [h/veh]). The red lines of those exhibits represent the constraints: the capacity constraint (Equation 3.8(b)-(c)), the minimum distance between stations (Equation 3.8(d)-(e)), and the minimum headway between vehicles (Equation 3.8(f)-(g)). The gray hatched area among the three red constraints defines the feasible region of solutions. Iso-lines in color gradient represent the total cost obtained from the objective function in which the black point is the optimal solution for a scenario that considers a specific technology and users' values of time in the concentric city.

For HRT systems, if the value of time takes low rates as in developing countries, subways cars will travel close to maximum capacity, as shown in Figure 4.19(a) and Figure 4.20(a). On the other hand, if the value of time increases to 5 or 10 [$/user·h] as in developed countries, the user's cost will make vehicles travel empties (lower demand) and frequencies increase as well (Figure 4.19(b)-(c) and Figure 4.20(b)-(c)). For LRT and BRT systems, users' costs increase with the optimal solution out the feasible region in the absence of constraints. In this case, two constraints are active (the minimum headway and capacity constraint), locating optimal solutions on the intersection of those constraints (Figure 4.19(d)-(i) and Figure 4.20(d)-(i)). By the way, the optimal results of a low travel time value are above the frequency constraint. The latter changes because the optimal solution approaches the minimum headway constraint if the travel time value increases.

4.2.5. Analysis

The proposed model for designing public transportation networks can adapt to non-homogeneously distributed demands, considering the local demand conditions over a city. The model is valid even in modeling scenarios where the generation/attraction rates are stable over the city because the density of trips is not homogeneous for the other three travel stages: waiting, in-vehicle trip, and transferring of users. For this reason, average demand values (i.e., a homogeneous distribution) will tend to underestimate real infrastructure needs where issues will increase when considering other demand distributions.

The feasibility of implementing a transit technology depends on the occupancy and operating constraints; therefore, the capacity of the technology is a critical parameter for the feasibility of a transit system. LRT and BRT systems have limited feasible spaces for radial corridors because their capacity is less than for an HRT. Moreover, some solutions for radial routes are not feasible for any of the three technologies analyzed in this dissertation instead of the ring routes that have an overlap of feasible areas.

The total costs obtained from the model show that LRT systems are only competitive for low levels of demand, and BRTs are competitive for high levels of demand if HRTs are not feasible. The results change considering the agency-by-user costs because HRTs are competitive for intermediate demand densities (between 1,000 and 2,000 [user/km^2]). On the other hand, an HRT system has a shorter average travel time if demand increases. LRTs and BRTs have become increasingly inefficient in these cases. Moreover, LRTs and BRTs rapidly saturate the capacity of vehicles if demand also increases, and infrastructure needs simultaneously increase in all cases.

In a homogeneous distribution, the distance between ring routes increases from the center to the periphery, although the transit frequency is less toward the periphery. Vehicle capacity constraints force the concentration of routes when travel density exceeds 500 [user/km^2]. The intermediate zone concentrates routes in terms of ring routes, while the radial route needs are in all zones. Therefore, these areas require a greater concentration of infrastructure or vehicles with greater capacity. Thus, the periphery requires an efficient system of feeder vehicles and radial transit systems.

The urban case with homogeneous demand is an idealized case. Urban cases with a monocentric or heterogeneous structure approach real structures but have higher total cost levels. The decentralized urban case that incorporates multi-subcenters reduces costs even equivalent to a homogeneous demand distribution. The effectiveness of subcenters depends on the size of these reducing costs and improvements in travel time. Regarding agency costs per user, if multi-subcenters increase their size, the cost reduction achieved the best levels for HRTs. However, the most significant percentage reductions give BRT and LRT systems. Thus, the multi-subcenters can even show better results than the idealized case in which the trips have a perfectly homogeneous distribution. Therefore, the generation of subcenters can become an attractive strategy for urban development.

4.3. Traffic network design

The modeling analyzes a circular city of 15 km of the radius (R), and its rush hour lasts 1.5 hours (T). The traffic network model assumes a trip has three stages: accessing to the nearest primary road, "regular" trip on a vehicle, and arriving at the trip destination, which includes the parking stage. The model can model different types of roads and vehicles as shown Medina and Robusté (2019b), analyzing two types of vehicles (connected and autonomous vehicles) and types of roads (freeways and arterial roads). However, this subchapter focuses on a specific case: conventional cars (manual vehicles) only traveling on freeways.

4.3.1. Demand density functions and parameters

The demand formulations come from density functions estimated for each stage of a private trip.

$$
\begin{aligned}
f^{F}_{c,v}(r,\theta) &= \int_{\theta-2}^{\theta+2}\int_{r}^{R} D(r,\theta,r_t,\theta_t)\, r_t\, dr_t\, d\theta_t \\
f^{F}_{r,v}(r,\theta) &= \int_{\theta-2}^{\theta+2}\int_{0}^{r} D(r,\theta,r_t,\theta_t)\, r_t\, dr_t\, d\theta_t + \int_{\theta+2}^{\theta-2+2\pi}\int_{0}^{R} D(r,\theta,r_t,\theta_t)\, r_t\, dr_t\, d\theta_t \\
f^{R}_{c,v}(r,\theta) &= \int_{\theta}^{\theta+2}\int_{r}^{R}\left\{\int_{\theta_t-2}^{\theta} D(r,\theta_f,r_t,\theta_t)\, r\, d\theta_f\right\} r_t\, dr_t\, d\theta_t + \int_{\theta}^{\theta+2}\left\{\int_{\theta_t-2}^{\theta}\int_{r}^{R} D(r_f,\theta_f,r,\theta_t)\, r_f\, dr_f\, d\theta_f\right\} r\, d\theta_t \\
&\quad + \int_{\theta-2}^{\theta}\int_{r}^{R}\left\{\int_{\theta}^{\theta_t+2} D(r,\theta_f,r_t,\theta_t)\, r\, d\theta_f\right\} r_t\, dr_t\, d\theta_t + \int_{\theta-2}^{\theta}\left\{\int_{\theta}^{\theta_t+2}\int_{r}^{R} D(r_f,\theta_f,r,\theta_t)\, r_f\, dr_f\, d\theta_f\right\} r\, d\theta_t \\
f^{R}_{r,v}(r,\theta) &= \int_{\theta-2}^{\theta+2}\int_{0}^{r}\left\{\int_{r}^{R} D(r_f,\theta,r_t,\theta_t)\, dr_f\right\} r_t\, dr_t\, d\theta_t + \int_{\theta+2}^{\theta-2+2\pi}\int_{0}^{R}\left\{\int_{r}^{R} D(r_f,\theta,r_t,\theta_t)\, dr_f\right\} r_t\, dr_t\, d\theta_t \\
&\quad + \int_{r}^{R}\left\{\int_{\theta-2}^{\theta+2}\int_{0}^{r} D(r_f,\theta_f,r_t,\theta)\, r_f\, dr_f\, d\theta_f\right\} dr_t + \int_{r}^{R}\left\{\int_{\theta+2}^{\theta-2+2\pi}\int_{0}^{R} D(r_f,\theta_f,r_t,\theta)\, r_f\, dr_f\, d\theta_f\right\} dr_t
\end{aligned}
\tag{4.2}
$$

$$
\begin{aligned}
f^{A}_{c,v}(r,\theta) &= \int_{\theta-2}^{\theta+2}\int_{r}^{R} D(r_f,\theta_f,r,\theta)\, r_f\, dr_f\, d\theta_f \\
f^{A}_{r,v}(r,\theta) &= \int_{\theta+2}^{\theta-2+2\pi}\int_{0}^{R} D(r_f,\theta_f,r,\theta)\, r_f\, dr_f\, d\theta_f + \int_{\theta-2}^{\theta+2}\int_{0}^{r} D(r_f,\theta_f,r,\theta)\, r_f\, dr_f\, d\theta_f
\end{aligned}
$$

Equation 4.2 contains demand density functions, whose explanation is in Appendix B. It is worth noting that the trip assignment assumes an incremental assignment in a continuous space. Section 3.3.2 (p. 58) explains the method.

Homogeneous demand function

Demand depends on both the width of road corridors and density functions. The demand density functions for a homogenous city generates and attracts the same density of trips in each point. However, the demand at each stage of a trip is not homogeneous over this city.

Figure 4.21 and Figure 4.22 show the density functions for a spatially homogeneous city of 1,000 [veh/km²·h] of generated trips obtained from Equations 4.2 (Appendix B). Firstly, Figure 4.21 shows demand density functions considering the all-or-nothing assignment method, which does not consider congestion. Secondly, Figure 4.22 presents the results of the incremental assignment method in which the assignment is progressive, considering increments in percentages: {50%, 25%, 15%, 5%, 3%, 2%}.

- In the first stage of a trip, the access density function in [veh/km²·h] for the all-or-nothing assignment method comes from the formulation presented in Equation 4.2. Figure 4.21(a) and (b) show the access demand densities for circular and radial roads in [veh/km²·h]. Figure 4.22(a) and (b) show the access demand densities for circular and radial roads in [veh/km²·h], considering the incremental assignment method.
- The second stage presents regular trip density surfaces in [veh/km·h] considering the width, in kilometers, of a traffic corridor at each city point (Equation 4.2). Figure 4.21(c) and (d) show the access demand densities for rings and radial roads in [veh/km·h] considering the all-or-nothing assignment. In this first case, the concentration of ring density is on the intermediate zone between the center and outer ring (Figure 4.21(c)), considering the intermediate ring has more likely to receive more trips in a scenario with homogeneous demand. Otherwise, radial trips increase in points close to the city center because it joins trips from the same city side and the opposite side (Figure 4.21(d)). Figure 4.22(c) and (d) show the access demand densities for circular and radial roads in [veh/km·h], considering the incremental assignment method. In this case, the intermediate ring density decreases, augmenting trips on ring roads at the periphery. On the other hand, for radial routes, trip density around the city center decreases regarding the first assignment method.
- In the third stage, the arriving density function (Equation 4.2) represents the user density, in [veh/km²·h], who arrive at the destination. The surface in Figure 4.21(c) and (d) show the arriving demand densities for rings and radial radials in [veh/km²·h] considering the all-or-nothing assignment. Figure 4.22(c) and (d) show the arriving demand densities for rings and radials in [veh/km²·h], considering the incremental assignment method.

Figure 4.21. Demand density surfaces of a homogeneous city (1,000 [user/km²·h]) obtained from the all-or-nothing assignment.

Figure 4.22. Demand density surfaces of a homogeneous city (1,000 [user/km²·h]), considering congestion.

Non-homogeneous demand function

The demand density functions come from the three scenarios presented in Section 4.1 (p. 72) in which the demand varies over the city as in the case of a transit system: heterogeneous, mono-centric, and multi-subcenters cities, considering a density rate of 1,000 [user/km^2·h] for a traffic network.

- *Heterogeneous city scenario*: In this case, the trip density of generation and attraction randomly varies at each point of the city. Figure 4.23 contains demand density functions for each stage of a trip in this urban case considering the all-or-nothing assignment method. After that, Figure 4.24 presents the demand density function obtained from the incremental assignment method. The demand densities also have a similar macro-structure compared to the previous case, although local conditions change at each point, modifying the regular structure of the homogeneous case (Figure 4.24(c) and (d)).
- *Mono-centric city scenario*: The central business district (CBD) of this scenario concentrates more trips than the rest of the city. Figure 4.25 shows demand density functions for each stage of a trip considering the all-or-nothing assignment method. On the other hand, Figure 4.26 presents the results of the assignment using the incremental method. The second case decreases the peak points. Notably, the incremental assignment reduces the maximum values of trips on radial routes around the city center because users choose shorter travel time trips.
- *Multi-subcenters city scenario*: The urban case has four subcenters in which trip densities around subcenters are more significant than the rest of the city points. Figure 4.27 shows demand density functions for each stage of a trip obtained from the all-or-nothing assignment method. Meanwhile, Figure 4.28 shows the demand density obtained from the incremental assignment method. The in-vehicle trip densities on circular services are in the intermediate zone. On the other hand, in-vehicle trip densities on radial services have a significant concentration on radial services where lie the subcenters, although the second assignment reduces the maximum values around subcenters.

Figure 4.23. Demand density surface of a heterogeneous city (1,000 [user/km²·hl) obtained from the all-or-nothing assignment.

Figure 4.24. Demand density surfaces of a heterogeneous city (1,000 [user/km²·hl), considering congestion.

Figure 4.25. Demand density surfaces of a mono-centric city (1,000 [user/km²·h]) obtained from the all-or-nothing assignment.

Figure 4.26. Demand density surfaces of a mono-centric city (1,000 [user/km²·h]), considering congestion.

Figure 4.27. Demand density surfaces of a multi-subcenters city (1,000 [user/km²·h]) obtained from the all-or-nothing assignment.

Figure 4.28. Demand density surfaces of a multi-subcenters city (1,000 [user/km²·h]), considering congestion.

Parameters

Table 4.6 shows the parameter list used by the model considering only mobility by cars on freeways. Firstly, the model considers that the travel time value will be equal for all users (Medina-Tapia & Robusté, 2018a, 2019b). For freeways, investigations show that freeways can reach the capacity of 2,099 [veh/lane·h], considering only manual vehicles (MVs). In the modeling, freeways have six lanes considering both directions (η^l).

Table 4.6. Traffic parameters to model a traffic system.

Parameter		Manual vehicles
T	[h]	1.5
η_u	[user/veh]	2.5
v_v^F	[km/h]	40
$v_{w,v}^{ff}$	[km/h]	80
v_v^p	[km/h]	10
v_v^A	[km/h]	40
v^a	[km/h]	3
d_p	[km]	0.2
$t_v^{F\prime}$	[h]	0.0125 (45 seg)
$t_v^{A\prime}$	[h]	0.0125 (45 seg)
a		0.15
b		3
k_v	[veh/lane·h]	2,099
η^l	[lane]	3
τ_v^i	[h/veh]	0
λ_P	[parking/km]	5

The model assumes some unitary costs presented in Table 4.7. The mileage in cars is 10 [km/L], the fuel price is 1 [$/L], and the parking fee is $\varphi^f = 1$ [$/h·veh]. Moreover, the basis of fixed unit cost values comes from the paved cost per linear meter built, and the lifetime of the road project divides it. Technical reports of Arkansas's Department of Transportation (2014) allow calculating costs per kilometer. The model considers that the variable unitary cost is 1% of fixed cost ($\varphi^{p(v)} = 0.01 \cdot \varphi^{p(f)}$ [$/km·h]).

Table 4.7. Unitary costs to model a traffic system.

Parameter		Manual vehicles
μ_v	[$/h]	10
φ_v^t	[$/km·veh]	0.1
φ_v^f	[$/h·veh]	1
$\varphi_v^{p(f)}$	[$/km]	$10.85 \cdot 10^6$
$\varphi_v^{p(v)}$	[$/km·h]	$\varphi_v^{p(f)} \cdot 1\%$

4.3.2. Spatially homogeneous demand case

Feasible and optimal solutions

Figure 4.29 shows the circular and radial optimal traffic structures regarding four demand scenarios: 100, 250, 500, and 1,000 [user/km²·h].

In Figure 4.29, black lines represent the optimal continuous density, considering rings in [corridor/km] and radial roads in [corridor/rad]. On those lines, black circles are discrete solutions obtained from the discretization method (Sub-chapter 3.4, p. 67). Red and blue lines represent the problem's two constraints (Equation 3.16, p. 62). The red lines show the minimal density curve in which the solution satisfies the saturation constraints (Equation 3.16(b) and (c)). Finally, the blue lines show the maximum density in which the solution reached the minimum separation of roads (Equation 3.16(d) and (e)).

In the exhibits in Figure 4.29, the maximum density for rings is 2.0 [corridor/km], i.e., the minimum distance between roads is 0.5 [km/corridor]. The minimum density increases if the demand density also increases, restricting the feasible space of solutions. Thus, optimal densities of circular roads does not reach the saturation constraints.

Regarding radial roads, the maximum density is at 4.0 [corridor/rad], i.e., 0.5 [km] from 2.0 km of radius to the city outer. On the other hand, the minimum density increases if the demand increases as well, i.e., the saturation constraint also rises to reduce the feasible solutions space in which the maximum saturation that defines the minimum road density is always active. The capacity constraint (minimum density) is active from 1,000 [user/km²·h] to 2,000 [user/km²·h]. After that, the problem has not a solution if urban demand density is higher than 2,000 [user/km²·h] in a homogeneous city case.

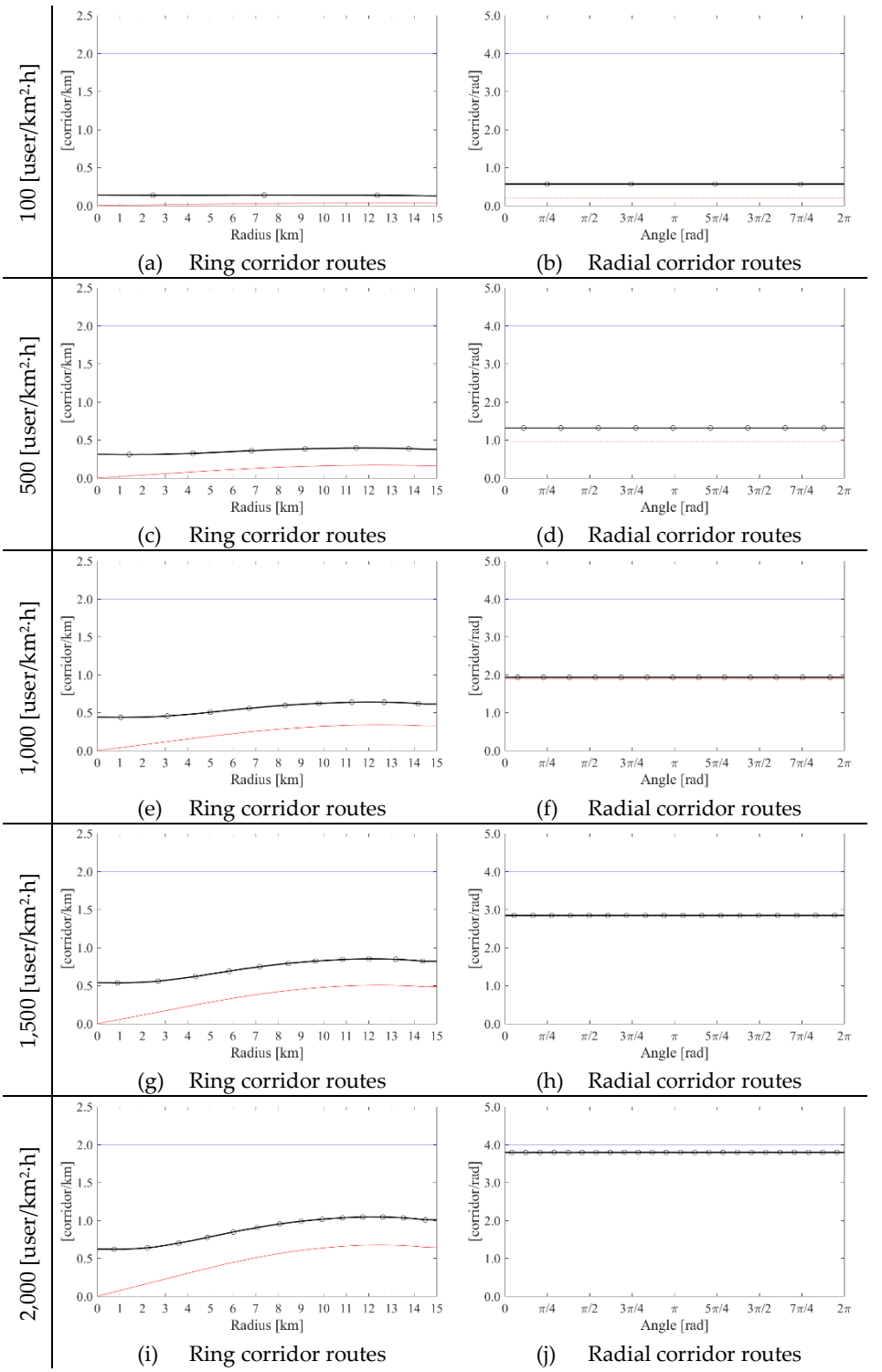

Figure 4.29. Optimal traffic structures regarding demand scenarios.

Effects of traffic on infrastructure

The exhibits of Figure 4.30 analyze the system costs considering progressive homogeneous demand scenarios.

- Figure 4.30(a) shows the total, user, and agency costs regarding progressive demand levels.
- Figure 4.30(b) represents the average cost by a user reaching the minimum values around 500 [user/km²·h].
- Figure 4.30(c) represents the agency cost divided by users allowing the comparison to other transportation modes. The minimum value is around 0.13 [$/user].

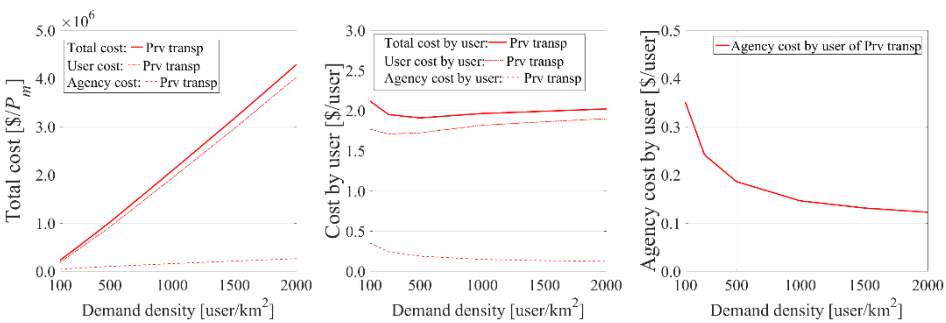

(a) Total cost (b) Total cost by user (c) Agency cost by user

Figure 4.30. Traffic system cost considering progressive homogeneous demand scenarios.

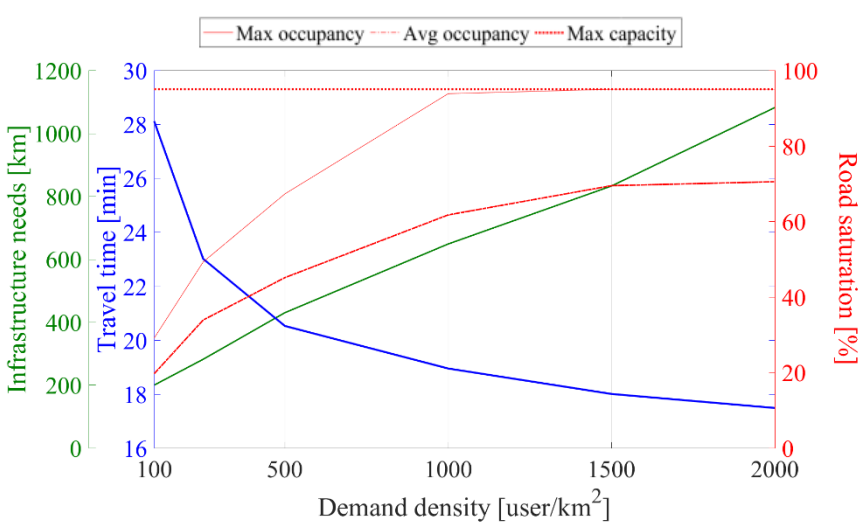

Figure 4.31. Traffic saturation and travel time according to progressive homogeneous demand scenarios.

Figure 4.31 shows demand effects on traffic and infrastructure, considering progressive demand levels. It is worth noting that each label color on the y-axis represents the line colors.

- Intuitively, the traffic saturation increases if demand densities also increase, reaching the maximum capacity at some city point when the density is higher than 1,000 [user/km²·h].
- The travel time decreases whether the demand increases due to the infrastructure increases as well.

4.3.3. Non-homogeneous demand case

The section also analyzes the same four scenarios of demand distribution presented in Section 4.1 (i.e., Hm, Ht, Mn, and Ms), in which the average generation rate is 1,000 [user/km²·h]. Figure 4.32 presents a comparison of the total cost for each urban scenario obtaining the following results:

- The decentralized cities (Hm, Ht, and Ms) are the best alternatives. It is worth noting that a Ht city presents multiple sub-centers or is entirely decentralized. The worst alternative is an Mn city.
- These results come from the reduction of the road saturation because trips in cars are flexible. The obtained outcomes are in opposition of transit results.
- An Ms city presents a cost reduction of 2.6% with respect to a Mn city. The critical factor is the saturation restriction, which allows infrastructure savings, although access costs increase at the origin and destination.

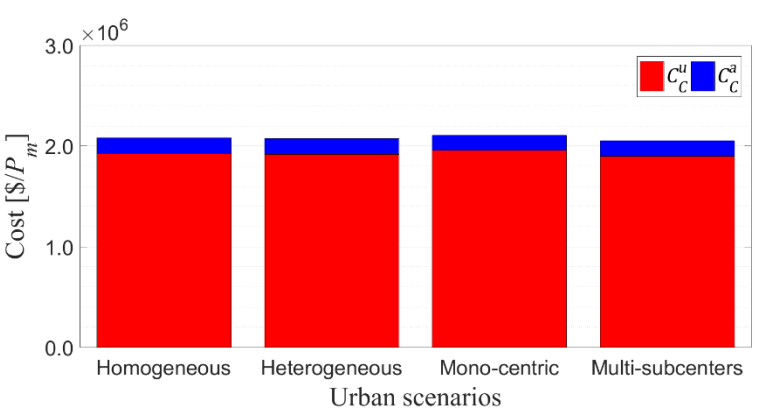

Figure 4.32. Costs of a traffic network considering four urban scenarios of a city with 1,000 [user/km²·h].

Figure 4.33 compares the four urban scenarios presented in Section 4.1 (Ht, Hm, Mn, and Ms) considering the size of CBD and subcenters, respectively. Both above progressively increase their demand from 5% (1.05x) to 25% (1.25x) regarding the number of trips.

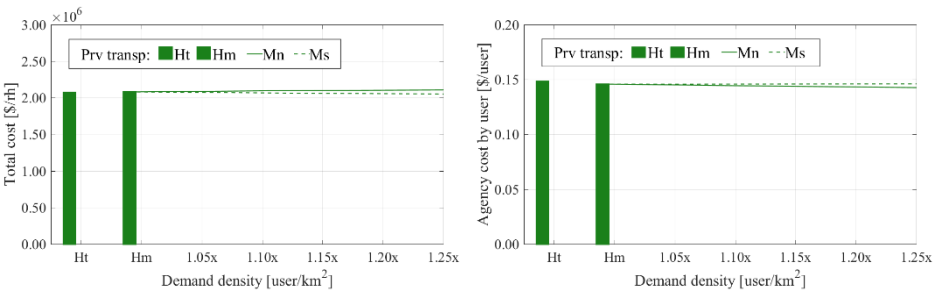

(a) Total cost (b) Agency cost by user

Figure 4.33. Traffic costs according to urban scenarios.

The previous plots show the following:

- *Total cost* (Figure 4.33(a)): Multi-subcenters slightly benefit to the system when subcenters size increases.
- *Agency cost by users* (Figure 4.33(b)): This plot shows Mn and Ms infrastructure are slightly cheaper than at Hm and Ht scenarios.

Effects on urban structure

The model proposes a specific road structure regarding the proposed scenarios of demand: Hm, Ht, Mn, and Ms. Figure 4.34 presents two components: the above exhibit shows the continuous optimal solutions, and the below exhibit shows the discrete road locations. In the above exhibit, blue lines represent the optimal density of ring roads in [corridor/km] and radial roads in [corridor/rad]. In the bottom exhibit, blue points represent road discrete locations obtained from the discretization process and explained in Section 3.4, including the total road number for each urban scenario next to the right axis.

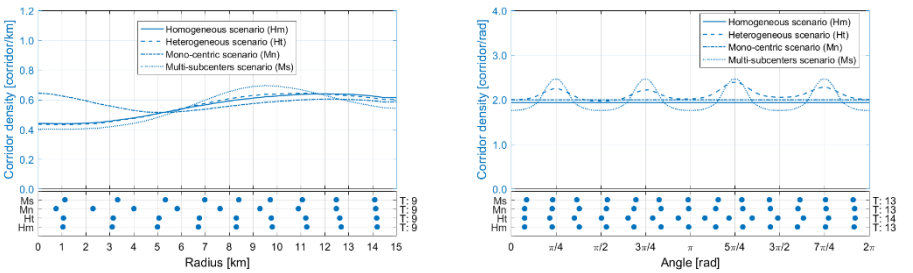

(a) Ring corridor routes (b) Radial corridor routes

Figure 4.34. Optimal solutions for a traffic network according to urban scenarios.

The previous exhibits show the following:

- For ring routes, Figure 4.34(a) shows all scenarios require the same number of main roads. However, the continuous densities have differences, increasing to the city outer for Hm, Ht, and Ms. A Mn city concentrates the density around the city center and decreases to the periphery. The Ms city increases the density at the intermediate zone of the city, considering the Ms city has the lowest density at the periphery.
- For radial routes, Figure 4.34(b) shows a uniform distribution for two urban cases: Hm and Mn. The Ht city requires more roads because the traffic flow for an Ht city adapts better than the Ms city.

Analysis of traffic saturation and travel time

Figure 4.35 presents the proposed locations of roads considering the four urban scenarios using the location presented in Section 3.4 (p. 67). The links show the saturation level using a color ramp between 0 and 1, in which the latter represents the maximum saturation.

Figure 4.36 shows the percentage of trips classified in time intervals. Each interval of the color ramp represents trips classified every 15 minutes. The bars compare the travel time among urban scenarios: Ht, Hm, and the progressive increment of Ms from 5% to 25% of trips regarding the total number of those. All cases in Figure 4.36 have a similar percentage of trips that last less than 15 minutes. However, Ht has a higher percentage of trips that last less than 30 minutes.

The implementation of subcenters is not attractive enough for private transportation because heterogeneous cities also show remarkable results.

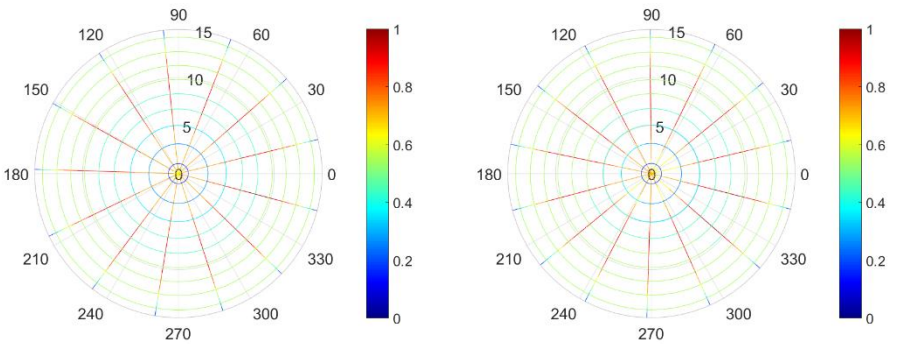

(a) Homogeneous scenario (b) Heterogeneous scenario

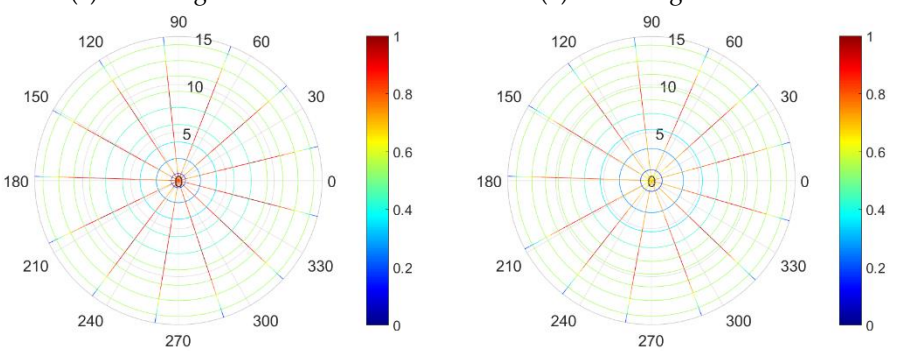

(c) Mono-centric scenario (d) Multi-subcenters scenario

Figure 4.35. Saturation levels of a traffic network according to urban scenarios.

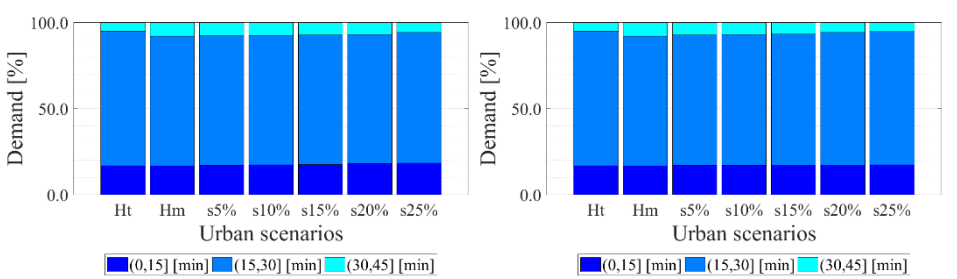

(a) Mono-centric scenario (b) Multi-subcenters scenario

Figure 4.36. Costs of a traffic network considering urban scenarios of a city with 1,000 [user/km²·h].

4.3.4. Sensitivity analysis

The analysis focuses on the value of time (μ) because it is one of the main parameters, analyzing the effects of the time value on optimal solutions for rings and radial roads.

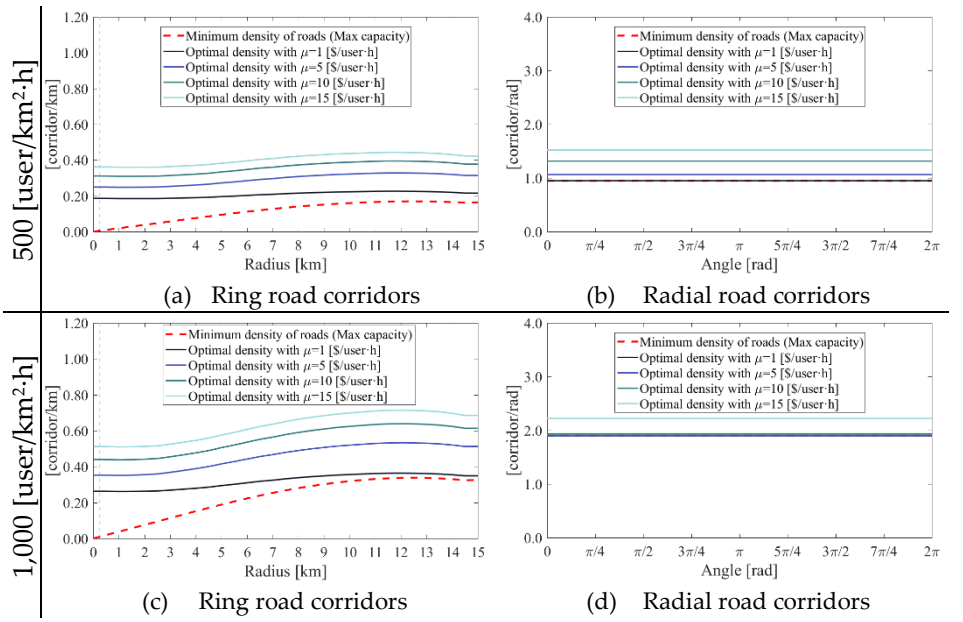

(a) Ring road corridors (b) Radial road corridors

(c) Ring road corridors (d) Radial road corridors

Figure 4.37. Sensibility analysis of optimal road densities.

Each exhibit in Figure 4.37 shows changes in the optimal road density for rings and radials, considering two homogeneous density scenarios (Hm): 500 and 1,000 [user/km²·h]. Moreover, dashed lines in red represent the minimum density of roads obtained from the maximum capacity constraints.

- For ring roads, road densities increase if the value of time (μ) increases as well. The increment increases even more to the outer city than around the city center.
- For radial roads, there are two cases. In the former, if the density is 500 [user/km²·h] and $\mu = 1$ [$/user·h], the density reaches the minimum density. In the latter, the demand density is higher and reaches the minimum density for $\mu = 1$, 5, and 10 [$/user·h].

4.3.5. Analysis

In a homogeneous demand distribution, radial roads firstly reach a road saturation level from 1,000 [user/km²·h]. However, the situation has no solution after 2,000 [user/km²·h] for any scenario.

Considering total costs, cities of 500 [user/km²·h] show optimal costs than cities of higher densities. If the demand increases, roads firstly reach saturation, increasing user costs as well. However, higher densities make profitable infrastructure costs.

As demand increases, infrastructure needs increase linearly. However, travel times decrease more slowly.

In a heterogeneous demand distribution, the model provides similar results for the analyzed four scenarios, but the best results are in decentralized cities. The Ht city needs more roads due to traffic flow adapts better than a Ms city. Thus, the cost of the system is lower in this case, but the cost of the agency is somewhat higher.

The cities Ht and Ms have slightly shorter times than Mn.

Considering variations in the travel time value, cities with a higher value, such as cities in developed countries, require a higher density of roads. On the other hand, cities with lower time values, such as Santiago of Chile, find a lower optimal road density. However, the problem is that the network quickly saturates from 500 [user/km^2·h] subject to the road capacity, making the system lose efficiency.

4.4. Summary

Regarding the transit network design, the outcomes from the modeling give the following conclusions.

- The feasibility of transit technologies depends on occupancy and operating constraints. LRT and BRT systems have a reduced feasible space due to the capacity is less than for HRTs.
- Regarding total costs, HRTs offer the best solution considering user and agency costs simultaneously. Regarding agency costs, BRTs are competitive at low levels of demand. If the demand increases, an HRT is the best technology, although the density must not exceed 2,000 [user/km^2]).
- Regarding operation results, HRTs have a shorter average travel time for high levels of demand. LRT and BRT systems are inefficient in these cases. Moreover, the latter systems saturate the capacity of vehicles when the demand also increases.
- The distance between ring routes for HRTs increases from the center to the periphery for a homogeneous distribution. However, the frequency also decreases toward the periphery.
- The intermediate zone also concentrates transit routes for ring routes of LRT and BRT systems. Therefore, these areas require a greater concentration of infrastructure or vehicles with higher capacity. Thus, the periphery requires an efficient system of feeder vehicles and radial transit systems.

Regarding traffic roads, the model allows giving the following conclusions.

- The feasibility of traffic networks is highly dependent on road saturation. Hence, if demand increases, the road capacity constraint will be active. Consequently, if demand increases even more, the model does not find a solution.
- Regarding total costs, the traffic network reaches reduced costs while the system does not have road saturation.
- Regarding operation results, distributed cities have slightly shorter times than concentrated cities as a mono-centric city.
- In a homogeneous distribution, the density between ring roads increases from the center to the periphery.
- Regarding four analyzed urban scenarios, rings concentrate their density to the periphery for decentralized cities. The unique exception is the monocentric city that concentrates the density in the city center. The radial roads tend to balance the number of roads. However, the heterogeneous city requires more infrastructure than the other urban models.

The global analysis, including public and private transportation analysis, gives the following assertions.

- The generation of a network design model that adapts their results to local conditions is valuable even in scenarios with generation/attraction rates are stable over the city. Thus, modeling average demand values—a homogeneous distribution—will tend to underestimate real infrastructure needs.
- The urban case with homogeneous demand is an idealized case. Urban cases with a mono-centric or heterogeneous structure approach real structures, showing total cost levels are higher.
- The implementation of decentralized urban structures provides significant results. Multi-subcenters reduce the level of costs being equivalent to a homogeneous demand distribution. The effectiveness of subcenters depends on the size of these reducing costs and improvements in travel time. Therefore, the generation of subcenters could be an attractive strategy for urban development.

5. Theoretical applications of some policies

In the 60s, the increment in demand for cars caused agencies proposed to build more roads to reduce congestion. Some years later, the demand increment continued, so the previous measure was ineffective. Therefore, experts began to propose measures to improve the management of the existing transportation infrastructure. However, the modification of infrastructure is not enough; in many cases, it is also necessary to modify the behavior of the users of a transportation system. Thus, the measures of experts pointed to measures of transportation demand management in the 80s. If the management measures are not enough, planning techniques are required, which are large-scale, expensive capital improvements.

The chapter has four parts. The first subchapter contains a discussion of policies considering different scales of time. The second and third subchapters analyze measures for public and private transportation. Finally, the last subchapter presents a statement of main points.

5.1. Discussion of policies

In a transportation system, policies want to increase safety, efficiency, and capacity integrating two types of measures: management and planning. The former includes measures in the system and demand without resorting to large-scale, expensive capital improvements. The latter connects urban planning and transportation in which the measures for solving those issues are in spatial planning instruments.

The tools of management are of two types: transportation systems management (TSM) and transportation demand management (TDM). Users are obliged to obey the TSM measures proposed by the agency, while TDM strategies seek to change user behavior, and users can choose to follow a measure.

TSM is a strategy aimed at improving the overall performance of an existing transportation system considering techniques from other disciplines. The measures include actions on the construction, operation, and institutional aspects of that transportation system. Some of the traditional types of TSM are the following.

- *Intelligent transportation system (ITS)*: Proposal solutions improve both the operation of traffic (e.g., lanes, speed, and others) and the safety of a transportation system.
- *Management in right movements*: The coordination of pickups and delivery of freight optimizes a transportation system.
- *Incident management*: Implementation of strategies for the removal of damaged vehicles from the road network.
- *Geometric network design*: An optimized urban design promotes the reduction of congestion and improvement of safety.
- *Improvements in signaling*: This considers the optimization of signals to improve the traffic flow on the road.
- *Intersection improvements*: The design of signals at intersections allows improving the flow and safety of pedestrians and drivers.

TDM is another strategy for modifying the travel behavior of users. Incentives or disincentives could allow reaching better levels of mobility, reducing the number of vehicles on roads. TDM measures prevent the costly expansion of a transportation system. Some of the classic types of TSM are the following. Some examples of TDM are the following.

- *Transport mode options*: This strategy strengthens areas with low public transportation coverage. For example, BRT systems, bicycling /walking (non-motorized travel), shuttle services, teleworking, intermodality, car-sharing, and car-pooling.
- *Incentives for alternative modes*: Agencies promote financial incentives for changes in the behavior of users. For example, integrated fare system, fuel taxes, flexible work schedules, variable price strategies (value pricing), and lane assignment (bus and bike lanes)
- *Parking management and land-use*: This policy encourages private transportation and improves the connection with other modes. For example, access restrictions, land use management, development of mixed uses areas, parking pricing, park-and-ride, and shared parking.
- *Governance (institutional policy)*: Agencies can define laws to reduce trips through land-use planning.

Both types of strategies aim to reduce congestion and maximize the efficiency of the existing infrastructure without investing in new infrastructure. In many situations, TDM and TSM work alongside urban planning instruments. In other cases, the strategies do not work because cities require infrastructure implementation. The above process is a triangulation among the types of management and urban planning (Figure 5.1).

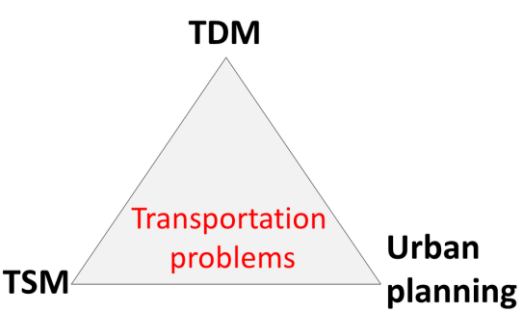

Figure 5.1. A proposal scheme to represent types of solutions for transportation.

The current chapter analyzes the implementation of two policies: subcenters and self-driving. The implementation of subcenters is mainly associated with measures established in spatial planning instruments (SPI). The above is partially correct, though operational aspects of the system also influence

through TSM measures. In parallel, TDM measures influence the behavior change in users to change the trip matrix. One of the future TSM measures is the implementation of autonomous vehicles in cities (self-driving). Undoubtedly, this measure will generate changes in the travel behavior of users. Moreover, our cities must adapt to this paradigm shift in mobility and transformation (Azolin, Rodrigues da Silva, & Pinto, 2020). The next two subchapters analyze those two policies and the effects on the urban structure.

5.2. A policy applied to public transportation: Urban subcenters

Modern cities inherit a foundational urban structure, which presents a central area that concentrates activities. This urban structure is observable around the world but especially in developing countries. The City council must face impacts of this type of urban structure such as congestion, transit issues, and others, which is worse in large and disperse cities.

The objective of subcenters aims to bring economic activities to peripheral inhabitants in cities. The implementation of urban subcenters is one of the most attractive urban planning tools. Unfortunately, few analyzes of the impact of subcenters on urban mobility exist in the previous literature. Medina-Tapia and Robusté (2019a) evaluate "the contribution to the mobility of implementing urban subcenters in a city." This paper bases the model on a total cost function on a circular city: ring and radial routes of a BRT system.

The objective function contains users and agency costs using the continuous approximation method. The problem is complex and holistic because it includes location, urban planning, and urban mobility. Moreover, there must be adequate investment in transport infrastructure, among other factors.

This subchapter has a basis on two scientific congresses (Medina-Tapia & Robusté, 2019a), a paper (Medina-Tapia et al., 2020), and a scientific conference (Medina-Tapia & Robusté, 2019c). Appendix F contains the details of this subchapter: overview, modeling, results, and conclusions.

5.2.1. Literature review

The literature presents a few contributions to this problem. Some first works were of German geographers between the late nineteenth and early twentieth

century, e.g., Lösch, Christaller, and von Thünen. More recently, McDonald (1987) proposed a methodology based on the detection of points of employment density in contiguous zones, which was subsequently replicated by McDonald and McMillen (1990).

For the identification of subcenters, some papers have used statistical-based methods using parametric and non-parametric procedures. McDonald and Prather (1994) base their work on differences between the real and estimated density under a negative exponential function. McMillen and McDonald (1998) developed one of the methodologies based on non-parametric methods. In this research, the authors perform a non-parametric estimation of the distribution of employment density with a locally or geographically weighted regression (the acronym in English is LWR or GWR). In this method, explanatory variables use Euclidean distances for the prediction of employment density from spatial units to the CBD. More recently, Sánchez et al. (2013) developed a subcenter identification model based on the work of McDonald (1987). This type of urban subcenter detection model uses Euclidean distances but does not consider travel times in a congestion scenario, multiple travel periods, multi-modes, and other essential elements of urban mobility. Nor are mechanisms to encourage the population to modify their travel patterns to use subcenters, e.g., determining the infrastructure endowment.

Regarding network design, Rodrigue et al. (2017) identified three essential structures: distributed, centralized, and decentralized networks. The first case has no subcenters. The second case has a highly demanded CBD. The third case also has a CBD, but the city also contains subcenters. Ouyang et al. (2014) design bus networks for an urban grid system considering non-homogeneous demand. Unfortunately, these demand functions are identical for generated and attracted trips; therefore, this does not allow us to analyze the behavior of subcenters and their impacts.

5.2.2. Implemented methodology

The model considers a concentric city, which has a transit with two types of services: ring and radial routes. The demand continuously varies over the city, i.e., non-homogeneous demand distribution. This assumption is the strength of the model and allows designing adapted transit networks to local conditions in a territory.

Mathematical formulation

The objective function contains two components—a user and agency cost—including three sets of constraints: vehicle capacity, the minimum distance between stations, and minimum time headway. It is worth mentioning that the two decision variables—d^c and Φ^r—varies at each point of the city. The condition allows for designing more flexible transit networks.

Regarding the solution of the mathematical problem, the model solution addresses mathematical optimization (Karush-Kuhn-Tucker conditions). The model evaluates a BRT network applied to scenarios of urban subcenters.

Application to case studies

The model evaluates eleven progressive scenarios of concentric cities. The city has a 15 [km] radius and a generation rate of 500 [user/km^2·h]. Figure 5.2—rows (i) and (ii)—represents a sequence of four cases from a city without subcenters to a city with a subcenter 1.25 times the CBD:

(A) A mono-centric city without subcenters in which the CBD is mainly a trip-attraction zone, i.e., the CBD attracts trip but generates few trips,
(B) A city that has a CBD and a subcenter locates in the southeast of the city. The CBD has mixed land use in which it generates and attracts trips, which is about 60% of the CBD (0.625xCBD),
(C) A city includes a CBD and a subcenter in which the subcenter is as high as the CBD (1.0xCBD), and
(D) A city includes a CBD and a subcenter in which the subcenter is 25% higher than the CBD (1.25xCBD).

Moreover, Figure 5.2—rows (iii) for ring routes and (iv) for radial routes—shows the continuous density functions of transit routes. For ring routes, the constraints are not active, but the optimal density is higher around 3 km from the center. For radial roads, the buses do not travel full during the first kilometers of a radial corridor. For progressive scenarios, the effect of one subcenter gradually increases. In the optimum, the headway reaches the minimum value.

The result of discretization (Figure 5.2, row (v)) shows the increase of new routes around subcenters, but those decreases in other urban areas. The solution is complicated because the cost savings of infrastructure might imply increasing in access cost.

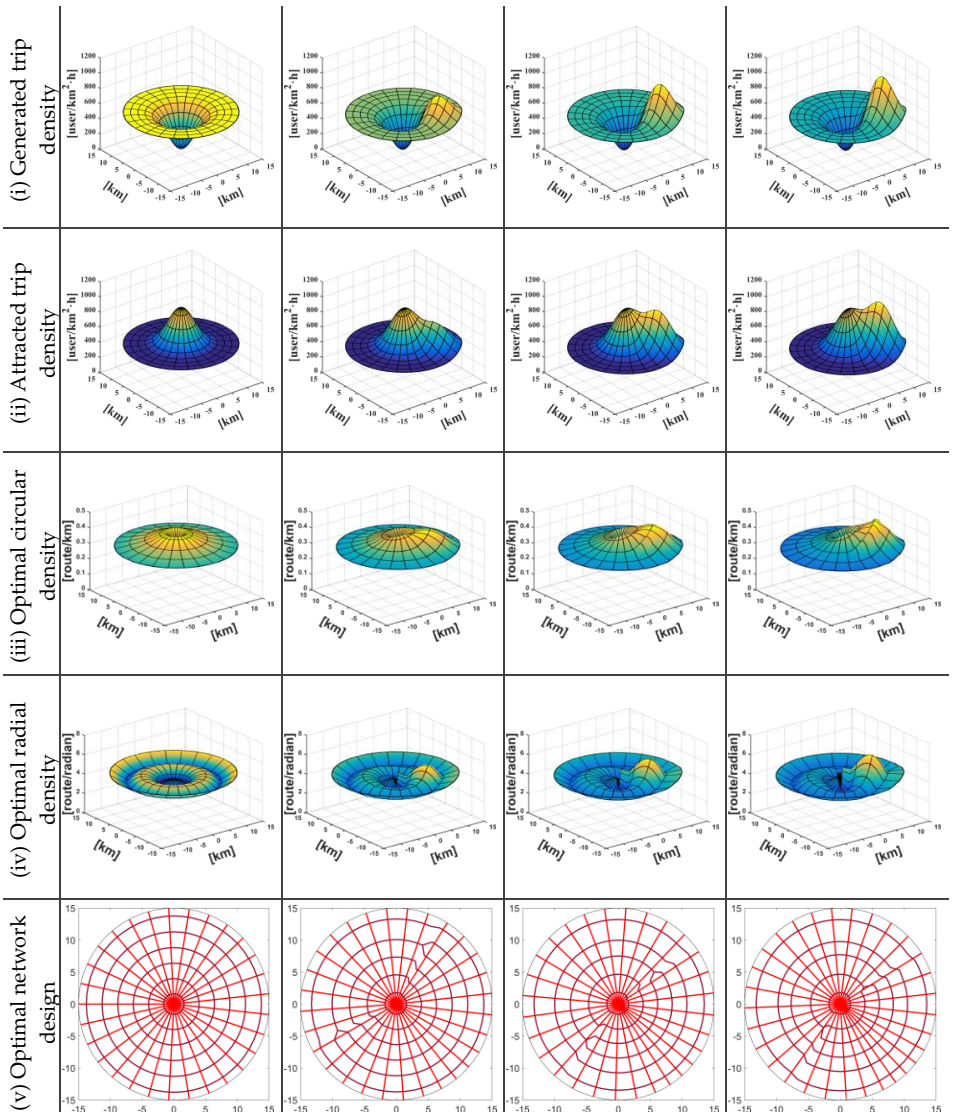

Figure 5.2. Urban scenarios and optimal transit networks, considering a subcenter policy.

5.2.3. Analysis of results

Regarding mobility patterns, many users take radial corridors from the periphery to the central zone, although full buses do not circulate on the first third of routes. The users mainly use ring routes to arrive closer to their destinations.

The subcenter policy gives savings in all scenarios: user mainly. For users, medium-size subcenters show the maximum savings, i.e., the access and travel time savings influence high savings. For the agency, savings are more significant when infrastructure includes subcenters, i.e., some transit routes share infrastructure in areas with low demand. Results presented in Figure F.3 (p. 252) show that scenario B obtains the most savings regarding the base scenario.

The modeling results show that the implementation of subcenters presents savings of 3.5% in rush hour, generating improvements in the functioning of a public transportation system. For total rush hours in a year, this policy might generate a saving of about $40MM. Although, the outcomes may be better with an urban pattern with subcenters and a transit scheme adapted to the demand needs.

5.3. A policy applied to private transportation: Autonomous cars

Urban mobility evolves slowly in which new technologies could progressively change the way users travel in a future city, although some scholars anticipate a paradigm change in urban mobility. In this line, cars will become autonomous, communicate with other vehicles and urban infrastructure, and cooperate among them.

Agencies will have an essential role in the implementation of those new technologies. Some scholars are optimistic and estimate autonomous cars will quickly insert into the market; other experts are not optimistic. Most probably, both types of vehicles will coexist in cities: manual (MVs) and autonomous vehicles (AVs), considering different levels of automatization (NHTSA, 2016).

The decision of agencies on the implementation of this policy will depend on the benefits of AVs. For this reason, the objective of this work is to assess the macroscopic effects of the implementation of AVs.

This subchapter has a basis on two scientific congresses (Medina-Tapia & Robusté, 2018a, 2018c) and two scientific conferences (Medina-Tapia & Robusté, 2018b, 2019b). Appendix G and Appendix H contain the basis of this work modeled for a circular city. Appendix G contains a preliminary view of the impacts that this paradigm shift could generate in urban mobility. Appendix H assess the neutral effects due to the implementation of AVs

The literature review presents a conceptual revision of AV implementation effects. The methodology subchapter presents the mathematical model based on the continuous approximation method (CA) to assess AVs' impact with total automatization. Finally, the next subchapter presents the analysis of modeling outputs and principal conclusions.

5.3.1. Literature review

AV (and connected car) implementation in urban areas will generate positive changes in transportation and mobility (e.g., Childress, Nichols, Charlton, & Coe, 2015; Kohli & Willumsen, 2016), but it also will produce non-desirable effects. Those effects have a broad discussion in the literature (Medina-Tapia & Robusté, 2018a, 2018b, 2018c, 2019b; Zakharenko, 2016). Bahamonde-Birke et al. (2018) gather the AV impacts on the effects of the first and second-order.

Direct effects

AV direct effects (or first-order effects) directly affect a transportation system. Five classes group these impacts:

1. *Reduction of generalized travel costs and energy*: This is one of the primary direct effects due to efficient driving, saving fuel costs, and travel time in all kinds of vehicles (cars, taxis, and public transport). In the case of cars, driving more efficiently could reduce the use of energy by 20 percent (Wadud, MacKenzie, & Leiby, 2016). Parking costs could also decrease due to AVs do the cruising for a parking space and parking maneuver in which both transport stages only begin when the user gets out of the car. In a Smart City, once the user has got out of an AV, the car will already have located a free parking spot (on-street or off-street). AVs will straight travel to the parking without passengers at top speed because the parking management of the Smart City will send this information to AVs (vehicle-to-Infrastructure communication, V2I).
2. *Efficiency increment and flexibility of modes*: In the case of taxis and public transportation, an autopilot permits efficiency in driving and flexibility in operations, but this could lead to a social problem due to a threat of unemployment. In the case of private AVs, the cost reduction due to the absence of a driver is not relevant as it is the same person as the primary user of a vehicle.
3. *Road capacity increment*: Scholars show different road capacity increments from 7% to 273% (Appendix H, p. 271). Their models consider the distance between cars, lane width, reduction of traffic interruptions due to braking,

change lanes, hesitation driving, and other factors (e.g., Kockelman, 2017). On the other hand, "*intersections are the bottlenecks of the urban road system*" (Lioris, Pedarsani, Tascikaraoglu, & Varaiya, 2017). This paper claims the capacity of an intersection could double or triplicate if vehicles cross it in platoons using adaptive cruise control (ACC). Even more, the headway will be shorter if cars include connected vehicle technology (CVT), such as the CACC system. In this line, Wadud et al. (2016) claim that platoons could create savings between 4 to 25 percent. Moreover, this could improve considering a smart city that will connect AVs and its infrastructure (V2I), optimizing crossroads.

4. *Pollution reduction*: Complementing the above mentioned, a significant efficiency in driving, in cooperation with other factors as the fleet renewal with electric vehicles, reduces pollutant emissions from cars, especially during rush hours. On the contrary, other experts predict an increment of this negative externality (Bahamonde-Birke et al., 2018; B. W. Smith, 2012; Wadud et al., 2016).
5. *Improvement in road safety*: Efficient driving should reduce human errors and negligence in driving for lowering the rate of road accidents. That could be achievable once the technology achieves the goal of systematizing the driving process and interaction with other vehicles and people on the road. AVs could reduce crash risks between 5 to 23 percent (Wadud et al., 2016).

There is no doubt that AV direct effects positively impact the paradigm shift of urban mobility. These positive changes encourage the implementation of new systems such as Mobility as a Service (MaaS), shared autonomous vehicles (SAV) as autonomous car-sharing systems (ACS or automated taxis), autonomous ridesharing (ARS), and others.

Indirect effects

AV indirect effects, called second-order or systemic effects in Bahamonde-Birke et al. (2018), will lead to changes in demand behavior, demand volume, new requirements in infrastructure in the long-run, and some cases, AVs will cause undesirable effects (Appendix H, p. 272):

1. *Reduction in the subjective value of travel time savings (VTTS)*: AVs will reduce the disutility of travel time because other tasks could be done instead of driving, reducing the stress levels (Kohli & Willumsen, 2016). That reduction implies other effects, one of them is the reduction of the generalized travel cost and the total cost, although changes in demand patterns could also be generated (generation, distribution, and modal split), from non-motorized to motorized modes or between motorized modes.

2. *A new system with new users*: Complementarily, AVs will permit that a broader range of users could use these vehicles, such as minors, the elderly, and disabled people (B. W. Smith, 2012).
3. *Demand increment*: Reduction in the value of time, congestion, and travel times plus induced demand will lead to an increase in trip generation. The increment of trip demand in AVs will have an impact on the use of public transportation. Thus, it will boost the vicious circle of transit, promoting the use of private transportation.
4. *Vehicle-kilometer traveled (VKT) increment*: At least three reasons provoke this increment, according to Smith (2012). First, splitting of trips, i.e., people traveling together, they will do it separately. Second, car trips without users (called "*ghost trips*") search autonomously for parking or because an empty car will return to the origin; so other family members could use it. Third, transportation costs will be lower because of the better amortization of a vehicle.
5. *Changes in trip distribution*: The reduction of general travel costs will promote longer trips. This consequence will imply changes in the origin, destination, or both (changes in trip generation and trip attraction).
6. *Changes in urban structure and activity system*: In the long run, if trips are longer than the current state, it will lead to an increment of the city size, modifying the place of residence, work, and activity system. From that point, new discontinuous and farther urban areas from the city could appear. It will change the urban model towards a dispersed model (urban sprawl).
7. *Other impacts*: AVs could generate social opposition to this paradigm shift in mobility because of ethics, legal, environmental, and territorial issues.

The development of transportation policies is necessary to avoid or reduce adverse impacts on AV indirect effects. Bahamonde-Birke et al. (2018) describe some of them. The Administration should prepare the cities for this new paradigm in urban mobility.

5.3.2. Implemented methodology

The model evaluates a concentric city of 15 [km] of the radius. The city homogeneously generates 500,000 trips in cars. The application analyses a current and future scenario. In the former, users only drive MVs in which the road capacity is 1,272 vehicles per lane. In the latter, the car users travel in AVs, considering 3,960 vehicles per lane of road capacity (Lioris et al., 2017).

In a Smart City with only CAVs, a central agency will assign the route for cars. In the proposed model, the assignment firstly considers the shortest

distance path with the all-or-nothing assignment method; secondly, the remaining trips consider a cost function through the incremental method.

Mathematical formulation

The objective function contains two components: a user and agency cost function. Two sets of constraints restrict the problem: the road capacity and the minimum distance between roads in which two decision variables—d_w^c and Φ_w^r—vary at each point of the city. The solution to the mathematical problem comes from Karush-Kuhn-Tucker conditions. After that, the process of discretization presents the optimal structure of the city.

Application to case studies

CAVs will influence different ways at each stage: access to main roads, regular trips, and arriving to trip destinations (Appendix H, p. 278).

In the first stage, users drive from the origin (household or place of residence) to the nearest main road. AVs could influence in two components:

1. The generalized cost functions will decrease due to the speed will increase, and the operation cost will decrease, and
2. The value of travel time will decrease because the users could do other activities during the travel, decreasing stress levels.

In the second stage, users are on a regular trip in a car, i.e., users travel using the main road structure: ring and radial routes. AVs could influence the local generalized travel cost function in five aspects:

1. The value of travel time will drop for AV users, as explained previously,
2. The speed of AV and CAVs will increase because AVs will be more efficient,
3. The road capacity will increase due to connected CAVs will travel in platoons,
4. The travel time when CAVs cross an intersection will decrease due to communication V2I (smart city), platoon formation, less reaction time, traffic lights coordination, and
5. The unitary operational cost will decrease because AVs will be more efficient.

The third stage considers the cost of arriving at the destination from the closest main road. In this case, AVs could influence in three aspects:

1. Drivers just get out of the car at the final destination,
2. The generalized cost will decrease due to AVs and CAVs will be more efficient, and
3. The users will not have to walk from the parking spot to the destination.

5.3.3. Analysis of results

The research exhibits the results of direct and indirect effects calculated through the analytical model considering three aspects: direct, indirect effects, and effects of progressive implementation (Appendix H, p. 283).

The direct effects mainly reduce road congestion and costs. In the former, the driving of AVs will be more efficient than MVs, and the increment of road capacity will cause that the road saturation by CAVs reduces between a third and a half of MV saturation. The latter is a consequence of the previous improvement in which the cost will decrease by about 30%.

The indirect effects of AVs and CAVs will influence the value of travel time, induced demand, increment of the VKT, changes in trip distribution and urban structure, and changes in trip distribution and urban structure. First, if the value of travel time decreases to 8 [$/h] in the model, then the total cost will decrease by 35%: Second, if the demand increases 50% (Induced demand), the total cost in the new equilibrium will be a little smaller than (or similar to) the current scenario. Third, VKT could increase if AVs started to look for a parking spot only once they get out of the car at the destination. This result could be relative, considering CAVs will connect infrastructure (V2I) in a smart city. Finally, the total cost will increase if a city grows, and the vicious cycle could be encouraged; therefore, the city size is as considerable as the induced demand. On the other hand, the average user cost per distance unit will slightly decrease due to the increment of the urban radius. The previous point will encourage longer trips, cause dispersion, and change in trip distribution and urban structure.

The progressive implementation analysis considers the analysis of the total cost and congestion level. Both of the previous variables will decrease if a city implements that technology considering a constant demand. The decrease is not a monotonous curve in which the gradual implementation could generate scenarios as bad as the initial state. The implementation forces agencies to mitigate imbalances between supply and demand for reducing the negative perception of AV implementation in the early years.

5.4. Summary

- The implementation of urban planning and management measures can simultaneously maintain mobility and safety in growing cities.
- Regarding the policy of subcenters, the implementation of those allows improving the mobility of inhabitants in scattered, large cities. Therefore, subcenters could become an opportunity to optimize transit systems.
- Urban subcenters, as large as a CBD, do not necessarily benefit a public transportation system. The results show that medium-sized subcenters obtain the maximum benefits and equilibrium between user and agency costs.
- Regarding the policy of autonomous cars, the work shows that in a future scenario with 50% more cars, the current scenario could have the same total cost as the future scenario with autonomous vehicles.
- Considering a reduction of the subjective value of time, the model shows that urban sprawl would compensate for the benefits given by autonomous cars.
- However, to the contrary, autonomous cars will encourage urban sprawl, which is already a profound problem in some cities, if agencies do not control it by urban planning measures.
- Regarding the application of the model in both cases, the proposed model based on the CA method allows analyzing benefits theoretically from implementing policies. Besides, the analysis is generic and independent of networks of particular cities.
- The results and analysis made from the application of the model are a contribution to the development of spatial planning instruments: Specifically, those works can support the definition of the objective image of a city (future urban planning scheme).

6. Application to Santiago, Chile

Santiago, Chile, is an extensive city of 850 km^2 with over 7 million inhabitants. The city's structuring road network tends to have a concentric structure defined from ancient roads that cross the city. However, only one ring is in the operation of those planned in spatial planning instruments. Regarding public transportation, *Red* (ex *Transantiago*) is the urban public transportation system that operates in Santiago's metropolitan area, the capital city of Chile.

Santiago's Metro articulates the *Red* system. Currently, Metro daily transports more than 2.6 million people on its seven lines extending 138 kilometers and 136 stations. Metro will continue to expand in the next decade to reach 220 kilometers of extension, including lines 7, 8, and 9, plus subways extensions of lines 2, 3, and 4.

The chapter analyses the current subway infrastructure in Santiago, Chile, using the formulated model to propose a required network. Mainly, the objective is to identify the needs for an adequate level of service in urban mobility and transportation, focusing on functionality and demand. The method uses the analytical formulations presented in previous chapters and transit information from the latest origin-destination survey in 2012.

The next section presents Santiago of Chile and its structure, delving into the public transportation network. After that, the section globally explains the methodology applied for Santiago, Chile. Finally, the chapter presents conclusions.

6.1. Santiago, Chile, its History, structure, and networks

6.1.1. Santiago's Metropolitan Region and its urban structure

Santiago, also called *Gran Santiago*, is the capital of Chile. The city belongs to the Metropolitan Region of Santiago, which has six provinces. The province of Santiago is the central province, which has 32 city councils called *Communes*. Figure 6.1 shows *Gran Santiago* includes these 32 zones plus two more zones (San Bernardo and Puente Alto). Santiago, founded in the 16th century on the banks of the Mapocho River, currently has a population of over 7 million inhabitants.

Regarding private transportation, Santiago concentrates 37% of the Chilean automobile market. The city has over eight hundred cars in which the car rate is one car per 7 inhabitants. The primary road is Bernardo O'Higgins Avenue, well-known as Alameda. This road locates from the southwest to the northeast direction of the city, connecting Los Pajaritos Avenue to the west and avenues Providencia and Apoquindo to the east (Figure 6.1).

Several longitudinal roads cross the main avenue from the north to the south of the city, e.g., General Velásquez, Panamericana, Independencia, Gran Avenida, Recoleta, Santa Rosa, Vicuña Mackenna, Macul, and Tobalaba. Finally, the ring road called Américo Vespucio surrounds the internal area of the city (Figure 6.1).

Most of these roads are very old, even some of them have a pre-Hispanic origin. The roads began to play an intercity role from the founding city to other towns. In recent decades, Santiago's urban growth and the country

caused a conurbation of Santiago and closer towns. Thus, the foundational Santiago is currently the central commune of the city, which is a small area of 3% of the total area of Santiago. Intercity roads become the primary urban road network of the city. For this reason, the town of Santiago tends to have a radial road structure, although the development of urban planning in Santiago has also developed other roads. The planning instruments in Santiago have defined several rings, but only one currently exists.

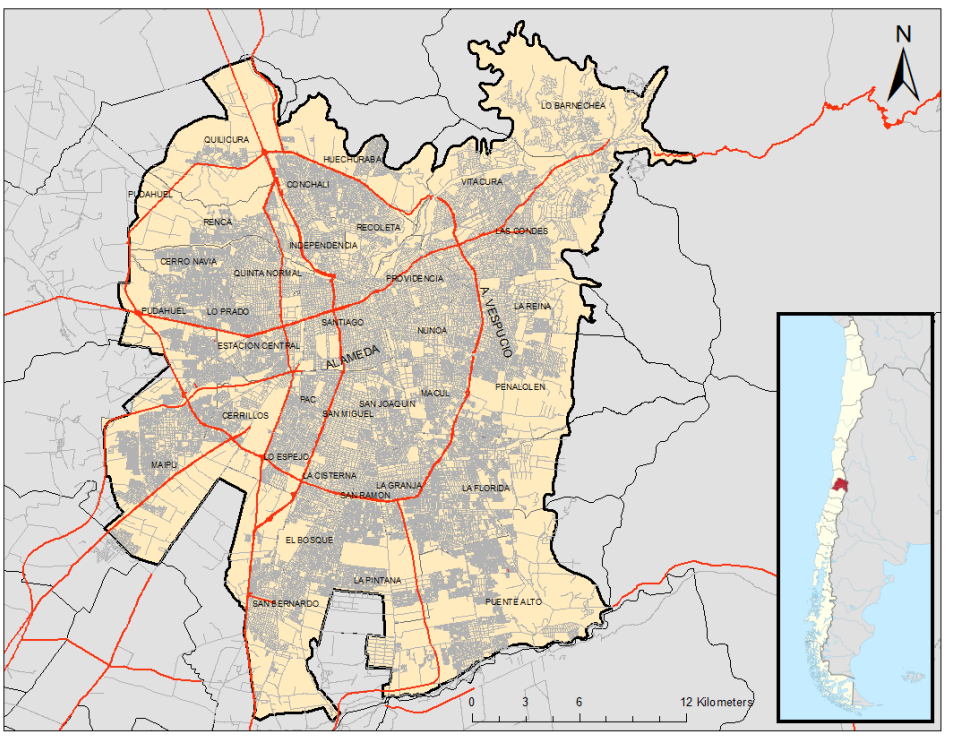

Figure 6.1. Santiago's urban structure and primary road network.

Since 2000, Santiago began the construction of tendered urban freeways. First, Central Freeway runs inside the city from north to south using the old Panamericana road, incorporating General Velásquez Avenue. Second, Américo Vespucio Avenue was transformed into a freeway and will soon be the first ring freeway in Chile. Third, the Norte Costanera freeway parallels the riverbed of Mapocho River and even runs under the river on a road segment. Subsequently, Santiago incorporates the San Cristóbal tunnel and the Access Northorient Highway. All freeways have a free flow toll system in an extension that exceeds 200 kilometers.

Furthermore, Santiago has a fleet of 25 thousand taxis and 11 thousand collective taxis. The latter mode refers to shared cars with a defined route. In

recent years, Santiago promotes using bicycles through an incipient network of bike-sharing and investments in cycleways.

Regarding public transportation, Santiago has a transportation system with extensive subway coverage and buses. Moreover, it has a commuter train. The next sub-section presents information about those in detail.

6.1.2. History of Public Transportation in Santiago, Chile

Until the early 1970s, Chilean State maintained total control in the passenger transportation industry in Santiago, Chile. The privatization of the urban transportation system began in 1975, increasing the bus fleet and, in the same way, the atomization of the system. In the same year, the operation of the first subway car runs a short stretch of the first line of the Chilean subway called Santiago's Metro. Three years later (1978), the agency inaugurated a second Metro line. By the early 1980s, the Metro was already an extension of 25 kilometers. On the other hand, surface transportation grouped small companies into Gremial Associations allowing a better operation to set fares and service routes (DTPM, 2019).

In 1989, Santiago's Metro became an independent company of the state apparatus. Metro continued to grow in the following years, incorporating a tunneling construction method without opening the surface and altering urban dynamics. The technique allowed the construction of Line 5 in 1997, starting the construction of Line 4 in 2002, and the extension of other lines.

On the other hand, the bus system has a new regulation process in 1990, unifying the system through the system so-called *Yellow Buses*. The new framework allows the fare integration between Metro and Bus through a new service called Metrobus. The latter opened the system incorporating foreign companies in 2003, consolidating integration creating intermodal stations (subway & bus) in 2004.

The year 2003 began the development of the bases of the urban transportation project called Transantiago, implemented in two primary stages. First, in 2005, the system incorporated the first articulated buses transforming transportation labor unions into traditional companies to operate the system. Also, the system created the financial manager (AFT). In a second phase, in 2007, Transantiago launched changes in the network structure and fare integration of all buses. Moreover, it incorporates a single means of access

and electronic payment, the so-called *Bip* card. Finally, the system created a specialized unit dedicated to plan and coordinate the system.

Transantiago covers an area of 2,353 km^2 called *Gran Santiago*. Initially, two sub-systems comprise Transantiago. The former is the trunk line network, whose basis is the Metro's network and bus services operating on the main roads of the city where some of them are BRT systems. The latter is the bus feeder network, consisting of local bus services operating on local streets of restricted geographical areas.

From 2010, the Chilean government adjusted the Transantiago system negotiating deals of transportation providers and complimentary services. The new deals came into force in 2012, eliminating the structure of trunk-feeder services and the exclusivity of the routes. Each company forms a business unit of transportation, which has a defined color. Moreover, 1,120 new high-tech buses entered with high levels of safety and comfort for users. In 2017, the suburban train service called Metrotren incorporated a train to Nos, which links Central Train Station with the southern part of the city.

In the following years, the system added new electric buses. Since March 2019, the system aims to grow in quality by renaming the Metropolitan Mobility Network, known as the "*Red*" system.

6.2. Spatial analysis of transit infrastructure

Santiago has three modes of public transportation: subway (Metro), buses (BRTs and traditional buses), and a commuter train (*MetroTren*).

6.2.1. Metro network

Metro's current network has seven lines; the opening of the last one (line 3) was in 2017. The future network plan incorporates three new lines and three extensions for old lines. Figure 6.2 presents the current subway network and the projected lines, including line extensions.

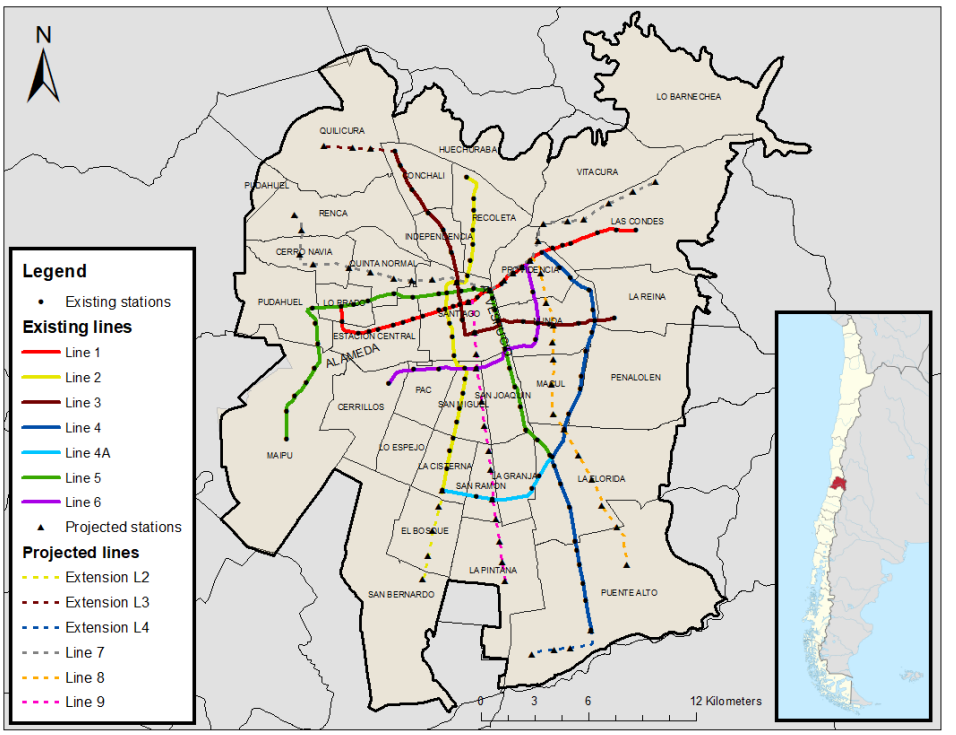

Figure 6.2. Metro network: existing lines and future projects.

6.2.2. Buses network

Public transport operators are companies regulated by the Ministry of Transportation and Telecommunications through the Executive Office called DTPM. Currently, the *Red* system has six business units, in which a company manages a set of bus services. The service identification is through numbers, letters, and colors. The buses meet the Euro VI emission standard, or some of them are electric. The most modern buses are red and white and have WIFI, USB ports and, air conditioning (DTPM, 2019).

The Santiago system has an infrastructure dedicated to bus services. The system has three types of infrastructure: corridors, exclusive roads, and bus lanes (FiscalizacionMTT, 2019).

- *Bus corridors*: Roads that have lanes exclusively for buses. These lanes are usually on the central zone of a road, separated from the rest of the lanes. The objective is to increase the commercial speed of buses.
- *Exclusive roads*: Roads that transit services use exclusively at a schedule.
- *Bus lanes*: Lanes for buses located on the right side of a road, according to the direction of traffic operating at all times and days of the week.

Figure 6.3 shows the infrastructure dedicated to transit services. Santiago has 19 corridors (red lines), 11 exclusive roads (blue lines), and 53 bus lanes (purple lines). The figure shows that the infrastructure dedicated exclusively to buses has a radial structure from the city center without ring corridors. Moreover, the transit infrastructure reaches neither continuity nor high coverage in the city.

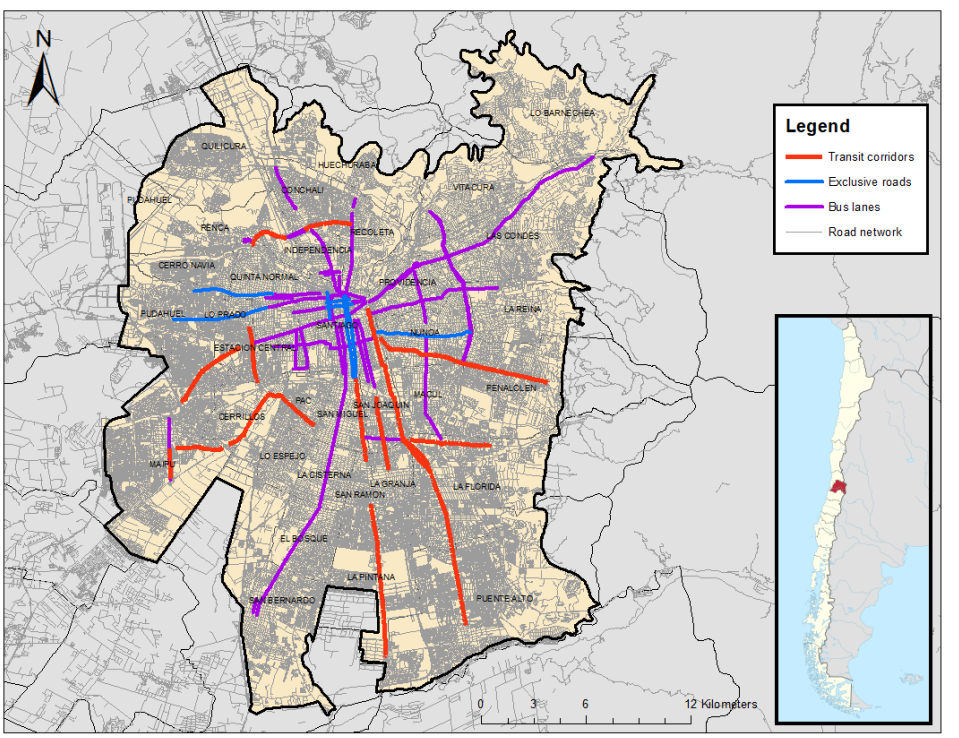

Figure 6.3. Buses networks: corridors, exclusive streets, and bus lanes.

6.3. Modeling

6.3.1. Parameters

The modeling considers Santiago's urban shape approaching a concentric city, explained by Medina-Tapia et al. (2021). The modeled city has a radius of 15 km (R), considering the rush hour lasts 1.5 hours (T). Table 6.1 shows the parameters in each stage of a trip, using the time perception from TRB (2013).

Table 6.1. Parameters used for user and agency cost functions.

Demand parameters												
T	α	β	γ	δ	v^w	χ^T	$v^a(r)$					
[h]	[dimensionless]	[dimensionless]	[dimensionless]	[dimensionless]	[km/h]	[m]	[km/h]					
1.5	2.2	2.1	1.0	2.5	3.0	40	$v^a(r) = 3.0 + 1.4\bar{6} \cdot r$					
Operational parameters												
v^t	a^a	a^d	τ	τ'	τ''	τ'''	τ^s	t^f	η^d	K^v	K^d	K^h
[km/h]	[m/s²]				[s/station]			[min]	[shift/veh]	[user/veh]	[km/route]	[s/veh]
80	1.3	1.3	19.2	5	35	0	42.1	6	1	1,494	0.481	123
Economic parameters												
μ	φ^k	φ^g	φ^o	$\varphi^{p(f)}$	φ^p	$\varphi^{s(f)}$	φ^s					
[$/user·h]	[$/veh]	[$/shift·h]	[$/km·veh]	[$/km·route·$P_m$]		[$/station·route·$P_m$]						
1.48	135.6	27	3.7	245.1	248.8	169.9	172.4					

6.3.2. Trip generation and attraction functions

The model considers a concentric city, which has a transit with two types of services: ring and radial routes. Santiago assimilates that urban form. The modeling considers dividing the city into 9 OD macro-zones: a central zone, four inner zones, and four outer zones (Figure 6.4).

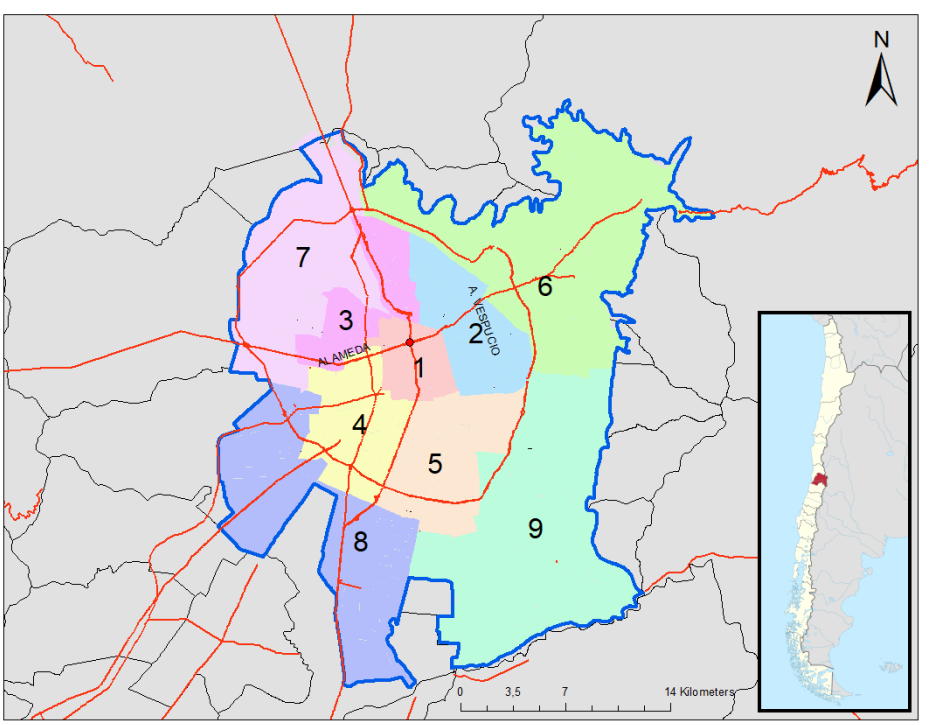

Figure 6.4. OD macro-zones used for the Santiago of Chile modeling.

The information of trips on the subway at rush hour obtained from the Santiago origin-destination survey (MTT, 2012) has a classification into the nine macro zones as shown in Table 6.2.

Table 6.2. Santiago's OD macro-matrix in [trip/P_m] obtained from OD Survey (MTT, 2012).

	1	**2**	**3**	**4**	**5**	**6**	**7**	**8**	**9**	**Total**
1	10575,5	7440,5	2346,0	1588,0	2728,5	9605,5	1326,4	624,7	1712,3	**37947,4**
2	22458,0	19583,3	1659,0	981,5	2973,0	9652,2	1023,6	609,0	4306,6	**63246,2**
3	12596,8	6248,9	9025,0	2018,6	727,9	3685,2	4103,0	974,6	694,6	**40074,7**
4	17550,9	5922,7	779,9	9656,3	3624,0	3462,8	1702,7	5936,3	2074,1	**50709,7**
5	14958,5	9937,8	494,7	1350,1	16573,4	7533,6	1859,1	1382,2	8933,3	**63022,7**
6	15385,9	16619,7	1985,5	1666,7	3754,5	24629,7	2246,1	334,7	2250,3	**68873,2**
7	20471,6	14257,2	13896,9	1983,4	1533,2	14097,3	32123,3	2548,4	374,4	**101285,8**
8	25495,8	13724,3	3938,1	8662,8	5836,0	7327,9	2766,1	50812,3	7306,0	**125869,4**
9	31559,0	30074,8	4648,4	5759,6	17143,4	18355,3	2062,1	3917,2	66970,2	**180490,0**
Total	**171052,0**	**123809,4**	**38773,5**	**33666,9**	**54893,9**	**98349,6**	**49212,4**	**67139,4**	**94621,9**	**731519,1**

The method calibrates a continuous function in which the total trips of each origin-destination is the value in the OD trip matrix (T_{ij} where i is the origin zone, and j is the destination zone), as shown in Table 6.2. Equation 6.1 represents the total trips between the origin and destination zones. The coordinates $\theta^i_{f(2)}$-$\theta^i_{f(1)}$ and $r^i_{f(2)}$-$r^i_{f(1)}$ defines the origin zone. Meanwhile, the coordinates $\theta^i_{t(2)}$-$\theta^i_{t(1)}$ and $r^i_{t(2)}$-$r^i_{t(1)}$ defines the destination zone.

$$T_{ij} = \int_{\theta^i_{f(1)}}^{\theta^i_{f(2)}} \int_{r^i_{f(1)}}^{r^i_{f(2)}} \int_{\theta^i_{t(1)}}^{\theta^i_{t(2)}} \int_{r^i_{t(1)}}^{r^i_{t(2)}} D(r_f, \theta_f, r_t, \theta_t)\, r_t\, dr_t\, d\theta_t\; r_f\, dr_f\, d\theta_f \qquad (6.1)$$

Using the function obtains the function of generated demand $\lambda(r,\theta)$ at a point (r,θ) in [user/km²·h] (Equation 6.2), and attracted demand $\rho(r,\theta)$ at a point (r,θ) in [user/km²·h] (Equation 6.3). Figure 6.5 shows the functions of trip generation (Figure 6.5(a)) and attraction (Figure 6.5(b)) obtained from Equations 6.2 and 6.3. Figure 6.5(c) represents the total trip density function, i.e., the sum of generated and attracted demand functions.

$$\lambda(r,\theta) = \int_0^{2\pi} \int_0^R D(r,\theta,r_t,\theta_t)\, r_t\, dr_t\, d\theta_t \qquad (6.2)$$

$$\rho(r,\theta) = \int_0^{2\pi} \int_0^R D(r_f,\theta_f,r,\theta)\, r_f\, dr_f\, d\theta_f \qquad (6.3)$$

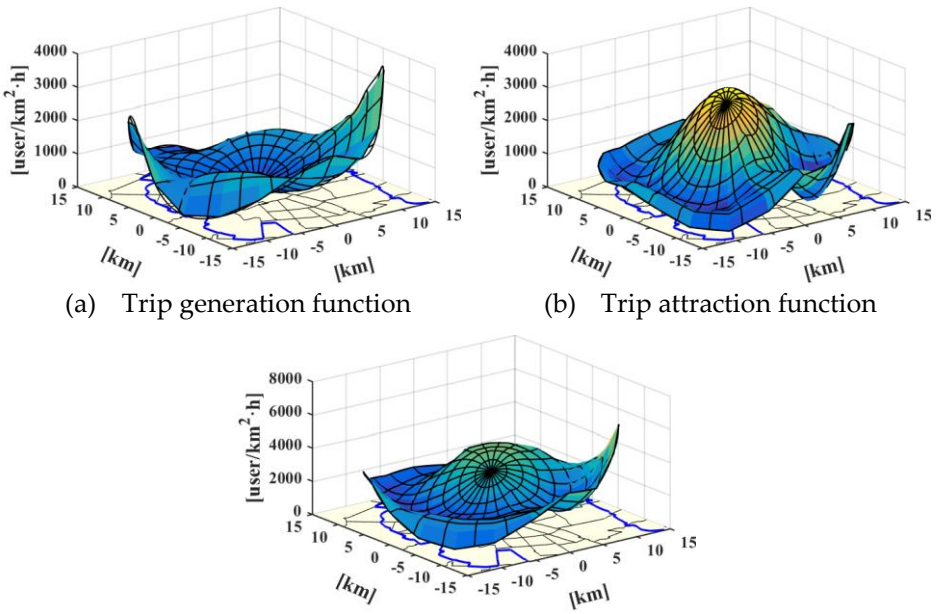

(a) Trip generation function (b) Trip attraction function

(c) Total trip function

Figure 6.5. Trip generation and attraction estimated functions from Santiago's OD matrix (MTT, 2012).

6.4. Analysis of infrastructure proposal

The objective function has two components (a user and agency cost function), including three sets of constraints: vehicle capacity, the minimum distance between stations, and minimum time headway. It is worth noting that the model has four decision variables: two spatial variables ($d^c(r)$ and $\Phi^r(\theta)$) and two temporary variables ($h^c(r)$ and $h^r(\theta)$). The solution to the mathematical problem comes from the mathematical optimization using Karush-Kuhn-Tucker conditions. The model definition is in Section 3.2 (p. 38).

Figure 6.6 presents the optimal transit structures for Santiago, Chile, obtained from the model. The blue line in Figure 6.6(a) represents the optimal ring route density, and Figure 6.6(b) represents the optimal solution for radial routes. The red points represent the optimal location of a route obtained from the discretization process (Section 3.4, p. 67). From optimal transit densities, Figure 6.7 shows occupation levels of transit corridors for Santiago, Chile.

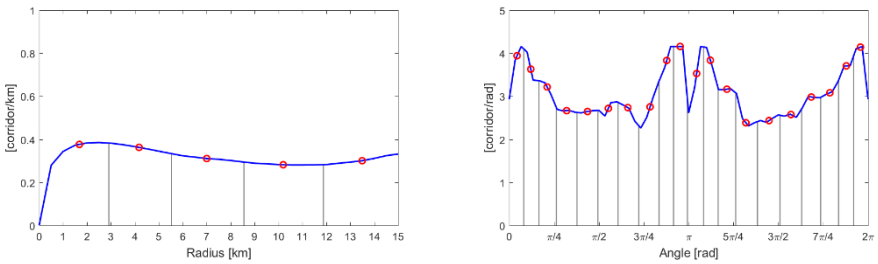

(a) Ring routes (b) Radial routes

Figure 6.6. Optimal transit densities for Santiago, Chile.

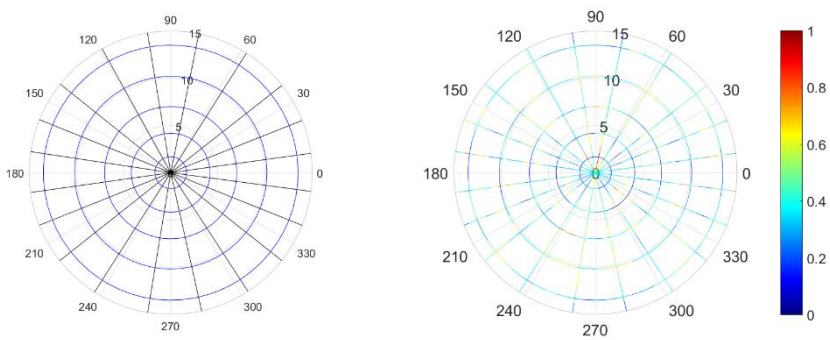

(a) Optimal transit structure (b) Occupation levels

Figure 6.7. Optimal transit structure for Santiago, Chile.

Regarding ring routes, the model proposes five transit corridors, which distribution is slightly higher around the city center. Regarding radial routes, the model proposes 20 corridors with non-homogeneous distribution with higher density in three zones: East zone (above 0 radians, including Providencia and Las Condes *communes*), West zone (above and below π radians, including Estación Central, Maipú, Pudahuel *communes*), and Southeast (below 0 radians, including La Florida and Puente Alto *communes*). It is worth noting that 20 radial lines represent ten lines from one side of the city to the opposite. Regarding occupation levels, rings have a maximum occupation of up 75%; however, the average occupation is around 25%. On the other hand, radial routes reach an occupation of up 92% with an average occupation around 37%. Therefore, the global transportation system is not stressed by high occupancy levels.

Figure 6.8 presents a comparison between the subway infrastructure proposal obtained from modeling and future subway projects for Santiago, Chile, presented in Section 6.2 (p. 137). Figure 6.8(a) shows blue lines representing the optimal transit structure, the red circle represents the analyzed area, and the map in the background is the *communes* of Santiago

city, Chile. Figure 6.8(b) also includes the current infrastructure and the future subway projects as brown lines for Santiago, Chile, where continuous lines are existing infrastructure, and dashed lines are the future projects. Currently, Santiago's Metro has seven lines (Section 6.2); however it represents nine existing radial routes, including their extensions, meanwhile the three new projected lines represent four more radial routes. Globally, the subway mobility plan proposes 13 radial routes, which should increase to 20 radial routes. Regarding rings, the transit system only proposes two incomplete rings, which should increase to 5 ring routes.

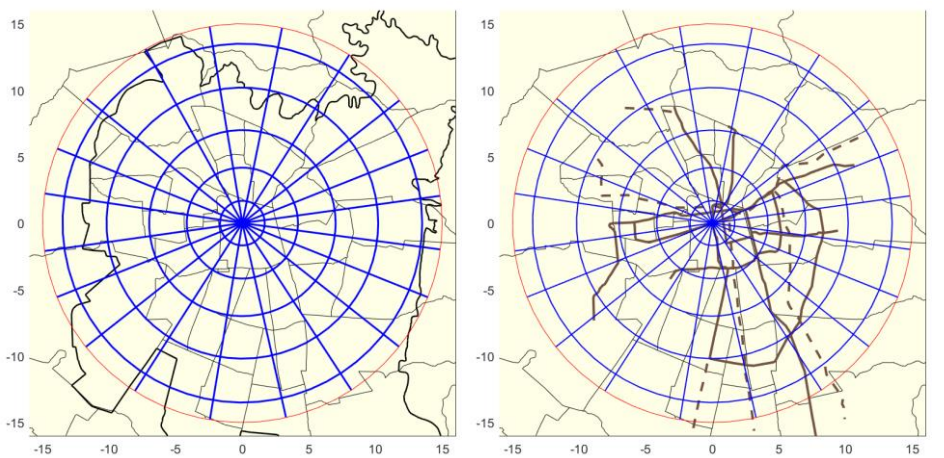

(a) Optimal transit structure (b) Comparison of proposal and subway infrastructure

Figure 6.8. Comparison between subway infrastructure proposal and current and future projects for Santiago, Chile.

6.5. Summary

- Santiago of Chile has a consolidated subway network of more than 50 years with seven lines currently operating. The investment plan considers the extension of some of these lines and the construction of three future projects.
- The modeling uses standard operating data. However, some parameters were adapted to the Chilean case, such as the value of time, the train capacity, and the transit demand.
- The continuous travel distribution function obtained from the travel matrix origin-destination between macro-zones allowed to represent the generation and attraction of trips. A territory is not a stepped structure with breaks between two OD-zones boundaries. On the contrary, demand

generally varies smoothly from one side of an OD zone boundary to the other side.

- The model obtained a macroscopic proposal for subway infrastructure needs, i.e., the modeling applied the theoretical mathematical model developed in the previous chapters, defining a relevant approach to determine the infrastructure needs for Santiago city.
- The proposed model for Santiago considers five rings and 20 radial routes. The comparison between this proposal and the current network plus the planned defines Santiago's infrastructure needs: 13 new radial routes (equivalent to 7 more lines) and four more rings. Future studies could study complementing these central services with tram services, particularly in Santiago's central commune.
- The proposal reduces occupation vehicle levels in comparison to the current operation: maximum occupation of rings is 75% and radials is 92%. The average occupation of rings is around 25%, and the average radial occupation is 37%.
- Therefore, Santiago of Chile should increase infrastructure supply for the subway network in future strategic planning.
- Future studies should analyze current services with complementary modes, e.g., tram services.

7. Conclusions and future research

Urban areas present massive challenges. One of the first is the need to place a large number of people in them. Secondly, population and activities rapidly increment in already congested cities. Both the previous issues and the influence of cars are fundamental causes of an inorganic dispersion called urban sprawl.

Urban planners constantly face a dilemma: dense or scattered cities. The advantages of the internet and other modern communications could justify that traditional concentrated cities are not necessary nowadays. From the above, it could seem reasonable to encourage urban sprawl, but land scarcity is another contemporary issue: territories need a balanced relation between the countryside and cities. Moreover, if the dispersion exceeds certain

thresholds, the distance will increase, and transportation problems will increase even more. Thus, concentrated areas present significant advantages in comparison to scattered cities. In a compact area, traveled distances are minimal, including mandatory trips; concentrated people attract diverse services, commercial and even factory activities, increasing business chances and new potential clients. Moreover, a new urbanization process is slow and lengthy in which short-term decisions tend to inhibit it.

It is worth noting that the dissertation provides an extensive analysis of urban design based on its functionality, considering that urban mobility is a dynamic system that has had a slow natural evolution and depends on urban density, operations, and infrastructure.

7.1. Methodological contributions

The research hypothesis exposes a question promoting a paradigm change in traditional urban planning: the need for a balance between the infrastructure and residential and non-residential densities to optimize the mobility for any purpose and mode. The dissertation work proves the research hypothesis using three analyses: theoretical approaches, application of some policies, and application to a real case. First, in Chapter 4, the theoretical schemes prove decentralized cities obtain significant results if infrastructure adapts to local urban conditions. Second, in Chapter 5, the model contributes to analyzing transportation issues that depend on service levels and urban structures. Thus, the modeling shows networks must consider as much the system operation as urban planning. Third, in Chapter 6, the application for a real case as Santiago, Chile, determines a more demanding scheme requiring more infrastructure corridors than the city's proposed network plan. Thus, networks adapting to local conditions try to optimize the systems under specific transit and private transportation conditions.

Four classes group the global contributions to the research line: urban network design based on city functionality.

Regarding the model, the dissertation focuses on using parsimonious models due to the continuous approximation method analytically proposes tractable models, obtaining continuous outcomes through an algorithm. This method speeds up the computation time compared to optimization methods, including those implemented in any software. Thus, the model combines the infrastructure and operation of a system to design public and private

transportation networks considering transportation network design depends on two components: the level of service and urban structure. Modeling transit and private systems consider the essential stages of a trip. Moreover, the agency costs also include relevant aspects such as capital, operation, and infrastructure. This relevant contribution identifies both nodal infrastructure costs (stations/stops) and linear corridors (routes/roads).

Regarding demand behavior over the city, only a few investigations on a continuous approach consider the effects of non-homogeneous demand over a city. The dissertation realizes the importance of considering heterogeneous demand because a homogeneous distribution underestimates the operation and infrastructure needs. Thus, the proposed model for designing transportation networks can adapt to non-homogeneously distributed demands, considering local demand conditions.

Regarding discretization of continuous outcomes over a city is another significant contribution to this research line. The proposal has a basis on two methods: the former aims the optimization, and the latter generates a heuristic that obtains its results in reduced times.

Regarding urban design, the implemented model allows the evaluation of mobility policies ranging from strategies to spatial planning instruments, from traditional measures (implementation of subcenters) to innovative measures toward the future (autonomous cars). Thus, decentralized urban structures give significant mobility levels, presenting a sustainable alternative to developing a scattered city (urban sprawl). The dissertation also seeks to break a theoretical analysis towards practical analyses defining an optimal strategic subway network for Santiago, Chile.

A matrix of origin-destination trips between macro-zones made it possible to fit a continuous travel distribution function. From this matrix, continuous functions graphically represent the generation and attraction of trips. Thus, the continuous representation of travel distribution functions is an effective tool. First, the continuous functions allow visualizing the mobility graphically that a city has, allowing comparing cities. Second, the computation of continuous functions yields interesting levels of calculation regarding large matrices.

7.2. Research findings

Many cities concentrate services at a zone or a few central zones. The latter is particularly observable in Latin American cities. Typically, the central business district (CBD) is the city zone that concentrates on business and service activities attracting many trips. Thus, cities require infrastructure, transportation, and logistics supply to proper functionality.

7.2.1. Transit system

For transit systems, the system feasibility depends on occupancy (demand) and operating constraints (technology). HRTs show larger feasible spaces respecting the three analyzed technologies, especially for radial routes.

BRT system is the most attractive for low demand, about 800 [user/km^2·h]. After that, LRT is competitive considering intermediate levels of demand less than 1,000 [user/km^2·h]. Finally, HRT is the best technology for a dense city with a density between 1,000 and 2,000 [user/km^2·h]. Another interesting point is BRTs are the unique feasible technology with super-high demand levels.

From the modeling results, the intermediate zone should concentrate transit routes for ring routes between 4 and 12 km from the central point. Moreover, the periphery needs efficient feeder systems connecting radial corridors because the system quickly loses competitiveness in the outskirts for a concentric city.

For subways and considering low time values as in developing countries (about 1 [$/user·h]), subway cars will travel close to maximum capacity. However, if the value of time increases to 5 or 10 [$/user·h] as in developed countries, vehicles travel with low levels of demand increasing frequencies.

A multi-subcenters city reduces from 6.9% for HRTs to 11.6% for BRTs of total costs regarding heterogeneous cities. Thus, multi-subcenter cities are the best alternatives for transit services.

Therefore, transit plays a significant role in an urban structure and mobility. Regarding technologies and considering the feasibility analysis, costs by user, operation variables, and adapting to different urban schemes, HRTs the best alternative for massive cities regarding the three analyzed technologies.

7.2.2. Traffic system

For traffic systems, the feasibility depends on the road saturation. Thus, density actives the capacity constraint from 1,000 to 2,000 [user/km²·h]. It is worth noting that the problem has no solution with a higher demand density than 2,000 [user/km²·h] for a homogeneous scenario. The latter constraint restricts cost reductions for the analyzed scenarios.

Regarding urban structure, distributed cities have slightly shorter times (about 2.6%) than concentrated cities. Generally, rings concentrate their density to the periphery for decentralized cities, except monocentric cities. However, a heterogeneous city needs more infrastructure in comparison to other urban scenarios.

Regarding the value of time, road densities for ring roads increase if the value increases even more to the outer city than in the city center. The density of radial roads reaches the minimum density for developing countries and low levels of demand because the system firstly saturates in this case; however, if the density increases rapidly active the minimum density of roads.

Overall, local conditions define generation/attraction rates, and network design must adapt to them. A homogeneous demand is an idealized urban scenario. However, homogeneous distributions will underestimate real infrastructure needs; thus, scientific researches should consider those limitations. This dissertation modeling gives value to a heterogeneous structure, which is a better approach for current urban conditions; however, cost levels are higher but more realistic. Regarding urban schemes, decentralized urban networks present highlighted results. Thus, multi-subcenters show better results than a homogeneous city. It is worth noting subcenter effectivity depends on the subcenter size to reduce costs and travel time. Therefore, subcenters can become a solution strategy for urban sprawl and dispersed cities.

The concentration of services, scattered growth of households, and transportation over-demand increase adverse effects on people's mobility. Therefore, transportation engineering and planning science jointly play a significant role in this systemic problem.

The problem is that cities heterogeneously expand to new areas due to environmental, social, and economic factors. Therefore, networks must adapt the schemes to heterogeneous demand patterns by considering the origin, destination, trip features, and transfers needed.

The scale of analysis is another aspect to consider in the design. Planning can be in macro, meso, or microscale. This research focuses on the former.

Different transportation technologies, however, are associated with varying speeds of travel and capacities. Transportation technology thus plays a significant role in defining urban form and the spatial pattern of various activities. However, public transit tends to reach a structuring role in many cities due to congestion, it allows massive transportation, and even users prefer it due to sustainability factors.

7.2.3. Applications on urban planning and new technologies

Regarding two policies analyzed in the dissertation, the implementation of subcenters and autonomous vehicles gives a complementary focus to the analysis. In the first work, subcenters are an opportunity to improve transit systems. The second work analyzes the impact of autonomous vehicles on a concentric city.

The implementation of subcenters gives savings of 3.5% in rush hour, improving the transit functionality. An interesting conclusion considers that the subcenter size is essential; however, medium-sized subcenters got better benefits balancing user and agency costs. Therefore, the analysis affirms public transportation significantly improves if the transit scheme adapted to the demand needs, considering an urban layout with subcenters.

Autonomous vehicles appear as a key factor for a paradigm change in urban mobility. However, the effects jointly give non-trivial results. On the one hand, direct effects would reduce road congestion increasing road capacity, travel costs, and energy, decreasing by about 30%. Moreover, the new technology would increase the efficiency and flexibility of modes, pollution reduction, and even road safety improvement. On the other hand, indirect effects would affect the value of travel time, induced demand, VKT increments, changes in trip distribution and urban structure, and changes in trip distribution and urban layouts.

The dissertation analyzes the indirect effects caused by the implementation of autonomous vehicles using the proposed model. Thus, reducing the value of travel time to 8 [$/h], the total cost would decrease by 35%. Inducing demand by 50%, the total cost would reach slightly lower cost levels than the initial scenario. Increasing VKT is relative, considering autonomous vehicles would have connections with infrastructure in a smart city (V2I), optimizing

the search for parking spots. This technology encourages urban sprawl in cities, deepening the vicious cycle and increasing the induced demand; however, the average user cost per distance would slightly decrease.

AVs impacts would show unequal results; these would encourage longer trips, urban dispersion, and changes in trip distribution and urban structure. Therefore, the implementation of connected and autonomous vehicles in cities could have neutral effects on the total travel time costs; an interesting conclusion gives for modeling and analysis of a concentric city.

7.2.4. Application to Santiago, Chile

Santiago of Chile has a consolidated subway network in which local authorities defined an investment plan, including extensions and future projects. The dissertation compares it with the theoretical model results, considering the city has a concentric structure.

The methodology presents a relevant proposal representing demand functions as continuous functions for Santiago, Chile: trip generation and attraction. An advantage of this analysis approach is a city is not a structure composed of isolated areas with breaks between two OD-zone boundaries. On the contrary, the distribution of demand in a city generally should vary smoothly from one side of a zone boundary to the other side. Thus, this spatial approach moves away from a stepped structure of discrete approaches.

The results from the model application are clear. The supply of infrastructure must increase to achieve balanced cost levels between users and the agency and reducing subway occupations. The outcomes determined the infrastructure needs for Santiago city, proposing 5 ring lines and 10 end-to-end longitudinal lines (20 radial routes). The continuous approximation (CA) method seeks to continuously balance the infrastructure over the city. Thus, the method recognizes the areas of the city without infrastructure. In particular, this result is observed for ring lines.

Considering the above, Santiago of Chile should increase infrastructure supply for the subway network. The results are considered a good preliminary solution; however, the research approach should be refined through complementary studies. These studies should consider information from all available origin-destination zones, periods, transport purposes, and others.

Therefore, the dissertation shows that the model, its implementation, analysis, and outcomes contribute to planning science. Moreover, this could enhance spatial planning instruments defining future urban planning schemes.

7.3. Future works

The proposed model and its applications allow opening several future work lines from methodological approaches to innovative applications.

The modeling can be extended to other urban forms for designing urban mobility networks, e.g., grilled cities and mixed urban structures, i.e., the downtown could be a grilled zone, and the periphery could be radial.

Consequently, the model will incorporate complementary transportation modes, flexible transportation schemes, multi-modes, and new technologies.

A trip distribution matrix can be generated dynamically in future research. Thus, exogenous attributes of a trip will define the attraction level of users. Particularly, the characteristics of land use for education and work purposes will allow modifying a distribution matrix. The modeling will dynamically consider the direct effects of changes in land use on the trip matrix for a city.

In a relevant improvement, the design modeling should simultaneously integrate both public and private transportation systems. It is worth mentioning that the current work presents complementary definitions between both systems. Thus, the integration is feasible.

The extension to model other urban structures and other current cities deepening the application to real cases. In this way, future works should reduce assumptions the model has.

The Macroscopic Fundamental Diagram (MFD) could improve the management of vehicular network dynamics for continuous mobility schemes. Behind this, new lines of research could arise if research analyzes the interrelationships between the model used and MFD concepts.

The approximation of the demand functions to real situations opens several investigations proposing a method for continuous travel

distribution functions. The latter would enable comparing travel generation and attraction functions between cities. These functions also allow modeling other aspects of demand, such as elastic demand, induced demand, and others.

The modeling challenges discussed previously will necessitate advances in the discretization processes. Thus, the research should deepen the determination of hierarchical networks that consider different levels of infrastructure.

For the Santiago case, future studies could study complementing current services with others, e.g., tram services. One of the research works currently is under development, analyzing personal mobility modes within a sustainability framework.

Regarding urban planning and transportation policies, this research line can allow the analysis of many strategies and urban planning measures. The study and modeling of new technologies will deepen in alternative scenarios in future works considering different heterogeneous demand; changes in user behavior in each trip stage; multi-modes (private, public, and freight transportation); different types of roads; the mobility as a service (MaaS); tactical urbanism, and finally, the simultaneous optimization of other scenarios and current cities.

References

Acheampong, R., & Silva, E. (2015). Land use–transport interaction modeling: A review of the literature and future research directions. *Journal of Transport and Land Use*, *8*(3). doi: 10.5198/jtlu.2015.806

Aldaihani, M. M., Quadrifoglio, L., Dessouky, M. M., & Hall, R. (2004). Network design for a grid hybrid transit service. *Transportation Research Part A: Policy and Practice*, *38*(7), 511–530. doi: 10.1016/J.TRA.2004.05.001

Arkansas, D. of T. (ARDOT). (2014). Estimated costs per mile. Retrieved June 1, 2018, from https://www.arkansashighways.com/

Arnott, R., & Rowse, J. (1999). Modeling parking. *Journal of Urban Economics*, *45*(1), 97–124. doi: 10.1006/juec.1998.2084

Australian Transport Council. (2006). *National Guidelines for Transport System Management in Australia* (2nd ed). Australian Transport Council. Retrieved from https://atap.gov.au/technical-support-library/ngtsm/index.aspx

Azolin, L. G., Rodrigues da Silva, A. N., & Pinto, N. (2020). Incorporating public transport in a methodology for assessing resilience in urban mobility. *Transportation Research Part D: Transport and Environment*, *85*, 102386. doi: 10.1016/j.trd.2020.102386

Badia, H. (2016). *Comparison of bus network structures versus urban dispersion: A monocentric analytical approach. Evidences from Barcelona's bus network* (Universitat Politècnica de Catalunya). Universitat Politècnica de Catalunya. Retrieved from https://upcommons.upc.edu/handle/2117/105285

Badia, H., Estrada, M., & Robusté, F. (2014). Competitive transit network design in cities with radial street patterns. *Transportation Research Part B: Methodological*, *59*, 161–181. doi: 10.1016/j.trb.2013.11.006

Badia, H., Estrada, M., & Robusté, F. (2016). Bus network structure and mobility pattern: A monocentric analytical approach on a grid street layout. *Transportation Research Part B: Methodological*, *93*, 37–56. doi: 10.1016/J.TRB.2016.07.004

Bahamonde-Birke, F., Kickhöfer, B., Heinrichs, D., & Kuhnimhof, T. (2018). A systemic view on autonomous vehicles: Policy aspects for a sustainable transportation planning. *DisP-The Planning Review*, *54*(3), 12–25. doi: 10.1080/02513625.2018.1525197

Brueckner, J., Fu, S., Gu, Y., & Zhang, J. (2015). *Measuring the stringency of land-use regulation and its determinants: The case of China's building-height limits*. Retrieved from http://www.socsci.uci.edu/~jkbrueck/China FAR.pdf

Buchanan, C. (1963). *Traffic in Towns: A study of the long term problems of traffic in urban areas* (1st ed). London: Her Majesty's Stationery Office.

Bull, A., & Thomson, I. (2002). La congestión del tránsito urbano: causas y consecuencias económicas y sociales. In *Revista de la CEPAL* (Vol. 76). Retrieved from https://repositorio.cepal.org/handle/11362/10804

Byrne, B. (1975). Public transportation line positions and headways for minimum user and system cost in a radial case. *Transportation Research*, *9*(2–3), 97–102. doi: 10.1016/0041-1647(75)90044-1

Byrne, B. (1976). Cost minimizing positions, lengths and headways for parallel public transit lines having different speeds. *Transportation Research*, *10*(3), 209–214. doi: 10.1016/0041-1647(76)90076-9

Chang, S., & Schonfeld, P. (1991). Multiple period optimization of bus transit systems. *Transportation Research Part B: Methodological*, *25*(6), 453–478. doi: 10.1016/0191-2615(91)90038-K

Chang, T. H., & Lai, I. S. (1997). Analysis of characteristics of mixed traffic flow of autopilot vehicles and manual vehicles. *Transportation Research Part C: Emerging Technologies*, *5*(6), 333–348. doi: 10.1016/S0968-090X(97)00020-X

Chen, H., Gu, W., Cassidy, M. J., & Daganzo, C. F. (2015). Optimal transit service atop ring-radial and grid street networks: A continuum approximation design method and comparisons. *Transportation Research Part B: Methodological*, *81*, 755–774. doi: 10.1016/j.trb.2015.06.012

Chien, S., & Qin, Z. (2004). Optimization of bus stop locations for improving transit accessibility. *Transportation Planning and Technology*, *27*(3), 211–227. doi: 10.1080/0308106042000226899

Childress, S., Nichols, B., Charlton, B., & Coe, S. (2015). Using an activity-based model to explore the potential impacts of automated vehicles. *Transportation Research Record: Journal of the Transportation Research Board*, *2493*, 99–106. doi: 10.3141/2493-11

Chiou, S.-W. (2008). A hybrid approach for optimal design of signalized road network. *Applied Mathematical Modelling*, *32*(2), 195–207. doi: 10.1016/J.APM.2006.11.007

Chua, T. A. (1984). The planning of urban bus routes and frequencies: A survey. *Transportation*, *12*(2), 147–172. doi: 10.1007/BF00167373

Clarens, G. C., & Hurdle, V. F. (1975). An operating strategy for a commuter bus system. *Transportation Science*, *9*(1), 1–20. doi: 10.1287/trsc.9.1.1

Daganzo, C. F. (2005). *Logistics systems analysis* (4th ed.). Berlin: Springer. doi: 10.1007/3-540-27516-9

Daganzo, C. F. (2010). Structure of competitive transit networks. *Transportation Research Part B: Methodological*, *44*(4), 434–446. doi: 10.1016/j.trb.2009.11.001

Daganzo, C. F., Gayah, V. V., & Gonzales, E. J. (2012). The potential of parsimonious models for understanding large scale transportation systems and answering big picture questions. *EURO Journal on Transportation and Logistics*, *1*(1–2), 47–65. doi: 10.1007/s13676-012-0003-z

Daganzo, C. F., & Pilachowski, J. (2011). Reducing bunching with bus-to-bus

cooperation. *Transportation Research Part B: Methodological*, *45*(1), 267–277. doi: 10.1016/j.trb.2010.06.005

Deluka Tibljaš, A., Giuffrè, T., Surdonja, S., & Trubia, S. (2018). Introduction of autonomous vehicles: Roundabouts design and safety performance evaluation. *Sustainability*, *10*(4), 1060. doi: 10.3390/su10041060

DTPM. (2019). Directorio de Transporte Publico Metropolitano, Santiago, Chile. Retrieved from http://www.dtpm.gob.cl/

Dupuy, G. (2008). *Urban networks : network urbanism* (1st ed; J. Van Schaick & I. T. Klaasen, Eds.). Amsterdam, The Netherlands: Techne Press.

Estrada, M., Roca-Riu, M., Badia, H., Robusté, F., & Daganzo, C. F. (2011). Design and implementation of efficient transit networks: Procedure, case study and validity test. *Transportation Research Part A: Policy and Practice*, *45*(9), 935–950. doi: 10.1016/j.tra.2011.04.006

Farahani, R. Z., Miandoabchi, E., Szeto, W. Y., & Rashidi, H. (2013). A review of urban transportation network design problems. *European Journal of Operational Research*, *229*(2), 281–302. doi: 10.1016/J.EJOR.2013.01.001

Ferguson, E. (2018). *Travel demand management and public policy* (2nd ed; Taylor & Francis Group, Ed.). New York: Routledge. Retrieved from http://library2.deakin.edu.au/record=b3932245~S1

Fernandez, R., & Planzer, R. (2002). On the capacity of bus transit systems. *Transport Reviews*, *22*(3), 267–293. doi: 10.1080/01441640110106328

Fielbaum, A. (2019). *Effects of the introduction of spatial and temporal complexity on the optimal design, economies of scale and pricing of public transport* (Universidad de Chile). Universidad de Chile. Retrieved from http://repositorio.uchile.cl/handle/2250/171789

FiscalizacionMTT. (2019). Programa de Fiscalización de Ministerio de Transporte y Telecomunicaciones. Retrieved from http://www.fiscalizacion.cl/

Foletta, N., Estrada, M., Roca-Riu, M., & Martí, P. (2010). New modifications to bus network design methodology. *Transportation Research Record: Journal of the Transportation Research Board*, *2197*(2197), 43–53. doi: 10.3141/2197-06

González-Guzmán, C., & Robusté, F. (2011). Road space reallocation according to car congestion externality. *Journal of Urban Planning and Development*, *137*(3), 281–290. doi: 10.1061/(ASCE)UP.1943-5444.0000070

Haight, F. A. (1964). Some probability distributions associated with commuter travel in a homogeneous circular city. *Operations Research*, *12*(6), 964–975. doi: 10.1287/opre.12.6.964

Ibarra-Rojas, O. J., Delgado, F., Giesen, R., & Muñoz, J. C. (2015). Planning, operation, and control of bus transport systems: A literature review. *Transportation Research Part B: Methodological*, *77*, 38–75. doi: 10.1016/J.TRB.2015.03.002

Inci, E. (2015). A Review of the Economics of Parking. *Economics of Transportation*, *4*(1), 50–63. doi: 10.1016/j.ecotra.2014.11.001

Jara-Díaz, S. (1982a). The estimation of transport cost functions: A methodological review. *Transport Reviews*, *2*(3), 257–278. doi: 10.1080/01441648208716498

Jara-Díaz, S. (1982b). Transportation product, transportation function and cost functions. *Transportation Science*, *16*(4), 522–539. doi: 10.1287/trsc.16.4.522

Jara-Díaz, S., & Basso, L. J. (2003). Transport cost functions, network expansion and economies of scope. *Transportation Research Part E: Logistics and Transportation Review*, *39*(4), 271–288. doi: 10.1016/S1366-5545(03)00002-4

Jara-Díaz, S., & Cortés, C. (1996). On the calculation of scale economies from transport cost functions. *Journal of Transport Economics and Policy*, *30*(2), 157–170. Retrieved from https://www.jstor.org/stable/20053107

Jara-Díaz, S., Fielbaum, A., & Gschwender, A. (2017). Optimal fleet size, frequencies and vehicle capacities considering peak and off-peak periods in public transport. *Transportation Research Part A: Policy and Practice*, *106*, 65–74. doi: 10.1016/J.TRA.2017.09.005

Jara-Díaz, S., & Gschwender, A. (2003a). From the single line model to the spatial structure of transit services: Corridors or Direct? *Journal of Transport Economics and Policy*, *37*(2), 261–277.

Jara-Díaz, S., & Gschwender, A. (2003b). Towards a general microeconomic model for the operation of public transport. *Transport Reviews*, *23*(4), 453–469. doi: 10.1080/0144164032000048922

Jara-Díaz, S., & Gschwender, A. (2009). The effect of financial constraints on the optimal design of public transport services. *Transportation*, *36*(1), 65–75. doi: 10.1007/s11116-008-9182-8

Jara-Díaz, S., & Tirachini, A. (2013). Urban Bus Transport: Open all doors for boarding. *Journal of Transport Economics and Policy*, *47*(1), 91–106. Retrieved from https://ideas.repec.org/a/tpe/jtecpo/v47y2013i1p91-106.html

Kockelman, K. (2017). *An assessment of autonomous vehicles: Traffic impacts and infrastructure needs*. Austin. Retrieved from http://library.ctr.utexas.edu/ctr-publications/0-6847-1.pdf

Kohli, S., & Willumsen, L. G. (2016). Traffic forecasting and automated vehicles. *44th European Transport Conference*. Barcelona: European Transport Conference. Retrieved from http://www.steerdaviesgleave.com/sites/default/files/elfinder/Traffic-forecasting-and-automated-vehicles-Kohli-Willumsen.pdf

Kuah, G. K., & Perl, J. (1988). Optimization of feeder bus routes and bus-stop spacing. *Journal of Transportation Engineering*, *114*(3), 341–354. doi: 10.1061/(ASCE)0733-947X(1988)114:3(341)

Larson, R., & Odoni, A. (2007). *Urban operations research* (2nd ed.). Belmont, Mass.: Dynamic Ideas.

Li, Z.-C., Chen, Y.-J., Wang, Y.-D., Lam, W. H. K., & Wong, S. C. (2013). Optimal density of radial major roads in a two-dimensional monocentric city with

endogenous residential distribution and housing prices. *Regional Science and Urban Economics*, *43*(6), 927–937. doi: 10.1016/j.regsciurbeco.2013.09.010

Lioris, J., Pedarsani, R., Tascikaraoglu, F. Y., & Varaiya, P. (2017). Platoons of connected vehicles can double throughput in urban roads. *Transportation Research Part C: Emerging Technologies*, *77*, 292–305. doi: 10.1016/j.trc.2017.01.023

Litman, T. (2016). *Transportation cost and benefit analysis techniques, estimates and implications*. Victoria. Retrieved from http://www.vtpi.org/tca/

Litman, T. (2018). *Autonomous vehicle implementation predictions: Implications for transport planning*. Victoria. Retrieved from https://www.vtpi.org/avip.pdf

Magnanti, T. L., & Wong, R. T. (1984). Network design and transportation planning: Models and algorithms. *Transportation Science*, *18*(1), 1–55. doi: 10.1287/trsc.18.1.1

Marshall, W. E., & Garrick, N. W. (2010). Street network types and road safety: A study of 24 California cities. *Urban Design International*, *15*(3), 133–147. doi: 10.1057/udi.2009.31

Martínez-Díaz, M., Soriguera, F., & Pérez, I. (2018a). Autonomous driving: a bird's eye view. *IET Intelligent Transport Systems*, 1–17. doi: 10.1049/iet-its.2018.5061

Martínez-Díaz, M., Soriguera, F., & Pérez, I. (2018b). Technology: A necessary but not sufficient condition for future personal mobility. *Sustainability*, *10*(11), 4141. doi: 10.3390/su10114141

Mathew, T. V., & Sharma, S. (2009). Capacity Expansion Problem for Large Urban Transportation Networks. *Journal of Transportation Engineering*, *135*(7), 406–415. doi: 10.1061/(ASCE)0733-947X(2009)135:7(406)

McDonald, J. (1987). The identification of urban employment subcenters. *Journal of Urban Economics*, *21*(2), 242–258. doi: 10.1016/0094-1190(87)90017-9

McDonald, J., & McMillen, D. (1990). Employment subcenters and land values in a polycentric urban area: the case of Chicago. *Environment and Planning A*, *22*(12), 1561–1574. doi: 10.1068/a221561

McDonald, J., & Prather, P. (1994). Suburban employment centres: The Case of Chicago. *Urban Studies*, *31*(2), 201–218. doi: 10.1080/00420989420080201

McMillen, D., & McDonald, J. (1998). Suburban subcenters and employment density in Metropolitan Chicago. *Journal of Urban Economics*, *43*(2), 157–180. doi: 10.1006/juec.1997.2038

Medina-Tapia, M. (2011). *Localización óptima de paradas de buses en corredor de transporte público en base a estructura de viajes en múltiples períodos: aplicación en corredor de transporte público de Avenida Grecia*. Thesis to obtain the Master's degree in Engineering, Pontificia Universidad Católica de Chile.

Medina-Tapia, M., Giesen, R., & Muñoz, J. C. (2013). Model for the optimal location of bus stops and its application to a public transport corridor in Santiago, Chile. *Transportation Research Record: Journal of the Transportation*

Research Board, *2352*, 84–93. doi: 10.3141/2352-10

Medina-Tapia, M., & Robusté, F. (2018a). Exploring paradigm shift impacts in urban mobility: Autonomous Vehicles and Smart Cities. *Proceedings of XIII Spanish Transportation Engineering Congress, Gijón, Spain*.

Medina-Tapia, M., & Robusté, F. (2018b). Exploring paradigm shift impacts in urban mobility: Autonomous Vehicles and Smart Cities. *Transportation Research Procedia*, *33*, 203–210. doi: 10.1016/j.trpro.2018.10.093

Medina-Tapia, M., & Robusté, F. (2018c). Impact assessment of autonomous vehicle implementation on urban road networks. *Proceedings of Pan-American Conference on Traffic, Transportation Engineering and Logistics*.

Medina-Tapia, M., & Robusté, F. (2019a). Diseño óptimo de redes de transporte público que se adaptan a condiciones locales y no-homogéneas en una ciudad circular. *III Campus Científico Del FIT*. Cercedilla, Madrid.

Medina-Tapia, M., & Robusté, F. (2019b). Implementation of connected and autonomous vehicles in cities could have neutral effects on the total travel time costs: modeling and analysis for a circular city. *Sustainability*, *11*(2), 482. doi: 10.3390/su11020482

Medina-Tapia, M., & Robusté, F. (2019c). Ingeniería de transporte y planificación urbana: Diseño de redes de transporte público en una ciudad concéntrica. *14th Edition of the CIMNE Coffee Talks*. Barcelona.

Medina-Tapia, M., Robusté, F., & Estrada, M. (2020). Modeling public transportation networks for a circular city: the role of urban subcenters and mobility density. *Transportation Research Procedia*, *47*, 353–360. doi: 10.1016/j.trpro.2020.03.109

Medina-Tapia, M., Robusté, F., & Estrada, M. (2021). Adaptive transit network design for spatially heterogeneous demand. *Submitted to a Journal for Publication*.

Meyer, J., Becker, H., Bösch, P. M., & Axhausen, K. W. (2017). Autonomous vehicles: The next jump in accessibilities? *Research in Transportation Economics*, *62*, 80–91. doi: 10.1016/J.RETREC.2017.03.005

Mills, E., & de Ferranti, D. (1971). Market choices and optimum city size. *The American Economic Review*, *61*(2), 340–345. Retrieved from http://www.jstor.org/stable/1817012

Miyagawa, M. (2018). Spacing of intersections in hierarchical road networks. *Journal of the Operations Research Society of Japan*, *61*(4), 272–280. doi: 10.15807/jorsj.61.272

MTT. (2012). *Encuesta Origen-Destino de Viajes 2012*. Santiago, Chile: Gobierno de Chile, Ministerio de Transportes y Telecomunicaciones.

National Highway Traffic Safety Administration (NHTSA). (2016). *Federal automated vehicles policy*. Washington, DC. Retrieved from https://one.nhtsa.gov/nhtsa/av/av-policy.html

Newell, G. F. (1971). Dispatching policies for a transportation route.

Transportation Science, *5*(1), 91–105. doi: 10.1287/trsc.5.1.91

Newell, G. F. (1973). Scheduling, location, transportation, and continuum mechanics: Some simple approximations to optimization problems. *SIAM Journal on Applied Mathematics*, *25*(3), 346–360. doi: 10.1137/0125037

Nourbakhsh, S. M. (2014). *Transit network design for areas with low and/or heterogeneous demand* (University of Illinois at Urbana-Champaign). University of Illinois at Urbana-Champaign. Retrieved from https://www.ideals.illinois.edu/handle/2142/73089

Ortúzar, J. de D., & Willumsen, L. G. (2011). *Modelling transport* (4th ed.). Chichester: United Kingdom: John Wiley.

Ouyang, Y., & Daganzo, C. F. (2006). Discretization and validation of the continuum approximation scheme for terminal system design. *Transportation Science*, *40*(1), 89–98. doi: 10.1287/trsc.1040.0110

Ouyang, Y., Nourbakhsh, S. M., & Cassidy, M. J. (2014). Continuum approximation approach to bus network design under spatially heterogeneous demand. *Transportation Research Part B: Methodological*, *68*, 333–344. doi: 10.1016/j.trb.2014.05.018

Pakusch, C., Stevens, G., Boden, A., & Bossauer, P. (2018). Unintended effects of autonomous driving: A study on mobility preferences in the future. *Sustainability*, *10*(7), 2404. doi: 10.3390/su10072404

Pilachowski, J. (2009). An Approach to Reducing Bus Bunching (University of California, Berkeley). University of California, Berkeley. Retrieved from https://escholarship.org/uc/item/6zc5j8xg

Portugal, L., Sarmiento, I., Florez, J., & Robusté, F. (1996). Estrategia para un uso modal y ambiental mas eficiente del espacio viario urbano. *Estudios de Transportes y Comunicaciones*, *1*(73), 7–34.

Precht, A., Reyes, S., & Salamanca, C. (2016). *El ordenamiento territorial de Chile* (1st ed). Santiago, Chile: Ediciones UC. Retrieved from https://www.jstor.org/stable/j.ctt1qv5p10

Pulido, R., Muñoz, J. C., & Gazmuri, P. (2015). A continuous approximation model for locating warehouses and designing physical and timely distribution strategies for home delivery. *EURO Journal on Transportation and Logistics*, *4*(4), 399–419. doi: 10.1007/s13676-014-0059-z

Roca-Riu, M., Estrada, M., & Trapote, C. (2012). The design of interurban bus networks in city centers. *Transportation Research Part A: Policy and Practice*, *46*(8), 1153–1165. doi: 10.1016/j.tra.2012.05.011

Rodrigue, J. P., Comtois, C., & Slack, B. (2017). *The Geography of transport systems* (4th ed). New York: Routledge. Retrieved from https://transportgeography.org/

Russo, F., & Musolino, G. (2012). A unifying modelling framework to simulate the Spatial Economic Transport Interaction process at urban and national scales. *Journal of Transport Geography*, *24*, 189–197. doi:

10.1016/J.JTRANGEO.2012.02.003

Saka, A. A. (2001). Model for Determining Optimum Bus-Stop Spacing in Urban Areas. *Journal of Transportation Engineering*, *127*(3), 195–199. doi: 10.1061/(ASCE)0733-947X(2001)127:3(195)

Sánchez, R., Velasco, F., & Medina-Tapia, M. (2013). Modelación espacial para la identificación de subcentros de empleo en el Gran Santiago. *Congreso Chileno de Ingeniería de Transporte*, (16). Santiago, Chile. Retrieved from https://congresotransporte.uchile.cl/index.php/CIT/article/view/28481

Schoon, J. (1996). *Transportation systems and service policy. A project-based introduction*. Springer US. doi: 10.1007/978-1-4615-4076-2

Sheshinski, E. (1973). Congestion and the optimum city size. *American Economic Review*, *63*(2), 61–66. Retrieved from http://search.ebscohost.com/login.aspx?direct=true&db=bth&AN=4504512&site=ehost-live&scope=site

Smeed, R. J. (1965). A theoretical model of commuter traffic in towns. *IMA Journal of Applied Mathematics*, *1*(3), 208–225. doi: 10.1093/imamat/1.3.208

Smeed, R. J. (1968). Traffic studies and urban congestion. *Journal of Transport Economics and Policy*, *2*(1), 33–70. Retrieved from http://www.jstor.org/stable/20052080

Smith, B. W. (2012). Managing autonomous transportation demand. *Santa Clara Law Review*, *52*(4), 1401–1422. Retrieved from http://digitalcommons.law.scu.edu/lawreview/vol52/iss4/8

Smith, R. (2014). *Large-scale transit service network design under continuous heterogeneous demand* (University of Illinois at Urbana-Champaign). University of Illinois at Urbana-Champaign. Retrieved from https://www.ideals.illinois.edu/handle/2142/49736

Snellen, D., Borgers, A., & Timmermans, H. (2002). Urban form, road network type, and mode choice for frequently conducted activities: A multilevel analysis using quasi-experimental design data. *Environment and Planning A: Economy and Space*, *34*(7), 1207–1220. doi: 10.1068/a349

Solow, R. (1972). Congestion, density and the use of land in transportation. *The Swedish Journal of Economics*, *74*(1), 161–173. doi: 10.2307/3439015

Solow, R. (1973). Congestion cost and the use of land for streets. *The Bell Journal of Economics and Management Science*, *4*(2), 602–618. doi: 10.2307/3003055

Solow, R., & Vickrey, W. (1971). Land use in a long narrow city. *Journal of Economic Theory*, *3*(4), 430–447. doi: 10.1016/0022-0531(71)90040-8

Thompson, G. L. (1977). Planning Considerations for Alternative Transit Route Structures. *Journal of the American Institute of Planners*, *43*(2), 158–168. doi: 10.1080/01944367708977773

Tientrakool, P., Ho, Y.-C., & Maxemchuk, N. F. (2011). Highway capacity benefits from using vehicle-to-vehicle communication and sensors for collision avoidance. *IEEE Vehicular Technology Conference (VTC Fall)*, 1–5. doi:

10.1109/VETECF.2011.6093130

Tirachini, A., Hensher, D. A., & Jara-Díaz, S. (2010). Comparing operator and users costs of light rail, heavy rail and bus rapid transit over a radial public transport network. *Research in Transportation Economics*, *29*(1), 231–242. doi: 10.1016/J.RETREC.2010.07.029

Transportation Research Board. (2010). *Highway Capacity Manual* (6th ed). Washington, D.C.: Transportation Research Board. Retrieved from http://www.trb.org/Main/Blurbs/175169.aspx

Transportation Research Board. (2013). *Transit Capacity and Quality of Service Manual* (3rd ed). Washington, D.C.: Transportation Research Board. doi: 10.17226/24766

Tsekeris, T., & Geroliminis, N. (2013). City size, network structure and traffic congestion. *Journal of Urban Economics*, *76*, 1–14. doi: 10.1016/j.jue.2013.01.002

UN-Habitat III. (2016). *New Urban Agenda* (1st ed). Quito, Ecuador: United Nations. Retrieved from www.habitat3.org

van Zuylen, H., & Taale, H. (2004). Urban networks with ring roads: Two-level, three-player game. *Transportation Research Record: Journal of the Transportation Research Board*, *1894*, 180–187. doi: 10.3141/1894-19

VanderWerf, J., Shladover, S., Kourjanskaia, N., Miller, M., & Krishnan, H. (2001). Modeling effects of driver control assistance systems on traffic. *Transportation Research Record: Journal of the Transportation Research Board*, *1748*, 167–174. doi: 10.3141/1748-21

VanderWerf, J., Shladover, S., Miller, M., & Kourjanskaia, N. (2002). Effects of adaptive cruise control systems on highway traffic flow capacity. *Transportation Research Record: Journal of the Transportation Research Board*, *1800*, 78–84. doi: 10.3141/1800-10

Vaughan, R. (1986). Optimum polar networks for an urban bus system with a many-to-many travel demand. *Transportation Research Part B: Methodological*, *20*(3), 215–224. doi: 10.1016/0191-2615(86)90018-4

Vuchic, V. (2007). *Urban Transit: Systems and Technology* (1st ed). New Jersey, EE.UU.: John Wiley & Sons, Inc.

Vuchic, V., & Newell, G. F. (1968). Rapid transit interstation spacings for minimum travel time. *Transportation Science*, *2*(4), 303–339. doi: 10.1287/trsc.2.4.303

Wadud, Z., MacKenzie, D., & Leiby, P. (2016). Help or hindrance? The travel, energy and carbon impacts of highly automated vehicles. *Transportation Research Part A: Policy and Practice*, *86*, 1–18. doi: 10.1016/J.TRA.2015.12.001

Wang, D. Z., & Lo, H. K. (2010). Global optimum of the linearized network design problem with equilibrium flows. *Transportation Research Part B: Methodological*, *44*(4), 482–492. doi: 10.1016/J.TRB.2009.10.003

Wegener, M., & Fürst, F. (2004). Land-use transport interaction: State of the Art.

In *SSRN Electronic Journal*. Dortmund. doi: 10.2139/ssrn.1434678

Wirasinghe, S. C. (1980). Nearly optimal parameters for a rail/feeder-bus system on a rectangular grid. *Transportation Research Part A: General*, *14*(1), 33–40. doi: 10.1016/0191-2607(80)90092-8

Wirasinghe, S. C., & Ghoneim, N. S. (1981). Spacing of bus-stops for many to many travel demand. *Transportation Science*, *15*(3), 210–221. doi: 10.1287/trsc.15.3.210

Wong, S. C. (1998). Multi-commodity traffic assignment by continuum approximation of network flow with variable demand. *Transportation Research Part B: Methodological*, *32*(8), 567–581. doi: 10.1016/S0191-2615(98)00018-6

Yang, H. (1997). Sensitivity analysis for the elastic-demand network equilibrium problem with applications. *Transportation Research Part B: Methodological*, *31*(1), 55–70. doi: 10.1016/S0191-2615(96)00015-X

Zakharenko, R. (2016). Self-driving cars will change cities. *Regional Science and Urban Economics*, *61*, 26–37. doi: 10.1016/J.REGSCIURBECO.2016.09.003

Zhang, W., Guhathakurta, S., Fang, J., & Zhang, G. (2015). Exploring the impact of shared autonomous vehicles on urban parking demand: An agent-based simulation approach. *Sustainable Cities and Society*, *19*, 34–45. doi: 10.1016/J.SCS.2015.07.006

Ziyou, G., & Yifan, S. (2002). A reserve capacity model of optimal signal control with user-equilibrium route choice. *Transportation Research Part B: Methodological*, *36*(4), 313–323. doi: 10.1016/S0191-2615(01)00005-4

Appendices

Appendix A. Nomenclature

1. General nomenclature

Table A.1. General parameters used for the modeling.

General parameters	
T	duration of the peak period or rush hour [h/P_m];
P_m	rush hour of the city that is the period of analysis.

2. Transit systems

Table A.2 and Table A.3 present the decision variables for two types of design problems of public transportation: fixed and flexible spatial transit systems, respectively.

Table A.2. Decision variables to model a fixed-spatial transit.

Variables	
$d^c(r)$	distance between ring transit routes with a radius r [km/route];
$\Phi^r(\theta)$	angle between radial routes with an angle θ [radian/route], which $d^r(r,\theta) = \Phi^r(\theta) \cdot r$, where $d^r(r,\theta)$ is the distance between radial routes at a point (r,θ);
$h^c(r)$	headway between vehicles at a circular route on r [h/veh];
$h^r(\theta)$	headway between vehicles at a radial route on θ [h/veh];

Table A.3. Decision variables to model a flexible-spatial transit.

Decision variables	
$d^c(r,\theta)$	distance between ring transit routes at a point (r,θ) [km/route];
$\Phi^r(r,\theta)$	angle between radial transit routes at a point (r,θ) [rad/route], which $d^r(r,\theta) = \Phi^r(r,\theta) \cdot r$, where $d^r(r,\theta)$ is the distance between radial routes at a point (r,θ);
H	headway between vehicles in the system [h/veh].

Table A.4, Table A.5, and Table A.6 contain the list of parameters used in the modeling: the density functions in each stage of a trip (access, waiting, in-vehicle travel, and transfer stage), the parameters to model the behavior of users, and the operation of the system, and the unitary costs for the objective function of the model.

Table A.4. Demand density functions of a transit system.

Demand functions	
$f^A(r,\theta)$	user density who board and alight from a transit vehicle [user/km²·h];
$f_l^W(r,\theta)$	user density who wait for a transit vehicle with direction $l \in L$ [user/km²·h];
$f_l^V(r,\theta)$	user density who travel on a transit vehicle with direction $l \in L$ [user/km·h];
$f_l^T(r,\theta)$	user density who transfer between two vehicles of transit with direction $l \in L$ [user/km²·h].

Table A.5. Parameters to model users and the operation of a transit system.

User and operational parameters	
α	perception of accessibility time by users [dimensionless];
β	perception of waiting time by users [dimensionless];
γ	perception of on-vehicle time by users [dimensionless];
δ	perception of transfer time by users [dimensionless];
$v^a(r)$	average access speed to access or egress in a route at radius r [km/h·route];
v^w	average walking speed of transferring between stations [km/h];
v^t	cruising speed of a transit vehicle [km/h];
τ	average time lost by braking ($v^t/2 \cdot a^d$) and acceleration ($v^t/2 \cdot a^a$) of a vehicle at a station where a^a is the acceleration when a transit vehicle leaves a station [km/h²] and a^d is the braking when a transit vehicle enters a station [km/h²]. Thus, $\tau = v^t \cdot (1/a^a + 1/a^d)/2$ [h/station].
τ'	average fixed dead time per station/stop by a transit vehicle [h/station];
τ''	stopping time by a transit vehicle at a station [h/station];
τ'''	the time lost by crossing an intersection [h/station];
t^f	positioning time at a terminal by a transit vehicle [h];
η^d	number of work shifts on a vehicle [shift/veh];
χ^T	average walking distance between two stops [km];
K^v	vehicle capacity [user/veh];
K^h	minimum time between consecutive vehicles [h/veh];
$K^{d(c)}$	minimum separation between two transit routes [km/route];
$K^{d(r)}$	minimum separation between two transit routes [rad/route], which $K^{d(r)} = K^{d(c)}/r_{min}$ where r_{min} is the minimum radius to lie a ring of the circular city.

Table A.6. Unitary costs of the objective function of a transit system.

Unitary cost parameters	
μ	travel time value by average user [$/user·h];
φ^k	unitary cost per vehicle [$/veh·$P_m$]. This cost ($\varphi^k = A + p_t \cdot s_t + p_b$) depends on the administration cost (A in [$/veh·$P_m$]), the cost of the terminal area (p_m in [$/m²·$P_m$]), the area per vehicle (s_t in [m²/veh]), and the vehicle price (p_b in [$/veh·$P_m$]);
φ^g	driver's wage per hour [$/shift·h];
φ^o	operating cost per kilometer traveled on a cruising speed [$/veh·km·route];
φ^p	linear infrastructure cost [$/km·route·$P_m$] which it considers a maintenance-fixed component ($\varphi^{p(f)}$ in [$/km·route·$P_m$]) and a maintenance variable cost ($\varphi^{p(v)}$ in [$/km·route·h]). Thus, $\varphi^p = \varphi^{p(f)} + \varphi^{p(v)} \cdot T$;
φ^s	nodal (stop or station) infrastructure cost [$/station·route· P_m] has two components: a fixed installation cost ([$/station·route·$P_m$]), and a maintenance (operation) variable cost ([$/station·route·h]). Thus, $\varphi^s = \varphi^{s(f)} + \varphi^{s(v)} \cdot T$.

Additionally, dependent variables use the previous parameters and variables. Table A.7 includes time functions in each stage of trips.

Table A.7. Time functions of a transit system modeling.

Time functions	
$t^A(r,\theta)$	average time spent by a user on access to the closest station and egress from this [h];
$t_l^W(r,\theta)$	average waiting time by a user at a station [h];
$t_l^V(r,\theta)$	travel time per kilometer incurred by a user on a transit vehicle with direction l [h/km];
$t_l^T(r,\theta)$	average transfer time function incurred by a user when he transfers between two modes [h];
$t_l^c(\cdot)$	cycle time a vehicle on a corridor line of type $l = \{c, r\}$ [h/route].

3. Traffic systems

Table A.8 presents the decision variables for designing private networks.

Table A.8. Decision variables to model traffic systems.

Decision variables	
$p^c(r)$	distance function between ring roads at the radius r km [km/road];
$\Psi^r(\theta)$	angle function between radial roads at an angle θ [radian/road] where $p^r(r,\theta) = \Psi^r(\theta) \cdot r$ is the distance between radial roads at a city point (r,θ) [km/road].

Table A.9, Table A.10, and Table A.11 contain the list of parameters used in the modeling: the demand density functions obtained from the assignment

method, the list of parameters used in the modeling, and the unitary costs for the objective function of the model.

Table A.9. Demand density functions of a traffic system.

Demand functions	
$f^F_{w,v}(r,\theta)$	density of vehicles of type $v \in V$ that access from the origin to the closest circular or radial primary road $w \in W$ [veh/km²·h];
$f^R_{w,v}(r,\theta)$	flow density of vehicles of type $v \in V$ that travel on a circular or radial primary road $w \in W$ considering its direction [veh/km·h];
$f^A_{w,v}(r,\theta)$	density of vehicles of type $v \in V$ that arrive from a circular or radial primary road to the destination $w \in W$ [veh/km²·h].

Table A.10. Parameters to model users and the operation of a traffic system.

User and operational parameters	
η_u	average number of users in a car of type $v \in V$ [user/veh];
v^F_v	car speed of type $v \in V$ to access main roads of a city [km/h];
v^A_v	car speed of type $v \in V$ to access local roads of a city [km/h];
v^{ff}_v	free-flow car speed of type $v \in V$ on a primary road [km/h];
v^p_v	cruising speed of a car $v \in V$ looking for a parking spot [km/h];
v^a	average walking speed for accessing the destination point from the parking site [km/h];
$t^{F\prime}_v$	average penalization time for accessing the primary road in a car $v \in V$ [h];
$t^{A\prime}_v$	average penalization time for accessing the local roads in a car $v \in V$ [h];
a and b	parameters of BPR volume-delay function [dimensionless];
k_v	capacity road per lane [veh/lane·h];
η^l	number of lanes at a road [lane];
τ^i_v	average time spent by a vehicle of type $v \in V$ when crosses a crossroad on the road [h/veh];
λ_P	average density of vacant parking space [parking/km];
d_p	distance before arriving at a destination where the drivers begin to look for a parking spot [km].

Table A.11. Unitary costs of the objective function of a traffic system.

Unitary cost parameters	
μ_v	value of travel time of users in a vehicle of type $v \in V$ [$/user·h];
φ^t_v	car cost of type $v \in V$ per distance unit [$/km·veh];
φ^f	parking fee [$/h·veh];
φ^p_v	linear infrastructure cost for a road and a car of type $v \in V$ [$/km], which it considers a maintenance-fixed component ($\varphi^{p(f)}_v$ in [$/km·road·$P_m$]) and a maintenance variable cost ($\varphi^{p(v)}_v$ in [$/km·road·h]). Thus, $\varphi^p_v = \varphi^{p(f)}_v + \varphi^{p(v)}_v \cdot T$.

Additionally, dependent variables use the previous parameters and variables. Table A.12 shows the cost functions of users. Table A.13 shows the generalized cost functions in which previous parameters and variables are part of these.

Table A.12. Cost functions of users of a traffic system.

User cost functions	
$c^F_{w,v}(r,\theta)$	average access cost of a car $v \in V$ for accessing to a circular or radial primary road $w \in W$ [$/veh];
$c^R_{w,v}(r,\theta)$	generalized travel cost of a car $v \in V$ on a circular or radial primary road $w \in W$ [$/km·veh];
$c^A_{w,v}(r,\theta)$	average destination cost of a car $v \in V$ when it arrives from a circular or radial primary road $w \in W$ [$/veh].

Table A.13. Generalized costs of a traffic system.

Generalized cost functions	
κ^F_v	unitary cost factor per accessing distance to the main road where $\kappa^F_v = \mu_v \cdot \eta_u / v^F_v + \varphi^t_v$ [$/km·veh];
$\kappa^{F\prime}_v$	penalty cost factor per accessing time to a main where $\kappa^{F\prime}_v = \mu_v \cdot \eta_u + v^F_v \cdot \varphi^t_v$ [$/h·veh];
κ^P_v	unitary cost of looking for a parking space where $\kappa^P_v = \mu_v / v^p_v + \varphi^t_v$ [$/km·veh];
κ^A_v	unitary cost factor per accessing distance to local roads where $\kappa^A_v = \mu_v / v^A_v + \varphi^t_v$ [$/km·veh];
$\kappa^{A\prime}_v$	unitary cost factor per accessing time to local roads where $\kappa^{A\prime}_v = \mu_v + v^F_v \cdot \varphi^t_v$ [$/h·veh].

Appendix B. Methods of demand modeling on continuous two-dimensional space

1. Introduction

The modeling of a transportation system requires quantifying the demand. One of the main parameters of the proposed model is the demand distribution function $D(r_f, \theta_f, r_t, \theta_t)$ in [user/km^4·h]. Vaughan (1986) proposed this trip density meaning the spatial density in polar coordinates of users per hour who begin a trip from an area $dr_f\ r_f\ d\theta_f$ in [km^2] about an origin (r_f, θ_f) to an area $dr_t\ r_t\ d\theta_t$ in [km^2] about a destination (r_t, θ_t). This function allows modeling the generation, attraction, and distribution of trips over continuous and two-dimensional space. Thus, the trip density function is an input for the continuous approximation method to design transportation networks.

In the literature, some investigations analyze this topic. Vaughan (1986) defines the criteria of the route taken by users to access the nearest destination considering polar coordinates. Using these criteria, Chen et al. (2015) determine the probability by demand takes a transit route. Nourbakhsh (2014) defines formulations for each stage of a trip in a concentric city. Unfortunately, Nourbakhsh (2014) does not consider the angle of origins depends on destinations (θ_t).

The objective is to develop a methodology to obtain demand densities over a continuous space for each stage of a public and private transportation trip through analytical functions considering the all-or-nothing assignment. The all-or-nothing assignment method considers that all users choose the shortest distance path, assuming an uncongested system.

The next point presents the formulation of analytical demand density functions for the all-or-nothing assignment method applied to the transit system on continuous space. Moreover, this appendix includes the analysis of this analytical methodology using a numerical example. Finally, the appendix presents conclusions on the proposed method.

2. All-or-nothing assignment model for transit systems on a continuous space

A trip on a transit system has four stages: accessing to/from a station, waiting for a transit vehicle, traveling on a transit vehicle, and transferring between routes.

2.1. Passenger density accessing to/from a station

In Equation B.1, the density of users at a point (r, θ) that access to and from the closest transit station ($f^A(r, \theta)$ in [user/km²·h]) represents the first stage of the classical transportation model, which considers the generation and attraction of trips.

$$f^A(r,\theta) = \int_0^{2\pi}\int_0^R D(r,\theta,r_t,\theta_t)\, r_t\, dr_t\, d\theta_t + \int_0^{2\pi}\int_0^R D\left(r_f,\theta_f,r,\theta\right) r_f\, dr_f\, d\theta_f \qquad (B.1)$$

Proof. The first integral in Equation B.1 represents users that travel from an origin point (r, θ) to the rest of a circular city. The second integral represents users that come from any point of the city to a destination (r, θ).

2.2. Passenger density waiting for a transit vehicle

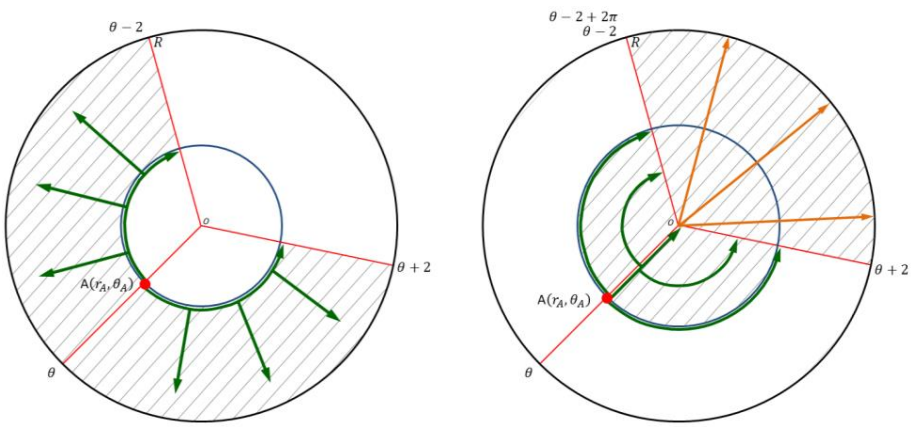

(a) Users board circular services. (b) Users board on radial services.

Figure B.1. Mobility patterns of users that wait and board a route.

- *Ring routes*: $f_c^W(r, \theta)$ represents the user density that waits for a circular service in [user/km²·h] (Equation B.2).

$$f_c^W(r,\theta) = \int_{\theta-2}^{\theta+2} \int_{r}^{R} D(r,\theta,r_t,\theta_t)\, r_t\, dr_t\, d\theta_t \qquad (B.2)$$

Proof. In Figure B.1(a), the green arrows represent the user density that will wait for a circular service if destinations are further to the central point than the origin, i.e., $r_t \geq r_f$ considering destinations are in the hatched zone between the angles $[\theta - 2; \theta + 2]$.

- *Radial routes*: $f_r^W(r,\theta)$ represents the density of users that waits for boarding a radial service ([user/km²·h]), which has two components. In Figure B.1(b), the green arrows represent the trip to the same city side, and the orange arrows are trips to the opposite side of a city.

$$f_r^W(r,\theta) = \int_{\theta-2}^{\theta+2} \int_{0}^{r} D(r,\theta,r_t,\theta_t)\, r_t\, dr_t\, d\theta_t + \int_{\theta+2}^{\theta-2+2\pi} \int_{0}^{R} D(r,\theta,r_t,\theta_t)\, r_t\, dr_t\, d\theta_t \qquad (B.3)$$

Proof. The first integral of Equation B.3 models the demand density of users that wait for a radial service whether the origin is further than the destination concerning the central point ($r_f \geq r_t$). The second integral models passengers that travel to any point of the opposite zone to a point (r,θ), which is the hatched region between $[\theta + 2; \theta - 2 + 2\pi]$.

2.3. Passenger density traveling on a transit vehicle

The density function of passengers traveling on a transit vehicle at a point (r,θ) is in [user/km·h].

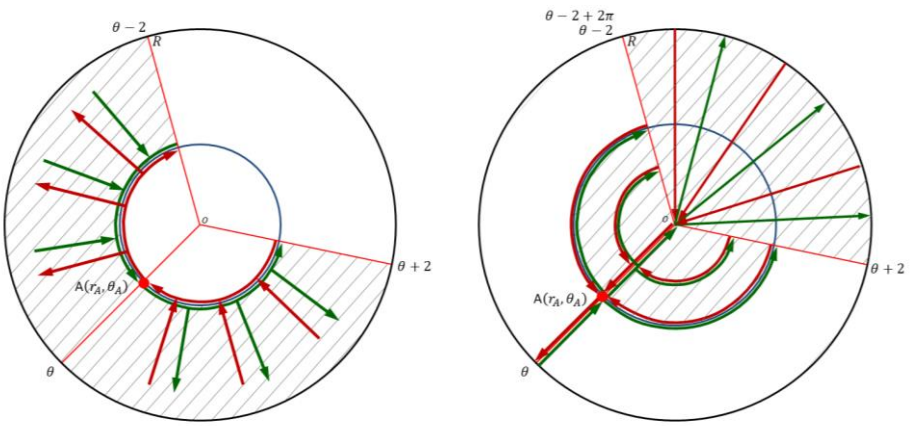

(a) User patterns traveling on rings. (b) User pattern traveling on radials.

Figure B.2. Mobility patterns of users traveling on ring and radial services.

- *Ring routes*: Figure B.2(a) shows the two types of trips on circular services: anticlockwise (the green arrows) and clockwise trips (the red arrows). The formulation bases the functions on Nourbakhsh (2014), but this dissertation considers that the angle of origins depends on destinations (θ_t).

Anticlockwise direction (c_a):

$$f_{c_a}^{V}(r,\theta) = \int_{\theta}^{\theta+2}\int_{r}^{R}\left\{\int_{\theta_t-2}^{\theta} D(r,\theta_f,r_t,\theta_t)\, r\, d\theta_f\right\} r_t\, dr_t\, d\theta_t + \int_{\theta}^{\theta+2}\left\{\int_{\theta_t-2}^{\theta}\int_{r}^{R} D(r_f,\theta_f,r,\theta_t)\, r_f\, dr_f\, d\theta_f\right\} r\, d\theta_t$$

Clockwise direction (c_c):

$$f_{c_c}^{V}(r,\theta) = \int_{\theta-2}^{\theta}\int_{r}^{R}\left\{\int_{\theta}^{\theta_t+2} D(r,\theta_f,r_t,\theta_t)\, r\, d\theta_f\right\} r_t\, dr_t\, d\theta_t + \int_{\theta-2}^{\theta}\left\{\int_{\theta}^{\theta_t+2}\int_{r}^{R} D(r_f,\theta_f,r,\theta_t)\, r_f\, dr_f\, d\theta_f\right\} r\, d\theta_t \quad \text{(B.4)}$$

Total ring density:

$$f_c^{V}(r,\theta) = f_{c_a}^{V}(r,\theta) + f_{c_c}^{V}(r,\theta)$$

Proof. First, in the anticlockwise function at the point (r,θ) (the green arrows in Figure B.2(a)), users directly board a clockwise circular service at the radius r between angles $\theta_t - 2$ and θ, and their destinations are in the hatched zone between θ and $\theta + 2$ (first integral in Equation B.4(r_a)). The anticlockwise circular corridor receives passengers from radial corridors between $\theta_t - 2$ and θ and destination are on the circular corridor between θ and $\theta + 2$ (second integral in Equation B.4(r_a)).

Second, in the clockwise function (the red arrows in Figure B.2(a)), the origins are between angles $\theta_t + 2$ and θ, and the destinations are in the hatched zone between $\theta - 2$ and θ (first integral in Equation B.4(r_c)), and the clockwise circular corridor also receives passengers from radial corridors between angles θ and $\theta_t + 2$ (second integral in Equation B.4(r_c)).

- *Radial routes*: The passenger load density at a point (r,θ) on radial services of transit have two components: the inside-direction (the green arrows in Figure B.2(b)) and the outside-direction trips (the red arrows in Figure B.2(b)).

Inside direction (r_i):

$$f_{r_i}^V(r,\theta) = \int_{\theta-2}^{\theta+2}\int_{0}^{r}\left\{\int_{r}^{R} D(r_f,\theta,r_t,\theta_t)\,dr_f\right\} r_t\,dr_t\,d\theta_t + \int_{\theta+2}^{\theta-2+2\pi}\int_{0}^{R}\left\{\int_{r}^{R} D(r_f,\theta,r_t,\theta_t)\,dr_f\right\} r_t\,dr_t\,d\theta_t$$

Outside direction (r_o):

$$f_{r_o}^V(r,\theta) = \int_{r}^{R}\left\{\int_{\theta-2}^{\theta+2}\int_{0}^{r} D(r_f,\theta_f,r_t,\theta)\,r_f\,dr_f\,d\theta_f\right\} dr_t + \int_{r}^{R}\left\{\int_{\theta+2}^{\theta-2+2\pi}\int_{0}^{R} D(r_f,\theta_f,r_t,\theta)\,r_f\,dr_f\,d\theta_f\right\} dr_t \quad \text{(B.5)}$$

Total radial density:

$$f_r^V(r,\theta) = f_{r_i}^V(r,\theta) + f_{r_o}^V(r,\theta)$$

Proof. First, the inside-direction corridor is used by users that directly boards to the central point on a radial corridor (green arrows in Figure B.2(b)). These trips finish in the same zone (first integral in Equation B.5(r_i)) or in the opposite zone (second integral in Equation B.5(r_i)).

Second, in the outside-direction corridor (red arrows in Figure B.2(b)), the users alight on the same corridor from the same zone (first integral in Equation B.5(r_o)) or the opposite zone (second integral in Equation B.5(r_o)).

2.4. Passenger density transferring between routes

Demand functions of transfers incorporate two cases: passengers who transfer from radial to circular routes, and passengers transfer from circular to radial services.

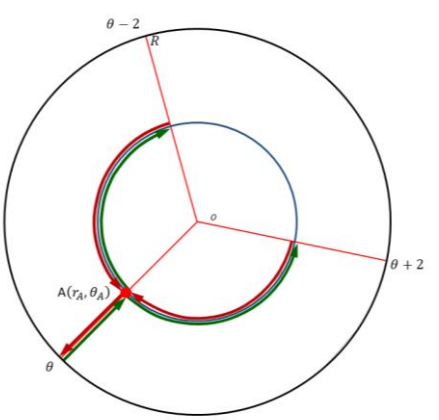

Figure B.3. Mobility patterns of users that transfer between services.

- *Ring routes*: The demand density ($f_c^T(r,\theta)$ in [user/km²·h]) of users can transfer from a radial to a circular service at a point A (the green arrows in Figure B.3).

$$f_c^T(r,\theta) = \int_r^R \int_{\theta-2}^{\theta+2} D(r_f,\theta,r,\theta_t)\, r_t\, d\theta_t\, dr_f \qquad (B.6)$$

Proof. Users board on a radial service with angle θ from the periphery to the point (r,θ), and the destination is on the circular arc with radius r between $\theta-2$ and $\theta+2$ (Equation B.6).

- *Radial routes*: The passenger demand ($f_r^T(r,\theta)$ in [user/km²·h]) can transfer from a circular to a radial service (the red arrows in Figure B.3).

$$f_r^T(r,\theta) = \int_{\theta-2}^{\theta+2} \int_r^R D(r,\theta_f,r_t,\theta)\, r_f\, dr_t\, d\theta_f \qquad (B.7)$$

Proof. Users board at a point on a circular service located on r between the angles $\theta-2$ and $\theta+2$, and the destination is on a radial corridor with angle θ (Equation B.7).

3. Incremental assignment model for traffic systems on a continuous space

For this dissertation, the incremental assignment method divides the distribution matrix at M_n factors ($\sum_n M_n = 1$, where n is the number of iterations). The method progressively assigns trips to the network using a part of the fractioned matrix.

At Step 0, the method uses the all-or-nothing method to assign the first fraction of the distribution matrix. In this step, a trip in a car has three stages explained in these three points: accessing the nearest primary road, traveling in a vehicle, and access to the destination, including parking operations. After that, the model calculates the optimal design problem that allowing determining the travel times considering congestion.

In the next steps, the method takes the next fraction of the matrix and assign trips considering the travel times of the previous step. The model assesses the minimum travel time point to point considering both types of paths: ring-radial and radial-ring streets. After that, the model updates the travel times

of the system. The algorithm finished when the method assigns all trips of the fractioned matrix.

3.1. Vehicle density that accesses a primary road

The vehicle density accessing the nearest primary road will depend on the type of road $f^F_{w,v}(r,\theta)$: ring and radial roads.

- *Ring roads*: The ring density function (Equation B.8 in [user/km²·h]) includes the density of drivers that begin their travels at a point (r,θ), and take a ring road because it is the nearest primary road.

$$f^F_{c,v}(r,\theta) = \int_{\theta-2}^{\theta+2} \int_{r}^{R} D(r,\theta,r_t,\theta_t)\, r_t\, dr_t\, d\theta_t \qquad (B.8)$$

Proof. The density of drivers at (r,θ) that begin their travels taking a ring meets two conditions to ensure that the shortest route begins with a ring. First, their destinations are between two angles $\theta+2$ and $\theta-2$. Second, their destinations are between two radii r and R.

- *Radial roads*: This density function (Equation B.9 in [user/km²·h]) groups users that take a radial road to the same side of a city and users that go to the opposite side, taking two radial roads.

$$f^F_{r,v}(r,\theta) = \int_{\theta-2}^{\theta+2} \int_{0}^{r} D(r,\theta,r_t,\theta_t)\, r_t\, dr_t\, d\theta_t + \int_{\theta+2}^{\theta-2+2\pi} \int_{0}^{R} D(r,\theta,r_t,\theta_t)\, r_t\, dr_t\, d\theta_t \qquad (B.9)$$

Proof. As previously explained, two types of users begin their trips taking the nearest radial road. The first integral of the density function comprises users that travel from (r,θ) to the same side of the city, but the destination is closer to the city center than the origin, i.e., destinations are in a zone between 0 and r. The second integral is composed of users that go to the opposite side, i.e., destinations are in the area between angles $\theta+2$ and $\theta-2+2\pi$.

3.2. Vehicle density in regular trips

The density function of passengers on a transit vehicle at a point (r,θ), in [user/km·h], is the density of users that are travel in a car at this point ($f^R_{w,v}(r,\theta)$). The users can travel on rings to two directions $i \in \{c_c =$

$clockwise, a_c = anticlockwise\}$. For radial corridors, there also are two directions $i \in \{r_i = inside, r_o = outside\}$.

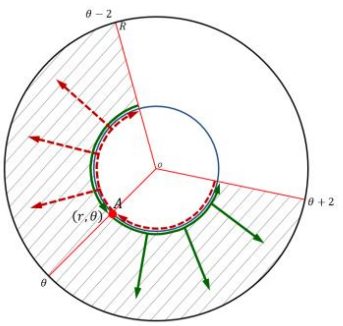

(a) Users drive to the hatched zone on a ring road.

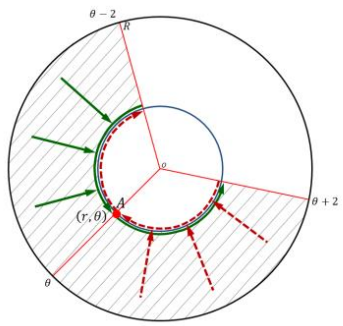

(b) Users drive from the hatched zone on a ring road.

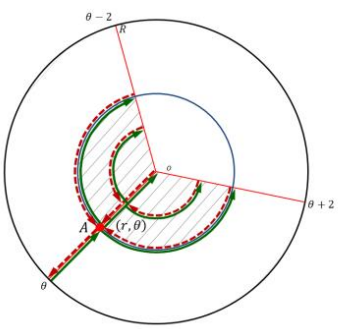

(c) Users drive from/to the hatched zone on a radial road.

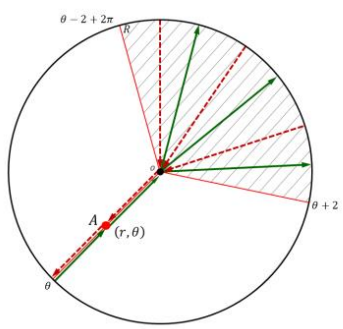

(d) Users drive to the opposite hatched zone on a radial road.

Figure B.4. Mobility patterns when users drive on ring or radial primary roads.

- *Ring roads*: Equations B.10 represent the two types of trips on circular services: anticlockwise (the green arrows in Figure B.4(a) and (b)) and clockwise trips (the red arrows in Figure B.4(a) and (b)). The formulation bases these functions on Nourbakhsh (2014), but this dissertation considers that the angle of origins depends on destinations (θ_t).

Anticlockwise direction (c_a):

$$f^R_{c_a,v}(r,\theta) = \int_{\theta}^{\theta+2}\int_{r}^{R}\left\{\int_{\theta_t-2}^{\theta} D(r,\theta_f,r_t,\theta_t)\, r\, d\theta_f\right\} r_t\, dr_t\, d\theta_t + \int_{\theta}^{\theta+2}\left\{\int_{\theta_t-2}^{\theta}\int_{r}^{R} D(r_f,\theta_f,r,\theta_t)\, r_f\, dr_f\, d\theta_f\right\} r\, d\theta_t$$

Clockwise direction (c_c):

$$f^R_{c_c,v}(r,\theta) = \int_{\theta-2}^{\theta}\int_{r}^{R}\left\{\int_{\theta}^{\theta_t+2} D(r,\theta_f,r_t,\theta_t)\, r\, d\theta_f\right\} r_t\, dr_t\, d\theta_t + \int_{\theta-2}^{\theta}\left\{\int_{\theta}^{\theta_t+2}\int_{r}^{R} D(r_f,\theta_f,r,\theta_t)\, r_f\, dr_f\, d\theta_f\right\} r\, d\theta_t \quad \text{(B.10)}$$

Total ring density:

$$f^R_{c,v}(r,\theta) = f^R_{c_a,v}(r,\theta) + f^R_{c_c,v}(r,\theta)$$

Proof. In a circular road on the radius r (Equation B.10), the first integral represents the density of users that come clockwise from the circular road to the external zone between r and R (green arrows in Figure B.4(a) and (b)). The second integral shows the users that come from the external hatched region to the circular road. The third integral represents the users that travel anticlockwise from the circular road to the external zone (red arrows in Figure B.4(a) and (b)). In the last integral, the users travel anticlockwise from the outer hatched zone to the circular road.

- *Radial roads*: The passenger load density at a point (r,θ) on a radial road has two components (Equations B.11): the inside-direction (the green arrows in Figure B.4(c) and (d)), and the outside-direction trips (the red arrows Figure B.4(c) and (d)).

Inside direction (r_i):

$$f^R_{r_i,v}(r,\theta) = \int_{\theta-2}^{\theta+2}\int_{0}^{r}\left\{\int_{r}^{R} D(r_f,\theta,r_t,\theta_t)\, dr_f\right\} r_t\, dr_t\, d\theta_t + \int_{\theta+2}^{\theta-2+2\pi}\int_{0}^{R}\left\{\int_{r}^{R} D(r_f,\theta,r_t,\theta_t)\, dr_f\right\} r_t\, dr_t\, d\theta_t$$

Outside direction (r_o):

$$f^R_{r_o,v}(r,\theta) = \int_{r}^{R}\left\{\int_{\theta-2}^{\theta+2}\int_{0}^{r} D(r_f,\theta_f,r_t,\theta)\, r_f\, dr_f\, d\theta_f\right\} dr_t + \int_{r}^{R}\left\{\int_{\theta+2}^{\theta-2+2\pi}\int_{0}^{R} D(r_f,\theta_f,r_t,\theta)\, r_f\, dr_f\, d\theta_f\right\} dr_t \quad \text{(B.11)}$$

Total radial density:

$$f^R_{r,v}(r,\theta) = f^R_{r_i,v}(r,\theta) + f^R_{r_o,v}(r,\theta)$$

Proof. In a radial road with angle θ (Equation B.11) to inside direction, users go to the city center (first integral), and users go to the opposite side (second

integral). In this case, users come from the external zone between radii r and R in both integrals (green arrows, Figure B.4(c) and (d), respectively).

Moreover, the density function is also formed by users that come from both the city center (first integral) and the opposite zone (second integral) and go to the zone around the radial road between radii r and R (red arrows, Figure B.4(c) and (d)).

3.3. Vehicle density that parks on-street

In Equation B.12 and B.13, the density of users at a point (r, θ) that access to a destination (r, θ) will depend on the type of roads ($f^A_{w,v}(r, \theta)$): ring or radial road.

- *Circular roads*: $f^A_{c,v}(r, \theta)$ in [user/km²·h] represents the density of trips that access to local roads from a ring (Equation B.12).

$$f^A_{c,v}(r, \theta) = \int_{\theta-2}^{\theta+2} \int_{r}^{R} D(r_f, \theta_f, r, \theta)\, r_f\, dr_f\, d\theta_f \qquad (B.12)$$

Proof. The circular road users (Equation B.12) come from the same side of the city, but the origin is further away from the circular center than the destination.

- *Radial roads*: $f^A_{r,v}(r, \theta)$ in [user/km²·h] represents the density of trips that access to local roads from a radial road (Equation B.13).

$$f^A_{r,v}(r, \theta) = \int_{\theta+2}^{\theta-2+2\pi} \int_{0}^{R} D(r_f, \theta_f, r, \theta)\, r_f\, dr_f\, d\theta_f + \int_{\theta-2}^{\theta+2} \int_{0}^{r} D(r_f, \theta_f, r, \theta)\, r_f\, dr_f\, d\theta_f \qquad (B.13)$$

Proof. The radial street users come from two different city zones (Equation B.13). Firstly, users drive from the same city side, but the origin is closer to the center than the destination (first integral). Secondly, drivers come from the opposite side of the circular city (second integral).

Appendix C. Formulation of urban scenarios

1. Introduction

Cities have heterogeneity regarding the distribution of demand. Particularly, Latin American cities have great inequality between different zones of cities regarding demand, services, equipment, and others. The origin-destination travel matrices reveal this inequality affecting the needs of infrastructure and transportation services. The network design obtained from the modeling requires the application of that on urban scenarios. For this reason, the formulation of several urban scenarios uses mathematical expressions to represent heterogeneous densities of demand on continuous concentric urban space. The analysis considers two types of scenarios: theoretical urban scenarios and the application to a real case: Santiago, Chile.

2. Theoretical scenarios

According to Chapter 4, the dissertation models four theoretical urban scenarios: homogeneous city, heterogeneous city, mono-centric city, and multi-subcenters city. Firstly, each point of a homogeneous city has a stable rate of trip generation and attraction. Secondly, a heterogeneous city is the opposite case to the previous scenario due to each city point has different densities of generation and attraction of trips. Thirdly, a mono-centric city has a central business district (CBD) in which this zone concentrates more trips than other zones of a city. Fourthly, the city contains many subcenters concentrating on economic activities.

The formulation of urban scenarios has a basis on Ouyang et al. (2014). The paper iteratively evaluates the proposed model to a square city. The mathematical expression considers that trip demand varies over space. Moreover, the authors analyze four types of cities, which have different spatial demand distributions: a mono-centric city, a twin city, an asymmetric mono-centric city, and a commuter city.

Equation C.1 contains the demand distribution function $D(x_1, y_1, x_2, y_2)$ from an origin point (x_1, y_1) to a destination point (x_2, y_2) in [user/km^4·h] represented in a Cartesian coordinate system. The function is equivalent to the function proposed by Ouyang et al. (2014); it only has changed on the

nomenclature. The function is the product of an origin ($i = 1$) and destination ($i = 2$) component. Each component contains six components. The first component a_{1i} depends on the type of point. The rest of the parameters depend on the number of points used in the calibration process (m). In that respect, m can be the number of travel generation / attraction zones.

$$D(x_1, y_1, x_2, y_2) = \prod_{i=1}^{2} \left(a_i^0 + \sum_{j=1}^{m} a_{ij}^1 \cdot e^{\left(b_{ij}' \cdot x_i - c_{ij}'\right)^2 + \left(b_{ij}'' \cdot y_i - c_{ij}''\right)^2} \right) \quad (C.1)$$

2.1. Homogeneous scenarios

Each point of a city has an equal rate of trip generation and attraction, i.e., $\lambda(r, \theta)$ and $\rho(r, \theta)$ expressed in Equations 3.2 and 3.3 (p. 38) are stable over the city. Figure C.1 shows an example of a concentric city, which has a radius of 15 km, in which the generation and attraction rate is 1,500 [user/km²·h], and the total trip distribution at each point is 3,000 [user/km²·h].

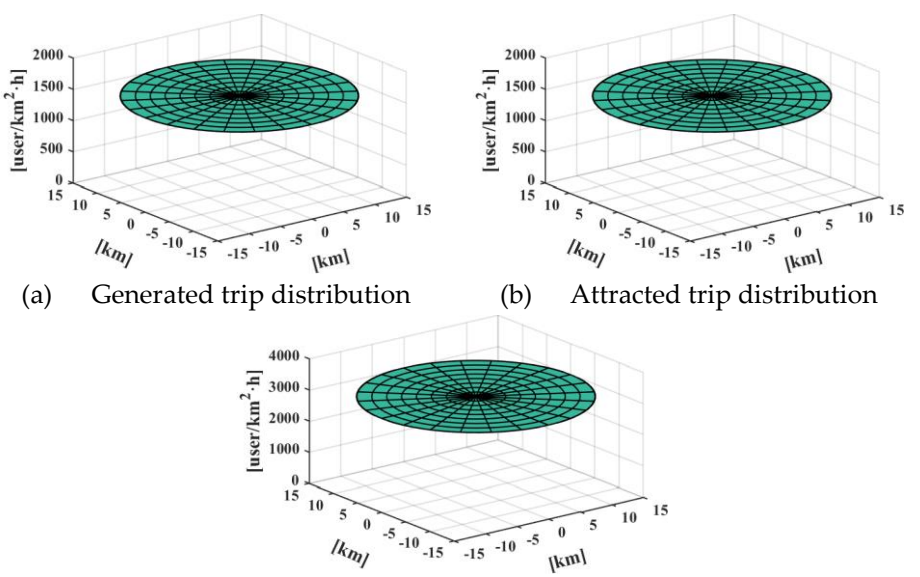

(a) Generated trip distribution (b) Attracted trip distribution

(c) Total trip distribution

Figure C.1. Homogeneous demand scenario that consider a generation/attraction rate of 1,500 [user/km²·h].

Table C.1 contains the list of parameters required by the demand function of Equation C.1 to formulate the continuous mathematical expression. The parameters allow determining a list of progressive urban scenarios in which the demand increases from 100 to 3,500 [user/km²·h]. Therefore, that process

gives equivalent figures to exhibits of **Figure C.1** for the progressive scenarios.

Table C.1. Parameters of demand functions for homogeneous scenarios.

Demand [user/km⁴·h]	m	a_i^0	a_{ij}^1	b'_{ij}	b''_{ij}	c'_{ij}	c''_{ij}
100	1	0.3761	0	0	0	0	0
		0.3761	0	0	0	0	0
250	1	0.5947	0	0	0	0	0
		0.5947	0	0	0	0	0
500	1	0.8410	0	0	0	0	0
		0.8410	0	0	0	0	0
1,000	1	1.1894	0	0	0	0	0
		1.1894	0	0	0	0	0
1,500	1	1.4567	0	0	0	0	0
		1.4567	0	0	0	0	0
2,000	1	1.6821	0	0	0	0	0
		1.6821	0	0	0	0	0
2,500	1	1.8806	0	0	0	0	0
		1.8806	0	0	0	0	0
3,000	1	2.0601	0	0	0	0	0
		2.0601	0	0	0	0	0
3,500	1	2.0601	0	0	0	0	0
		2.0601	0	0	0	0	0

2.2. Non-homogeneous scenarios

The dissertation concentrates its analysis on three types of non-homogeneous scenarios: heterogeneous, mono-centric, and multi-subcenters city. The analysis of the latter two scenarios incorporates a progressive implementation of a mono-center and subcenters, respectively.

Heterogeneous city scenario

The formulation of this scenario comes from a random process considering the same total number of generated/attracted trips in comparison to the homogeneous city. Table C.2 contains the parameters used in this scenario, considering 9 points. The function using these parameters obtains continuous surfaces of trip generation density, attraction density, and total trip densities presented in Figure C.2.

Table C.2. Parameters of a demand function for a heterogeneous scenario.

Demand [user/km⁴·h]	m	a_i^0	a_{ij}^1		b'_{ij}		b''_{ij}		c'_{ij}		c''_{ij}	
1,000	9	1.1475 1.1475	-0.355	0.355	0.3	0.3	0.3	0.3	0	0	0	0
			-0.455	-0.455	0.3	0.3	0.3	0.3	0.8	0.7	0.6	0.7
			0.455	0.455	0.3	0.3	0.3	0.3	-0.7	-0.7	0.7	0.7
			-0.455	0.455	0.3	0.3	0.3	0.3	-0.7	-0.7	-0.7	-0.7
			-0.455	0.455	0.3	0.3	0.3	0.3	0.7	0.7	-0.7	-0.7
			0.275	0.355	0.3	0.3	0.3	0.3	2.0	2.0	2.0	2.0
			0.255	0.255	0.3	0.3	0.3	0.3	-2.0	-2.3	2.0	2.3
			0.355	0.255	0.3	0.3	0.3	0.3	-2.0	-2.0	-2.0	-2.0
			0.355	-0.355	0.3	0.3	0.3	0.3	1.8	2.2	-1.8	2.2

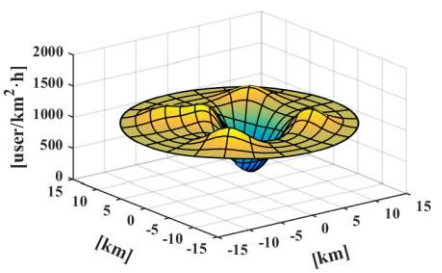

(a) Generated trip distribution

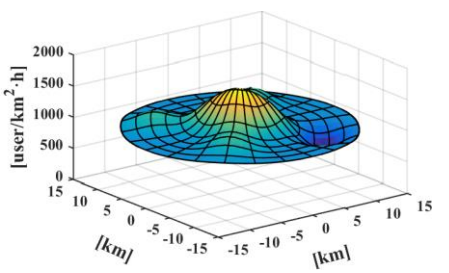

(b) Attracted trip distribution

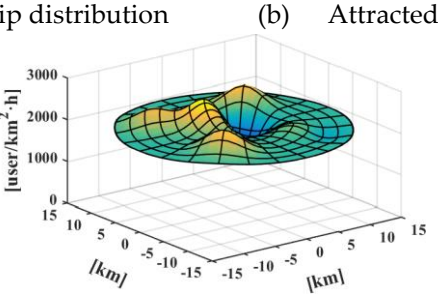

(c) Total trip distribution

Figure C.2. Heterogeneous demand scenario that consider an average generation/attraction rate of 1,000 [user/km²·h].

Mono-centric city scenario

The mono-centric scenarios come from the parameters presented in Table C.3 evaluated in Equation C.1, transforming the function from Cartesian coordinates to polar coordinates. These parameters allow obtaining a set of progressive mono-centric cities illustrated in Figure 4.2 (p. 74). From those exhibits, Figure C.3 shows a mono-centric in which the central business district (CBD) occupies 25% of the total trips (1.25x scenario) in a concentric city considering an average generation and attraction rates of 1,000 [user/km²·h].

Table C.3. Parameters of demand functions for mono-centric scenarios.

Demand [user/km⁴·h]	m	a_i^0	a_{ij}^1		b'_{ij}		b''_{ij}		c'_{ij}		c''_{ij}	
1,000	2	1.1894	0	0	0.3	0.3	0.3	0.3	0	0	0	0
Hm scenario		1.1894	0	0	0	0	0	0	0	0	0	0
1,000	2	1.1735	0.21	0.42	0.3	0.3	0.3	0.3	0	0	0	0
1.05x scenario		1.1735	0	0	0	0	0	0	0	0	0	0
1,000	2	1.1577	0.42	0.85	0.3	0.3	0.3	0.3	0	0	0	0
1.10x scenario		1.1577	0	0	0	0	0	0	0	0	0	0
1,000	2	1.1420	0.64	1.28	0.3	0.3	0.3	0.3	0	0	0	0
1.15x scenario		1.1420	0	0	0	0	0	0	0	0	0	0
1,000	2	1.1264	0.85	1.70	0.3	0.3	0.3	0.3	0	0	0	0
1.20x scenario		1.1264	0	0	0	0	0	0	0	0	0	0
1,000	2	1.1108	1.06	2.12	0.3	0.3	0.3	0.3	0	0	0	0
1.25x scenario		1.1108	0	0	0	0	0	0	0	0	0	0

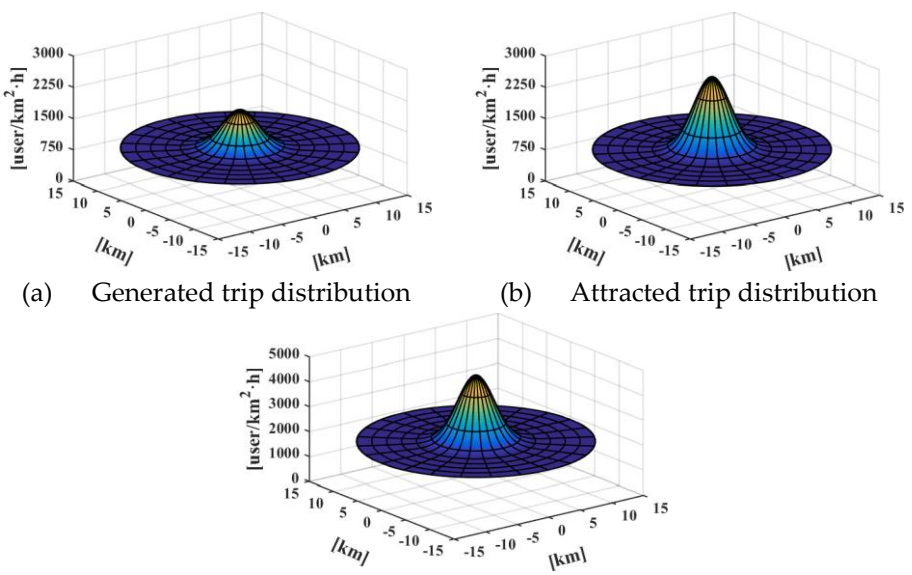

(a) Generated trip distribution (b) Attracted trip distribution

(c) Total trip distribution

Figure C.3. Mono-centric demand scenario that consider an average generation/attraction rate of 1,000 [user/km²·h] considering 1.25x scenario.

Multi-subcenters city scenario

The multi-subcenters scenario includes four subcenters. The role of subcenters is to "bring economic activities (e.g., services, employment, and others) closer to people who live in peripheral urban spaces" (Medina-Tapia et al., 2020).

Table C.4 presents the list of parameters used by the demand function (Equation C.1) for multi-subcenters scenarios considering 5 points. The

parameters of the scenarios formulate a progressive implementation from the homogeneous scenario. The scenarios of subcenters increase its size from 5% of the total trips to a scenario in which multi-subcenters consider 25% of total trips.

Table C.4. Parameters of demand functions for multi-subcenters scenarios.

Demand [user/km⁴·h]	m	a_i^0	a_{ij}^1		b'_{ij}		b''_{ij}		c'_{ij}		c''_{ij}	
			0	0	0.3	0.3	0.3	0.3	0	0	0	0
			0	0	0.3	0.3	0.3	0.3	2.0	2.0	2.0	2.0
1,000 Hm scenario	5	1.1894 1.1894	0	0	0.3	0.3	0.3	0.3	-2.0	-2.0	2.0	2.0
			0	0	0.3	0.3	0.3	0.3	-2.0	-2.0	-2.0	-2.0
			0	0	0.3	0.3	0.3	0.3	2.0	2.0	-2.0	-2.0
			0	0	0.3	0.3	0.3	0.3	0	0	0	0
			0.24	0.24	0.3	0.3	0.3	0.3	2.0	2.0	2.0	2.0
1,000 1.05x scenario	5	1.1410 1.1410	0.24	0.24	0.3	0.3	0.3	0.3	-2.0	-2.0	2.0	2.0
			0.24	0.24	0.3	0.3	0.3	0.3	-2.0	-2.0	-2.0	-2.0
			0.24	0.24	0.3	0.3	0.3	0.3	2.0	2.0	-2.0	-2.0
			0		0.3	0.3	0.3	0.3	0	0	0	0
			0.47	0.47	0.3	0.3	0.3	0.3	2.0	2.0	2.0	2.0
1,000 1.10x scenario	5	1.0958 1.0958	0.47	0.47	0.3	0.3	0.3	0.3	-2.0	-2.0	2.0	2.0
			0.47	0.47	0.3	0.3	0.3	0.3	-2.0	-2.0	-2.0	-2.0
			0.47	0.47	0.3	0.3	0.3	0.3	2.0	2.0	-2.0	-2.0
			0	0	0.3	0.3	0.3	0.3	0	0	0	0
			0.69	0.69	0.3	0.3	0.3	0.3	2.0	2.0	2.0	2.0
1,000 1.15x scenario	5	1.0533 1.0533	0.69	0.69	0.3	0.3	0.3	0.3	-2.0	-2.0	2.0	2.0
			0.69	0.69	0.3	0.3	0.3	0.3	-2.0	-2.0	-2.0	-2.0
			0.69	0.69	0.3	0.3	0.3	0.3	2.0	2.0	-2.0	-2.0
			0		0.3	0.3	0.3	0.3	0	0	0	0
			0.90	0.90	0.3	0.3	0.3	0.3	2.0	2.0	2.0	2.0
1,000 1.20x scenario	5	1.0137 1.0137	0.90	0.90	0.3	0.3	0.3	0.3	-2.0	-2.0	2.0	2.0
			0.90	0.90	0.3	0.3	0.3	0.3	-2.0	-2.0	-2.0	-2.0
			0.90	0.90	0.3	0.3	0.3	0.3	2.0	2.0	-2.0	-2.0
			0		0.3	0.3	0.3	0.3	0	0	0	0
			1.09	1.09	0.3	0.3	0.3	0.3	2.0	2.0	2.0	2.0
1,000 1.25x scenario	5	0.9764 0.9764	1.09	1.09	0.3	0.3	0.3	0.3	-2.0	-2.0	2.0	2.0
			1.09	1.09	0.3	0.3	0.3	0.3	-2.0	-2.0	-2.0	-2.0
			1.09	1.09	0.3	0.3	0.3	0.3	2.0	2.0	-2.0	-2.0

Figure 4.3 (p. 75) shows a list of exhibits representing the progressive implementation of multi-subcenters presented in Table C.4. Finally, Figure C.4 shows the latest demand scenario in which the average generation/attraction rate is 1,000 [user/km2·h] and multi-subcenters representing 25% of the total trips.

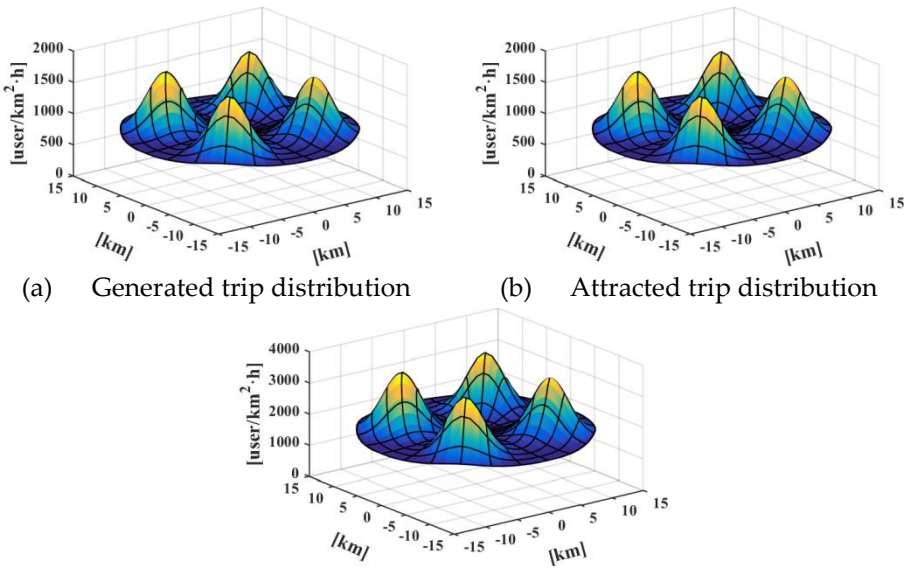

(a) Generated trip distribution (b) Attracted trip distribution

(c) Total trip distribution

Figure C.4. Multi-subcenters demand scenario that consider an average generation/attraction rate of 1,000 [user/km²·h] considering 1.25x scenario.

3. Application to Santiago, Chile

Santiago of Chile adjusts to concentric city and adapted to a circular form, considering ring and radial routes. The modeling divides the city into 9 OD macro-zones: a central zone, 4 inner zones, and 4 outer zones. The trips on the subway at rush hour comes from the Santiago origin-destination survey (MTT, 2012).

The method calibrates a continuous function meeting the total trips of each origin-destination is the value in the OD trip matrix (T_{ij} where i is the origin zone, and j is the destination zone). Equation 6.1 represents the total trips between the origin and destination zones in polar coordinates. First, the coordinates $\theta^i_{f(2)} - \theta^i_{f(1)}$ and $r^i_{f(2)} - r^i_{f(1)}$ defines the origin zone. Second, the coordinates $\theta^i_{t(2)}$-$\theta^i_{t(1)}$ and $r^i_{t(2)}$-$r^i_{t(1)}$ defines the destination zone.

$$T_{ij} = \int_{\theta^i_{f(1)}}^{\theta^i_{f(2)}} \int_{r^i_{f(1)}}^{r^i_{f(2)}} \int_{\theta^i_{t(1)}}^{\theta^i_{t(2)}} \int_{r^i_{t(1)}}^{r^i_{t(2)}} D(r_f, \theta_f, r_t, \theta_t)\, r_t\, dr_t\, d\theta_t\; r_f\, dr_f\, d\theta_f \qquad (C.2)$$

Appendix D. Adaptive transit network design for spatially heterogeneous demand[1]

Abstract: Cities have always had a concentrating effect on population and services. Public transportation is the most sustainable way of transporting large quantities of users. Even worse, cities increase their population through a dispersed distribution, in which their demand density has a heterogeneous distribution throughout the space. Therefore, the design of public transportation schemes must adapt to local conditions of demand over the territory. The objective of this research is to propose a methodology through continuous analytical functions in order to identify the lowest-cost structure (users and agency costs), considering three primary technologies of transit (subways, tramways, and BRT systems). As a first contribution, the transit design adapts its optimal structure to non-homogeneous demand distribution in a concentric city (ring and radial routes). As a second contribution, the network design simultaneously determines spatial and temporary transit components. Finally, as a third contribution, considering the continuous approximation method, an algorithm determines the discrete location of radial and ring routes. The results show that the optimal solutions are not stable values, even for homogeneous cities. The density of rings and headways will increase their values if the radius increases toward the outer areas of the city. Therefore, a concentric city must encourage transit rings in the periphery. Some urban density structures allow better performance than other urban structures. Regarding a heterogeneous demand distribution, the reduction of total costs due to the implementation of a multi-subcenter structure ranges from 7.8% to 11.7%. Therefore, multi-subcenters can compete with a homogeneous scheme because the system achieves more efficiency than the other urban scenarios.

Keywords: Public transportation network design; Continuous approximation method; Non-homogeneous demand; Concentric city.

1. Introduction

Nowadays, more than half of the world's people live in cities, and cities will grow even more. The problem is the cities heterogeneously expand to new areas due to environmental, social, and economic factors. Public transportation is one of the main components of transportation systems in

[1] Paper submitted to a journal:

- Medina-Tapia, M., Robusté, F., Estrada, M. (2021). Adaptive transit network design for spatially heterogeneous demand.

most cities, and this structure in urban mobility will keep in the future. Therefore, transit networks must adapt new infrastructure and schemes to heterogeneous demand patterns by considering the origin, destination, and trip features.

The planning process is essential for the correct functioning of a public transportation system. One of the first early stages of planning is the strategic design for any transit structure, i.e., a linear transit route (e.g., Medina-Tapia et al., 2013), a grid network, or a ring-radial network (e.g., Chen et al., 2015). Regarding grid networks, Badia (2016) identifies four types of schemes: radial, direct trip-based, hybrid, and grid structure. Considering a ring-radial street pattern, we identify works grouped into a similar classification to the former: radial (Badia, 2016; Byrne, 1975), direct trip-based (Badia, 2016), hybrid structure (Badia, 2016; Chen et al., 2015), and ring-radial structure (Nourbakhsh, 2014; Vaughan, 1986). Regarding urban form, many cities have a radio-centric structure, for example, Milan, Moscow (Badia et al., 2014), Canberra, Chengdu, and Santiago of Chile (Medina-Tapia & Robusté, 2019b).

For strategic planning decisions, the transit design aims to determine spatial and temporary variables (Ibarra-Rojas et al., 2015). This problem is a transit network design and frequency setting sub-problem (TNDSP) in which simultaneously determines routes and preliminary frequencies (R. Smith, 2014). Discrete and analytical models can solve TNDSP (Ibarra-Rojas et al., 2015). Parsimonious models are analytical models that rely on a few parameters and assumptions to study macroscopic transportation systems (Daganzo et al., 2012). The transit design has a diverse list of parsimonious models: Chang and Schonfeld (1991), Daganzo (2010), Estrada et al. (2011), Badia et al. (2014, 2016), and others. In this framework, the Continuous Approximation method (henceforth CA) may be one of the best tools to optimize the macroscopic design of transit networks. Newell's paper (1971) contains one of the first works that applied this method. The CA method solves the problem on a local cost basis using variables that are densities (Daganzo, 2005). If there is no perfect information—such as the arrival of passengers, traffic conditions, and others—it is possible to model with smooth and continuous functions because the information is not accurate (Newell, 1973). These are common conditions in the design of transit networks.

In the literature of network design, three modeling approaches simplify the demand distribution. First, the demand is spatially homogeneous over a town (e.g., S. Chang & Schonfeld, 1991; Daganzo, 2010). Second, the demand is variable and symmetric, where the maximum value linearly or

exponentially decreases from the center to the suburbs (e.g., Byrne, 1975). Finally, in the third case, the city has a spatially continuous, two-dimensional, and non-symmetric demand. In this paper, we use the third alternative because it is more realistic than an idealized demand distribution. Moreover, our network design model may reduce the total system cost in comparison to a homogenous distribution (Ouyang et al., 2014).

A few contributions analyze the transit design considering spatially, non-homogeneous demand using the CA method. In one of the first works, Vaughan (1986) analyzes the ring and radial behavior on a network in which a continuum function represents a *many-to-many* demand with buses that run at a fixed speed. More recently, Smith (2014) evaluates the impact of spatially heterogeneous demand over a hybrid transit system and the transit network design with spatially elastic demand. Ouyang et al. (2014) formulated a method based on continuum approximations, which designs bus networks for an urban grid system with heterogeneous demand. Also, Nourbakhsh (2014) proposed several methods of transit network design to improve transit, considering low and heterogeneous spatial demand. Unfortunately, these papers do not consider that time headways must vary considering local conditions within a city. Moreover, no works have expressed an analytical formulation that represents the optimal needs of transit infrastructure, adapting to a heterogeneous and non-symmetric demand over a town. Finally, the discretization method is relevant if variables of a network spatially vary over a city depending on attributes of transit technologies needed: speeds and operating attributes, the capacity of vehicles and operation, frequencies, costs of capital, operation, and infrastructure of a transit system.

The problem then, to be studied in this paper, is to propose a methodology through continuous analytical functions to identify the lowest-cost configuration pattern that adapts to the demand distribution, which spatially varies over a city. The idea is to deploy more density of stops and routes where the concentration of potential users is also higher. Regarding a ring and radial transit configuration, we compare results from the model for three types of transit modes.

The next section details preliminary concepts and presents the cost functions of our model. From this conceptualization, we formulate the proposed model and expose the optimization methodology, including the discussion of analytical results. To better understand the outcomes, we formulate four urban scenarios and analyze the numerical results. Finally, we present the conclusions of our research.

2. Methodology

2.1. Preliminary concepts

The region of analysis is a concentric city of radius R ([km]), which has ring and radial transit services. Users have a continuous distribution over the city, considering four scenarios of different patterns of demand. The generated demand $\lambda(r,\theta)$ at a point (r,θ), which it is in polar coordinates, is a density function in [user/km²·h]. This condition is essential, considering the imperfect distribution of the demand over the territory. This approach also allows correctly characterizing the demand to obtain adapted transit schemes. The period of the analysis is the rush hour (P_m) because the peak period defines the required infrastructure.

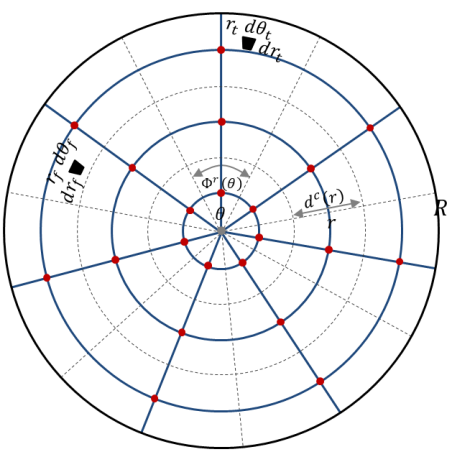

Figure D.1. Transit structure: ring, radial services, and transfer points.

We assume passengers can travel on two types of transit routes represented by blue lines in Figure D.1: ring and radial routes ($l = \{c, r\}$) in four directions. Each line only serves an area called a *transit corridor* that contains the origin or destination of a trip. On circular routes, users can travel clockwise or anticlockwise direction ($c = \{c_c: clockwise, c_a: anticlockwise\}$). On radial routes, users can go to the center or come out from this ($r = \{r_i: inside, r_o: outside\}$).

In this problem, four variables define the network scheme of a transit: two spatial variables (Figure D.1) and two temporary variables that define the operation of a system.

$d^c(r)$: distance between ring transit routes with a radius r [km/route];

$\Phi^r(\theta)$: the angle between radial routes with an angle θ [radian/route], which $d^r(r,\theta) = \Phi^r(\theta) \cdot r$, where $d^r(r,\theta)$ is the distance between radial routes at a point (r,θ);

$h^c(r)$: time headway between vehicles at a ring route on r [h/veh];

$h^r(\theta)$: time headway between vehicles at a radial route on θ [h/veh].

All vehicles of the transit system are identical, although we compare results among different types of transit modes: Heavy Rail Transit as a metro (HRT), Light Rail Transit as a tramway (LRT), and Bus Rapid Transit (BRT). Each type of service has defined a cruising speed (v^t), capacity (K^v), and other operational attributes that allow obtaining the commercial speed. By the way, the model, through constraints, ensures that vehicles reach the cruising speed between stops/station (K^d) and avoids frequencies that could be dangerous for the operation of the system, especially in railway services (K^h). The transit system has implemented a fixed stop system in which the vehicles lose time (τ^s in [h/station]) due to acceleration, braking, maneuvers when getting to a station, boarding, alighting, and transferring passengers between transit routes. Red points in Figure 3.4 represent stations where passengers board, alight, or transfer between transit lines. Finally, each type of transit mode has specific parameters of costs considering capital, salary, operational, and two types of infrastructure (stops, stations, railway lines, and roads according to the transit mode).

Demand distribution

The demand distribution function $D(r_f, \theta_f, r_t, \theta_t)$ in [user/km^4·h] (Vaughan, 1986) represents the spatial density in polar coordinates of passengers per hour who begin a trip from an area $dr_f\ r_f\ d\theta_f$ in [km^2] about an origin point (r_f, θ_f) to an area $dr_t\ r_t\ d\theta_t$ in [km^2] about a destination point (r_t, θ_t) (Figure 3.4). Any method of interpolation from an origin-destination survey allows calculating this function, e.g., using bicubic spline interpolation. In consequence, Δ is the total trip demand, [user/h], in a concentric city with radius R (Equation D.1). Considering this formulation, we obtain the function of generated demand $\lambda(r,\theta)$ at a point (r,θ) in [user/km^2·h] (Equation D.2).

$$\Delta = \int_0^{2\pi} \int_0^R \int_0^{2\pi} \int_0^R D(r_f, \theta_f, r_t, \theta_t)\ r_t\ dr_t\ d\theta_t\ \ r_f\ dr_f\ d\theta_f \qquad (D.1)$$

$$\lambda(r,\theta) = \int_0^{2\pi} \int_0^R D(r, \theta, r_t, \theta_t)\ r_t\ dr_t\ d\theta_t \qquad (D.2)$$

Based on the demand distribution function, we can obtain four demand density functions that represent the demand in each stage of a trip: access, waiting, in-vehicle travel, and transfer function. These density functions allow calculating how many people compose the generalized cost of the system at a city point.

$f^A(r,\theta)$: the density of users who board and alight from a transit vehicle [user/km²·h];
$f_l^W(r,\theta)$: the density of users who wait for a transit vehicle of corridor $l \in \{c,r\}$ [user/km²·h];
$f_l^V(r,\theta)$: the density of users who travel on a transit vehicle of corridor $l \in \{c,r\}$ [user/km·h]; and
$f_l^T(r,\theta)$: the density of users who transfer between two vehicles of transit of corridor $l \in \{c,r\}$ [user/km²·h].

Assumptions

Users take the shortest route riding on a ring, a radial, or both types of routes. If we assume that passengers choose the path that minimizes the distance, the modeling of travel demand considers the next mobility patterns:

- If the destination is on the same side of the city between $\theta - 2$ and $\theta + 2$ angles, and the trip destination is closer to the central point than the trip origin, then users will initially use the radial route and the ring route secondly. It is worth mentioning that if the difference of an angle between two points ($\Delta\theta$) is less than two radians $(r \cdot \Delta\theta < 2r)$, the shortest route is by a ring route.
- Users should use a ring route firstly and a radial route secondly. If the destination is in the same city side, and the origin is closer to the concentric city center than the destination.
- Users will take to radial routes if the destination is in the opposite city side between $\theta + 2$ and $\theta - 2 + 2\pi$, i.e., these angles have at least two radians of difference concerning the radial axis of a point (r,θ).

Considering these mobility patterns, the model obtains demand density functions: $f^A(r,\theta)$, $f_l^W(r,\theta)$, $f_l^V(r,\theta)$, and $f_l^T(r,\theta)$. Otherwise, the following points present a list of assumptions of this work about demand and costs.

- The passenger arrival rate at each point is deterministic and high. Therefore, the model considers a transit operation by frequency.
- Passengers who board and alight at a transit station are fixed and known. Therefore, we do not model user reassignment on the network.
- Users can take one or two services performing up to one transfer between routes.

- The users' cost is independent of age, socioeconomic level, time of the day (period), or other conditions.
- The driver's salary is a fixed value. In other words, salaries do not depend on the number of passengers transported.
- The unitary cost of operations is the same when a vehicle travels at cruising speed when a vehicle accelerates and brakes at a station, and when users board and alight at a station.

2.2. Cost functions

User Costs

The total time of users ($T_T^u = T_A + T_W + T_V + T_T$ in [user·h/P_m] where P_m is the rush hour and lasts T [h/P_m]) has four components: accessibility time (T_A), waiting time (T_W), travel time (T_V), and transfer time (T_T).

a) Access time

This component captures the total time spent by users that access from an origin (places of residence for home-based trips) to the closest transit station/stop and egress from this facility to the destination (T_A in [user·h/P_m], Eq. D.3). The continuous local cost function is the product of two elements that depend on each type of route: ring and radial. First, $f^A(r,\theta)\cdot T$ in [user/km²·P_m] is the user density in the rush hour that board and alight at a point (r,θ). Second, the average time spent on accessing and egressing from the closest station ($t^A(r,\theta)$ in [h]).

$$T_A = \int_0^{2\pi}\int_0^{R} f^A(r,\theta)\cdot T\cdot t^A(r,\theta)\ r\ dr\ d\theta \qquad (D.3)$$

The density of transit users ([user/km²·h]) includes two types of trips. First, passengers that travel from an origin point (r,θ) to the rest of a concentric city (first integral in Eq. D.4). Second, the users come from any point of the city to a destination (r,θ) (second integral in Eq. D.4).

$$f^A(r,\theta) = \int_0^{2\pi}\int_0^{R} P(r,\theta,r_t,\theta_t)\ r_t\ dr_t\ d\theta_t + \int_0^{2\pi}\int_0^{R} P\left(r_f,\theta_f,r,\theta\right) r_f\ dr_f\ d\theta_f \qquad (D.4)$$

The average access time at a point (r,θ) (Eq. D.5) is half of the maximum access distance $(d^c(r)/2 + \Phi^r(\theta)\cdot r/2)$ on a local road network at an access

speed $v^a(r)$ (e.g., Kuah & Perl, 1988; Wirasinghe & Ghoneim, 1981). The access speed varies according to the radius in a city ($v^a(r)$) because we assume that users access the stations on foot around the city center, but in the periphery, the users access using a feeder bus or a private vehicle. Therefore, the access speed will be higher in the periphery than in the center, but the access distance will also be higher. Moreover, users differently perceive the time in each part of a trip (TRB, 2013); hence, a time perception factor (α) multiplies the function.

$$t^A(r,\theta) = \alpha \cdot \frac{d^c(r) + \Phi^r(\theta) \cdot r}{4 \cdot v^a(r)} \qquad (D.5)$$

b) Waiting time

The component is the time spent by users waiting for the next arriving of a transit vehicle (T_W in [h], Eq. D.6). The user density that boards a vehicle during the rush hour is $f_l^W(r,\theta) \cdot T$ in [user/km²·P_m] and the average waiting time at a station is $t_l^W(r,\theta)$ in [h] for the route l. Finally, we independently calculate the transfer time regarding the waiting time.

$$T_W = \int_0^{2\pi} \int_0^R \sum_{l \in \{c,r\}} f_l^W(r,\theta) \cdot T \cdot t_l^W(r,\theta)\ r\, dr\, d\theta \qquad (D.6)$$

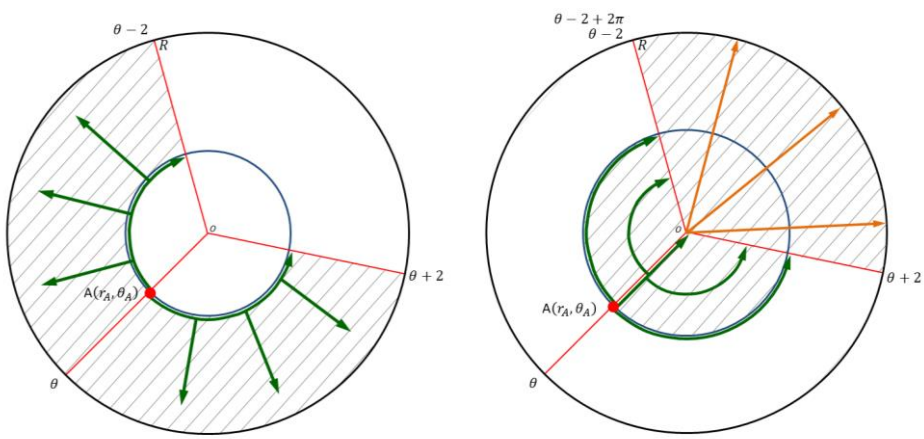

(a) Users board ring services. (b) Users board on radial services.

Figure D.2. Mobility patterns of users that wait and want to board a ring and radial route.

In Figure D.2(a), the user density will wait for a ring service ([user/km²·h]) if destinations are further to the central point than the origin A in the hatched zone between $[\theta - 2; \theta + 2]$ (green arrows and Eq. D.7).

$$f_c^W(r,\theta) = \int_{\theta-2}^{\theta+2} \int_{r}^{R} P(r,\theta,r_t,\theta_t)\, r_t\, dr_t\, d\theta_t \qquad (D.7)$$

In Figure D.2(b), the density of users that board a radial service ([user/km²·h]) has two components. First, the green arrows (first integral in Eq. D.8) represent users that wait for a radial service, whether the origin is further than the destination concerning the central point ($r_f > r_t$). Second, the orange arrows (second integral in Eq. D.8) show passengers that travel to any point in the opposite zone of the city (the hatched region between $[\theta + 2; \theta - 2 + 2\pi]$ in Figure D.2).

$$f_r^W(r,\theta) = \int_{\theta-2}^{\theta+2} \int_{0}^{r} P(r,\theta,r_t,\theta_t)\, r_t\, dr_t\, d\theta_t + \int_{\theta+2}^{\theta-2+2\pi} \int_{0}^{R} P(r,\theta,r_t,\theta_t)\, r_t\, dr_t\, d\theta_t \qquad (D.8)$$

The average waiting time function (Eq. D.9) linearly increases according to the headway between vehicles and the time perception factor (β) (TRB, 2013). It depends on the type of route. We have assumed that the headways are deterministic and perfectly regular, i.e., the average waiting time per user is $1/2$ headway (e.g., Larson & Odoni, 2007; Medina-Tapia et al., 2013).

$$t_l^W(\cdot) = \beta \cdot \frac{h^l(\cdot)}{2} \quad l \in \{c, r\} \qquad (D.9)$$

c) In-vehicle travel time

The local travel time per kilometer depends on two components: the user density on a transit vehicle in rush hour ($f^V_{l\in\{c,r\}}(r,\theta)\cdot T$ in [user/km·P_m]), and the travel time per kilometer incurred by a user on a vehicle ($t^V_{l\in\{c,r\}}(r,\theta)$ in [h/km]). In radial corridors, the user density depends on the area of a corridor between r and R. This area is a circular trapezoid in which the width of the corridor varies according to the radius. In the model, we use the average width of this shape, i.e., $\Phi^r(\theta)\cdot(R+r)/2 \cdot= \Phi^r(\theta)\cdot(R/r+1)\cdot r/2$. Finally, the total in-vehicle travel time (T_V in [user·h/P_m]) is the result of the integration of the local function over the circular region (Eq. D.10).

$$T_V = \int_0^{2\pi} \int_0^{R} f_c^V(r,\theta)\cdot T\cdot t_c^V(r,\theta) + \frac{1}{2}\cdot\left(\frac{R}{r}+1\right)\cdot f_r^V(r,\theta)\cdot T\cdot t_r^V(r,\theta)\; r\, dr\, d\theta \qquad (D.10)$$

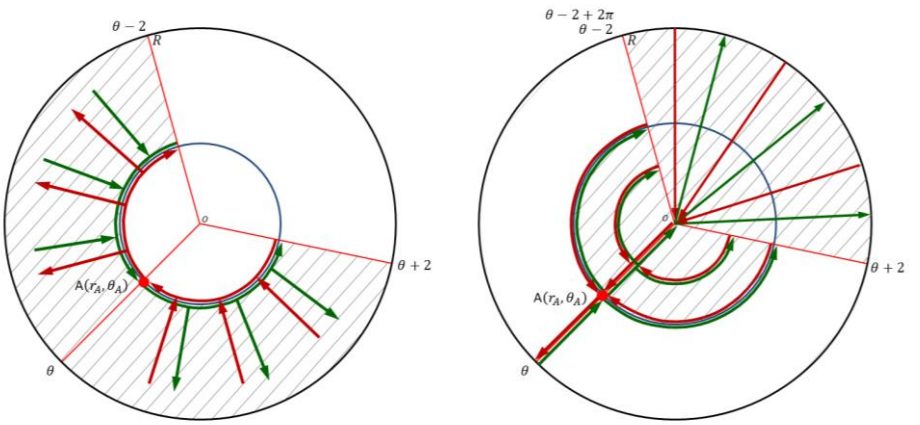

(a) User patterns traveling on rings. (b) User patterns traveling on radials.

Figure D.3. Mobility patterns of users that travel on ring and radial services.

The load-passengers density function at a point (r, θ) in [user/km·h] is the density of users that are traveling on a vehicle of transit at this point. Ring services have two types of trips: $f_c^V(\cdot) = f_{c_a}^V(\cdot) + f_{c_c}^V(\cdot)$. Firstly, the anticlockwise function ($f_{c_a}^V(\cdot)$) at point (r, θ) contains two types of trips. Green arrows in Figure D.3(a) are users that directly board a clockwise circular service at the radius r between angles $\theta_t - 2$ and θ, and their destinations are in the hatched zone between θ and $\theta + 2$ (first integral in Eq. D.11($l = c_a$)). The anticlockwise circular corridor receives passengers from radial corridors between $\theta_t - 2$ and θ and destination are on the ring corridor between θ and $\theta + 2$ (second integral in Eq. D.11($l = c_a$)). Secondly, in the clockwise function ($f_{c_c}^V(\cdot)$) (red arrows in Figure D.3(a)), the origins are between angles $\theta_t + 2$ and θ, and the destinations are in the hatched zone between $\theta - 2$ and θ (first integral in Eq. D.11($l = c_c$)); and a clockwise circular corridor also receives passengers from radial corridors between angles θ and $\theta_t + 2$ (second integral in Eq. D.11($l = c_c$)). The formulation of these functions has a basis on Nourbakhsh (2014), but we have adjusted bounds of integrals. If an origin angle (θ) changes on a ring route, the destination will also change (θ_t), always conserving an angle of 2 radians.

$$f_l^V(r,\theta) = \begin{cases} \int_{\theta}^{\theta+2} \int_{r}^{R} \left(\int_{\theta_t-2}^{\theta} P(r,\theta_f,r_t,\theta_t)\, r\, d\theta_f \right) r_t\, dr_t\, d\theta_t + \int_{\theta}^{\theta+2} \left(\int_{\theta_t-2}^{\theta} \int_{r}^{R} P(r_f,\theta_f,r,\theta_t)\, r_f\, dr_f\, d\theta_f \right) r\, d\theta_t & l = c_a \\ \int_{\theta-2}^{\theta} \int_{r}^{R} \left(\int_{\theta}^{\theta_t+2} P(r,\theta_f,r_t,\theta_t)\, r\, d\theta_f \right) r_t\, dr_t\, d\theta_t + \int_{\theta-2}^{\theta} \left(\int_{\theta}^{\theta_t+2} \int_{r}^{R} P(r_f,\theta_f,r,\theta_t)\, r_f\, dr_f\, d\theta_f \right) r\, d\theta_t & l = c_c \end{cases} \quad \text{(D.11)}$$

The load-passenger density at a point (r,θ) on radial transit services has two components: $f_r^V(\cdot) = f_{r_i}^V(\cdot) + f_{r_o}^V(\cdot)$. Firstly, the direction-inside corridor is used by users that directly boards to the central point on a radial corridor (green arrows in Figure D.3(b)). These trips finish in the same zone (first integral in Eq. D.12($l = r_i$)) or the opposite zone (second integral in Eq. D.12($l = r_i$)). Secondly, in the direction-outside corridor (red arrows in Figure D.3(b)), the users alight on the same corridor from the same zone (first integral in Eq. D.12($l = r_o$)) or from the opposite zone (second integral in Eq. D.12($l = r_o$)).

$$f_l^V(r,\theta) = \begin{cases} \int_{\theta-2}^{\theta+2}\int_{0}^{r}\left(\int_{r}^{R} P(r_f,\theta,r_t,\theta_t)\,dr_f\right) r_t\,dr_t\,d\theta_t + \int_{\theta+2}^{\theta-2+2\pi}\int_{0}^{R}\left(\int_{r}^{R} P(r_f,\theta,r_t,\theta_t)\,dr_f\right) r_t\,dr_t\,d\theta_t & l = r_i \\ \int_{r}^{R}\left(\int_{\theta-2}^{\theta+2}\int_{0}^{r} P(r_f,\theta_f,r_t,\theta)\,r_f\,dr_f\,d\theta_f\right)dr_t + \int_{r}^{R}\left(\int_{\theta+2}^{\theta-2+2\pi}\int_{0}^{R} P(r_f,\theta_f,r_t,\theta)\,r_f\,dr_f\,d\theta_f\right)dr_t & l = r_o \end{cases} \quad \text{(D.12)}$$

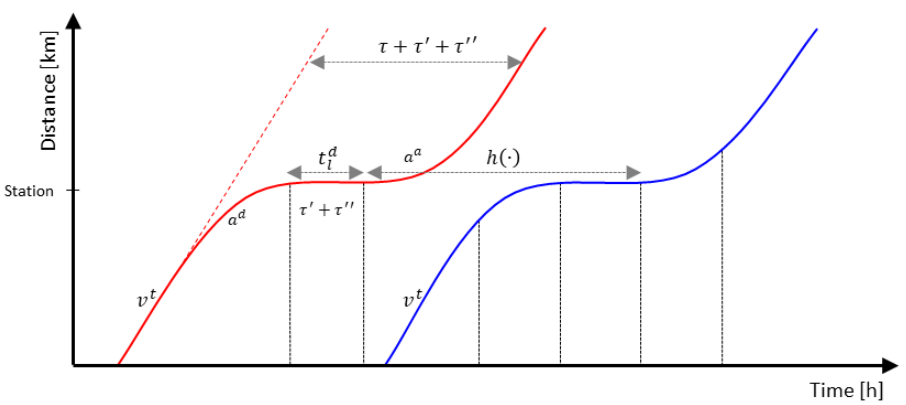

Figure D.4. Components of in-vehicle travel time based on Medina-Tapia et al. (2013).

The trip time estimation depends on a density function (Eq. D.13 expressed in [h/km]), which has four additive components similar to Daganzo (2010), in which γ is the time perception factor (TRB, 2013).

$$t_l^V(r,\theta) = \begin{cases} \gamma\cdot\left(\frac{1}{v^t} + \frac{\tau}{\Phi^r(\theta)\cdot r} + \frac{t^d}{\Phi^r(\theta)\cdot r} + \frac{\tau'''}{\Phi^r(\theta)\cdot r}\right) & l = c \\ \gamma\cdot\left(\frac{1}{v^t} + \frac{\tau}{d^c(r)} + \frac{t^d}{d^c(r)} + \frac{\tau'''}{d^c(r)}\right) & l = r \end{cases} \quad \text{(D.13)}$$

- *Travel time density based on cruising speed*. Travel time per kilometer spent by a user at a constant cruising speed v^t ($1/v^t$ in [h/km], Figure D.4).
- *Time density by acceleration and braking operations*. The additional time represented in the second term of Eq. D.13 depends on the parameter τ

([h/station], Figure D.4), and the station density ([station/km]). This value ($\tau = v^t \cdot (1/a^a + 1/a^d)/2$ has a component by deceleration and acceleration of a vehicle at a station (e.g., Chien & Qin, 2004; Vuchic, 2007; Wirasinghe & Ghoneim, 1981).

- *Dwell time density by passengers that board and alight at stops/stations*. The third term is $t^d/\Phi^r(\theta) \cdot r$ for rings and $t^d/d^c(r)$ for radial services ([h/km]), where the dwell time ($t^d = \tau' + \tau''$ in [h/station]) is the sum of a dead time (τ') and a minimum stopping time (τ'') due to boarding and alighting by users (Figure D.4) considering a sequential boarding operation of users (Fernandez & Planzer, 2002).
- *Time density lost crossing an intersection*. The fourth term in Eq. D.13 includes the time density lost by crossing an intersection, $\tau'''/\Phi^r(\theta) \cdot r$ for rings, and $\tau'''/d^c(r)$ for radial services, where τ''' represents the average lost time crossing an intersection.

d) Transfer time

The transfer cost (T_T in [user·h/P_m], Eq. D.14) is the lost time of users due to changes between service routes. This function is composed of two factors: the passenger density in rush hour that transfers at each point ($f^T_{l\in\{c,r\}}(r,\theta) \cdot T$ in [user/km^2· P_m]), and the average transfer time incurred by a passenger ($t^T_{l\in\{c,r\}}(r,\theta)$ in [h]). A factor multiplies the passenger density representing the average width of the area between r and R ($\Phi^r(\theta) \cdot (R + r)/2$).

$$T_T = \int_0^{2\pi} \int_0^R \frac{1}{2} \cdot \left(\frac{R}{r} + 1\right) \cdot f_c^T(r,\theta) \cdot T \cdot t_c^T(r,\theta) + \frac{1}{2} \cdot \left(\frac{R}{r} + 1\right) \cdot f_r^T(r,\theta) \cdot T \cdot t_r^T(r,\theta)\ r\, dr\, d\theta \quad \text{(D.14)}$$

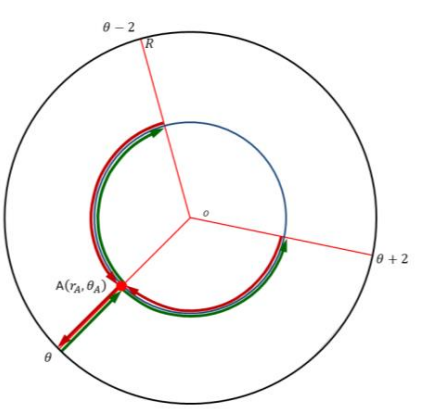

Figure D.5. Mobility patterns of users that transfer between services.

Transfer demand functions incorporate two cases: the passengers who transfer from radial to ring routes and the passengers who transfer from ring to radial services. Firstly, in Eq. D.15, the demand density ([user/km²·h]) of users transfers from a radial to a ring service at a point A, i.e., green arrows in Figure D.5. This behavior represents users that board a radial service with angle θ from the periphery to the point (r, θ), and whose destination is on the circular arc with radius r between $\theta - 2$ and $\theta + 2$.

$$f_c^T(r,\theta) = \int_r^R \int_{\theta-2}^{\theta+2} P\left(r_f, \theta, r, \theta_t\right) r_t \, d\theta_t \, dr_f \tag{D.15}$$

Secondly, in Eq. D.16, the passenger demand ([user/km²·h]) transfers from a ring to a radial service (red arrows in Figure D.5). Users board at a point on a ring service located on r between the angles $\theta - 2$ and $\theta + 2$, and the destination is on the radial corridor with angle θ.

$$f_r^T(r,\theta) = \int_{\theta-2}^{\theta+2} \int_r^R P\left(r, \theta_f, r_t, \theta\right) r_f \, dr_t \, d\theta_f \tag{D.16}$$

The average transfer-time function per user has three components. The first term is the passenger perception of the time (δ) (TRB, 2013). Second, the average walking time between two stops (e.g., χ^T/v^w). Third, the average waiting time is deterministic and perfectly regular on a ring ($h^c(r)/2$) or a radial route ($h^r(\theta)/2$).

$$t_l^T(\cdot) = \delta \cdot \left(\frac{\chi^T}{v^w} + \frac{h^l(\cdot)}{2}\right) \quad l \in \{c, r\} \tag{D.17}$$

Agency Costs

The cost spent by the agency, which operates the transit system, has three components ($C_T^a = C_K + C_O + C_I$ in [\$/P_m]): capital (C_K), vehicle operation (C_O), and infrastructure (C_I).

a) Capital cost

The capital cost prorated to the rush hour (C_K in [\$/P_m], Eq. D.18) depends on the fleet size ($F = F_c + F_r$ in [veh]) and the cost per vehicle (φ^k in [\$/veh·P_m]).

$$C_K = (F_c + F_r) \cdot \varphi^k \tag{D.18}$$

The fleet size in a corridor route (Eq. D.19 in [veh]) is the ratio between the cycle time ($t_c^C(r)$ or $t_r^C(\theta)$ in [h/route]) and the headway ($h^c(r)$ or $h^r(\theta)$ in [h/veh]) in rush hour. Moreover, each route is distanced by $d^c(r)$ or $\Phi^r(\theta)$.

$$F_l = \begin{cases} \int_0^R \frac{t_c^C(r)}{h^c(r)} \cdot \frac{1}{d^c(r)}\ dr & l = c \\ \int_0^{2\pi} \frac{t_r^C(\theta)}{h^r(\theta)} \cdot \frac{1}{\Phi^r(\theta)}\ d\theta & l = r \end{cases} \tag{D.19}$$

Three elements compose the cycle time functions on a corridor (Eq. D.20 in [h/route]): the time at cruising speed, the positioning time at terminals (t^f), the lost time by acceleration and braking before a station, the dwell time due to boarding and alighting of users, and the time lost by crossing an intersection.

$$t_l^C(\cdot) = \begin{cases} t_c^C(r) = 2 \cdot \int_0^{2\pi} \frac{1}{v^t} + \frac{t^f}{2\pi r} + \frac{\tau + \tau' + \tau'' + \tau'''}{\Phi^r(\theta) \cdot r}\ r\ d\theta & l = c \\ t_r^C(\theta) = 2 \cdot \int_0^{R} \frac{1}{v^t} + \frac{t^f}{R} + \frac{\tau + \tau' + \tau'' + \tau'''}{d^c(r)}\ dr & l = r \end{cases} \tag{D.20}$$

b) Operational cost

The operational cost ($C_O = C_G + C_V$ in [\$/P_m]) depends on two factors: the driver salary (C_G), and the operation cost of vehicles (C_V).

- **On-vehicle crew cost.** The cost of total salary in rush hour (C_G in [\$/P_m]) is in proportion to three components. Firstly, the fleet ($F_l \in \{c, r\}$) that depends on the type of corridor route. Secondly, the number of work shifts on a vehicle (η^d). Third, the salary earned during a rush hour by a driver is $T \cdot \varphi^g$ (in [\$/shift·P_m]).

$$C_G = (F_c + F_r) \cdot \eta^d \cdot T \cdot \varphi^g \tag{D.21}$$

- **In-operation vehicle cost.** The total operating cost in a route (C_V in [\$/P_m]) depends on the cost of ring and radial corridor routes. The cost of a route is composed of two components: the number of vehicles ($2 \cdot T/h^c(r)$ and $2 \cdot T/h^r(\theta)$ in [veh/P_m]), and the unitary cost (φ^o in [\$/veh·km·route]) considering the width of a transit corridor $d^c(r)$ or $\Phi^r(\theta)$.

$$C_V = \int_0^{2\pi} \int_0^R \left(\frac{2 \cdot T \cdot \varphi^o}{h^c(r) \cdot d^c(r)} + \frac{2 \cdot T \cdot \varphi^o}{h^r(\theta) \cdot \Phi^r(\theta) \cdot r} \right) \cdot r\ dr\ d\theta \tag{D.22}$$

c) Infrastructure cost

The total infrastructure cost for public transportation systems ($C_I = C_P + C_S$ in [\$/P_m]) consists of two other sub-costs: the road cost (C_P), and the station or stop cost (C_S).

- **Linear infrastructure.** The road infrastructure cost proportionally divide the rush hour ($C_P = C_c^P + C_r^P$ in [\$/P_m]) into two components according to the type of transportation corridor: rings (C_c^P) and radials (C_r^P). The corridor density, i.e., the inverse of the separation between routes ($d^c(r)$ or $\Phi^r(\theta)$), is multiplied by the unitary cost per km in the rush hour ($\varphi^p = \varphi^{p(f)} + \varphi^{p(v)} \cdot T$ in [\$/km·route·P_m]).

$$C_P = \begin{cases} 2 \cdot \int_0^{2\pi} \int_0^R \frac{1}{d^c(r)} \cdot \varphi^p \; r \, dr \, d\theta & l = c \\ 2 \cdot \int_0^{2\pi} \int_0^R \frac{1}{\Phi^r(\theta)} \cdot \varphi^p \; dr \, d\theta & l = r \end{cases} \quad (D.23)$$

- **Nodal infrastructure.** The cost of stations prorated in rush hour ($C_S = C_c^S + C_r^S$ in [\$/P_m]) depends on the separation of transportation routes ($\Phi^r(\theta)$ or $d^c(r)$), and the separation between facilities $\Phi^r(\theta)$ and $d^c(r)$ in which each corridor has two stops by direction. Each station has a unitary cost ($\varphi^s = \varphi^{s(f)} + \varphi^{s(v)} \cdot T$ in [\$/station·route·P_m]).

$$C_S = 4 \cdot \int_0^{2\pi} \int_0^R \frac{1}{\Phi^r(\theta)} \cdot \frac{1}{d^c(r)} \cdot \varphi^s \; dr \, d\theta \quad (D.24)$$

3. Problem formulation and optimization

The transit network design and frequency setting problem minimizes the total cost of the system, considering a heterogeneous demand for this research. The formulation of the total cost of a transit system ($TC_T = \mu \cdot T_T^u + C_T^a$) in monetary units ([\$/ P_m] contains a user cost component (T_T^u in [user·h/P_m]), which is multiplied by the travel time value (μ in [\$/user·h]), and an agency cost component (C_T^a in [\$/ P_m]) (Eq. D.25(a)). As previously described, the problem has four decision variables ($d^c(r), \Phi^r(\theta), h^c(r), h^r(\theta)$) according to the spatial and temporal deployment of resources.

$$Min\ TC_T = \mu \cdot (T_A + T_W + T_V + T_T) + (C_K + C_V + C_I) \quad \text{(a)}$$

s.t.

$$\max_{\theta, l \in L_c} \left(f_l^V(r,\theta) \cdot d^c(r) \cdot h^c(r) \right) \leq K^v \quad \forall\, r \quad \text{(b)}$$

$$\max_{r, l \in L_r} \left(f_l^V(r,\theta) \cdot \Phi^r(\theta) \cdot \frac{R+r}{2} \cdot h^r(\theta) \right) \leq K^v \quad \forall\, \theta \quad \text{(c)} \qquad \text{(D.25)}$$

$$d^c(r) \geq K^{d(c)} \quad \forall\, r \quad \text{(d)}$$

$$\Phi^r(\theta) \geq K^{d(r)} \quad \forall\, \theta \quad \text{(e)}$$

$$h^c(r) \geq K^h \quad \forall\, r \quad \text{(f)}$$

$$h^r(\theta) \geq K^h \quad \forall\, \theta \quad \text{(g)}$$

The problem has three sets of constraints. The first of these (Eq. D.25(b) and (c)) ensures that occupancy does not exceed the capacity of each vehicle (K^v [user/veh]). Second, the minimum distance between stations ensures that transit vehicles reach the cruising speed before arriving at the next station (Eq. D.25(d) and (e)). In the case of radial routes (Eq. D.25(e)), $K^{d(r)} = K^{d(c)}/r_{min}$, where r_{min} is a minimum radius in which this constraint is applied. Finally, the operator requires a minimum separation (time) between consecutive vehicles (TRB, 2013). Equations D.25(f) and (g) ensure that the optimum frequency is feasible.

3.1. Method for solving the problem

The mathematical problem is a nonlinear system with inequality constraints replacing the user and agency sub-cost functions on the objective function (Eq. D.25(a)). The Karush-Kuhn-Tucker (KKT) conditions allow finding the necessary conditions to solve it. The first-order optimization conditions enable obtaining optimized analytical functions, and it will permit getting the optimal value of overall city points. The necessary conditions are not sufficient for optimality, but all local minimum satisfies them. Therefore, a convexity analysis of the problem is required to find the optimal solution.

In the CA method, the $tc(r,\theta)$ is a local cost function at a point (r,θ). Equations D.26 shows the set of KKT conditions considering the number of variables n_v and constraints n_c. The stationarity conditions (Eq. D.26(a)) come from the local cost function considering multipliers ($\lambda_j^\circ(\cdot)$) and constraints for ring ($c_j^c(r,\theta)$) and radial ($c_j^r(r,\theta)$) routes. The second condition (Eq. D.26(b)) contains the constraints (c_j°). The third condition (Eq. D.26(c)) is a complementary slackness expression. If an inequality constraint becomes equality (tight), its slack is zero, and its multiplier takes any non-negative

value (Eq. D.26(d)). Finally, each decision variable (x_i°) must be higher than a K^{min} (K^v, K^h, $K^{d(c)}$,$K^{d(r)}$, respectively; Eq. D.26(e)).

$$\begin{aligned}
&\frac{\partial\, tc(r,\theta)}{\partial\, x_i^\circ(\cdot)} + \sum_{j=1}^{n_c} \lambda_j^c(r) \cdot \frac{\partial\, c_j^c(r,\theta)}{\partial\, x_i^\circ(\cdot)} + \sum_{j=1}^{n_c} \lambda_j^r(\theta) \cdot \frac{\partial\, c_j^r(r,\theta)}{\partial\, x_i^\circ(\cdot)} = 0 \quad \forall\, i = 1, \dots, n_v && \text{(a)}\\
&c_j^\circ(r,\theta) - K_j \le 0 \quad \forall\, j = 1, \dots, n_c && \text{(b)}\\
&\lambda_j^\circ(\cdot) \cdot \left(c_j^\circ(r,\theta) - K_j\right) = 0 \quad \forall\, j = 1, \dots, n_c && \text{(c)}\\
&\lambda_j^\circ(\cdot) \ge 0 \quad \forall\, j = 1, \dots, n_c && \text{(d)}\\
&x_i^\circ(\cdot) > K^{min} \quad \forall\, i = 1, \dots, n_v && \text{(e)}
\end{aligned} \qquad \text{(D.26)}$$

where $n_v = 4, n_c = 6$,
$x_i^\circ(\cdot) = \{d^c(r), \Phi^r(\theta), h^c(r), h^r(\theta)\}$
$\lambda_j^\circ(\cdot) = \{\lambda_1^c(r), \lambda_2^c(r), \lambda_3^c(r), \lambda_1^r(\theta), \lambda_2^r(\theta), \lambda_3^r(\theta)\}$

3.2. Optimal analytical solutions

Using the formulation of Equation D.26(a), we obtain the optimal analytical functions for each decision variable: the distance between routes and the headway between vehicles on each type of corridor.

Optimal distance function between routes

From stationarity conditions, we isolate the variable $d^c(r)$ representing it as a square root of an analytical ratio (Eq. D.27). The numerator of this ratio is a cost function ([$]) obtained from two components. The first component is the cost due to users on radial routes that arrive at a station within a ring corridor. The second cost is the operation and infrastructure cost on a ring route at r. The denominator, which is multiplied by the travel time value, represents the total time per square kilometer due to access of all users to a station ([h·user/km²]). Moreover, the denominator contains two more components: user density per kilometer on a vehicle multiplies by a Lagrange multiplier ($\lambda_1^c(r)$), and a second Lagrange multiplier ($\lambda_2^c(r)$).

$$\boldsymbol{d^c(r)} = \sqrt{\frac{\int_0^{2\pi} \left(\mu \cdot \gamma \cdot \frac{1}{2} \cdot \left(\frac{R}{r} + 1\right) \cdot f_{L_r}^V(r,\theta) \cdot T \cdot \tau^s + 2 \cdot \left(\left(\frac{1}{v^t} + \frac{t^f}{2\pi r} + \frac{\tau^s}{\boldsymbol{\Phi^r(\theta)} \cdot r}\right) \cdot \frac{\varphi^v}{\boldsymbol{h^c(r)}} + \frac{\tau^s \cdot \varphi^v}{\boldsymbol{\Phi^r(\theta)} \cdot r \cdot \boldsymbol{h^r(\theta)}} + \frac{T \cdot \varphi^o}{\boldsymbol{h^c(r)}} + \varphi^p + \frac{2 \cdot \varphi^s}{\boldsymbol{\Phi^r(\theta)} \cdot r}\right)\right) \cdot r\, d\theta}{\mu \cdot \int_0^{2\pi} \frac{\alpha \cdot f^A(r,\theta) \cdot T}{4 \cdot v^a(r)}\, r\, d\theta + \boldsymbol{\lambda_1^c(r)} \cdot \max_{\theta, l \in L_c}\left(f_l^V(r,\theta)\right) \cdot \boldsymbol{h^c(r)} - \boldsymbol{\lambda_2^c(r)}}} \qquad \text{(D.27)}$$

In Eq. D.27, including Equations D.28, D.29, and D.30, we have defined two new parameters. First, the time lost at a station ($\tau^s = \tau + \tau' + \tau'' + \tau'''$ in

[h/station]). Second, we have grouped the cost per vehicle and the salary cost per vehicle in rush hour ($\varphi^v = \varphi^k + \eta^d \cdot T \cdot \varphi^g$ in [\$/veh·P_m]).

In the second case, from the local cost function of radial routes, the expression of the optimal angle between radial corridor lines ($\Phi^r(\theta)$, Eq. D.28) has an analytical structure that is similar to the previous function, but each component represents the cost of the angle between radial routes. Moreover, there are two aggregated factors in the denominator, which contain the multipliers $\lambda_1^r(\theta)$ and $\lambda_2^r(\theta)$.

$$\boldsymbol{\Phi^r(\theta)} = \sqrt{\frac{\int_0^R \left(\mu \cdot \gamma \cdot f_{L_c}^V(r,\theta) \cdot T \cdot \tau^s + 2 \cdot \left(\left(\frac{1}{v^t} + \frac{t^f}{R} + \frac{\tau^s}{\boldsymbol{d^c(r)}}\right) \cdot \frac{\varphi^v}{\boldsymbol{h^r(\theta)}} + \frac{\tau^s \cdot \varphi^v}{\boldsymbol{h^c(r)} \cdot \boldsymbol{d^c(r)}} + \frac{T \cdot \varphi^o}{\boldsymbol{h^r(\theta)}} + \varphi^p + \frac{2 \cdot \varphi^s}{\boldsymbol{d^c(r)}}\right)\right) dr}{\mu \cdot \int_0^R \frac{\alpha \cdot f^A(r,\theta) \cdot T \cdot r}{4 \cdot v^a(r)} \cdot r \; dr + \boldsymbol{\lambda_1^r(\theta)} \cdot \max_{r,l \in L_r} \left(f_l^V(r,\theta) \cdot \frac{R+r}{2}\right) \cdot \boldsymbol{h^r(\theta)} - \boldsymbol{\lambda_2^r(\theta)}}} \tag{D.28}$$

Optimal headway function on routes

The optimal headway has the same structure for rings (Eq. D.29) and radial (Eq. D.30) routes. The numerator is the time per kilometer that is multiplied by the cost. The denominator is the user density per kilometer that waits or transfers at a station, which is multiplied by the travel time value. Moreover, the denominator includes two factors, and Lagrange multipliers multiply these factors.

$$\boldsymbol{h^c(r)} = \sqrt{\frac{2 \cdot \int_0^{2\pi} \left(\left(\frac{1}{v^t} + \frac{t^f}{2\pi r} + \frac{\tau^s}{\boldsymbol{\Phi^r(\theta)} \cdot r}\right) \cdot \varphi^v + T \cdot \varphi^o\right) \cdot \frac{1}{\boldsymbol{d^c(r)}} \; r \, d\theta}{\mu \cdot \int_0^{2\pi} \left(\frac{\beta}{2} \cdot f_{L_c}^W(r,\theta) \cdot T + \frac{\delta}{4} \cdot \left(\frac{R}{r} + 1\right) \cdot f_{L_c}^T(r,\theta) \cdot T\right) \cdot r \, d\theta + \boldsymbol{\lambda_1^c(r)} \cdot \max_{\theta, l \in L_c} \left(f_l^V(r,\theta)\right) \cdot \boldsymbol{d^c(r)} - \boldsymbol{\lambda_3^c(r)}}} \tag{D.29}$$

$$\boldsymbol{h^r(\theta)} = \sqrt{\frac{2 \cdot \int_0^R \left(\left(\frac{1}{v^t} + \frac{t^f}{R} + \frac{\tau^s}{\boldsymbol{d^c(r)}}\right) \cdot \varphi^v + T \cdot \varphi^o\right) \cdot \frac{1}{\boldsymbol{\Phi^r(\theta)}} \; dr}{\mu \cdot \int_0^R \left(\frac{\beta}{2} \cdot f_{L_r}^W(r,\theta) \cdot T + \frac{\delta}{4} \cdot \left(\frac{R}{r} + 1\right) \cdot f_{L_r}^T(r,\theta) \cdot T\right) \cdot r \, dr + \boldsymbol{\lambda_1^r(\theta)} \cdot \max_{r,l \in L_r} \left(f_l^V(r,\theta) \cdot \frac{R+r}{2}\right) \cdot \boldsymbol{\Phi^r(\theta)} - \boldsymbol{\lambda_3^r(\theta)}}} \tag{D.30}$$

In previous functions, it is worth mentioning that an optimal analytical function ($d^c(r), \Phi^r(\theta), h^c(r), h^r(\theta)$) dependent on each other. Thus, the solution of one type of route—i.e., rings or radial routes—will depend on the result of the other type of route.

3.3. Solution methodology

The optimal functions $d^c(r)$ and $h^c(r)$ (Eqns. D.27 and D.29) have a common factor $\lambda_1^c(r) \cdot \max_{\theta, l \in L_c} \left(f_l^V(r,\theta) \right)$. If we equate these two expressions using this factor, we will obtain Equation D.31(a). Therefore, from KKT conditions (Eq. D.26), we formulate the equation system to solve the problem of ring services in the set of Equations D.31, where Equations D.31(b) are the constraints, the set of Equations D.31(c) is the complementary slackness, and Equations D.31(d) is the integrality of multipliers.

$$
\begin{aligned}
&\boldsymbol{d^c(r)^2} \cdot \int_0^{2\pi} \frac{\mu \cdot \alpha \cdot f^A(r,\theta) \cdot T}{4 \cdot v^a(r)} \cdot r \, d\theta - \boldsymbol{d^c(r)} \cdot \boldsymbol{h^c(r)} \cdot \int_0^{2\pi} \mu \cdot \left(\frac{\beta}{2} \cdot f_{L_c}^W(r,\theta) \cdot T + \frac{\delta}{4} \cdot \left(\frac{R}{r} + 1 \right) \cdot f_{L_c}^T(r,\theta) \cdot T \right) \cdot r \, d\theta \\
&+ \boldsymbol{d^c(r)} \cdot \left(\boldsymbol{\lambda_3^c(r)} - \boldsymbol{\lambda_2^c(r)} \right) - \int_0^{2\pi} \left(\frac{1}{2} \cdot \mu \cdot \gamma \cdot f_{L_r}^V(r,\theta) \cdot \left(\frac{R}{r} + 1 \right) \cdot T \cdot \tau^s + \frac{2 \cdot \tau^s \cdot \varphi^v}{\Phi^r(\theta) \cdot r \cdot h^r(\theta)} + 2 \cdot \varphi^p + \frac{4 \cdot \varphi^s}{\Phi^r(\theta) \cdot r} \right) \cdot r \, d\theta = 0 \quad \forall r
\end{aligned} \tag{a}
$$

$$
\begin{aligned}
\max_{\theta, l \in L_c} \left(f_l^V(r,\theta) \cdot \boldsymbol{d^c(r)} \cdot \boldsymbol{h^c(r)} \right) &\leq K^v \quad \forall r \\
\boldsymbol{d^c(r)} &\geq K^d \quad \forall r \\
\boldsymbol{h^c(r)} &\geq K^h \quad \forall r
\end{aligned} \tag{b}
$$

$$
\begin{aligned}
\boldsymbol{\lambda_1^c(r)} \cdot \left(\max_{\theta, l \in L_c} \left(f_l^V(r,\theta) \cdot \boldsymbol{d^c(r)} \cdot \boldsymbol{h^c(r)} \right) - K^v \right) &= 0 \quad \forall r \\
\boldsymbol{\lambda_2^c(r)} \cdot \left(-d^c(r) + K^{d(c)} \right) &= 0 \quad \forall r \\
\boldsymbol{\lambda_3^c(r)} \cdot \left(-h^c(r) + K^h \right) &= 0 \quad \forall r
\end{aligned} \tag{c}
$$

$$
\begin{aligned}
\boldsymbol{\lambda_1^c(r)} &\geq 0 \quad \forall r \\
\boldsymbol{\lambda_2^c(r)} &\geq 0 \quad \forall r \\
\boldsymbol{\lambda_3^c(r)} &\geq 0 \quad \forall r
\end{aligned} \tag{d}
$$

(D.31)

For the radial routes case, analytical development is similar to the circular case. Therefore, we also formulate the analytical equation system that solves the problem of radial services in the set of Equations D.32, where the meaning of the equations is similar to the previous case. Equations D.32(b) are the constraints, Equations D.32(c) represents the complementary slackness conditions, and Equations D.32(d) is the integrality of multipliers.

$$
\begin{aligned}
&\boldsymbol{\Phi^r(\theta)^2} \cdot \int_0^{R} \frac{\mu \cdot \alpha \cdot f^A(r,\theta) \cdot T \cdot r}{4 \cdot v^a(r)} \cdot r \; dr - \boldsymbol{\Phi^r(\theta)} \cdot \boldsymbol{h^r(\theta)} \cdot \int_0^{R} \mu \cdot \left(\frac{\beta}{2} \cdot f_{L_r}^W(r,\theta) \cdot T + \frac{\delta}{4} \cdot \left(\frac{R}{r} + 1 \right) \cdot f_{L_r}^T(r,\theta) \cdot T \right) \cdot r \; dr \\
&+ \boldsymbol{\Phi^r(\theta)} \cdot \left(\boldsymbol{\lambda_3^r(r)} - \boldsymbol{\lambda_2^r(r)} \right) - \int_0^{R} \left(\mu \cdot \gamma \cdot f_{L_c}^V(r,\theta) \cdot T \cdot \tau^s + \frac{2 \cdot \tau^s \cdot \varphi^v}{h^c(r) \cdot d^c(r)} + 2 \cdot \varphi^p + \frac{4 \cdot \varphi^s}{d^c(r)} \right) dr = 0 \quad \forall \theta
\end{aligned} \tag{a}
$$

$$
\begin{aligned}
\max_{r, l \in L_r} \left(f_l^V(r,\theta) \cdot \boldsymbol{\Phi^r(\theta)} \cdot \frac{R + r}{2} \cdot \boldsymbol{h^r(\theta)} \right) &\leq K^v \quad \forall \theta \\
\boldsymbol{\Phi^r(\theta)} &\geq K^{d(r)} \quad \forall \theta \\
\boldsymbol{h^r(\theta)} &\geq K^h \quad \forall \theta
\end{aligned} \tag{b}
$$

$$
\begin{aligned}
\boldsymbol{\lambda_1^r(\theta)} \cdot \left(\max_{r, l \in L_r} \left(f_l^V(r,\theta) \cdot \boldsymbol{\Phi^r(\theta)} \cdot \frac{R + r}{2} \cdot \boldsymbol{h^r(\theta)} \right) - K^v \right) &= 0 \quad \forall \theta \\
\boldsymbol{\lambda_2^r(r)} \cdot \left(-\boldsymbol{\Phi^r(\theta)} + K^{d(r)} \right) &= 0 \quad \forall r \\
\boldsymbol{\lambda_3^r(r)} \cdot \left(-\boldsymbol{h^r(\theta)} + K^h \right) &= 0 \quad \forall r
\end{aligned} \tag{c}
$$

$$
\begin{aligned}
\boldsymbol{\lambda_1^r(\theta)} &\geq 0 \quad \forall \theta \\
\boldsymbol{\lambda_2^r(\theta)} &\geq 0 \quad \forall \theta \\
\boldsymbol{\lambda_3^r(\theta)} &\geq 0 \quad \forall \theta
\end{aligned} \tag{d}
$$

(D.32)

Each set of Equations D.31 and D.32 contains a system with inequalities that allow obtaining the optimal solution. In consequence, we formulate an algorithm based on the CA method. Algorithm 1 in Figure D.6 consists of iterating the analytical expressions of ring and radial corridors until reaching the convergence.

The method has two phases. The first stage consists of the initialization of variables in which a feasible solution uses the minimum value of each variable, respectively: $\{K^d, K^h\}$. Moreover, the algorithm creates a variable that stores the number of iterations (i). The second stage is an iterative process in which the model calculates the four decision variables. The process will iterate while the solutions are feasible, and the error is higher than the tolerance for each variable. The first sub-problem calculates the two variables $(d^{c(i)}(r), h^{c(i)}(r))$ for a set of ring corridor routes ($r \in [0 \dots R]$) if there are feasible solutions and first-order optimization conditions are satisfied. After that, the section includes the convexity of the problem and the search for the optimal solution. In the case of radial services, the process is identical. After that, the variable will increase by one unit. Finally, the algorithm will stop when the error is less than the tolerance.

Algorithm 1: Solution of the continuous problem

Initialize $d^{c(0)}(r) = K^{d(c)}$; $\Phi^{r(0)}(\theta) = K^{d(r)}$; $h^{c(0)}(r) = K^h$; $h^{r(0)}(\theta) = K^h$
i := 1
while (abs($d^{c(i)}(r) - d^{c(i-1)}(r)$) > tolerance or abs($\Phi^{r(i)}(\theta) - \Phi^{r(i-1)}(\theta)$) > tolerance or
abs($h^{c(i)}(r) - h^{c(i-1)}(r)$) > tolerance or abs($h^{r(i)}(\theta) - h^{r(i-1)}(\theta)$) > tolerance)

for each $r \in [0 \dots R]$ **do**
$\{d^{c(i)}(r), h^{c(i)}(r)\} \leftarrow$ *SystemOfEquations*($\{\Phi^{r(i-1)}(\theta), h^{r(i-1)}(\theta)\}$)
end for

for each $\theta \in [0 \dots 2\pi]$ **do**
$\{\Phi^{r(i)}(\theta), h^{r(i)}(\theta)\} \leftarrow$ *SystemOfEquations*($\{d^{c(i-1)}(r), h^{c(i-1)}(r)\}$)
end for

i := i + 1
end while

Figure D.6. The algorithm based on successive approximations numerically solves the problem.

The discretization of continuum results from the model allows the location of corridors, routes, and the transit service frequency. Medina-Tapia et al. (2013) proposed a method based on the disk model (Ouyang & Daganzo, 2006). For this paper, we propose a method using the inverse of optimal continuous

functions (density functions of ring or radial corridor routes), and we calculate the area below the function's curve. This algorithm searches similar areas, i.e., the integral of an area gives a unitary value or close to one. Figure D.7 shows the density function $\delta(x)$ (the blue line) that represents the inverse of the distance between ring routes ($1/d^c(r)$), or the angle between radial routes ($1/\Phi^r(\theta)$). The x-axis represents the distance of a corridor route in kilometers or radians. Moreover, the gray zones in the plot symbolize the area below the density curve between the two following thresholds. A black point represents the position of a route at the point $x_{2\cdot i}$, in which each zone Z_i is defined between $x_{2\cdot i-1}$ and $x_{2\cdot i+1}$ (red points). Therefore, using a system of inequalities for rings (Eq. D.33) and radial (Eq. D.34) routes, we obtain the position of $x_{2\cdot i-1}$, $x_{2\cdot i}$, and $x_{2\cdot i+1}$.

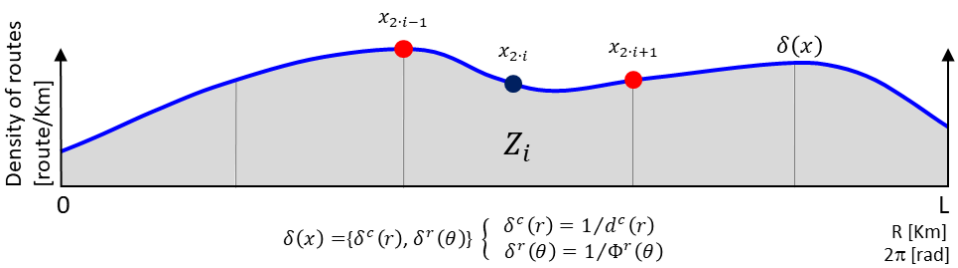

Figure D.7. Graphical representation of the discretization process of a density function using a system of inequalities.

$$\int_{x_{2\cdot i-1}}^{x_{2\cdot i}} \delta^c(r)\,dr \le \frac{1}{2}\cdot(1+\xi) \quad \forall\, Z_i \qquad \text{(a)}$$

$$\int_{x_{2\cdot i}}^{x_{2\cdot i+1}} \delta^c(r)\,dr \le \frac{1}{2}\cdot(1+\xi) \quad \forall\, Z_i \qquad \text{(b)} \qquad \text{(D.33)}$$

$$\int_{x_{2\cdot i-1}}^{x_{2\cdot i+1}} \max_{\theta, l\in L_c}\left(f_l^V(r,\theta)\cdot h^c(x_{2\cdot i})\right) dr \le K^v \quad \forall\, Z_i \qquad \text{(c)}$$

$$\int_{x_{2\cdot i-1}}^{x_{2\cdot i}} \delta^r(\theta)\,d\theta \le \frac{1}{2}\cdot(1+\xi) \quad \forall\, Z_i \qquad \text{(a)}$$

$$\int_{x_{2\cdot i}}^{x_{2\cdot i+1}} \delta^r(\theta)\,d\theta \le \frac{1}{2}\cdot(1+\xi) \quad \forall\, Z_i \qquad \text{(b)} \qquad \text{(D.34)}$$

$$\int_{x_{2\cdot i-1}}^{x_{2\cdot i+1}} \max_{r, l\in L_r}\left(f_l^V(r,\theta)\cdot\frac{R+r}{2}\cdot h^c(x_{2\cdot i})\right) d\theta \le K^v \quad \forall\, Z_i \qquad \text{(c)}$$

In the first stage of the discretization of a continuous density function ($\delta(x)$), the total area under the density function determines the number of zones. Second, each zone takes equidistant borders as a feasible initial solution. Third, the set of inequalities for rings (Eq. D.33) and radial routes (Eq. D.34) allow determining a discrete solution. The inequalities (a) and (b) have slack or tolerance (ξ), and inequality (c) is strict. The solution cannot be unique.

4. Application to cases

4.1. Parameters

The modeling analyzes a concentric city that has a radius of 15 km (R), considering the rush hour lasts 1.5 hours (T). Each stage of a trip requires a list of parameters (Table D.1) that depend on three types of modal services: HRT, LRT, and BRT.

Table D.1. Parameters used for user and agency cost functions.

Demand parameters

	T	α	β	γ	δ	v^w	χ^T	$v^a(r)$
	[h]		[dimensionless]			[km/h]	[m]	[km/h]
HRT							50	$v^a(r) = 3.0 + 1.4\bar{6} \cdot r$
LRT	1.5	2.2	2.1	1.0	2.5	3.0	75	
BRT							100	

Operational parameters

	v^t	a^a	a^d	τ	τ'	τ''	τ'''	τ^s	t^f	η^d	K^v	K^d	K^h
	[km/h]	[m/s²]		[s/station]					[min]	[shift/veh]	[user/veh]	[km/route]	[s/veh]
HRT	90	1.3	1.3	19.2	45	35	0	69.2	12	1	750	0.481	123
LRT	50	1.0	1.3	12.2	30	45	30	52.2	8	1	190	0.171	118
BRT	30	0.8	1.0	9.3	15	60	30	39.3	4	1	101	0.079	60

Economic parameters

	μ	φ^k	φ^g	φ^o	$\varphi^{p(f)}$	φ^p	$\varphi^{s(f)}$	φ^s
	[$/h]	[$/veh]	[$/shift·h]	[$/km·veh]	[$/km·route·$P_m$]		[$/station·route·$P_m$]	
HRT		135.6	27	3.7	306.4	309.5	169.9	214.4
LRT	10	83.8	25	2.6	169.6	171.3	8.3	8.4
BRT		38.5	23	1.6	141.3	142.7	1.6	1.6

The first demand parameters are time perception with their values based on TRB (2013). Considering the accessibility, we assumed that that speed would linearly increase from the city center to the periphery. At the city center, the speed will be 3.0 [km/h], which is about 83 [cm/s]. At the outer line, the speed will be 25 [km/h] because the user could take a feeder bus or another vehicle; therefore, the access speed function is $v^a(r) = 3.0 + 22/15 \cdot r$. Respect to the operation parameters, the values are based on TRB (2013). The cruising speed (v^t) depends on the type of vehicle. At a station, the average time τ lost by deceleration and acceleration. The average fixed dead time and the minimum stopping time at a station use standard values. According to transit infrastructure costs, fixed values are based on Australian technical report ATC (2006) for linear and nodal infrastructures and variable costs, assuming by 1% of the fixed cost. The model's constraints require a threshold in each modal scenario. The thresholds K^v and K^h come from ATC (2006), but K^d was calculated using the acceleration and deceleration to reach the cruising speed.

In the unitary cost parameters, the value of travel time takes a standard while the rest of the parameters have a basis on ATC (2006). Finally, in these applied cases, we assumed that long-term urban changes would not affect the structure of unitary costs.

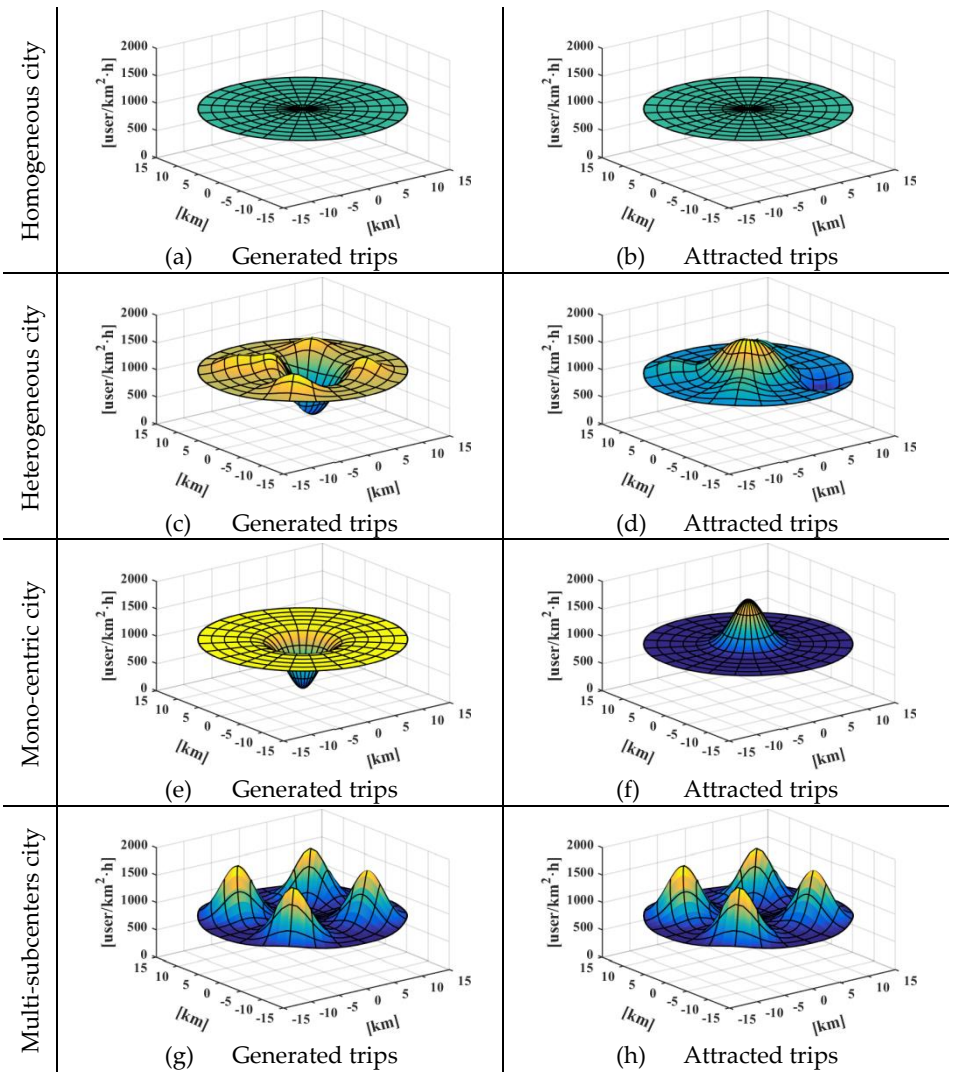

Figure D.8. Types of scenarios analyzed with spatially homogeneous and heterogeneous demand: the case of 1,000 [user/km²·h].

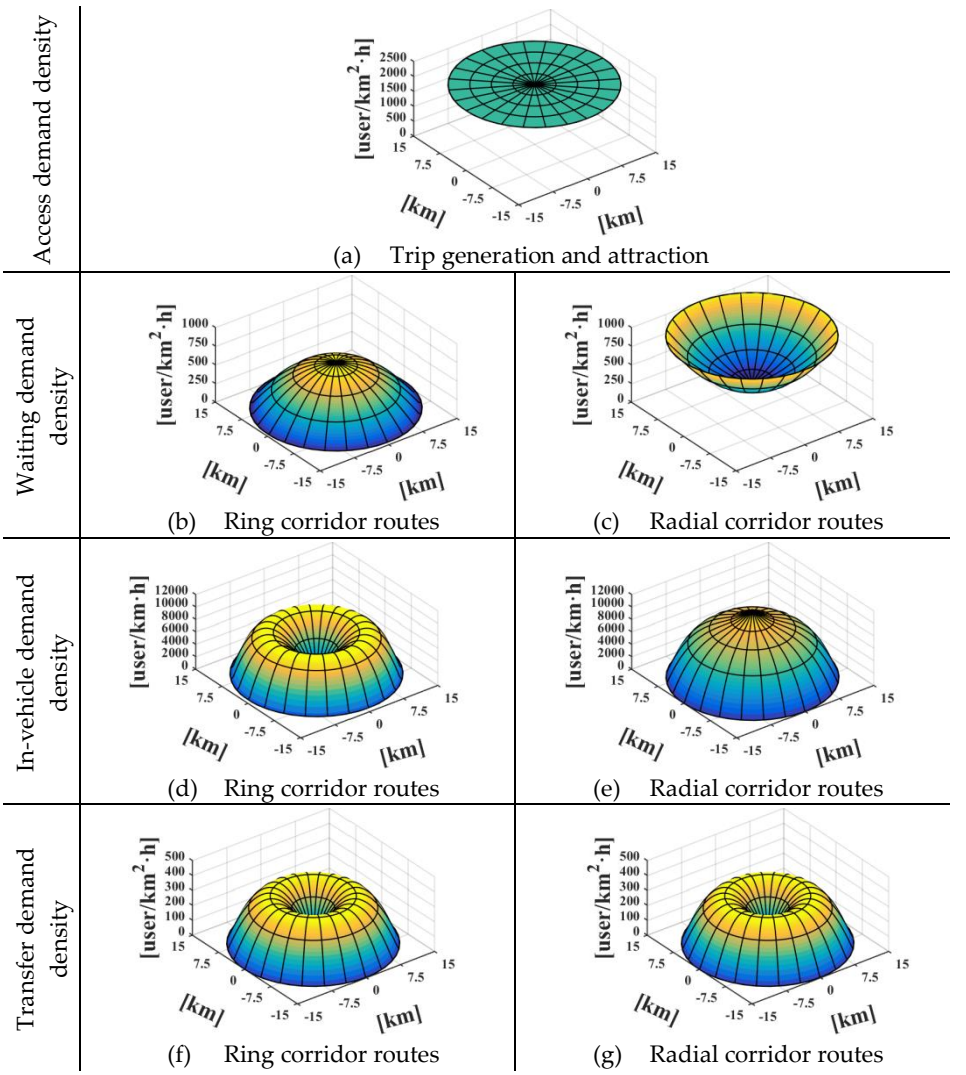

Figure D.9. Demand density functions calculated for the case of 1,000 [user/km²·h].

Scenarios of demand

We analyze four scenarios of cities: homogeneous city, heterogeneous city, mono-centric city, and multi-subcenters city (Figure D.8). First, in a homogeneous city, each point of a city has a stable trip generation and attraction density; in this case, the rate is 1000 [user/km²·h]. Second, the heterogeneous city is a case opposite to the homogeneous city in which each point on the city has different densities of generation and attraction of trips. The selection of this case was random, respecting the same total number of generated/attracted trips in comparison to the homogeneous city. Third, the

mono-centric city contains a central business district (CBD) that generates and attracts more trips than the rest of the city. Finally, the multi-subcenters city contains a CBD as the previous case and four subcenters. The role of urban subcenters is to "bring economic activities (e.g., services, employment) closer to people who live in peripheral urban spaces" (Medina-Tapia et al., 2020).

Demand density functions

The demand density functions represent the mobility in a city in each stage of a trip. These functions depend on the width of a transit corridor. In this section, we have analyzed the case with homogenous demand over the city, i.e., each point at the city generates/attracts the same density of trips. Figure D.9 shows the density function with a spatially homogeneous density of 1,000 [user/km^2·h] generated trips. In the case of access density (Figure D.9(a)), the function $f^A(r,\theta)$ in [user/km^2·h] shows a constant value of 2,000 [user/km^2·h] over the city and depends on generated and attracted trips (boarding and alighting) for both types of corridor routes.

In Figure D.9(b), the demand density of passengers that wait for a ring route ($f_l^W(r,\theta)$ expressed in [user/km^2·h]) increases closer to the city center than the outskirts of the city because the probability of starting a trip and finish is higher around the center than in the city periphery. The opposite happens in radial transit, where the probability is higher in the periphery than in the city center (Figure D.9(c)).

In Figure D.9(d), the trip density surface shows the "regular" trip density per kilometer of the width of a transit corridor at each city point ($f_l^V(r,\theta)$ in [user/km·h]). In ring roads, the density is concentrated on an intermediate ring between the center and outer ring because the intermediate ring has more likely to receive more trips in a scenario with homogeneous demand. Furthermore, radial trips increase in points close to the city center because this zone joins trips from the same city side and the opposite side (Figure D.9(e)).

The transfer density function ($f_l^T(r,\theta)$) represents the density of users in [user/km^2·h] that transfer between two types of routes. The surface is similar in both types of corridor services considering a homogeneous demand (Figure D.9(f) and (g)) because the density functions are equivalent if a user transfers from a ring to a radial service or vice versa.

Therefore, these plots show that although the demand generated and attracted is a fixed value, the demand at each stage of the trip is not constant over the city. It is interesting to analyze the effect that has these high and low values that demand functions present in the exhibit.

4.2. Spatially homogeneous demand case

Feasible and optimal solutions

This section analyzes the case of a concentric city in which the homogeneous trip generation rate is 1,000 [user/km²·h] in each city point. In the design problem, the constraints of the model define areas in Figure D.10 representing feasible regions for each transit technology: HRT (green area), LRT (blue area), and BRT (red area). First, the spatial and temporal minimum constraints have equivalent values between ring and radial routes (Eqns. D.25(d-g)). On the other hand, the occupancy density ($f_c^v(r,\theta)$ in Eq. D.25(b)) varies according to a ring corridor even in the homogeneous case; therefore, the maximum iso-capacity curve will also change for different rings. Thus, plot (a) only shows the feasible region for the radius 7.5 [km], and plot (b) shows it for the angle π [rad].

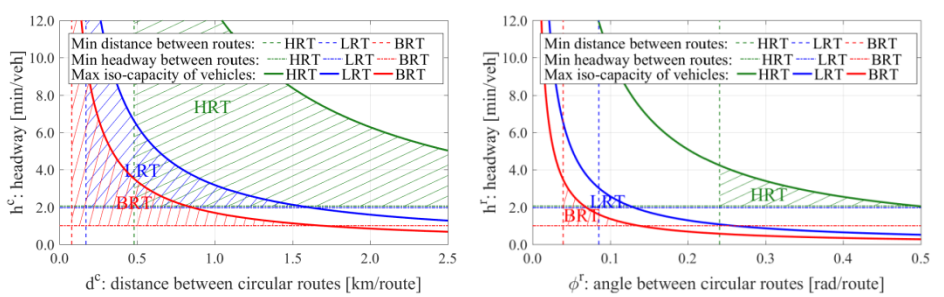

(a) Ring route at a radius 7.5 [km] (b) Radial route at an angle π [rad]

Figure D.10. Feasible region for a homogeneous city (1000 [user/km²·h]) considering three transit technologies.

The demand density for radial routes is stable, but demand for radials is higher than for ring routes (Figure D.9(d) and (e)). Therefore, the iso-capacity curve is more restrictive in the case of radial routes, e.g., in a balanced scenario, a bus system with a headway of 2 [min/veh] requires corridors separated by about 1 [km] (0.069 [rad]) at the periphery. Therefore, the feasible regions are more significant for ring routes than in radial routes for the three technologies. Finally, the case (a), we can see overlapping areas

among transit technologies, but the technologies analyzed in this paper do not cover all space of solutions for case (b).

Figure D.11 shows optimal solutions for a homogeneous city previously described considering the feasible regions for each type of corridor route (Figure D.9). The iso-capacity constraints change at each radius due to the variation of demand density; for this reason, the exhibit includes only four iso-capacity constraints at radii 3, 6, 9, and 12 km. Although the generation and attraction rates are constant throughout the city, the solutions for ring routes vary according to the radius. The first exhibit (Figure D.11(a)) shows the curve that contains the optimal solutions for ring routes considering different radii, and the second exhibit (Figure D.11(b)) shows the optimal solutions for a radial route at the angle π because the solution at radial routes is stable for all points.

In Figure D.11(a) for ring routes, feasible regions are more significant at the extremes of routes than at the intermediate zone, which is the most charged zone of passengers. The temporary constraints are active from the city center to 12 km of radius. At the city center, the BRT's headways are lower, but the constraint is not active until 4 km from the city center. In the outskirts zone, the spatial distributions are more relevant for BRT, LRT, and HRT—in this order—than at the city center, considering even less frequency. Consequently, the density of rings and headways will increase its value if the radius increases toward the outer of the city. Therefore, a concentric city must encourage transit rings in the periphery. For radial routes (Figure D.11(b)), optimal solutions are stable for all angles; this is the opposite in comparison to ring routes. HRT systems activate both minimum spatial and temporary constraints. On the other hand, LRTs and BRTs have two active constraints: maximum occupancy and minimum headway.

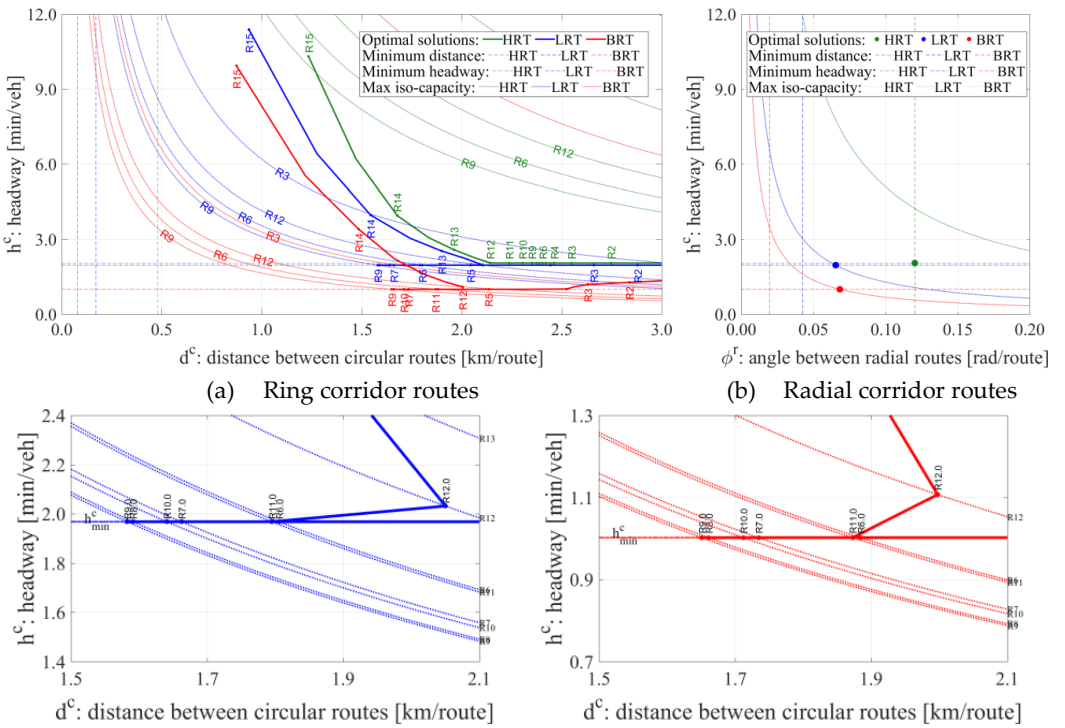

(a) Ring corridor routes (b) Radial corridor routes

(c) Case LRT (d) Case BRT

Figure D.11. Optimal solutions calculate for a homogeneous city with a generation rate of 1,000 [user/km²·h].

Considering the exhibit in Figure D.11(a), two highlighted cases show the effects of the active capacity constraints for LRT and BRT systems. In the LRT case (Figure D.11(c)), the temporary and capacity constraints are both active within 5 and 11 km of radius due to the high density at the intermediate zone of the city, causing the density of ring routes to increase in this zone. In the BRT case (Figure D.11(c)), the only capacity constraint is active from 4 km of radius, reducing the headway and distance simultaneously. After that, as in the case mentioned above, both constraints are also active between 6 and 11 km.

Figure D.12 shows feasible regions of the network design problem considering the constraints for each transit technology: HRT, LRT, and BRT. Each region feasible has three constraints: dotted lines represent iso-capacity curves obtained from vehicle capacity constraints (Eqns. D.25(b) and (c)), dashed lines represent the spatial constraints (Eqns. D.25(d) and (e)), and dash-dot lines represent the minimum time headways (Eqns. D.25(f) and (g)). The iso-capacity curves have distances and headways in which the capacity constraint is active according to the transit technologies. Moreover, the iso-capacity curves consider a progressive demand increment from 500 to 3500

[user/km^2·h]. Thus, the dotted lines depend on the demand, i.e., if the demand increases, the feasible region decreases in size. In Figure D.12, blue dotted lines represent unfeasible solutions because the capacity constraint is smaller than the minimum distance and headway. The previous definition appears on at least one of the two types of routes, particularly, radial routes which firstly achieve the infeasibility of solutions. Therefore, the maximum feasible demand is 2,000 [user/km^2·h] for HRTs, 1,500 [user/km^2·h] for LRTs, and 3,000 [user/km^2·h] for BRTs. At least in a homogeneous distribution scheme, the bus at a BRT system is the one that has less individual capacity but offers greater capacity for the system.

For ring routes, the implementation of BRT must reach a high frequency, and the corridors should close to each other, while an HRT system has an implementation with less frequency, and the distance is higher from each other than BRT and LRT systems. In radial routes, the demand of users is higher, and so transit modes have more differences than in the previous case. For low demand levels, the constraints are not all active. The temporary and capacity constraints are active over 1,000 [user/km^2·h] for LRT and BRT systems. In the case of HRT systems, the temporary and spatial constraints are active over 1,000 [user/km^2·h], although ring routes only have active the temporary constraint. For this reason, the minimum distance between vehicles for HRT systems is significant in the network design; on the contrary, the restriction prevents it would be able to reach higher levels of demand. On the other hand, adding more oversized vehicles in the transit system (higher capacity of buses or tramways) will be able to feasible areas more significant for BRTs and LRTs.

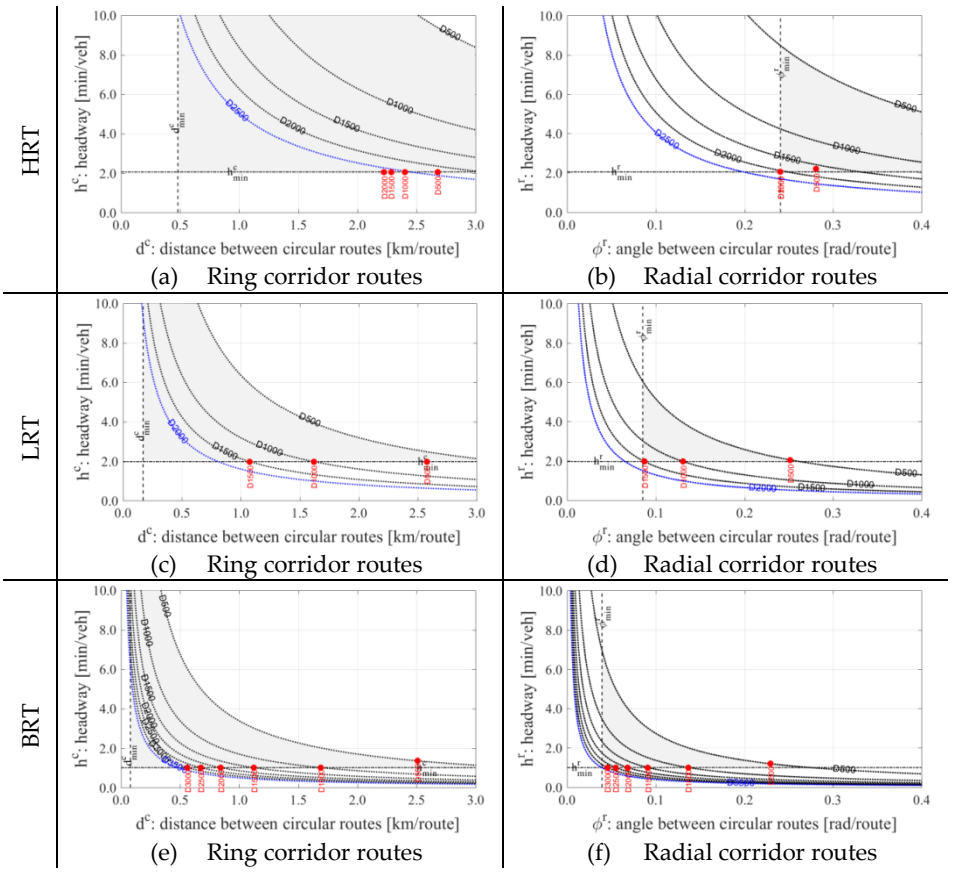

Figure D.12. Feasible regions for each transit technology, considering the set of constraints.

Figure D.13 represents the density of corridors considering different levels of demand for a ring city with a homogeneous trip distribution. In these exhibits, points represent the discrete location obtained from the algorithm in Figure D.6. The levels of demand progressively increase, considering the existence of a feasible space for solutions explained at the previous point. Figure D.13(a) shows that optimal density curves are continuous because they are no active, as Figure D.12(a) showed it. On the other hand, Figure D.13(a) shows the same density for cities over D1000 [user/km^2·h], although the occupancy also increases, reducing the available capacity of each subway car. Figure D.13(b) and (e) show the effects of activation of temporary and capacity constraints around the central ring zone. Thus, LRT's and BRT's ring density of D1000 [user/km^2·h] show the consequences explained previously. In radial densities, route density increases rapidly if the city's homogeneous demand also increases.

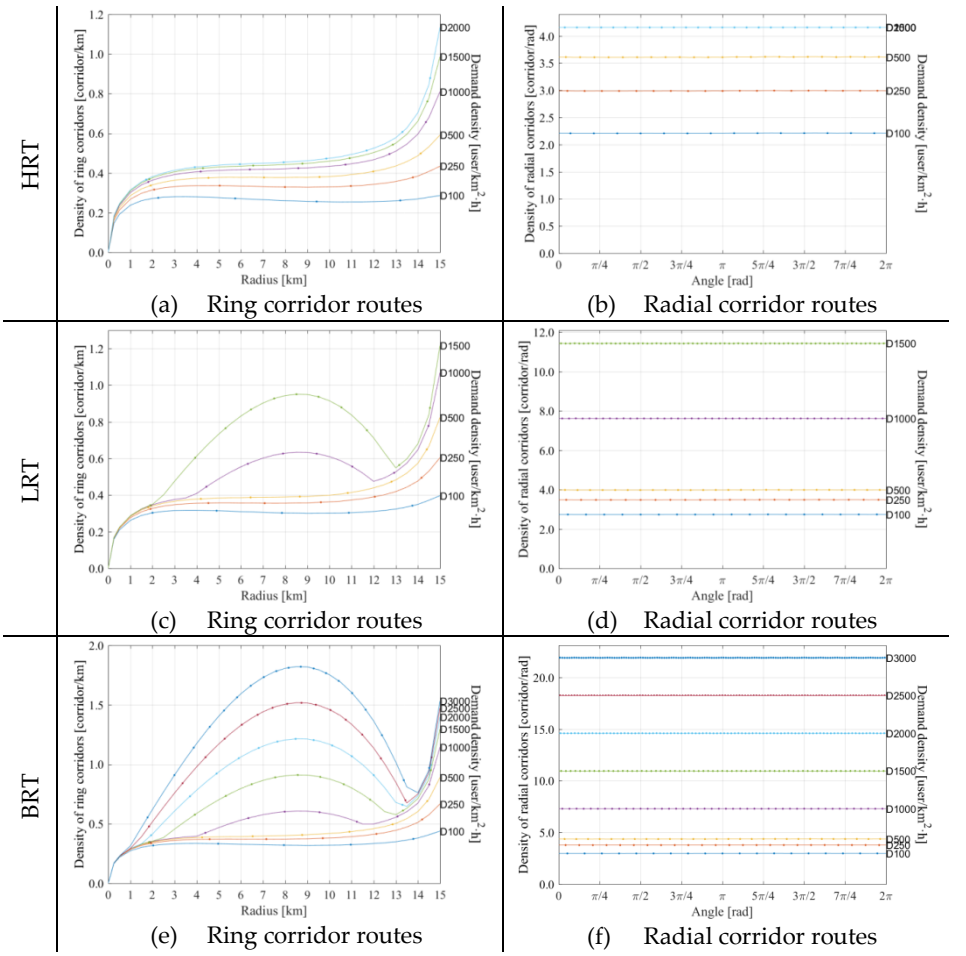

(a) Ring corridor routes (b) Radial corridor routes

(c) Ring corridor routes (d) Radial corridor routes

(e) Ring corridor routes (f) Radial corridor routes

Figure D.13. Optimal transit structures regarding homogeneous demand scenarios.

Effects of transit operation on infrastructure

The exhibits of Figure D.14 allow analyzing the system costs considering the three transit technologies. Figure D.14(a) shows the behavior of the total, user, and agency costs regarding levels of demand that progressively increase, considering the system feasibility. LRT has less cost at low levels of demand. HRT is more suitable in intermediate and high levels of demand, but HRT is unfeasible in very high levels of demand; in this case, the only alternative is a BRT system. Figure D.14(b) represents the average cost by a user in which the green curve (HRT) decreases concerning the demand. The BRT system reaches the minimal values at approximately 1,000 [user/km²·h]; after that, the average cost increase, and the BRT system is less efficient. Figure D.14(c) represents the agency cost divided by users; it could represent

the fare of the transit. In this exhibit, the BRT system is more attractive for low and super high levels of demand when this is the unique transit feasible. LRT is less expensive if demand is a little less than 1,000 [user/km²·h]. Finally, HRT is the most expensive in low levels of demand, but this situation improves regarding the demand; this is the best transit alternative between 1,000 and 2,000 [user/km²·h].

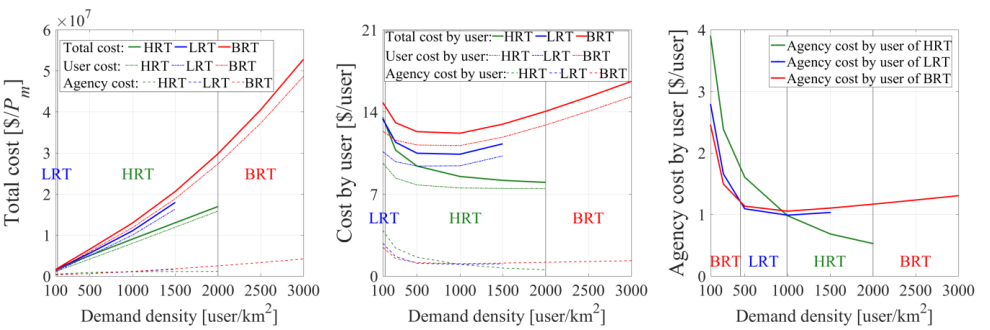

(a) Total cost (b) Total cost by user (c) Agency cost by user

Figure D.14. System cost considering progressive homogeneous demand scenarios.

Figure D.15 shows some effects of transit operation (Figure D.15(a) HRT, (b) LRT, and (c) BRT) on infrastructure considering different levels of demand. The color of the lines represents each label on the y-axis. The transit occupation increases if the demand densities also increase but do not reach the maximum capacity for an HRT system. On the contrary, LRT and BRT systems reach saturation quickly if demand exceeds 1,000 and 500 [user/km²·h], respectively. The travel time decreases whether the demand increases in the case of HRTs because the infrastructure increases as well. For the case of LRT and BRT, the travel time decreases to reach a minimal value (1000 and 1500 [user/km²·h], respectively); after that, the systems are inefficient.

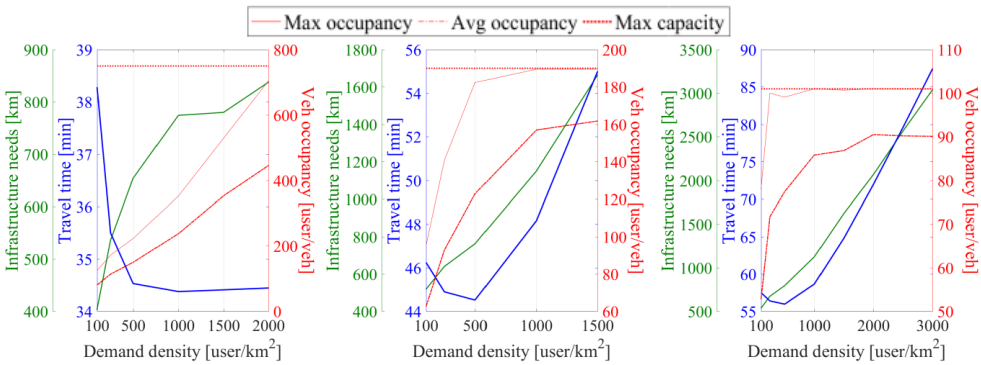

(a) HRT (b) LRT (c) BRT

Figure D.15. Transit occupation and travel time according to progressive homogeneous demand scenarios.

4.3. Non-homogeneous demand systems

Using the network design model, we analyze four scenarios of demand distribution in which the city has a generating rate of 1,000 [user/km²·h] (Figure D.8): homogeneous city (Hm), heterogeneous city (Ht), mono-centric city (Mn), and multi-subcenters city (Ms). Figure D.16 shows a comparison of the total cost regarding each urban scenario and transit technologies. The implementation of HRT systems presents the least cost of all types of cities. A city, which has its demand perfectly distributed (Hm), is the best alternative for almost all types of technologies. This conclusion seems to be logical due to it prevents or reduces the saturation and costs due to the concentration of passengers at specific points in the city. This condition contrasts against the heterogeneous city (Ht), which has the highest total costs. The best alternatives are those that implement downtown and subcenters (Mn and Ms), although a muti-subcenters city have an equivalent total cost regarding a homogeneous city. The encouragement of an Mn city generates a reduction in costs. The reduction ranges from 7.8% for HRTs to 11.7% for LRTs, according to a Ht city. Even in the case of HRT systems, the muti-subcenters city provides the best alternative reducing the cost by 37.7% regarding the worst-case analyzed in this paper (BRT for a Ht city).

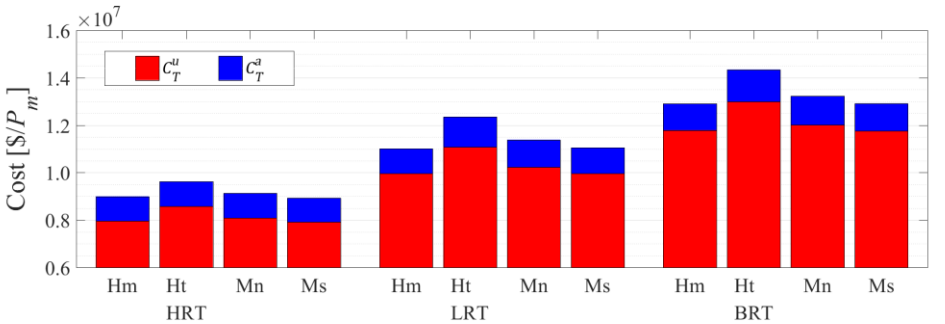

Figure D.16. Costs among transit technologies at a city with 1,000 [user/km²·h].

The results of the implementation of a CBD/subcenters change depending on the size of these. Figure D.17 shows the comparison of the four urban scenarios explained previously (Ht, Hm, Mn, and Ms). The two latter have a progressive implementation in the analysis taking into account the size of the CBD or subcenters. The size of the CBD/subcenters progressively increases from 5% (1.05x) to 25% of the total trips (1.25x). Figure D.17(a) mainly presents two ideas: the total cost of a monocentric city increases if the size of the CBD also increases considering the total number of trips; and otherwise, the total cost of a multi-subcenters city decreases if the subcenters size increases. Even the cost is less than at a homogeneously distributed city, reaching a reduction of 2.2% for an HRT system. Therefore, a decentralized city is more effective than policies that seek the concentration of equipment and services at specific points in a city. Figure D.17(b) represents a comparison of costs regarding the agency cost by users in which the cost per user makes a system economically sustainable. The exhibit allows for proving three assertions. First, the implementation of a homogeneous city reduces costs for BRT and LRT technologies in comparison to a heterogeneous case. Second, the implementation of small subcenters (less than 10% of total trips) generates similar levels of costs in comparison to the homogeneous case. Finally, if the multi-subcenters grow up due to the generation/attraction of trips, the cost reduces regarding a monocentric demand structure. Even in the case of HRTs, the subcenters structure improves the system better than the homogeneous case, reducing the cost by 1.7% concerning the most idealized case.

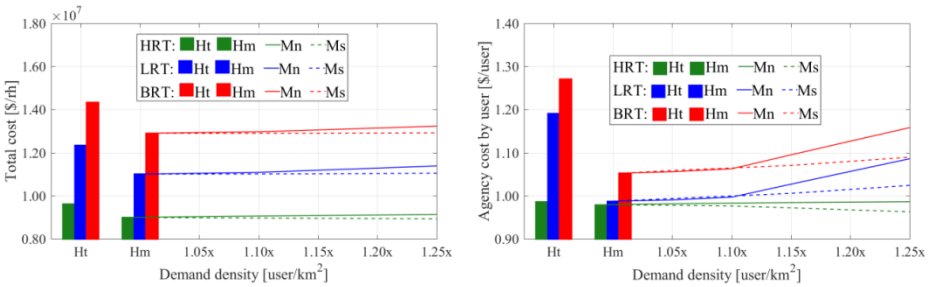

(a) Total cost (b) Agency cost by user

Figure D.17. Cost of the system according to urban scenarios and transit systems.

Effects on urban structure and frequency

Each scenario of demand (Hm, Ht, Mn, and Ms) requires a specific structure of transit. Each exhibit of Figure D.18 represents the solutions for each technology and type of route, which has two elements: the above exhibit contains the continuous optimal solutions for spatial and temporary variables, and the below exhibit contains discrete locations of corridors. In the above exhibit, the blue lines represent the optimal density of rings in [corridor/km] and radial routes in [corridor/rad]; on the other side, the orange lines represent the headways along a transit corridor. In the bottom exhibit, the blue points represent the discrete location of corridors using the discretization algorithm presented previously. Finally, this exhibit also includes the number of corridors, which is next to the right axis.

For HRTs, in Figure D.18(a), a homogeneous scenario of demand (solid lines) homogeneously distributes corridors at the intermediate zone (about 0.5 [corridor/km]). However, the density decreases approaching the city center, which tends to zero and increases towards the periphery (about 0.8 [corridor/km], almost double of the intermediate zone). Moreover, time headway reaches the value of the minimum headway constraint (2.05 [min/veh]) and rapidly rises towards the city center and the periphery for all technologies. In a mono-centric scenario (dash-dot lines), the central area concentrates ring routes reducing the density outer, but this is not enough to save infrastructure (all scenarios have the same number of rings). Thus, Ms reaches as ring corridors as the Hm scenario for all technologies. Secondly, Figure D.18(b) shows a uniform distribution for Hm, Mn, and Ht cases reaching the maximum density (4.158 [corridor/rad], which is the minimum distance between routes) and the minimum headway between vehicles (2.052 [min/veh]). The only exception is the Ms scenario, in which the model saves one radial route. The advantage of a multi-sub-center structure is to provide

more supply in areas of higher demand than other zones that have less demand. A homogeneous distribution means an idealized scheme, which is challenging to implement as an urbanism strategy; therefore, multi-subcenters is a competitive strategic solution to a homogeneous scheme.

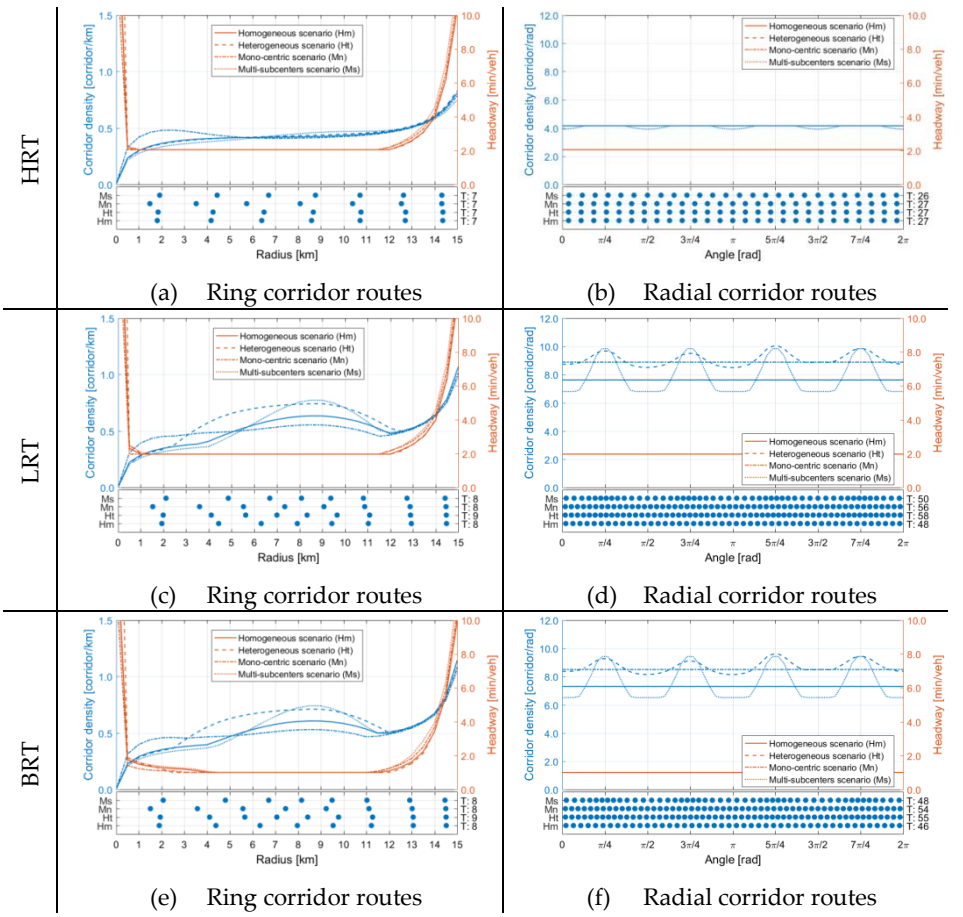

(a) Ring corridor routes (b) Radial corridor routes

(c) Ring corridor routes (d) Radial corridor routes

(e) Ring corridor routes (f) Radial corridor routes

Figure D.18. Optimal solutions for transit technologies according to urban scenarios.

For LRTs, the saturation of the vehicle capacity causes an alteration of the ring density in the intermediate zone of the city (Figure D.18(c)). The mono-centric structure is the least affected scenario because it reduces the demand in this area, increasing the demand towards the city center. In any case, the Mn case has as rings as the Mn and Ms. In radial routes (Figure D.18(d)), Hm and Mn have a uniform distribution of the route density. Ms has a better distribution of the demand and allows grouping the infrastructure offer making it more efficient. In Figure D.18(e) and (f), the BRT system has similar route densities for rings in comparison to the LRT system, but radials are less than in the previous case. Moreover, the headways are smaller than the

headways of LRTs. Finally, Figure D.19 shows the location of transit corridors considering a multi-subcenters demand structure. The discretization algorithm gives the location presented in Figure D.6. Moreover, the link of the transit network contains the saturation level using a color ramp from 0 to 1 in which the occupancy and capacity are equal.

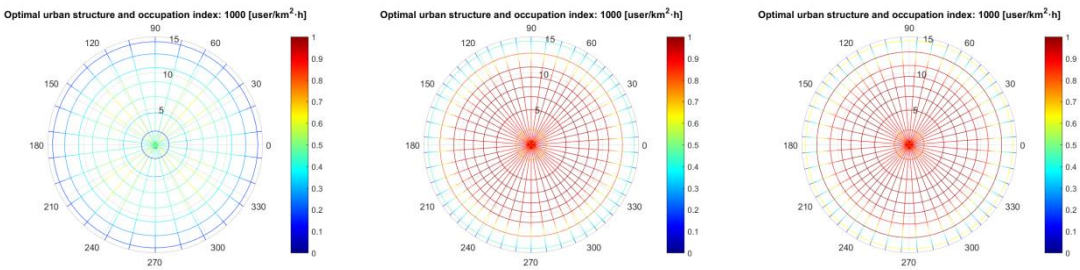

(a) HRT (b) LRT (c) BRT

Figure D.19. Saturation levels of transit corridors for a multi-subcenters city.

Analysis of transit occupation and travel time

In Figure D.20, the bars show the percentage of trips classified in time intervals. Each interval of the color ramp represents trips lasting 15 minutes. The bars in the exhibit compare the travel time among city scenarios for the three transit technologies: homogeneous (Ht), heterogeneous (Hm), and the progressive increment of multiple subcenters from 5% to 25% of trips with respect to the total number of these.

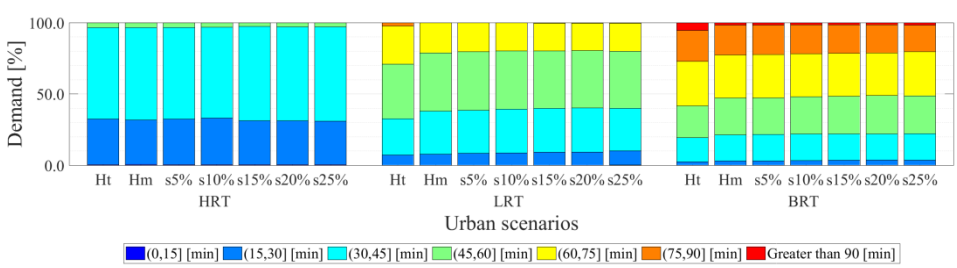

Figure D.20. Costs among transit technologies in a city with 1,000 [user/km²·h].

HRT is the only system with trips that last less than 15 minutes, while longer trips last between 45 and 60 minutes. The implementation of LRTs increases the travel time in comparison to HRTs in which longer trips take between 75 and 90 minutes for the heterogeneous case, although the implementation of subcenters reduces them even more. The case of BRT has the worst performance considering travel time because the maximum travel time

exceeds 90 minutes. However, a homogeneous distribution also reduces the duration of travel; the implementation of the subcenters improves them even more. The above is observable in all technological cases, even in HRTs, where the maximum time bars (green color) decrease as well. This problem is most significant in the case of BRT because analyzed urban strategies do not eliminate times higher than 90 min.

5. Conclusions

The proposed model for designing public transportation networks can adapt to non-homogeneously distributed demands, considering the local demand conditions over a city. The model is valid even in modeling scenarios where the generation/attraction rates are stable over the city because the density of trips is not homogeneous for the other three travel stages: waiting, in-vehicle trip, and transferring of users. For this reason, average demand values (i.e., a homogeneous distribution) will tend to underestimate real infrastructure needs where issues will increase when considering other demand distributions.

The feasibility of implementing a transit technology depends on the occupancy and operating constraints; therefore, the capacity of the technology is a critical parameter of the feasibility of a transit system. For radial corridors, LRT and BRT systems have limited feasible spaces because their capacity is less than that of HRTs. Besides, some solutions for radial routes are not feasible for any of the three technologies analyzed in this paper, as opposed to the ring routes that have an overlap of feasible areas.

The total costs obtained from the model show that LRT systems are only competitive for low levels of demand, and BRTs are competitive for high levels of demand if HRTs are not feasible. The results change if we analyze agency-by-user costs where HRTs are competitive for intermediate demand densities (between 1,000 and 2,000 [user/km^2]). On the other hand, an HRT system has a shorter average travel time if the level of demand increases. LRTs and BRTs rise increasingly inefficient in these cases. Moreover, LRTs and BRTs rapidly saturate the capacity of vehicles if demand also increases, and infrastructure needs simultaneously increase in all cases.

In the case of a homogeneous distribution, the distance between ring routes decreases from the center to the periphery, although the transit frequency is less toward the periphery. Vehicle capacity constraints force the concentration of routes when travel density exceeds 500 [user/km^2]. In the

case of ring routes, the intermediate zone concentrates many routes, but the requirements of radial routes are in all zones. Therefore, these areas require a greater concentration of infrastructure or vehicles with higher capacity. Thus, the periphery requires an efficient system of feeder vehicles and radial transit systems.

The urban case with homogeneous demand is an idealized case. Urban cases with a monocentric or heterogeneous structure approach real structures but have higher total cost levels. The decentralized urban case that incorporates multi-subcenters reduces the level of costs being equivalent to a homogeneous demand distribution. The effectiveness of subcenters depends on the size of these reducing costs and improvements in travel time. Regarding agency costs per user, if the multi-subcenters increase their size, cost reduction achieved the best levels for the case of HRTs (reduction of 2.4%). However, the most significant reductions in percentage are observed for BRT and LRT, decreasing by about 16%. The multi-subcenters can even show better results than the idealized case in which the trips have a perfectly homogeneous distribution. Therefore, the generation of subcenters can become an attractive strategy for urban development.

Appendix E. Traffic system design modeling

Abstract: Congestion is one of the main problems for traffic systems in cities. Urban planning proposes solutions for congestion in which the design of strategic road networks presents a set of techniques to overcome the issue. One of these approaches is the continuous approximation method (CA). The paper develops an analytical model using CA to replicate a private transportation system of a radio-centric city with a pattern of non-homogeneous demand. The model considers radial and circular primary roads and allows obtaining the optimal configuration of infrastructure, balancing the total costs of users and the agency. The solution to the mathematical problem uses the Karush-Kuhn-Tucker (KKT) conditions. KKT conditions allow finding the necessary conditions of optimization and getting the optimal value on each city point.

Keywords: Private transportation network design; Continuous approximation method; Non-homogeneous demand; Concentric city.

1. Introduction

Traffic systems have significant problems in cities; one of them is the congestion identified since the '60s by Colin Buchanan (1963). Solutions come from transportation demand management (TDM). However, urban planning and transportation engineering may give adequate solutions to private systems.

Some previous papers study designing road network patterns. A group of these analyzes the street capacity expansion, e.g., Mathew and Shrama (2009), Wang and Lo (2010), and González and Robusté (2011). In this line, Li et al. (2013) and Miyagawa (2018) model the hierarchy of a road network. The former optimizes the density of strategic road networks. The latter papers model the optimal spacing among roads considering hierarchical road networks with minor and major roads. The "macroscopic fundamental diagram" (MFD) allows analyzing the relation between traffic and land use applied to a concentric city (Tsekeris & Geroliminis, 2013). One topic is relevant for the model: cars have to park in the city. Arnott and Rowse (1999) present a simple parking model that models when the drivers realize a trip in private transportation and need a vacant parking spot.

The section develops an analytical model that replicates the performance of a private transportation system for a radio-centric city with radial and circular primary roads. The model aims to identify the optimal configuration of infrastructure in a city by considering a pattern of non-homogeneous demand and balancing the costs of users and the agency.

Cars park in house garages, and the trip model considers three components: time spent cruising for parking, time spent in "regular" car travel, and time spent walking from the parking location to the destination and back again. The dissertation assumes that drivers know the probability of finding a vacant space; besides, the finding-a-vacant-parking-space probability is independent of each other. The cruising for parking is one of the most studied topics in the economics of parking (Inci, 2015) because it causes several transportation problems.

The next section explains the proposed method that uses the continuous approximation method considering non-homogeneous demand over a concentric city. After that, the section explains the formulation and optimization of the problem. The current appendix finalizes presenting their conclusions.

2. Methodology

2.1. Preliminary concepts

The total cost has two components: user and agency costs. The governmental agency considers the private transportation infrastructure cost. However, the model does not consider urban freight distribution. The users take the shortest route to the destination by both circular and radial street corridors.

Demand distribution

The demand distribution function $D(r_f, \theta_f, r_t, \theta_t)$ in [user/km^4·h] (Vaughan, 1986) represents the spatial density in polar coordinates of users per hour who begin a trip from an area $dr_f\ r_f\ d\theta_f$ in [km^2] about an origin point (r_f, θ_f) to an area $dr_t\ r_t\ d\theta_t$ in [km^2] about a destination point (r_t, θ_t). Using the function obtains the total trip demand (Δ in [user/h]) for a concentric city of radius R (Equation E.1).

$$\Delta = \int_0^{2\pi} \int_0^{R} \int_0^{2\pi} \int_0^{R} D(r_f, \theta_f, r_t, \theta_t)\, r_t\, dr_t\, d\theta_t\; r_f\, dr_f\, d\theta_f \qquad (E.1)$$

The above function also allows obtaining the function of generated demand $\lambda(r,\theta)$ at a point (r,θ) in [user/km²·h], and attracted demand $\rho(r,\theta)$ at a point (r,θ) in [user/km²·h].

The model has three types of demand density functions obtained from the assignment method.

$f_{w,v}^{F}(r,\theta)$: density function of vehicles of type $v \in V$ accessing from the origin to the closest circular or radial primary road $w \in W$ [veh/km²·h];

$f_{w,v}^{R}(r,\theta)$: density flow of vehicles of type $v \in V$ traveling on a circular or radial primary road $w \in W$ considering its direction [veh/km·h];

$f_{w,v}^{A}(r,\theta)$: density function of vehicles of type $v \in V$ arriving from a circular or radial primary road to the destination $w \in W$ [veh/km²·h].

Assumptions

The dissertation assumes the following assumptions.

- The private transport demand at each point of the city during a given period is a known deterministic function that varies according to the position.
- Car users take the cheapest route (minimum generalized cost) to the destination, and they can use ring streets, radial streets, or both of them.
- The travel time value is the same for all users, regardless of age, socioeconomic status, or period of the day.
- The road capacity is proportional to the number of lanes.
- Drivers that look for a parking space cannot stop and wait for vacant parking spots; drivers cannot return either (Arnott & Rowse, 1999). Moreover, these vehicles park on service streets; therefore, the vehicles looking for parking do not reduce road capacities.
- Vehicles park on service streets; therefore, they do not cause a reduction in road capacity. The model does not consider the parking capacity.
- The model does not include urban freight distribution and public transportation costs.

2.2. Cost functions

The total cost function ($TC_C = C_C^u + C_C^a$ in [\$/P_m]) has two elements at the peak hour P_m: the cost of users (C_C^u in [\$/P_m]) and the agency cost (C_C^a in [\$/P_m]).

User costs

The cost functions represent the total cost for all stages of a trip using cars. The functions come from the integration of the local cost function over the circular region of the city. The formulation is similar to the case of public transportation.

a) Access cost to main roads

The local access cost function has two components: the demand density in rush hour ($f^F_{w,v}(r,\theta)\cdot T/\eta_u$ in [veh/km^2·P_m]), and the average access cost per vehicle ($c^F_{w,v}(r,\theta)$) in [$/veh]). The access cost to the main road is the integration of the local access cost over the city region considering the types of vehicles $v \in V$ (C_F in [$/$P_m$]).

$$C_F = \int_0^{2\pi}\int_0^{R}\sum_{w\in W}\sum_{v\in V}\frac{1}{\eta_u}\cdot f^F_{w,v}(r,\theta)\cdot T\cdot c^F_{w,v}(r,\theta)\;\; r\,dr\,d\theta \qquad (E.2)$$

b) Regular trip cost

The total trip cost (C_R in [$/$P_m$]) is the integration of a local cost function over the circular region. The local cost function comes from the demand density in rush hour ($f^R_{w,v}(r,\theta)\cdot T/\eta_u$ in [veh/km·P_m]) and the local generalized travel cost for all roads ($c^R_{w,v}(r,\theta)$ in [$/km·veh]).

$$C_R = \int_0^{2\pi}\int_0^{R}\frac{1}{\eta_u}\cdot\sum_{v\in V} f^R_{c,v}(r,\theta)\cdot T\cdot c^R_{c,v}(r)+\frac{1}{2}\cdot\left(\frac{R}{r}+1\right)\cdot f^R_{r,v}(r,\theta)\cdot T\cdot c^R_{r,v}(r,\theta)\;\; r\,dr\,d\theta \qquad (E.3)$$

c) Arriving cost to trip destinations

The arriving cost (C_A in [$/$P_m$]) is the integration of the local cost composed of the demand function in the rush period ($f^A_{w,v}(r,\theta)\cdot T/\eta_u$ in [veh/P_m]), and the expected walking cost and parking fee ($c^A_{w,v}(r,\theta)$ in [$/veh]).

$$C_A = \int_0^{2\pi}\int_0^{R}\sum_{w\in W}\sum_{v\in V}\frac{1}{\eta_u}\cdot f^A_{w,v}(r)\cdot T\cdot c^A_{w,v}(r)\;\; r\,dr\,d\theta \qquad (E.4)$$

Agency costs

The agency cost (C_I in $[\$/P_m]$ is the multiplication of the cost per linear kilometer and the road density ($1/p^c(r)$ or $1/r \cdot \Psi^r(\theta)$). The unitary cost contains two parts: a fixed and a variable element, i.e., $\varphi_v^p = \varphi_v^{p(f)} + \varphi_v^{p(v)} \cdot T$.

$$C_I = 2 \cdot \int_0^{2\pi} \int_0^{R} \sum_{v \in V} \frac{\varphi_v^p}{p^c(r)} + \frac{\varphi_v^p}{r \cdot \Psi^r(\theta)} \; r \, dr \, d\theta \qquad \text{(E.5)}$$

3. Problem formulation and optimization

3.1. Method for solving the problem

The mathematical problem is a nonlinear system with inequality constraints. The Karush-Kuhn-Tucker (KKT) conditions allow finding the necessary conditions to solve it.

3.2. Optimal analytical solutions

If the mathematical problem is a nonlinear system without constraints. The conditions of the first-order optimization allow obtaining the optimized analytical functions. These functions allow getting the optimal value on all city road corridors. The model uses the derivatives of local functions regarding $p^c(r)$ and $\Psi^r(\theta)$. These analytical functions are necessary conditions for the optimal solution (Equations E.6 and E.7).

Optimal distance function between ring roads

$$\frac{\partial \, ct(r)}{\partial \, d_c(r)} = a_c(r) \cdot p^c(r)^{b-1} - c_c(r) \cdot p^c(r)^{-2} + b_c(r) = 0$$

where

$$a_c(r) = \int_0^{2\pi} \sum_{w \in W} \sum_{v \in V} \frac{1}{\eta_u} \cdot f_{c,v}^R(r,\theta) \cdot T \cdot \frac{\mu_v \cdot a \cdot b}{v_{w,v}^c} \cdot \left(\frac{\frac{1}{\eta_u} \cdot f_{c,v}^R(r,\theta)}{K_{c,w}^V(r,\theta)} \right)^{b-1} \; r \, d\theta$$

$$c_c(r) = \int_0^{2\pi} \sum_{w \in W} \sum_{v \in V} \frac{1}{\eta_u} \cdot f_{r,v}^R(r,\theta) \cdot T \cdot \mu_v \cdot \tau_{w,v}^i + \sum_{w \in W} \sum_{v \in V} \left(\varphi_{w,v}^{h(f)} + \varphi_{w,v}^{h(v)} \cdot T \right) \cdot \eta_w \; r \, d\theta \qquad \text{(E.6)}$$

$$b_c(r) = \int_0^{2\pi} \sum_{v \in V} \frac{1}{4} \cdot \left(\frac{1}{\eta_u} \cdot f_{c,v}^F(r,\theta) \cdot T + \frac{1}{\eta_u} \cdot f_{c,v}^A(r,\theta) \cdot T \right) \cdot \Psi_v^F \; r \, d\theta$$

Optimal distance function between radial roads

$$\frac{\partial\, ct(\theta)}{\partial\, \Phi_r(\theta)} = a_r(\theta)\cdot \Psi^r(\theta)^{b-1} - c_r(\theta)\cdot \Psi^r(\theta)^{-2} + b_r(\theta) = 0$$

where

$$a_r(\theta) = \int_0^R \sum_{w\in W}\sum_{v\in V} \frac{1}{\eta_u}\cdot f^R_{r,v}(r,\theta)\cdot T\cdot \frac{\mu_v\cdot a\cdot b}{v^c_{w,v}}\cdot \left(\frac{\frac{1}{\eta_u}\cdot f^R_{r,v}(r,\theta)\cdot r}{K^V_{r,w,v}(r,\theta)}\right)^{b-1} dr$$

$$c_r(\theta) = \int_0^R \sum_{w\in W}\sum_{v\in V} \frac{1}{\eta_u}\cdot f^R_{c,v}(r,\theta)\cdot T\cdot \mu_v\cdot \tau^i_{w,v}\cdot \frac{1}{r} + \sum_{w\in W}\sum_{v\in V}\left(\varphi^{h(f)}_w + \varphi^{h(v)}_w\cdot T\right)\cdot \eta_w\cdot \frac{1}{r}\; dr \qquad (E.7)$$

$$b_r(\theta) = \int_0^R \sum_{v\in V} \frac{1}{4}\cdot \left(f^F_{r,v}(r,\theta) + f^A_{r,v}(r,\theta)\right)\cdot T\cdot \Psi^F_v\cdot r\;\; dr$$

3.3. Solution methodology

If $a = 2$ and $b = 3$, then Equation E.6 is a compound quadratic polynomial. Introducing a new variable $u = {d_c}^2$, the equation becomes a quadratic function. The solution has one solution (Equation E.8) and three non-valid ones (negative and complex roots). The solution has three components: $a_c(r)$, $b_c(r)$, and $c_c(r)$. Firstly, $a_c(r)$ will show the total cost density of vehicles that drive on a circular corridor multiplied by a factor representing the congestion density. Secondly, $b_c(r)$ represents the total cost density of drivers that leave their origin and arrive at the destination point. Finally, $c_c(r)$ expresses the total cost of two components: the cost of drivers that cross an intersection by a radial road; and the cost of construction and maintenance.

$$p^{c(*)}(r) = \sqrt{\frac{-b_c(r) + \sqrt{b_c(r)^2 - 4\cdot a_c(r)\cdot c_c(r)}}{2\cdot a_c(r)}}$$

$$because\ of\ c_c < 0\ and\ \sqrt{b_c(r)^2 - 4\cdot a_c(r)\cdot c_c(r)} > b_c(r)$$

where

$$a_c(r) = \int_0^{2\pi} \sum_{w\in W}\sum_{v\in V} \frac{1}{\eta_u}\cdot f^R_{c,v}(r,\theta)\cdot T\cdot \frac{6\cdot \mu_v}{v^c_{w,v}}\cdot \left(\frac{\frac{1}{\eta_u}\cdot f^R_{c,v}(r,\theta)}{K^V_{c,w}(r,\theta)}\right)^3 r\, d\theta$$

$$b_c(r) = \int_0^{2\pi} \sum_{v\in V} \frac{1}{4}\cdot \left(\frac{1}{\eta_u}\cdot f^F_{c,v}(r,\theta)\cdot T + \frac{1}{\eta_u}\cdot f^A_{c,v}(r,\theta)\cdot T\right)\cdot \Psi^F_v\; r\, d\theta \qquad (E.8)$$

$$c_c(r) = -\int_0^{2\pi} \sum_{w\in W}\sum_{v\in V} \frac{1}{\eta_u}\cdot f^R_{r,v}(r,\theta)\cdot T\cdot \mu_v\cdot \tau^i_{w,v} + \left(\varphi^{h(f)}_{w,v} + \varphi^{h(v)}_{w,v}\cdot T\right)\; r\, d\theta$$

The optimal formulation of Ψ^r is similar to the previous case (Equation E.9). The formulation has three components. The first one ($a_r(\theta)$) represents the total cost density of cars that travel on a radial road. Secondly, $b_r(\theta)$ shows the total cost density of vehicles that leave and arrive at a point. Finally, $c_r(\theta)$

expresses two components: the cost density of cars that cross an intersection by a circular road; and the cost density of construction and maintenance.

$$\Psi^{r(*)}(\theta) = \sqrt{\frac{-b_r(\theta) + \sqrt{b_r(\theta)^2 - 4 \cdot a_r(\theta) \cdot c_r(\theta)}}{2 \cdot a_r(\theta)}}$$
$$because\ of\ c_r(\theta) < 0\ and\ \sqrt{b_r(\theta)^2 - 4 \cdot a_r(\theta) \cdot c_r(\theta)} > b_r(\theta)$$

where

$$a_r(\theta) = \int_0^R \sum_{w \in W} \sum_{v \in V} \frac{1}{\eta_u} \cdot f_{r,v}^R(r,\theta) \cdot T \cdot \frac{6 \cdot \mu_v}{v_{w,v}^c} \cdot \left(\frac{\frac{1}{\eta_u} \cdot f_{r,v}^R(r,\theta) \cdot r}{K_{r,w,v}^V(r,\theta)} \right)^3 dr \qquad (E.9)$$

$$b_r(\theta) = \int_0^R \sum_{v \in V} \frac{1}{4} \cdot \left(\frac{1}{\eta_u} \cdot f_{r,v}^F(r,\theta) + \frac{1}{\eta_u} \cdot f_{r,v}^A(r,\theta) \right) \cdot T \cdot \Psi_v^F \cdot r \ dr$$

$$c_r(\theta) = -\int_0^R \sum_{w \in W} \sum_{v \in V} \frac{1}{\eta_u} \cdot f_{c,v}^R(r,\theta) \cdot T \cdot \mu_v \cdot \tau_{w,v}^i \cdot \frac{1}{r} + \left(\varphi_w^{h(f)} + \varphi_w^{h(v)} \cdot T \right) \cdot \frac{1}{r} \ dr$$

The method has two phases. The first stage consists of the initialization of variables. A feasible solution uses the minimum value of each variable, respectively: $\{K^d\}$. Moreover, the algorithm creates a variable that stores the number of iterations (i). The second stage is an iterative process in which the model calculates the two decision variables.

Algorithm: Solution of the continuous traffic problem

Initialize $p^{c(0)}(r) = K^{d(c)}$; $\Psi^{r(0)}(\theta) = K^{d(r)}$
for 1... n
    m $\leftarrow M_n$
    $D^{\circ} \leftarrow D(r_f, \theta_f, r_t, \theta_t)$×m

    $i \coloneqq 1$
    while (abs($p^{c(i)}(r) - p^{c(i-1)}(r)$) > tolerance or
            abs($\Psi^{r(i)}(\theta) - \Psi^{r(i-1)}(\theta)$) > tolerance)
        for each $r \in [0 \ldots R]$ **do**
            $p^{c(i)}(r) \leftarrow$ *SystemOfEquations*($\Psi^{r(i-1)}(\theta)$)
        end for

        for each $\theta \in [0 \ldots 2\pi]$ **do**
            $\Psi^{r(i)}(\theta) \leftarrow$ *SystemOfEquations*($p^{c(i-1)}(r)$)
        end for

        $i \coloneqq i + 1$
    end while
end for

Figure E.1. Algorithm for solution of the traffic network design based on successive approximations.

The process will iterate while the solutions are feasible, and the error is higher than the tolerance for each variable. The first sub-problem calculates the variable for a set of circular corridor routes ($r \in [0 \ldots R]$) if there are feasible solutions and first-order optimization conditions are satisfied. After that, the section analyzes the convexity of the problem, finding the optimal solution. In the case of radial services, the process is identical. After that, the variable i will increase by one unit. Finally, the algorithm will stop when the error is less than the tolerance.

4. Conclusions

The model allows adapting the transportation network design to non-homogeneously distributed demands. The modeling considers the local demand conditions over a city and the essential stages of a trip: access cost to main roads, regular trip cost, and arriving cost to trip destinations. The model includes the agency's costs, such as capital, operation, and infrastructure. Notably, the model considers the congestion using a flow-delay function based on a BPR function. Finally, the modeling finalizes with the discretization of continuous results.

Appendix F. Modeling public transportation networks for a circular city: the role of urban subcenters and mobility density[2]

Abstract: The concentration of both employment and services in a specific area of a town generates positive effects but also impacts (congestion, transit issues, and others). Urban subcenters seek to approach economic activities to residents in peripheral urban spaces. The objective of this research is to evaluate the contribution to the mobility of implementing urban subcenters in a city. The model has a total cost function (users and agency costs) on a circular city (ring and radial routes) formulated using the continuous approximation method. The model solution addresses mathematical optimization. The model evaluates a BRT network applied to scenarios of urban subcenters. The results of the modeling show that the implementation of subcenters obtains savings of 3.5% in rush hour. Thus, this strategy of urban planning generates improvements in the functioning of a public transportation system. Moreover, the maximum benefits came out in medium-sized subcenters in comparison to the CBD, which allows balancing user and agency costs. Therefore, the outcomes may be better with an urban pattern with subcenters, and a transit scheme adapted to the demand needs.

Keywords: Public transportation network design; Urban subcenter; Continuous approximation method

[2] Paper presented at two scientific congress (Campus FIT 2019 and EWGT 2019), a paper, and a scientific conference, and published in a journal:

- Medina-Tapia, M., & Robusté, F. (2019a) Diseño óptimo de redes de transporte público que se adaptan a condiciones locales y no-homogéneas en una ciudad circular. Proceedings of III Campus Científico Foro de Ingeniería del Transporte 2019, Madrid, Spain.
- Medina-Tapia, M., & Robusté, F. (2019c) Ingeniería de transporte y planificación urbana: Diseño de redes de transporte público en una ciudad concéntrica. 14th edition of the CIMNE Coffee Talks, Universitat Politècnica de Catalunya, Barcelona, Spain.
- Medina-Tapia, M., Robusté, F., & Estrada, M. (2020) Modeling public transportation networks for a circular city: the role of urban subcenters and mobility density. Transportation Research Procedia, 47, 353-360.

1. Introduction

Nowadays, contemporary cities face several problems. One of them is the extreme concentration of urban services in a specific area called the central business district (CBD) in a specific period of the day (peak period). In some cases, a transportation strategy may solve these issues, i.e., demand and transportation systems management (TDM, TSM). In other cases, we should apply urban planning tools such as the implementation of urban subcenters. Urban subcenters aim to bring economic activities (e.g., services, employment) closer to people who live in peripheral urban spaces. The implementation of new subcenters seeks to balance attractiveness among all zones in a city in order to reach a balance between trip attraction and generation. Thus, new areas in a city will have an urban dynamic more efficiently. Unfortunately, there is not a quantitative evaluation of results that could have this policy.

Russo and Musolino (2012) proposed a unifying modeling framework to model interactions between spatial economic and transport systems simultaneously. Rodrigue et al. (2017) identified three basic network structures: distributed, centralized, and decentralized networks. The first case has no subcenters. The second case has a highly demanded CBD. The third case also has a CBD, but the city also contains subcenters. Transportation network design depends on the level of service required and its urban structure (Rodrigue et al., 2017). Several works have analyzed BRT networks. It highlights papers such as Daganzo (2010) and Tirachini et al. (2010). The former proposed a hybrid grid transit on a square region with constant demand. If a city is neither big nor has low demand, then the BRT system can compete with cars. The latter compares transit modes (bus, tramway, and metro) considering a radial system with a CBD in a circular city. The results of several scenarios show that BRT is the best alternative.

Ouyang et al. (2014) formulated a method based on continuum approximations that design bus networks for an urban grid system with non-homogeneous demand. Unfortunately, the non-homogeneous demand functions are identical for generated and attracted trips; therefore, this does not allow us to analyze the behavior of subcenters and their impacts. The authors formulated a mathematical model using the continuous approximation (CA) method. This method will be useful regardless of whether the information inputs are perfect. In this case, information of user arriving, traffic conditions, and others are not accurate; therefore, it is valid to model with smooth and continuous functions. These conditions are standard results in a macroscopic problem of network design. The CA

method assumes that inputs slowly vary over the domain; the total cost can be the aggregation of small sub-region costs, which depend on local characteristics (Daganzo, 2005). This method has applications in solving transit problems (e.g., Medina-Tapia et al., 2013), logistics problems (e.g., Pulido et al., 2015), and private transportation issues as well (e.g., Medina-Tapia & Robusté, 2019b).

The objective of the investigation is to evaluate the impact of the implementation of urban subcenters for the improvement of a BRT network, although the model can also apply to other transit modes (e.g., tramway, subway). The authors formulate a CA model considering the spatial design as well as the operation design of a transit system. The analysis considers a set of urban subcenter scenarios to evaluate the improvements in mobility.

The next section will expose the main attributes of the model and its results. Finally, this section will end with conclusions and further research.

2. Methodology

The region of analysis is a circular city of radius R [km], which has ring and radial transit services. The model implemented in polar coordinates assumes that passengers can travel on these two types of transit routes in four directions. Users can travel clockwise/anticlockwise direction ($L_c = \{l_c: clockwise, l_a: anticlockwise\}$) on circular routes or users can go to the center or come out from this ($L_r = \{l_i: inside, l_o: outside\}$) on radial routes. Users have a continuous distribution over the city considering three scenarios with a heterogeneous pattern of demand. Thus, the demand $D(r_f, \theta_f, r_t, \theta_t)$ in polar coordinates represents the density of trips from an origin (r_f, θ_f) to a destination (r_t, θ_t) (Vaughan, 1986). Therefore, the distribution of demand over the territory is imperfect. This approach also allows obtaining adapted transit schemes to demand when city planners implement new subcenters. From this, we obtain the generated demand function $\lambda(r, \theta)$ at a point (r, θ) in [user/km^2·h] (Equation F.1). The mobility pattern supposes that passengers travel using the shortest route through circular, radial, or both types of transit services. The period of the analysis is the rush hour of a town (P_m) because the peak period defines the required infrastructure.

$$\lambda(r, \theta) = \int_0^{2\pi} \int_0^R D(r, \theta, r_t, \theta_t)\, r_t\, dr_t\, d\theta_t \qquad (F.1)$$

The mathematical formulation has two components, user (T_T^u in [user·h/P_m]) and agency (C_T^a in [\$/P_m]) costs and three decision variables, two spatial variables, and one operational variable (e.g., Estrada et al., 2011).

Table F.1. Nomenclature.

Decision variables:	
$d^c(r,\theta)$	distance between circular transportation routes at a point (r,θ) [km/route]
$\Phi^r(r,\theta)$	angle between radial routes at a point (r,θ) [radian/route], which $d^r(r,\theta) = \Phi^r(r,\theta)\cdot r$, where $d^r(r,\theta)$ is the distance between radial corridor routes at a point (r,θ)
H	headway between vehicles at the system [h/veh]
Parameters:	
T	duration of the peak period or rush hour [h/P_m]
$\alpha,\beta,\gamma,\delta$	perception of access (α), waiting (β), travel (γ), and transfer (δ) time by users [dimensionless]
$v^a(r)$	average access speed of accessing or egressing on a route at radius r [km/h·route]
v^w	average walking speed to transfer between stations [km/h]
v^t	cruising speed of a transit vehicle [km/h]
τ^s	average time lost at a station [h/station]
t^f	positioning time at a terminal by a transit vehicle [h]
η^d	number of work shifts on a vehicle [shift/veh]
χ^T	average walking distance between two stops [km]
K^v	capacity of a vehicle [user/veh]
K^h	minimum time between consecutive vehicles [h/veh]
K^d	minimum separation between two transit routes [km/route]
Unitary cost parameters:	
μ	travel time value by average user [\$/user·h]
φ^k	unitary cost per vehicle [\$/veh·P_m]
φ^g	driver's wage per hour [\$/shift·h]
φ^o	operating cost per kilometer traveled on a cruising speed [\$/veh·km·route]
φ^p	linear infrastructure cost [\$/km·route·P_m]
φ^s	nodal (stop or station) infrastructure cost [\$/station·route·P_m]

2.1. User costs

The total time of users (T_T^u in [user·h/P_m], Equation F.2) has four elements: access, waiting, trip, and transfer time.

$$T_T^u = \int_0^{2\pi}\int_0^R \left(T^A(r,\theta) + \sum_{l\in\{L_c,L_r\}} \left(T_l^W(r,\theta) + T_l^V(r,\theta) + T_l^T(r,\theta) \right) \right) \cdot r \, dr \, d\theta$$

where

$$\begin{aligned} T^A(r,\theta) &= f^A(r,\theta)\cdot T \cdot t^A(r,\theta) \\ T_l^W(r,\theta) &= f^W(r,\theta)\cdot T \cdot t^W(r,\theta) \\ T_l^V(r,\theta) &= K_l \cdot f_l^V(r,\theta)\cdot T \cdot t^V(r,\theta) \\ T_l^T(r,\theta) &= \frac{1}{2}\cdot\left(\frac{R}{r}+1\right)\cdot f_l^T(r,\theta)\cdot T \cdot t^T \end{aligned} \quad (F.2)$$

- *Access/egress time*: In Equation F.2, the access time depends on the demand and the average access time per user. The demand access a station during rush hour ($f^A(r,\theta)\cdot T$ in [user/km²]) is the density of users that board and alight at a station. The average access time ($t^A(r,\theta) = \alpha \cdot (d^c(r,\theta) + \Phi^r(r,\theta)\cdot r)/4 \cdot v^a(r)$) depends on the time perception α (TRB, 2013), the average distance between the origin/destination and the closest bus-stop (a quarter of the maximum walking distance, $(d^c(r,\theta) + \Phi^r(r,\theta)\cdot r)/4$), and the access speed ($v^a(r)$).
- *Waiting time*: In Equation F.2, the user density $f_l^W(r,\theta)\cdot T$ ([user/km²]) at the direction $l = \{L_c, L_r\}$ waits $1/2$ headway, which depends on user perception ($t^W = \beta \cdot H/2$). The model assumes that the headways are deterministic and perfectly regular (e.g., Medina-Tapia et al., 2013).
- *In-vehicle travel time*: The transit is a BRT system that does not share infrastructure; therefore, congestion will not affect the system. In Equation F.2, the local travel time per kilometer depends on two components: the user density on a bus during rush hour ($f_l^V(r,\theta)\cdot T$ at the direction l in [user/km]), and the travel time per kilometer ($t_l^V(r,\theta)$ in [h/user·km], Equation F.3) incurred by a user on a vehicle considering a factor γ. The user density is multiplied by a factor K_l ($K_{L_c} = 1$; $K_{L_r} = (R/r+1)/2$) because the corridor width in radial routes increase to the periphery.

$$t_l^V(r,\theta) = \begin{cases} \gamma\cdot\left(\frac{1}{v^t} + \frac{\tau^s}{\Phi^r(r,\theta)\cdot r}\right) & l = L_c \\ \gamma\cdot\left(\frac{1}{v^t} + \frac{\tau^s}{d^c(r,\theta)}\right) & l = L_r \end{cases} \quad (F.3)$$

- *Transfer time*: In Equation F.2, the transfer depends on the user density that transfers at a point ($f_l^T(r,\theta)\cdot T$ in [user/km²]), and the average transfer time ($t^T(r,\theta) = \delta\cdot(\chi^T/v^w + H/2)$).

2.2. Agency costs

The agency cost has three components (C_T^a in [\$/P_m]): capital, operational, and infrastructure cost (Equation F.4).

$$C_T^a = \int_0^{2\pi}\int_0^R \sum_{l\in\{L_c,L_r\}} \left(\left(\frac{t_l^C(r,\theta)\cdot\varphi^k}{H} + \frac{t_l^C(r,\theta)\cdot\eta^d\cdot T\cdot\varphi^g}{H} + \frac{2\cdot T\cdot\varphi^o}{H} + 2\cdot\varphi^p \right)\cdot\frac{1}{d^l(r,\theta)} \right) + \left(\frac{4\cdot\varphi^s}{\Phi^r(r,\theta)\cdot r\cdot d^c(r,\theta)} \right)\cdot r\, dr\, d\theta \quad (F.4)$$

- *Capital cost*: In Equation F.4, it depends on the fleet (t_l^C/H in [veh] in which t_l^C is the cycle time at route $l \in \{L_c, L_r\}$), and the cost per vehicle (φ^k). Three elements compose the cycle time at a route l (Equation F.5): the time at cruising speed, the positioning time at terminals (t^f), the lost time by a bus-stop (τ^s).

$$t_l^C(r,\theta) = \begin{cases} 2\cdot\left(\frac{1}{v^t} + \frac{t^f}{2\pi r} + \frac{\tau^s}{d^c(r,\theta)}\right) & l = L_c \\ 2\cdot\left(\frac{1}{v^t} + \frac{t^f}{R} + \frac{\tau^s}{\Phi^r(r,\theta)\cdot r}\right) & l = L_r \end{cases} \quad (F.5)$$

- *Operational cost*: It has two components: the on-vehicle crew cost and the operation cost of a vehicle. The total salary ($t_l^C\cdot\eta^d\cdot T\cdot\varphi^g/H$ at route l, Equation F.4) is in proportion to the fleet, number of work shifts on a vehicle (η^d), and the salary in the rush hour ($T\cdot\varphi^g$). The total operating cost depends on three components: the number of vehicles that run during the rush hour ($2\cdot T/H$), and the operation cost per unit of distance traveled (φ^o).
- *Infrastructure cost*: Firstly, the road cost also has two components related to each type of corridor: the corridor density ($1/d^c(r,\theta)$ or $1/\Phi^r(r,\theta)\cdot r$), and the unitary cost (φ^p) in Equation F.4. Secondly, the density of stations ($1/\Phi^r(r,\theta)\cdot r\cdot d^c(r,\theta)$) and the unitary cost ($\varphi^s$) compose the local station cost in Equation F.4.

2.3. Mathematical formulation

The mathematical problem ($TC = \mu\cdot T_T^u + C_T^a$) is a nonlinear system with inequality constraints (Equation F.6). In the objective function, the travel time value multiplies the user cost function (μ in [$/user·h]) and the agency costs. The problem has three sets of constraints. The first set (Equation F.6(b) and (c)) ensures that the demand does not exceed the capacity of a vehicle (K^v). The second set (Equation F.6(d) and (e)) makes sure a minimum distance between stations to reach the cruising speed before arriving at the next station (K^d). The third constraint (Equation F.6(f)) makes sure that the optimum headway has a minimum separation (time) between vehicles (K^h) (TRB, 2013).

$$Min\ TC = \mu \cdot T_T^u + C_T^a \quad \text{(a)}$$

s.t.

$$\max_{(r,\theta),l\in L_c} \left(f_l^V(r,\theta)\cdot d^c(r,\theta)\cdot H\right) \le K^v \quad \text{(b)}$$

$$\max_{(r,\theta),l\in L_r} \left(f_l^V(r,\theta)\cdot \Phi^r(r,\theta)\cdot \frac{R+r}{2}\cdot H\right) \le K^v \quad \text{(c)} \qquad \text{(F.6)}$$

$$d^c(r,\theta) \ge K^{d(c)} \quad \forall\,(r,\theta) \quad \text{(d)}$$

$$\Phi^r(r,\theta) \ge K^{d(r)} \quad \forall\,(r,\theta) \quad \text{(e)}$$

$$H \ge K^h \quad \text{(f)}$$

Karush-Kuhn-Tucker (KKT) conditions allow finding the necessary conditions. The first-order optimization conditions enable obtaining optimized analytical functions, and it will permit getting the optimal value on each city point. The necessary conditions are not sufficient for optimality, but all local minimum satisfies these conditions. To find the optimal solution is required to analyze the convexity of the problem. In the CA method, the minimized function is $tc(r,\theta)$ that is the local cost at the point (r,θ), in which the problem has three continuous decision variables $(d^c(r,\theta), \Phi^r(r,\theta), H)$. From the continuous solution, the authors applied three sequential steps for obtaining the discrete location of routes. First, the inverse of optimal continuous variables allows obtaining density functions of routes in [route/km] or [route/rad], i.e., the area below of these curves is the total number of routes (N). Second, the total area can divide into N sub-areas, which each one represents a route corridor, i.e., the value of the integral over each area will be about one. Third, the solution of this sub-problem is through a system of inequalities on a differential radius for ring routes and a differential angular for obtaining radial routes. Therefore, the system of inequalities defines the location of routes and the border of each route corridor.

3. Application to a case study

3.1. Scenarios and parameters

The research analyzes a progressive of eleven scenarios of concentric cities with a radius of 15 [km] and generates 500 [user/km²·h]. This progressive set presents from a city without subcenters to a city with a subcenter 1.25 times the CBD. Figure F.1 represents this sequence through four cases:

(a) A mono-centric city without subcenters (A), although the CBD attracts many users, although it is not a trip-generating zone,

(b) A city, which includes a CBD and a subcenter, generates and attracts users by about 60% of the CBD (0.625xCBD) (B),
(c) A city with a CBD and a subcenter that has the same size as the CBD (1.0xCBD) (C), and
(d) A city that has a subcenter 25% higher than the CBD (1.25xCBD) (D).

Moreover, exhibits in row (i) represent generated trips, and exhibits in row (ii) are attracted trips.

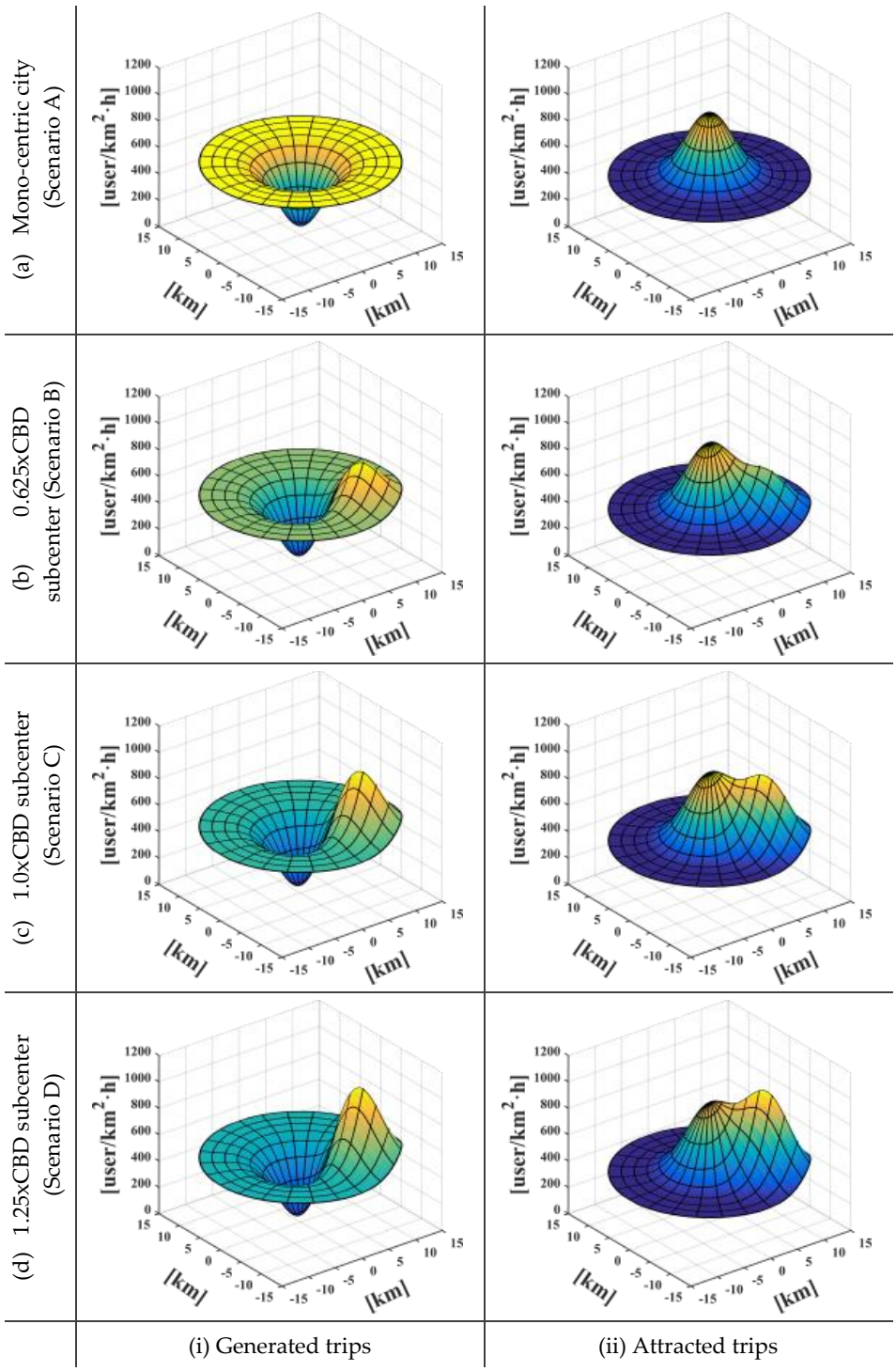

Figure F.1. Scenarios modeled for the subcenter policy.

Table F.2 presents the parameters used in the modeling of a BRT system.

Table F.2. Parameters used in the modeling of a BRT system.

Parameter	Value
T	1.5 [h/P_m]
$\alpha, \beta, \gamma, \delta$	2.2, 2.1, 1.0, 2.5
$v^a(r)$	$3 + 1.4\bar{6} \cdot r$ [km/h·route]
v^t	90 [km/h]
v^w	3.0 [km/h]
τ^s	49 [s/station]
t^f	5 [min]
η^d	1 [shift/veh]
K^v	101 [user/veh]
K^d	0.079 [km/route]
K^h	60 [seg/veh]
μ	1.48 [$/user·h]
φ^k	37.9 [$/veh·$P_m$]
φ^g	23 [$/shift·h]
φ^o	1.6 [$/veh·km·route]
φ^p	62.1 [$/km·route·$P_m$]
φ^s	6.2 [$/station·route·$P_m$]

3.2. Results and discussion

The model gets two optimal results: headway and continuous density functions of the distance between transit routes. The headway reaches the minimum value. Figure F.2 shows optimal route densities (the inverse of the distance between routes) for ring and radial routes (i-ii) and each urban scenario: (a-d). Figure F.2(iii) contains the optimal objective function values (OFV). Consequently, we obtain a discrete solution from continuous functions for each type of route. Figure F.2(iv) presents the optimal network scheme and includes both transit routes.

In scenario A, the constraints are not active over the urban region for ring roads (Figure F.2(i)-(a)). The optimal density is higher around 3 km from the center, but this decreases abruptly toward the center and slowly toward the periphery. For radial roads, the buses do not travel full during the first kilometers of a radial corridor (≈ 4 km). After that, the demand dominates the optimal density of radial routes (Figure F.2(ii)-(a)). In the other scenarios, Figure F.2(i-ii)-(b-d) shows the progressive effect of a subcenter. The result of discretization (Figure F.2(iv)) shows the effect of the implementation of subcenters. In scenarios A, B, and C, the city needs 29 radial routes, although these are more concentrated in the subcenter area when its density increases.

If the subcenter is more significant than the CBD, the city needs 30 radial routes (scenario D). Concerning ring routes, all scenarios require six routes, although the system can share the infrastructure in an area without subcenters for scenarios B, C, and D. These save infrastructure costs but increase the access cost.

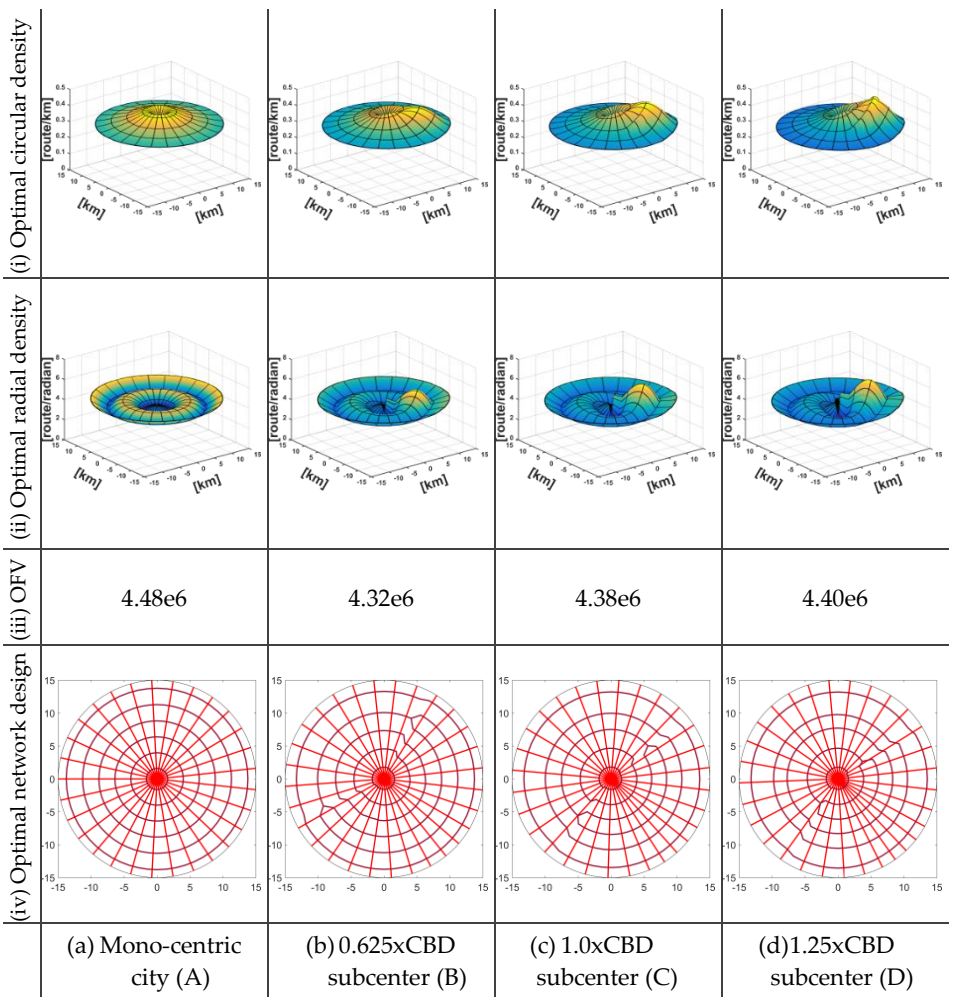

Figure F.2. Optimal transit network design: BRT system for the subcenter policy.

Figure F.3 shows a comparison of costs and travel time between urban scenarios. Figure F.3(a) shows the evolution of user, agency, and total savings concerning scenario A. The progressive scenarios consider the increment of the subcenter size from 0.125 (1/8xCBD) to 1.25 times the CBD (5/4xCBD, scenario D). The implementation of subcenters presents savings in all scenarios. For users, the maximum savings appear with medium-size subcenters (0.5x to 0.75x). For the agency, more significant savings appear

when the subcenters are big, and the system reduces the infrastructure in areas with low demand. Thus, the peak saving appears in scenario B in comparison to scenario A (3.49%). Figure F.3(b) compares savings between scenarios A and B. All stages of a trip have savings except access (0.22%) and operating cost (0.25%). The most significant savings are in the infrastructure because some routes share infrastructure on the opposite side of the sub-center.

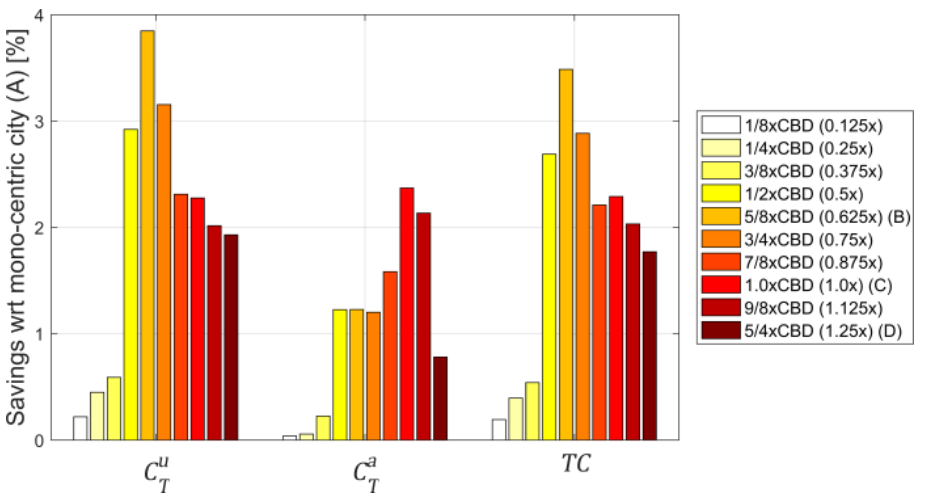

(a) Cost savings wrt the mono-centric city (only CBD)

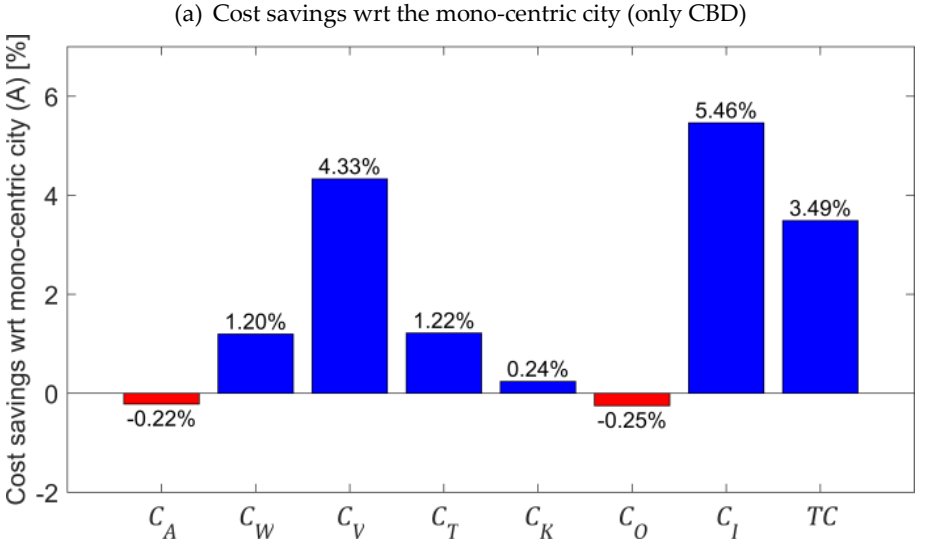

(b) Comparison of costs between (A) and (B) scenarios

Figure F.3. Cost savings considering a set of urban scenarios.

Figure F.4(a) represents infrastructure needs considering the progressive set of urban scenarios. The first four scenarios maintain the same needs of infrastructure. After that, the BRT system can merge services at the same corridor in areas with low demand, which reduces linear infrastructures, and

BRT stops. The minimum number of stops is between 0.875x and 1.125x of the CBD. In the last scenario (1.25xCBD), transit requires a new radial corridor. Figure F.4(b) represents time savings regarding scenario A. Access and travel time savings influence these savings.

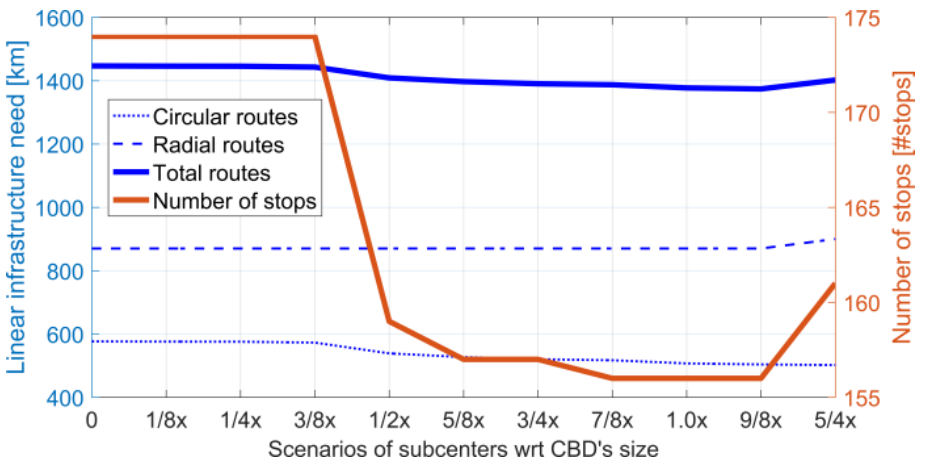

(a) Infrastructure needs

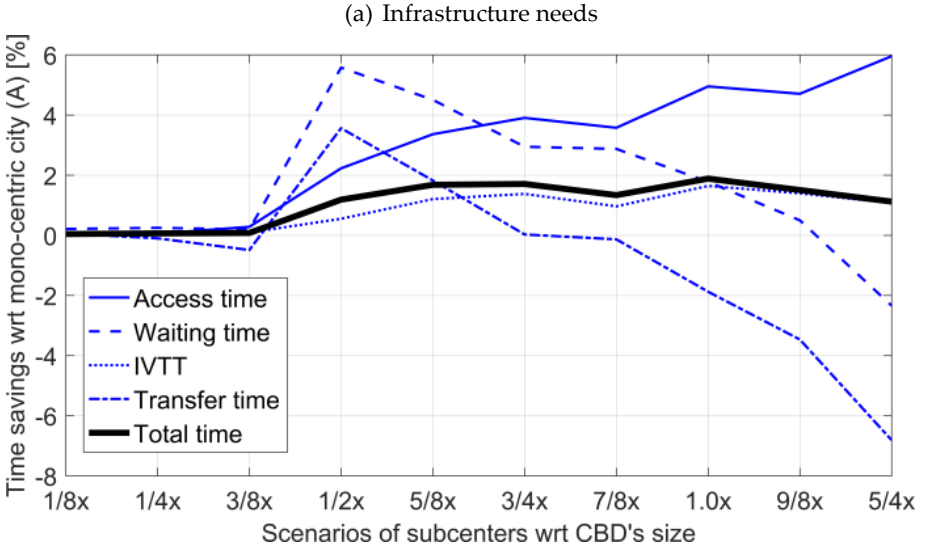

(b) Comparison of travel time

Figure F.4. Infrastructure needs and travel time considering a set of scenarios.

4. Conclusions

The proposed methodology based on the CA method allows us to analyze improvements for the mobility of a city or quantify the required primary infrastructure. Moreover, the results of the model can contribute to the

development of spatial planning instruments, which require several studies to define an objective image of a city (future urban planning scheme) that can include urban subcenters. The results show how radial corridors allow massive trips of users from the periphery to central areas of a city, although buses only circulate full during 2/3 of a route. On the other hand, circular routes bring passengers closer to their destinations, e.g., CBD or urban subcenters. However, ring routes also have a significant role in the city periphery. The role of subcenters makes it possible to improve the mobility of inhabitants in scattered, large cities. Besides, subcenters create an opportunity to optimize transit systems. The results show that this strategy of urban planning allows for obtaining a savings of 3.5% in rush hour. These savings are about $40MM in a year, considering a subcenter in just morning's peak periods. Another relevant aspect is the size of the subcenters. The results show that subcenters as large as the CBD (or even larger) do not necessarily cause benefits to a public transportation system. The maximum benefits are obtained in medium-sized subcenters in comparison to the CBD because there must be a balance between user and agency costs. In future works, the application to a specific case will improve the analysis considering real cities in current and future mobility scenarios. The application of this model is macroscopic for an entire city or a specific zone. The model allows for determining the density of transit services necessary to satisfy demand with a balance of adequate total costs. Moreover, the analytical formulation of the model allows identifying key elements that could generate problems or conflicts between a transportation system and an urban system.

Appendix G. Exploring paradigm shift impacts on urban mobility: autonomous vehicles and smart cities[3]

Abstract: Urban mobility is a dynamic system that has had a (slow) natural evolution. Scientists and engineers are currently developing new mobility technologies. A progressive paradigm shift will change everything from the fuel type to the way of driving vehicles. Vehicles will progressively become autonomous and will communicate and cooperate among cars. In the long run, profound changes will appear as mobility as a service.

Furthermore, urban areas will have a higher level of development, and cities will likely turn into smart cities in which the vehicles will interact with the urban infrastructure. The main objective of this paper is to explore the macroscopic effects of mobility interaction in a radial-circular urban road system for current and future cities (smart cities). In the literature, there is documentation of the direct effects of autonomous vehicles, but some indirect effects will cause undesirable impacts such as an increase in demand and more congestion, which change the demand behavior and the urban structure. Finally, this paper exhibits the results of direct and indirect effects calculated through analytical tools (continuous approximation method). Thus, the research shows that if demand increases by about 50%, the current scenario could have the same total cost as the future scenario with autonomous vehicles. Besides, if both the city radius increases by about 33% and the subjective value of time decreases by about 20%, then it will compensate benefits of the implementation of autonomous cars. Therefore, the paper proves that autonomous vehicles could encourage urban sprawl in the long run. Finally, Administrations should define transport strategies and policies to control these externalities because autonomous driving could deteriorate mobility even worse than it is now.

Keywords: Urban road network; Autonomous car; Continuous approximation

---

[3] Paper presented at two scientific congresses and published in a journal:

- Medina-Tapia, M., & Robusté, F. (2018a). Exploring paradigm shift impacts in urban mobility: autonomous vehicles and smart cities. Proceedings of XIII Spanish Transportation Engineering Congress, Gijón, Spain.
- Medina-Tapia, M., & Robusté, F. (2018b). Exploring paradigm shift impacts in urban mobility: autonomous vehicles and smart cities. Transportation Research Procedia, 33, 203–210.
- Medina-Tapia, M., & Robusté, F. (2018c). Impact assessment of autonomous vehicle implementation on urban road networks. Proceedings of Pan-American Conference on Traffic, Transportation Engineering and Logistics.

1. Introduction

In the 1960s, the renowned English engineer Colin Buchanan had already pointed out that traffic congestion was one of the most significant problems in cities nowadays (Buchanan, 1963). Administrations have traditionally applied several strategies to control it. Recently, the implementation and the effects of new technologies as autonomous vehicles are an essential topic of discussion by scientists. Autonomous vehicles will come to our cities in the coming years. Some experts estimate that it will be during the next decade, while others are not so optimistic. One thing is for sure; there would be a transition period in which two types of vehicles will coexist, manual (MVs) and autonomous vehicles (AVs) with different levels of automatization (NHTSA, 2016).

Urban mobility has had a slow, natural evolution. The next challenge to face is a technological jump; it brings together a change of paradigm in urban mobility, which makes it necessary to evaluate it and get used to it, at the same time, our cities and infrastructures do. The primary objective of the research is to assess AV implementation and its possible macroscopic impacts on the decongestion and efficiency of an urban network and potential benefits for society. The research has two stages. The first one is a conceptual revision of AV implementation effects, while the second stage proposes a mathematical model to assess the impact of those effects. For this, the Continuous Approximation Method (CA) allows for modeling a continuous and two-dimensional space through a circular-radial network to explore and compare results between a base scenario with only MVs and a future scenario (smart cities) with AVs provided with total automatization.

The next section shows a conceptual and systematic analysis of AVs. The following section explains the mathematical model developed. In the fourth section, the model allows assessing the two urban scenarios mentioned. Finally, the last section discusses the main conclusions of the paper.

2. AV direct and indirect effects

AVs (and vehicles communicated among them, V2V) will generate positive changes in transportation and mobility (e.g., Childress et al., 2015; Kockelman, 2017; Kohli & Willumsen, 2016), but it also will produce non-desirable effects. Bahamonde-Birke et al. (2018) gather the AV impacts on the effects of the first and second-order.

2.1. Direct effects

AV direct effects (or first-order) directly impact one attribute of the transportation system. Five items contain the direct impacts that researchers have widely discussed in the literature:

- The automatization of the driving process (AVs) will reduce the generalized travel costs,
- The operation of taxis and public transportation will be more efficient and flexible than MVs,
- AVs will allow increasing the urban road capacity due to platoon formations in urban roads,
- Reduction of pollution, and
- Improvement of road safety.

2.2. Indirect effects

AV indirect effects, called second-order or systemic in Bahamonde-Birke et al. (2018), will lead to changes in demand behavior, demand volume, new requirements in infrastructure in the long run, and some cases, undesirable effects will be caused (B. W. Smith, 2012):

- AVs will reduce the value of travel time (VTTS) due to the reduction of driving disutility.
- New users (minors, the elderly, disabled people, and induced demand) could use AVs (B. W. Smith, 2012).
- AVs will produce an increment of induced demand due to the reduction in congestion, so the value of time and travel times will cause an increase in the trip generation (induced demand).
- AVs will increase vehicle-kilometer traveled (VKT) due to trips without users and others (B. W. Smith, 2012).
- The reduction of costs, congestion levels, and the value of travel time will generate longer trips than at this time. These effects will produce changes in the trip generation, attraction, and distribution matrix.
- The changes in trip distribution will cause changes in the urban structure and the activity system in the long run due to more dispersed cities (urban sprawl), changes in place of residence, and employment (B. W. Smith, 2012).

3. An analytical model to analyze AV effects

3.1. Continuous Approximation Method (CA)

The methodological focus of this work is in a two-dimensional and continuous analysis; therefore, it was appropriate to use the CA Method. If we have no accurate information, CA will be valid (Newell, 1973). CA resolves a problem based on local costs, which have a density structure (Daganzo, 2005). CA has several applications in transportation and logistics. For instance, Pilachowski (2009) optimizes the bus bunching process. Medina-Tapia et al. (2013) simultaneously optimize the location of bus stops and the headways (operation). Pulido et al. (2015) locates warehouses and designs distribution strategies for a freight system with time windows.

Table G.1. Nomenclature.

Decision variables:	
$d_c(r)$	distance function between circular roads at the radius r km [km/street]
$d_r(r,\theta)$	distance function between radial roads at a city point (r,θ) [km/street]
$\Phi(\theta)$	angle function between radial roads at a city point with angle θ [radian/street]
Parameters:	
T	duration of period [h]
v_f	car speed to access main roads of the city [km/h]
v_c	free-flow car speed on the main road [km/h]
v_p	cruising speed looking for a parking spot [km/h]
v_a	average walking speed for accessing a destination point from the parking site [km/h]
a and b	parameters of BPR volume-delay function [dimensionless]
c	congestion parameter that represents the effect of cars looking for a parking spot [dimensionless]
k_V	capacity road per lane [veh/lane·h]
τ_V	average time spent by a vehicle when crosses a crossroad [h/street]
λ_P	mean density of vacant parking space [parking/km]
d_p	distance before arriving at the destination where the drivers begin to look for a parking spot [km]
d_s	distance (width) of influence between the main road and the destination point [km]
Unitary cost parameters:	
μ	value of travel time [$/h]
φ^t	car cost per distance unit [$/km]
φ^p	parking fee [$/veh·h]

3.2. Proposed model

Table G.1 describes the parameters used to assess two mobility scenarios: the current case with only MVs (the driver without passengers) and the future case with only AVs with Level 5 of automation.

The modeling assumes a circular city with a radius of R km and a circular-radial road system. The demand density function $P(r_f, \theta_f, r_t, \theta_t)$ in polar coordinates represents the density of car trips from an area $dr_f\ r_f\ d\theta_f$ about the origin (r_f, θ_f) to an area $dr_t\ r_t\ d\theta_t$ at a destination (r_t, θ_t) (Vaughan, 1986). In Equation G.1, Δ represents the total trips in the city.

$$\Delta = \int_0^{2\pi R} \int_0^{2\pi R} P(r_f, \theta_f, r_t, \theta_t)\ r_t\ dr_t\ d\theta_t\ r_f\ dr_f\ d\theta_f \qquad (G.1)$$

Car users choose the shortest route (minimum distance) between two points. Therefore, there are three private mobility patterns: radial-circular, circular-radial, and radial-radial trips (Medina-Tapia & Robusté, 2018a).

3.3. User costs

The model only includes private transportation costs. The total cost of car users (C_C^u) is the addition of three sub-costs: accessibility cost to main roads (C_F), regular car trip cost (C_V), and cost for arriving at the destination (C_A).

Accessibility cost to main roads

In this section, we have calculated the cost expended when users drive from the origin (household or place of residence) to the nearest main road. The demand function ($[veh/km^2 \cdot h]$) represents the vehicle density that accesses the main road on circular ($f_F^c(r,\theta)$) and radial road corridors ($f_F^r(r,\theta)$) (Medina-Tapia & Robusté, 2018a).

Average cost ($[\$/veh]$) for accessing to circular ($c_F^c(r)$) and radial road ($c_F^r(r,\theta)$) (Equation G.2) depends on the distance between the origin and the main street ($d_c(r)/4$ or $d_r(r,\theta)/4$), and the generalized cost per kilometer (Ψ^F). This generalized cost has two components: travel cost at a speed v_f, and monetary cost of operation (φ^t).

$$c_F^k(r)=\begin{cases}\dfrac{d_c(r)\cdot\Psi^F}{4}=\dfrac{d_c(r)}{4}\cdot\left(\dfrac{\mu}{v_f}+\varphi^t\right) & k=c:circular\\ \dfrac{r\cdot\Phi(\theta)\cdot\Psi^F}{4}=\dfrac{d_r(r,\theta)}{4}\cdot\left(\dfrac{\mu}{v_f}+\varphi^t\right) & k=r:radial\end{cases} \quad (G.2)$$

AVs should impact local cost function in two aspects:

- Reduction of generalized cost (Ψ^F): the speed (v_f) should increase, and the operation cost (φ^t) should decrease.
- Reduction of the value of travel time (μ): AVs will allow users to do other activities during a trip.

Finally, the total cost of accessibility (C_F in [$]) is the integration of local cost function (demand density, period, and the average cost of accessibility) on the urban area (Equation G.3).

$$C_F=\int_0^{2\pi}\int_0^R\frac{1}{4}\cdot\left(f_F^c(r,\theta)\cdot T\cdot d_c(r)+f_F^r(r,\theta)\cdot T\cdot r\cdot\Phi(\theta)\right)\cdot\Psi^F\, r\, dr\, d\theta \quad (G.3)$$

Regular trip cost

Vehicle flow density function ($[veh/km\cdot h]$) at a point has different formulations for circular ($f_V^c(r,\theta)$) and radial road corridors ($f_V^r(r,\theta)$) (Medina-Tapia & Robusté, 2018a).

Local generalized travel costs ($[\$/km\cdot veh]$) has three components (Equation G.4). Firstly, we model the travel cost through a BPR function (Bureau of Public Roads). The free-flow travel cost per kilometer (μ/v_c, $[\$/km]$) is multiplied by the congestion factor. This factor depends on the car flow: regular travel flow ($F_V^c(r,\theta)=f_V^c(r,\theta)\cdot d_c(r)$ or $F_V^r(r,\theta)=f_V^r(r,\theta)\cdot d_r(r,\theta)$), and cruising flow for parking ($F_P^c(r,\theta)$ or $F_P^r(r,\theta)$). The car flow also depends on the road capacity ($K_V^c(r,\theta)$ or $K_V^r(r,\theta)$). Secondly, the function contains a component for crossing regulated crossroads. The formulation of the function presents a ratio between time spent by crossing a road intersection and road density ($1/d_c(r)$ or $1/d_r(r,\theta)$). Finally, the function contains a monetary component of operation travel cost (φ^t).

$$c_V^k(r)=\begin{cases}\dfrac{\mu}{v_c}\cdot\left(1+a\cdot\left(\dfrac{F_V^c(r,\theta)+c\cdot F_P^c(r,\theta)}{K_V^c(r,\theta)}\right)^b\right)+\dfrac{\mu\cdot\tau_V}{r\cdot\Phi(\theta)}+\varphi^t & k=c:circular\\ \dfrac{\mu}{v_c}\cdot\left(1+a\cdot\left(\dfrac{F_V^r(r,\theta)+c\cdot F_P^r(r,\theta)}{K_V^r(r,\theta)}\right)^b\right)+\dfrac{\mu\cdot\tau_V}{d_c(r)}+\varphi^t & k=r:radial\end{cases} \quad (G.4)$$

AVs should impact on local generalized travel cost function in seven aspects:

- The reduction of the value of travel time (μ).
- Speed increase due to efficient driving (v_c).
- The increment of vehicles that are looking for a parking spot ($F_P^c(r,\theta)$, $F_P^r(r,\theta)$) due to "ghost trips" (empty cars) to the origin point.
- The reduction of congestion impacts due to AVs will have perfect information on the parking location ($c = 1$).
- Road capacity increase due to platoons, less headway, and others ($K_V^c(r,\theta)$ and $K_V^r(r,\theta)$).
- Reduction of time for crossing intersections (τ_V) due to platoons, traffic lights coordination, less reaction time, communication V2I, and others (Smart City).
- The reduction of car operational cost due to efficient driving (φ^t).

About the demand functions of users that look for a parking spot, there are two types of functions (Medina-Tapia & Robusté, 2018a). AVs will not have to look for a parking space before the destination ($d_p = 0$) because the vehicles will directly arrive at the destination and, after that, they will go to a parking spot without users (Medina-Tapia & Robusté, 2018a). In the modeling, the model assumes that drivers neither can stop and wait for a parking site nor can come back upstream (Arnott & Rowse, 1999).

Finally, the total travel cost in the urban system (C_V in [$]) is the double integral of the local cost function on circular city area, which includes the demand density, duration of the period, and local generalized travel cost (Equation G.5).

$$C_V = \int_0^{2\pi}\int_0^R \left(f_V^c(r,\theta)\cdot T\cdot c_V^c(r) + f_V^r(r,\theta)\cdot T\cdot c_V^r(r,\theta)\right) r\, dr\, d\theta \qquad (G.5)$$

Arriving cost to the destination

The density of users ($[veh/km^2\cdot h]$) that arrive at a circular ($f_A^c(r,\theta)$) or a radial road ($f_A^r(r,\theta)$) is calculated (Medina-Tapia & Robusté, 2018a).

$$c_A^k(r) = \begin{cases} \left(\frac{d_c(r)-d_p}{4}\right)\cdot\Psi^F + \frac{1}{\lambda_P}\cdot\Psi^P + \left(\frac{2\cdot e^{-\lambda_P\cdot d_p}}{\lambda_P} + d_p - \frac{1}{\lambda_P}\right)\cdot\Psi^A + \varphi^p & k = c : circular \\ \left(\frac{r\cdot\Phi(\theta)-d_p}{4}\right)\cdot\Psi^F + \frac{1}{\lambda_P}\cdot\Psi^P + \left(\frac{2\cdot e^{-\lambda_P\cdot d_p}}{\lambda_P} + d_p - \frac{1}{\lambda_P}\right)\cdot\Psi^A + \varphi^p & k = r : radial \end{cases} \qquad (G.6)$$

The average cost function per vehicle at the destination has four elements (Equation G.6). Firstly, the cost of driving by secondary roads from a main

road to the destination and without cruising for a parking spot ($(d_c(r) - d_p)/4$) multiplied by generalized cost ($\Psi^F = \mu/v_f + \varphi^t$). Secondly, the cost of cruising for a parking site depends on the average distance where there is vacant parking ($1/\lambda_P$) and the generalized cost ($\Psi^P = \mu/v_p + \varphi^t$). Thirdly, the walking cost from the parking site to the destination point depends on the expected walking distance that is multiplied by the generalized cost ($\Psi^A = \mu/v_a$). Arnott and Rowse (1999) determined the expected walking distance from parking ($(2 \cdot e^{-\lambda_P \cdot d_p})/\lambda_P + d_p - 1/\lambda_P$); if a driver parks before destination point ($x < d$), he will step $d - x$ km; in another case, the driver will walk $x - d$ km. Finally, the last component is the car parking fee (φ^p).

In the case of AVs, these vehicles should impact local cost function in three aspects:

- Drivers in a Smart City will get out of the car neither before the destination nor after it ($d_p = 0$).
- The generalized cost of AVs will decrease (Ψ^F and Ψ^P), and the component μ/v_p is null in the generalized cost Ψ^P.
- The component $((2 \cdot e^{-\lambda_P \cdot d_p})/\lambda_P + d_p - 1/\lambda_P)$ is null because they do not have to walk from the parking spot.

The total cost of cruising for parking, parking on the spot, and walking to the destination (C_A) come from integrating the demand in rush hour and the average cost per vehicle at the destination (Equation G.7).

$$C_A = \int_0^{2\pi} \int_0^R \left(f_A^c(r,\theta) \cdot T \cdot c_A^c(r) + f_A^r(r,\theta) \cdot T \cdot c_A^r(r,\theta) \right) r \, dr \, d\theta \qquad (G.7)$$

4. Quantitative estimation of AV effects

4.1. Parameters

We model a circular city with five zones: a Central Business District (CBD) and four external zones. The radius of the city is 15 km (R), and the CBD has a radius of about 6.7 km ($R_c = R/\sqrt{5}$). The city has 500,000 car users of MVs distributed homogeneously (Medina-Tapia & Robusté, 2018a).

Table G.2. Parameters in each analyzed scenario.

Parameters		Manual vehicle Case	Autonomous vehicle Case
$d_c(r)$	[km/street]	1.0	1.0
$\Phi(\theta)$	[radian/street]	0.12	0.12
T	[h]	1.5	1.5
μ	[$/hr]	10	[5…10]
v_f	[km/h]	20	20
v_c	[km/h]	45	50
v_p	[km/h]	10	10
v_a	[km/h]	3	3
d_p	[km]	0.2	0.0
a		2	2
b		3	3
c		3	1
k_V	[veh/lane·h]	1,272	3,960
τ_V	[h/veh·street]	0.0125	0.0125·70%
λ_P	[parking/km]	5	5
d_s	[km]	0.2	0.2
φ^t	[$/km]	0.1	0.1·70%
φ^p	[$/veh·h]	1	1

In the current scenario (MVs), the road capacity is 1,272 per lane (k_V). In a future scenario (AVs), the road capacity will be 3,960 (k_V); it is three times bigger than the current scenario (Lioris et al., 2017).

4.2. Influence of AV implementation

Influence of direct effects

In the discussion previously made about AV impacts on urban mobility, we presented five direct effects, but three of them we have analyzed in this paper.

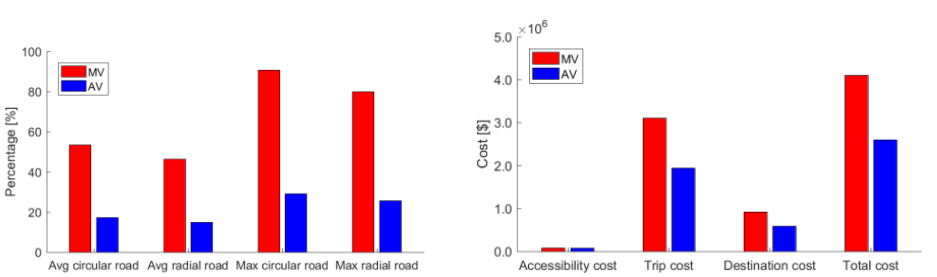

(a) MV and AV saturation percentage (b) Travel stage cost of MVs and AVs

Figure G.1. Impacts of direct effects.

- *Congestion reduction*: If the driving of AVs is more efficient than MVs, the road capacity per lane will increase, and the congestion will decrease (Figure G.1(a)).
- *Travel cost reduction*: If VTTS takes the same value as the base scenario ($\mu = 10\ [\$/h]$), the total cost will decrease by 33.7%, but the travel cost reduction will be more significant, 37.1% (Figure G.1(b)). The accessibility cost also decreases in a lower percentage than other trip stages (5%).
- *Parking cost reduction*: Costs of looking for parking in the AV scenario also decrease notoriously regarding the MV case (28.8%) because AVs look for parking without passengers; hence there are only operational costs.

Influence of indirect effects

In a complementary way to the previous point, AVs also cause indirect effects on the urban transport system; positive results of direct effects have compensation due to indirect effects (Bahamonde-Birke et al., 2018).

- *VTTS reduction*: Kohli and Willumsen (2016) have pointed the VTTS could decrease by 20% in the AV scenario; hence, if $\mu = 8$ in our model, the total cost is reduced by 40.6% and the travel cost by 46.6%. There is a trade-off between longer trips without drivers (AVs) and an increment of walking time (MVs).
- *VKT increment*: After the user arrives at the destination, AVs will look for a parking spot without passengers, and the Smart City (V2I) will assign the nearest free spot. Our model indicates AVs will travel 66,722.9 km more than the MVs because these cars begin to look for parking before the destination (d_p).
- *Travel distribution pattern changes*: If the value of travel time and congestion decreases, new users will use AVs. According to the model (Figure G.2(a)), a significant increment of demand density could compensate for the reduction of costs by direct effects. Figure G.2(b) simultaneously shows the value of travel time and the increment of the demand on the total cost with AVs (blue lines) in comparison to the total cost using MVs (red symbol and lines).
- *Travel distribution and urban structure changes*: City size affects the length of trips and, therefore, the total cost of the system. Figure G.2(c) shows that the total cost will increase if the urban radius also increases, but this value will be similar to the cost of the base scenario (MVs) at the radius of about 35 km with $\mu = 8\ [\$/h]$. It could be inferred that the city size effects are more significant on the total cost value than the effects of the induced demand. In Figure G.2(d), the average user cost per kilometer will slightly decrease if the urban radius increases and the average costs of AVs are smaller than the costs of the base scenario (blue point). In other words, if the generalized

costs are smaller included the value of time, the trips will tend to be longer, and the users will change the destination. This reduction will cause urban problems, and the urban structure could also change in the long term; in other words, these problems are early phases of profound urban problems as spatial segregation and urban sprawl.

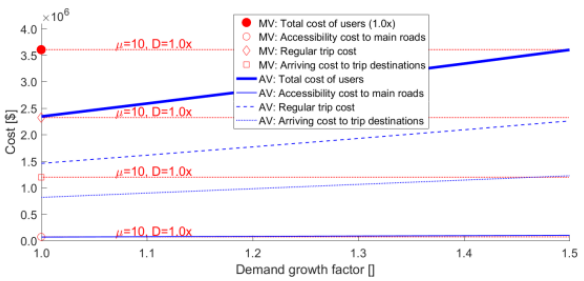

(a) Impact of demand increment on the total cost in each travel stage

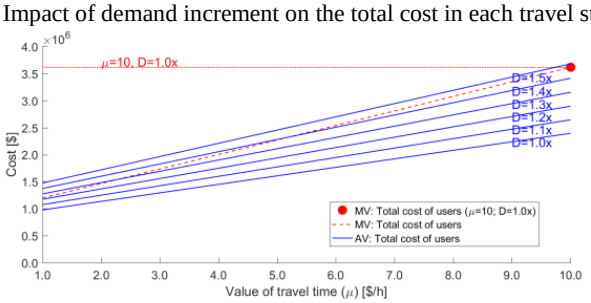

(b) Impact of variation in the value of travel time and demand increment on the system total costs

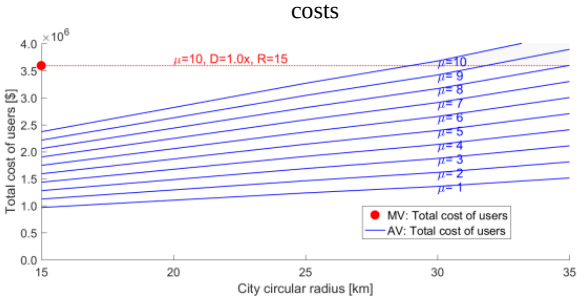

(c) Effect of the urban radius on the total cost of users

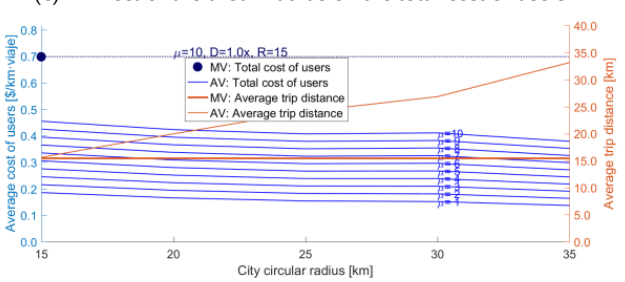

(d) Effect of the urban radius and the average travel distance on the average cost of users

Figure G.2. Impact of demand increment and urban structure.

5. Conclusions

The paradigm shift in urban mobility is a broad and dynamic concept in which AVs play a relevant role. They present direct and indirect effects. Our results show that the direct effects will be positive for the urban system. However, the indirect effects will change the equilibrium between transport supply and demand, with externalities reaching far beyond the private transport system, as it also influences the urban structure and the urban activity system. According to our results, the effect of system user costs due to urban growth is more significant than the increment of users by induced demand. These impacts will deteriorate the current negative externalities that already encourage private transportation (vicious circle of public transportation). Moreover, a city with only AVs and without other complementary modes (private, public, and shared transportation) is unsustainable in the long run.

The proposed model is a contribution to the analysis of AVs' impacts on urban structure. However, it also allows the analysis of a broad spectrum of scenarios, possibilities, measures, or strategies to improve the urban transport system and strategic-level infrastructures of real cities. Therefore, according to our results, if Administrations do not implement regulatory measures and urban planning, the urban problems will be multiplied twice or three times in comparison to the current state. Urban planners and transport engineers should design policies and actions that anticipate problems of the AV implementation in mainly four aspects. Firstly, governments should design transport demand policies such as incentives or restrictions on private and public transportation. Secondly, they should design types of transport systems such as private or sharing AVs, complementing with other freight and passenger transportation systems. Thirdly, urban infrastructure should adapt to new systems or a complete urban redesign. Finally, urban policies should design following the type of urban development—dense or dispersed cities—and the size and form of cities. This last point is the least studied and, at the same time, a key factor for the correct functioning of a new transport system.

New technologies such as AVs, smart cities, and MaaS will work neither in the short run nor simultaneously. Instead, there will be a transitional period where AVs and MVs will share streets. For this reason, our analysis and modeling in future works will deepen in alternative scenarios such as non-homogeneous demand multi-modes (private, public, and freight transportation); different types of roads; the mobility as a service (MaaS); and finally, the optimization of the system.

Acknowledgments

This study was supported and granted from Project 061312MT of the Departamento de Investigaciones Científicas y Tecnológicas (DICYT) of the Vicerrectoría de Investigación, Desarrollo e Innovación of the Universidad de Santiago de Chile (USACH). It was also supported by CONICYT PFCHA/BCH, No. 72160291.

Appendix H. Implementation of connected and autonomous vehicles in cities could have neutral effects on the total travel time costs: modeling and analysis for a circular city[4]

Abstract: Autonomous vehicles promise to revolutionize the automobile market, although their implementation could take several decades in which both types of cars will coexist on the streets. We formulate a model for a circular city based on continuous approximations, considering demand surfaces over the city. Numerical results from our model predict some direct and indirect effects of connected and autonomous vehicles. Direct effects will be positive for our cities: (a) less street supply is necessary to accommodate the traffic; (b) congestion levels decrease, travel costs may decrease by 30%. Some indirect effects will counterbalance these positive effects: (c) a decrease of 20% in the value of travel time can reduce the total cost by a third. (d) induced demand could be as high as 50%, bringing equivalent total costs in the future scenario; (e) the vehicle-kilometers traveled could also affect the future scenario; and (f) increment in city size and urban sprawl. Regarding conclusions, the implementation of autonomous vehicles could be neutral for the cities regarding travel time costs. City planning agencies still have to promote complementary modes such as active mobility (walking and bicycle), transit (public transportation), and shared mobility (shared autonomous vehicles and mobility as a service).

Keywords: Urban road network; Connected and autonomous car; Continuous approximation

1. Introduction

In recent years, experts have discussed the implementation of autonomous vehicles (AVs) and their benefits for decongesting cities. For this reason, in some countries, the planning agencies are designing long-term plans, and these agencies need modeling tools that anticipate the impact they may have on transportation networks (Childress et al., 2015). AVs have different levels of automation, and there are multiple definitions for them; NHTSA (2016) proposes to use the SAE International's classification that defines five levels

[4] Paper published in a journal:

- Medina-Tapia, M., & Robusté, F. (2019b). Implementation of connected and autonomous vehicles in cities could have neutral effects on the total travel time costs: Modeling and analysis for a circular city. Sustainability, 11(2), 482.

of automation, and the cars are entirely autonomous when they reach level five (L5).

Some experts believe that these cars will widely enter the automotive market during the next decade. However, other scholars are not optimistic. Inevitably, AVs will arrive in our cities, and both types of vehicles will share the streets: autonomous and connected vehicles (CAVs) and manual vehicles (MVs) (Martínez-Díaz, Soriguera, & Pérez, 2018b; Medina-Tapia & Robusté, 2018b).

Implementation of CAVs will need new technical requirements, which Martínez-Díaz et al. (Martínez-Díaz, Soriguera, & Pérez, 2018a) explain in detail, e.g., a new onboard architecture, sensing system, new communications, cloud requirements, infrastructure needs, and others. These conditions will allow these new cars could generate positives changes in transportation and urban mobility. For example, the reduction of the generalized transportation cost and parking cost of private vehicles, reduction of disutility on travel time, reduction of polluting emissions, improvement in road safety, induced demand, and improvement in road capacity because the distance among vehicles can be less than nowadays (Childress et al., 2015; Kockelman, 2017).

Several previous researchers have determined the impact of AVs on isolated sections of a highway. The main objective of this research is to analyze the effects of the implementation of CAVs on an urban network. The paper assesses how CAVs will deploy and will share the infrastructure with MVs by considering three aspects: the potential benefits for the optimal urban structure, the assessment of the direct and indirect impacts of AVs on the efficiency of a network, and the probable effects of the progressive implementation of CAVs. As its focus, this work presents a strategic and macroscopic analysis of CAVs, using a continuous, two-dimensional, total-cost function applied to a circular city. The analysis does not consider other topics such as safety or livability.

2. Theoretical CAV impacts on urban mobility

The classification of AV impacts depends on the type of connection between AVs and the transportation system. AVs should produce positive effects, but some of them will generate non-desirable impacts (Medina-Tapia & Robusté, 2018a, 2018b; Pakusch, Stevens, Boden, & Bossauer, 2018).

2.1. Direct effects

Firstly, some consequences will directly impact a transportation system; they are positive in general terms, as the literature describes it (Bahamonde-Birke et al., 2018). Five groups contain these direct effects (Medina-Tapia & Robusté, 2018a, 2018b):

1. *Reduction of generalized travel costs*: Efficient driving will create savings in fuel costs and increment the travel speed in all types of vehicles. Furthermore, in a Smart City with V2I communication (vehicle-to-infrastructure), the cars will find a vacant parking spot quickly (on-street or off-street), and the CAVs will directly travel to the parking spot without users at top speed.
2. *An increment of efficiency and flexibility*: Driverless vehicles will permit flexibility in operations for transit and taxis, but this could generate a social problem (unemployment). In private AVs, this reduction of cost is not relevant.
3. *Road capacity increment*: Previous papers show different results (Kockelman, 2017). Chang and Lai (1997) analyzed the mixed traffic flow in a freeway section; the results show that the increment of road capacity is close to 33%. VanderWerf et al. (2001; 2002) studied the impact of autonomous adaptive cruise control (AACC) and cooperative adaptive cruise control (CACC) using traffic simulation. The results show that AACC vehicles will increase the capacity of about 7% if the AACC rate is between 40% and 60%; meanwhile, CACC vehicles will increment the capacity to near 102% when all cars are communicated (VanderWerf et al., 2002). Tientrakool et al. (2011) estimated that the road capacity would increase by 43% with AVs and 273% with V2V vehicles. Lioris et al. (2017) stressed that an intersection is the bottleneck of the road capacity. If vehicles with AACC crossed an intersection in a platoon, then the road capacity would increase to double or triple. Even if cars have CACC technology, the headways will be shorter. In a smart city, CAVs will be more efficient at intersections for V2I technology. On the other hand, other authors disagree and think that AVs would not reduce the congestion because AVs will drive rather cautiously; moreover, it is likely to increase the vehicle-kilometers traveled (Martínez-Díaz et al., 2018b).
4. *Pollution reduction*: Some authors estimate that pollution could decrease (Martínez-Díaz et al., 2018b; Pakusch et al., 2018) due to these cars will be electric vehicles (optimization of energy consumption) (Martínez-Díaz et al., 2018a). On the contrary, other experts predict an increment of this negative externality (Bahamonde-Birke et al., 2018; Wadud et al., 2016).
5. *Improvement in road safety*: AVs correctly implemented will reduce human errors and negligence in comparison to manual driving (Martínez-Díaz et al., 2018b; Pakusch et al., 2018), although some estimations have determined

that the crash number at roundabouts increases when AVs increase as well (Deluka Tibljaš, Giuffrè, Surdonja, & Trubia, 2018).

2.2. Indirect effects

Secondly, indirect effects will change demand behavior (Bahamonde-Birke et al., 2018). Indirect effects of AVs will cause changes in the system equilibrium between transportation supply and demand (Medina-Tapia & Robusté, 2018a, 2018b). As a result, new requirements for infrastructure will be necessary for the long-term (B. W. Smith, 2012):

1. *Reduction in the subjective value of travel time savings (VTTS)*: Ortúzar and Willumsen (2011) define VTTS as "*the willingness to pay to reduce travel time by one unit*" (Ortúzar & Willumsen, 2011). It was first formulated by English Economists: Becker (1965), Johnson (1966), Oort (1969), DeSerpa (1971), and Evans (1972) (Ortúzar & Willumsen, 2011). Users of AVs will do other tasks instead of driving, reducing the disutility of the travel time (Kohli & Willumsen, 2016).
2. *New users to the vehicle system*: AVs will expand the range of users that will use these cars (e.g., minors, the elderly, and disabled people) (B. W. Smith, 2012).
3. *Induced demand*: A reduction of the value of time, congestion, and travel times will cause an increment of trip demand in AVs and CAVs. The changes in travel patterns will impact the reduction of transit users (Pakusch et al., 2018), and AV and CAVs could increase. Therefore, this phenomenon will encourage the vicious circle of public transportation (Ortúzar & Willumsen, 2011).
4. *The increment of vehicle-kilometers traveled (VKT)*: The increment of the VKT has at least three reasons (2012). First, the splitting of joint trips (Bahamonde-Birke et al., 2018) in which two or more members of a family that are currently traveling together could travel separately with AVs. Second, AVs will move without passengers ("*ghost trips*") (Bahamonde-Birke et al., 2018; Pakusch et al., 2018). Moreover, transportation costs will be lower due to better vehicle amortization (Martínez-Díaz et al., 2018b).
5. *Changes in trip distribution*: The improvements due to direct effects, such as the reduction of congestion, costs, and the value of travel time, will cause longer trips. Changes in the place of residence, work, or both will imply changes in the generation and attraction of trips.
6. *Changes in the urban structure and urban activity system*: Changes in trip distribution will imply an increment in the city size in the long-term. The urban model will change to a dispersal model (urban sprawl) because new urban areas will be built in places far away from the city center (Meyer,

Becker, Bösch, & Axhausen, 2017; B. W. Smith, 2012; Zakharenko, 2016; Zhang, Guhathakurta, Fang, & Zhang, 2015).

7. *Other impacts*: These are no less important than the previous ones. First, it could generate social opposition to this paradigm shift in mobility due to ethics, legal, environmental, and territorial issues (Martínez-Díaz et al., 2018a).

3. Mathematical modeling

This section describes the mathematical formulation. The total cost function ($TC = C_C^u + C_C^a$) has two elements: the total cost of users (C_C^u in [$]) and the agency cost ($C_C^a$ in [$]). The model uses continuous spatial variables (Table H.1); secondly, Table H.2 describes the demand density functions obtained from the assignment method. Finally, Table H.3 presents the list of parameters used in the modeling of a circular city.

Table H.1. Variables used in the modeling of a circular city.

Variables	
$d_w^c(r)$	distance function between circular roads of type $w \in W$ at the radius r km [km/road]; and
$\Phi_w^r(\theta)$	angle function between radial roads of type $w \in W$ at a city point with angle θ [radian/road], which $d_r(r,\theta) = \Phi_r(\theta) \cdot r$ is the distance function between radial roads at a city point (r,θ) [km/road].

Table H.2. Demand density functions come from the assignment method.

Demand Functions	
$f_{k,v}^F(r,\theta)$	vehicles density of type $v \in V$ that access from the origin to a circular ($k = c$) or radial ($k = r$) primary road [veh/km²·h];
$f_{k,d,v}^R(r,\theta)$	vehicle flow density of type $v \in V$ that travel on a circular ($k = c$) or radial ($k = r$) primary road considering the direction d [veh/km·h]; and
$f_{k,v}^A(r,\theta)$	vehicles density of type $v \in V$ that arrive from a circular ($k = c$) or radial ($k = r$) primary road to the destination [veh/km²·h].

Table H.3. Parameters used in the modeling of a circular city.

Other Parameters	
T	duration of period [h];
μ_v	value of travel time of users in vehicle v [$/h];
v_v^F	car speed of type v to access main roads of the city [km/h];
$v_{w,v}^{ff}$	free-flow car speed of type v on a primary road of type w [km/h];
v_v^p	cruising speed of a car v looking for a parking spot [km/h];
v^a	average walking speed for accessing the destination point from the parking site [km/h];
$t_{w,v}^F$	average time for accessing the primary road w of a car v [h];
$t_{w,v}^A$	average time for accessing the local roads from a road w of a car v [h];
a and b	parameters of BPR volume-delay function [dimensionless];
$k_{w,v}$	capacity road per lane of type w [veh/lane·h];
η_w	number of lanes at a road w [lane];
$\tau_{w,v}^i$	average time spent by a vehicle of type v when crosses a crossroad on a road of type w [h/veh];
λ_P	average density of vacant parking space [parking/km];
d_p	distance before arriving at the destination where the drivers begin to look for a parking spot [km];
d_w^p	the expected walking distance after parking the vehicle has two cases [km];
φ_v^t	car cost of type v per distance unit [$/km·veh];
φ^p	parking fee [$/h·veh];
$\varphi_{w,v}^{h(f)}$	maintenance fixed cost by road infrastructure for a road w and a car v [$/km]; and
$\varphi_{w,v}^{h(v)}$	maintenance variable cost by road infrastructure for a road w and a car v [$/km·h].

3.1. Users costs

The total user cost function ($C_C^u = C_F + C_R + C_A$ in [$]) contains three elements: accessibility cost to a primary road (C_F), cost spent on a regular car trip (C_R), and arriving cost at the destination (C_A).

Accessibility cost to main roads

The average access cost (Equation H.1 in [$/veh]) for accessing a circular ($c_{c,w,v}^F(r)$) or a radial road ($c_{r,w,v}^F(r,\theta)$) has two components. First, cars travel a quarter of the distance between the origin and the closest primary road. The average travel cost is the multiplication of this distance and the generalized cost Ψ_v^F ($\Psi_v^F = \mu_v/v_v^F + \varphi_v^t$ in [$/km·veh]). Second, the users incur a cost for accessing the primary road ($t_{w,v}^F \cdot \Psi_{w,v}^c$ where $\Psi_{w,v}^c = \mu_v + v_v^F \cdot \varphi_v^t$ in [$/h·veh]).

$$c^F_{k,w,v}(\cdot) = \begin{cases} \dfrac{d^c_w(r)}{4} \cdot \Psi^F_v + t^F_{w,v} \cdot \Psi^c_{w,v} & k = c \\ \dfrac{r \cdot \Phi^r_w(\theta)}{4} \cdot \Psi^F_v + t^F_{w,v} \cdot \Psi^c_{w,v} & k = r \end{cases} \quad \text{(H.1)}$$

The local accessibility cost function has two components: the demand density in rush hour ($f^F_{k,v}(r,\theta) \cdot T$) and the average access cost per vehicle ($c^F_{k,w,v}(r)$). This cost is the integration of a local cost over the city area for all types of roads w and vehicles v (Equation H.2).

$$C_F = \int_0^{2\pi} \int_0^R \sum_{w \in W} \sum_{v \in V} f^F_{c,v}(r) \cdot T \cdot c^F_{c,w,v}(r) + f^F_{r,v}(r,\theta) \cdot T \cdot c^F_{r,w,v}(r,\theta)\ \ r\ dr\ d\theta \quad \text{(H.2)}$$

Regular trip cost

In regular trips, the generalized travel cost function has three elements (Equation H.3 in [$/km·veh]). The first component is a Bureau of Public Roads (BPR) function that represents the congestion effects. The free-flow travel cost per kilometer is the inverse of free-flow speed multiplied by the value of travel time ($\mu_v / v^{ff}_{w,v}$). The congestion level depends on the traffic flow ($F^R_{c,w,d,v}(r,\theta) = f^R_{c,d,v}(r,\theta) \cdot d^c_w(r)$ and $F^R_{r,w,d,v}(r,\theta) = f^R_{r,d,v}(r,\theta) \cdot r \cdot \Phi^r_w(\theta)$) and the capacity of the road type w ($K^R_{d,w,v}(r,\theta)$) where the vehicles can travel in two directions: $d \in \{d_1 = clockwise, d_2 = anticlockwise\}$ on circular roads, and $d \in \{d_1 = inside, d_2 = outside\}$ on radial roads. Secondly, the unitary cost of a regulated crossroad by traffic lights is the ratio between the cost spent by crossing the road ($\mu_v \cdot \tau^i_{w,v}$) and the distance between roads ($r \cdot \Phi^r_w(\theta)$ or $d^c_w(r)$). Finally, the last component is the operational cost (φ^t_v).

$$c^R_{k,d,w,v}(r,\theta) = \begin{cases} \dfrac{\mu_v}{v^{ff}_{w,v}} \cdot \left(1 + a \cdot \left(\dfrac{F^R_{c,d,v}(r,\theta)}{K^R_{d,w,v}(r,\theta)}\right)^b\right) + \dfrac{\mu_v \cdot \tau^i_{w,v}}{r \cdot \Phi^r_w(\theta)} + \varphi^t_v & k = c \\ \dfrac{\mu_v}{v^{ff}_{w,v}} \cdot \left(1 + a \cdot \left(\dfrac{F^R_{r,d,v}(r,\theta)}{K^R_{d,w,v}(r,\theta)}\right)^b\right) + \dfrac{\mu_v \cdot \tau^i_{w,v}}{d^c_w(r)} + \varphi^t_v & k = r \end{cases} \quad \text{(H.3)}$$

Similar to the previous case, the total trip cost (C_R in [$]) is the integration of the local cost function. The elements of the local cost function are the demand density in rush hour and the local generalized travel cost in each type of road w (Equation H.4).

$$C_R = \int_0^{2\pi} \int_0^R \sum_{d \in D} \sum_{w \in W} \sum_{v \in V} f^R_{c,d,v}(r,\theta) \cdot T \cdot c^R_{c,d,w,v}(r) + f^R_{r,d,v}(r,\theta) \cdot T \cdot c^R_{r,d,w,v}(r,\theta)\ r\ dr\ d\theta \quad \text{(H.4)}$$

Arriving cost to trip destinations

After that, a user parks his car paying for the parking fee, and has to walk to the final destination. The average destination cost has five elements. Firstly, the users incur a cost for accessing local roads ($t^A_{w,v} \cdot \Psi^c_{w,v}$ where $\Psi^c_{w,v} = \mu_v + v^F_v \cdot \varphi^t_v$ in [$/h·veh]). Secondly, the driving cost on local streets before the users start to look for a vacant parking spot. This sub-cost is composed of the average distance (e.g., $(d^c_w(r) - d_p)/4$) and the generalized cost ($\Psi^F_v = \mu_v/v^F_v + \varphi^t_v$). Thirdly, the cost incurred by users, which are looking for a parking space, is the multiplication of the average distance between vacant spots ($1/\lambda_P$) and the generalized cost ($\Psi^P_v = \mu_v/v^p_v + \varphi^t_v$). Fourthly, the user walking cost, which is the distance between the user parked and the destination, is the multiplication of the expected walking distance and the generalized cost ($\Psi^A_v = \mu_v/v^a$). According to Arnott and Rowse (1999), the expected walking distance after parking the vehicle has two cases (d^p_w). If a driver finds a vacant space before his destination ($x < d$) then this driver will walk $d - x$ km. In another case, the driver will walk $x - d$ km to the destination. Finally, the cost includes the car-parking fee (φ^p). Equation H.5 shows the average local destination cost ([$/veh]) for each road type.

$$c^A_{k,w,v}(r) = \begin{cases} t^A_{w,v} \cdot \Psi^c_{w,v} + \left(\dfrac{d^c_w(r) - d_p}{4}\right) \cdot \Psi^F_v + \dfrac{\Psi^P_v}{\lambda_P} + d^p_w \cdot \Psi^A_v + \varphi^p & k = c \\ t^A_{w,v} \cdot \Psi^c_{w,v} + \left(\dfrac{r \cdot \Phi^r_w(\theta) - d_p}{4}\right) \cdot \Psi^F_v + \dfrac{\Psi^P_v}{\lambda_P} + d^p_w \cdot \Psi^A_v + \varphi^p & k = r \end{cases} \quad \text{(H.5)}$$

where

$$d^p_w = \frac{2 \cdot e^{-\lambda_P \cdot d_p}}{\lambda_P} + d_p - \frac{1}{\lambda_P}$$

The total arriving cost (C_A in [$], Equation H.6) is the integration of the local cost composed of the demand function in the rush period ($f^A_{k,v}(r,\theta) \cdot T$), and the expected walking cost and parking fee ($c^A_{k,w,v}(r,\theta)$).

$$C_A = \int_0^{2\pi} \int_0^R \sum_{w \in W} \sum_{v \in V} f^A_{c,v}(r) \cdot T \cdot c^A_{c,w,v}(r) + f^A_{r,v}(r,\theta) \cdot T \cdot c^A_{r,w,v}(r,\theta) \;\; r \, dr \, d\theta \quad \text{(H.6)}$$

3.2. Agency costs

In the agency cost (C_I in [$], Equation H.7), the local cost function ([$/km^2]) is the multiplication of the cost per linear kilometer and the road density ($1/d^c_w(r)$ or $1/r \cdot \Phi^r_w(\theta)$). The unitary cost contains two parts: a fixed and a variable element.

$$C_I = \int_0^{2\pi} \int_0^{R} \sum_{w \in W} \sum_{v \in V} \frac{\varphi_{w,v}^{h(f)} + \varphi_{w,v}^{h(v)} \cdot T}{d_w^c(r)} + \frac{\varphi_{w,v}^{h(f)} + \varphi_{w,v}^{h(v)} \cdot T}{r \cdot \Phi_w^r(\theta)} \, r \, dr \, d\theta \qquad \text{(H.7)}$$

3.3. Mathematical formulation

The nonlinear system has n decision variables ($x_i(\cdot) = \{d_w^c(r), \Phi_w^r(\theta)\}, \; w \in W$) and m constraints. The set of Equations H.8 shows the mathematical formulation. The first expression is the objective function (H.8(a)). Regarding the constraints, the model also considers that the congestion should not overtake 90 percent of capacity for both roads (H.8(b) and (c)). Finally, the decision variables are no negative (H.8(d) and H.8(e)).

$$Min\ TC = C_C^u + C_C^a \qquad \text{(a)}$$

s.t.

$$\max_{\theta} \left(\frac{f_{c,d,v}^R(r,\theta) \cdot d_w^c(r)}{K_{d,w,v}^R(r,\theta)} \right) \leq 0.9 \qquad \forall\, r,d,w,v \qquad \text{(b)}$$

$$\max_{r} \left(\frac{f_{r,d,v}^R(r,\theta) \cdot \Phi_w^r(\theta) \cdot r}{K_{d,w,v}^R(r,\theta)} \right) \leq 0.9 \qquad \forall\, \theta,d,w,v \qquad \text{(c)} \qquad \text{(H.8)}$$

$$d_w^c(r) \geq 0 \qquad \text{(d)}$$

$$\Phi_w^r(\theta) \geq 0 \qquad \text{(e)}$$

The set of Equations H.9 shows the formulation of a solution, in which H.9(a) presents the first condition for each one of the decision variables when they are no negative (H.9(e)). The second condition contains the constraints c_j (H.9(b)). The third condition set is the complementary slackness (H.9(c)); if the inequality constraint is active, its slack is zero, and its multiplier ($\lambda_j(\cdot)$) takes any non-negative value (H.9(d)). In Equation H.9, the expression contains an equation system with inequalities. This system of equations allows obtaining the optimal solution through the method of successive approximations.

$$\nabla tc\big(x_i(\cdot)\big) + \sum_j^m \lambda_j(\cdot) \cdot \nabla c_j\big(x_i(\cdot)\big) = 0 \quad \forall\, i = 1, \dots, n \text{ (a)}$$

$$c_j(r,\theta) - b_j \leq 0 \quad \forall\, j = 1, \dots, m \text{ (b)}$$

$$\lambda_j(\cdot) \cdot \big(c_j(r,\theta) - b_j\big) = 0 \quad \forall\, j = 1, \dots, m \text{ (c)} \qquad \text{(H.9)}$$

$$\lambda_j(\cdot) \geq 0 \quad \forall\, j = 1, \dots, m \text{ (d)}$$

$$x_i(\cdot) > 0 \quad \forall\, i = 1, \dots, n \text{ (e)}$$

3.4. Impacts of CAVs on urban mobility

CAVs will impact in different ways at each stage (Medina-Tapia & Robusté, 2018b). The following points describe these effects.

- *First stage*: access to main roads.
  1. The generalized cost functions (Ψ_v^F and $\Psi_{w,v}^c$) will decrease due to v_v^F will increase, and the operation cost (φ_v^t) will decrease, and
  2. The value of travel time (μ_v) will decrease because the users could do other activities during the travel, and it will decrease the stress level.
- *Second stage*: regular trips.
  1. The value of travel time (μ_v) will drop for AV users, as explained previously,
  2. The speed of AV and CAVs will increase because AVs will be more efficient ($v_{w,v}^{ff}$),
  3. The road capacity will increase due to connected CAVs will travel in platoons ($K_{d,w,v}^R(r,\theta)$),
  4. The travel time when CAVs cross an intersection will decrease ($\tau_{w,v}^i$) due to communication V2I (Smart City), platoon formation, less reaction time, traffic lights coordination, and
  5. The unitary operational cost will decrease because AVs will be more efficient (φ_v^t).
- *Third stage*: arriving at a trip destination.
  1. Drivers get out of the car at the final destination ($d_p = 0$),
  2. The generalized cost will decrease (Ψ_v^F and Ψ_v^P) due to AVs and CAVs will be more efficient. Moreover, the ratio μ_v/v_v^p will be null in the generalized cost Ψ_v^P, and
  3. The users will not have to walk from the parking spot to the destination. Therefore, $((2 \cdot e^{-\lambda_P \cdot d_p})/\lambda_P + d_p - 1/\lambda_P)$ is null.

4. Application to a case study

This section has five parts: a description of the case study, parameters, and three points with the results of the modeling.

4.1. Description

The analyzed case is a circular city with nine zones: a Central Business District (CBD), four internal zones, and four external zones (Figure H.1(a) and (b)). If the city radius is 15 km (R) with a homogeneous trip density, then the CBD radius will be 5 km ($R_1 = R_2/\sqrt{5}$), and the external radius will be about 11.2 km ($R_2 = R \cdot \sqrt{5}/3$). The distribution matrix is symmetric and has 405,000 private trips per hour (Figure H.1(c)).

The distribution of trip demand (generation, attraction, and trip distribution) allows obtaining the demand density function using the incremental assignment method. Figure H.2 shows the density of vehicles that access main roads, the density of vehicles that travel on main roads, and the density of vehicles that arrive at main roads. Moreover, Table H.3 shows the list of parameters for both types of vehicles used by the model.

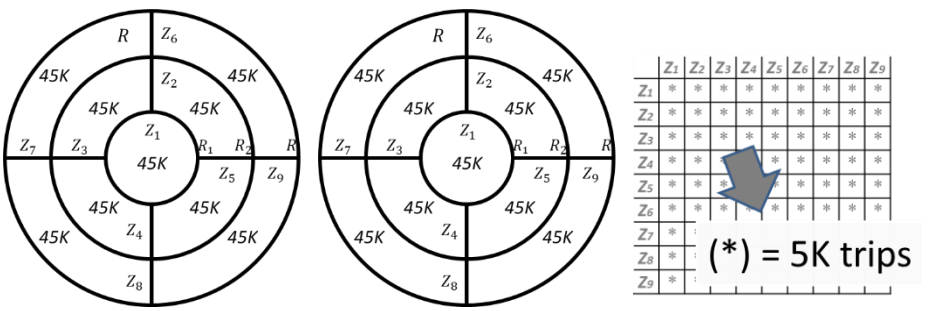

(a) Generation (b) Attraction (c) Trip distribution

Figure H.1. Demand scenario used for the CAV policy.

4.2. Demand

Figure H.2 shows the homogeneous demand density with only MVs in each car trip stage using the incremental assignment method. In Stage 1, the density of generated and attracted trips in an infinitesimal area ([veh/km²·h)]) is concentrated on the central zone for trips that access major circular roads (Figure H.2(a)) and on the periphery for radial roads (Figure H.2(b)). In Stage 2, an internal zone for circular roads concentrates the regular trip density ([veh/km·h)]) at each city point (Figure H.2(c)). On the other hand, the zone around the city center concentrates radial trips (Figure H.2(d)). In Stage 3, the density represents attracted trips around a point ([veh/km²·h)]) concerning trips that arrive from circular (Figure H.2(e)) and radial roads (Figure H.2(f)). Similar to Stage 1, the majority of attracted trips from circular roads are around the central area, whereas the most density of radial trips is in external zones (Medina-Tapia & Robusté, 2018a).

Stage 1

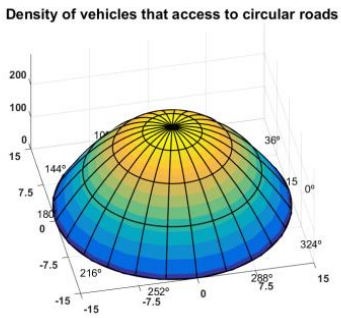

(a) Vehicle density that accesses circular roads

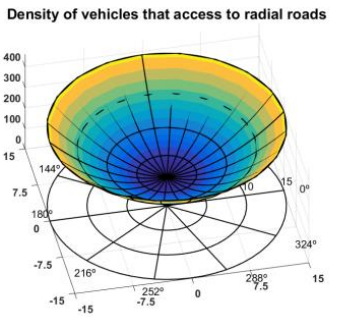

(b) Vehicle density that accesses radial roads

Stage 2

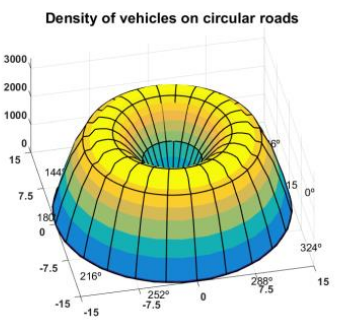

(c) Vehicle density that travels on circular roads

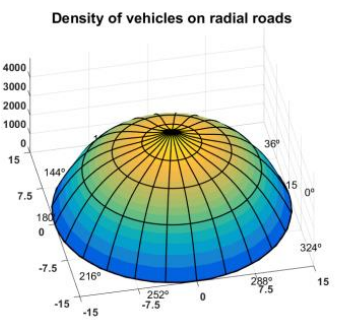

(d) Vehicle density that travels on radial roads

Stage 3

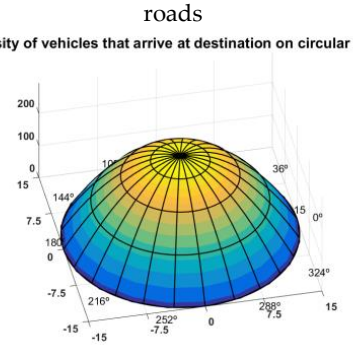

(e) Vehicle density that arrives at the destination on circular roads

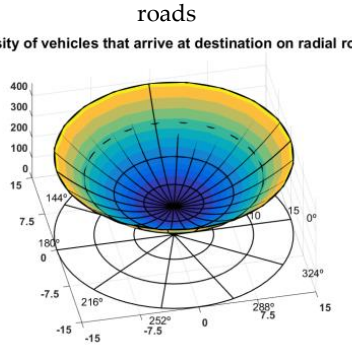

(f) Vehicle density that arrives at the destination on radial roads

Figure H.2. Traffic density assignment for the CAV policy.

4.3. Parameters

Table H.4 shows the parameter list of both types of vehicles used by the model. Our model considers that the value of travel time will be equal for each type of car user (Medina-Tapia & Robusté, 2018a). Litman's report (2016) gives an average value.

Table H.4. Parameters of the model used in each scenario for the CAV policy.

Parameters		Case of MVs	Case of CAVs
T	[h]	1.5	1.5
μ_v	[$/h]	10	8
v_v^F	[km/h]	25	30
$v_{w,v}^{ff}$	[km/h]	a: 45; f: 95	a: 50; f: 100
v_v^p	[km/h]	10	30
v^a	[km/h]	3	3
$t_{w,v}$	[h]	a: 45/3600; f: 5/60	a: 45/3600; f: 5/60
a		2	2
b		3	3
$k_{w,v}$	[veh/lane·h]	a: 1,272; f: 2,099	a: 3,960; f: 4,259
η_w	[lane]	a: [0…6]; f: [0…8]	a: [0…6]; f: [0…8]
$\tau_{w,v}^i$	[h/veh]	a: 0.0125; f: 0	a: 0.0125·70%; f: 0
λ_P	[parking/km]	5	5
d_p	[km]	0.2	0.0
φ_v^t	[$/km·veh]	0.1	0.1·50%
φ^p	[$/h·veh]	1	1
$\varphi_{w,v}^{h(f)}$	[$/km]	a: $5.680 \cdot 10^6$; f: $10.85 \cdot 10^6$	$\varphi_{w,MV}^{h(f)} \cdot 1.25$
$\varphi_{w,v}^{h(v)}$	[$/km·h]	$\varphi_{w,MV}^{h(f)} \cdot 1\%$	$\varphi_{w,MV}^{h(v)} \cdot 1.25$

In arterial roads, the capacity of urban roads depends on the intersection capacity (Lioris et al., 2017). AACC allows the formation of platoons, although the headway could improve if the cars have CACC. In the current scheme with only MVs, the capacity of streets is 1,272 per lane ($k_{w,v}$) (Lioris et al., 2017). In a future scenario with AVs, the road capacity will be 3,960 ($k_{w,v}$); it is three times bigger than the present scenario as stated in Lioris et al. (2017). For freeways, the investigations show that MVs can reach the capacity of 2,099 [veh/lane·h]. On the other hand, AACC vehicles will increase the road capacity by about 7% if the ratio of AACC is between 40% and 60% (2001, 2002), while the CACC vehicles increase the capacity by about 102% when all vehicles are communicated (4,259 [veh/lane·h]). Therefore, in modeling, the case of AVs includes connected and automated vehicles (CAVs). In the modeling, arterial roads have six lanes, and freeways have eight lanes. The lanes will distribute between MVs and AVs because the number of lanes depends on the type of road and the penetration of AVs. In AV lanes, these cars will form platoons.

The model assumes that the mileage in MVs is 10 km/L, and the fuel price is 1 $/L. Moreover, the model assumes that AVs will save 50% in comparison to a conventional car (Litman, 2018). Moreover, the model assumes that the parking fee is $\varphi^p = 1$ [$/veh·h]. Furthermore, the fixed unit cost value is based on the paved cost per linear meter built, and the lifetime of the road project

divides it. The cost per kilometer is based on technical reports of Arkansas's Department of Transportation (2014). The model assumes that the variable unitary cost is 1% of fixed cost ($\varphi^{h(v)} = 0.01 \cdot \varphi^{h(f)}$ in [$/km·h]). Finally, the model assumes that the infrastructure cost for AVs is 25% more expensive than the infrastructure for MVs.

Scenario with only MVs:

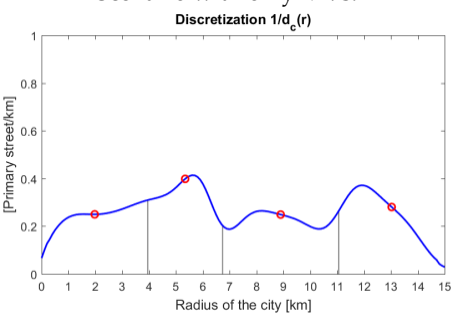

(a) MV density of circular roads

Scenario with only CAVs:

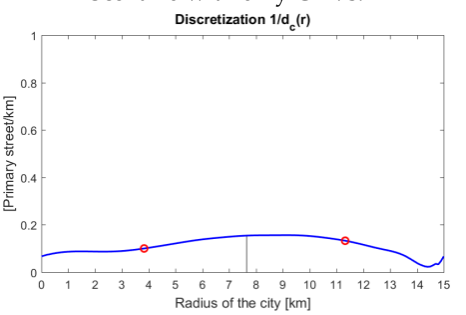

(b) MV density of circular roads

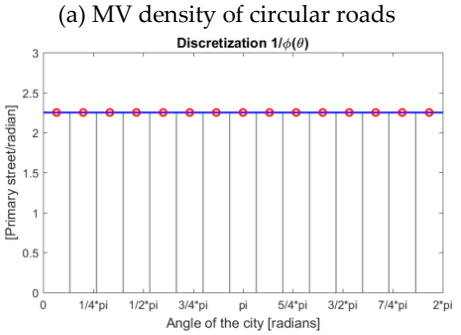

(g) MV density of radial roads

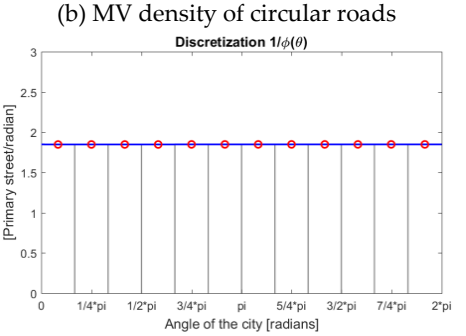

(h) MV density of radial roads

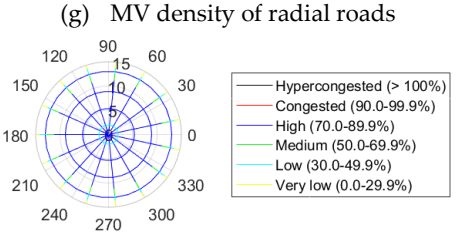

(i) Optimal urban structure with only MVs and its congestion level

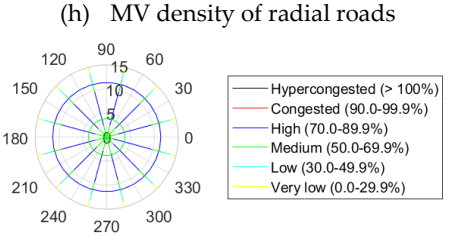

(j) optimal urban structure with only CAVs and its congestion level

Figure H.3. Comparison of results between MVs and CAVs.

4.4. Optimal urban structure

Figure H.3 represents the comparison between the results of the optimization with only MVs and CAVs (Level 5 of automation and connected vehicles). The exhibit (Figure H.3) shows the inverse of the optimal decision variables: the distance between circular ((a) and (b)) and radial roads ((c) and (d)). The average of the optimal distance between circular roads is 3.8 km in the base

scenario and 7.5 km in the future scenario reducing by half the number of primary roads. In radial roads, the results are similar in both cases. The average optimal distance between radial roads is 2.1 km at a radius of 5 km, 4.1 at 10 km, and 6.2 at 15 km for the current scenario. In the scenario with CAVs, the distance for radial roads is 2.6 km at a radius of 5 km, 5.2 at 10 km, and 7.8 at 15 km. In the discretization, the gray lines represent the border between corridors, and the area in this zone is approximately a unit, while the red points represent the location of optimal major roads.

Finally, the circular exhibits (e) and (f) represent the congestion levels on all optimal primary roads of both scenarios. The exhibits reveal that the saturation of the future scenario drops, even if there is less road infrastructure supply than in the base scenario.

4.5. Effects on the urban network

AV direct effects

This section explains some results of direct effects on urban mobility (Medina-Tapia & Robusté, 2018a, 2018b).

- *Reduction of road congestion*: If the driving of AVs is more efficient than MVs, then the road capacity will rise, and the congestion will drop (Medina-Tapia & Robusté, 2018c). The reduction of road saturation by CAVs can reach between a third and a half of MV saturation (Figure H.4(a)).
- *Reduction of costs*: Because of the previous improvement, the operation cost will also decrease. The cost functions will decrease by about 30%, as shown in Figure H.4(b).

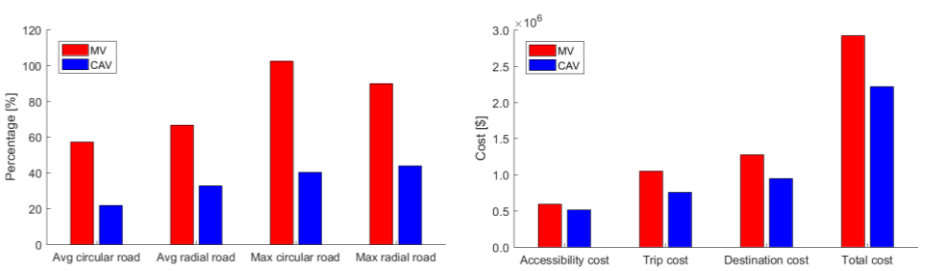

(a) Saturation percentage of MVs and CAVs (b) Travel stage cost of MVs and CAVs

Figure H.4. Influence of direct effects of MVs and CAVs for the CAV policy.

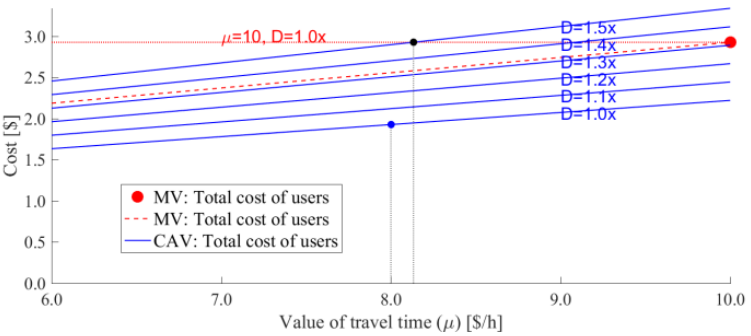

(a) Variation of the value of travel time and demand on the cost function

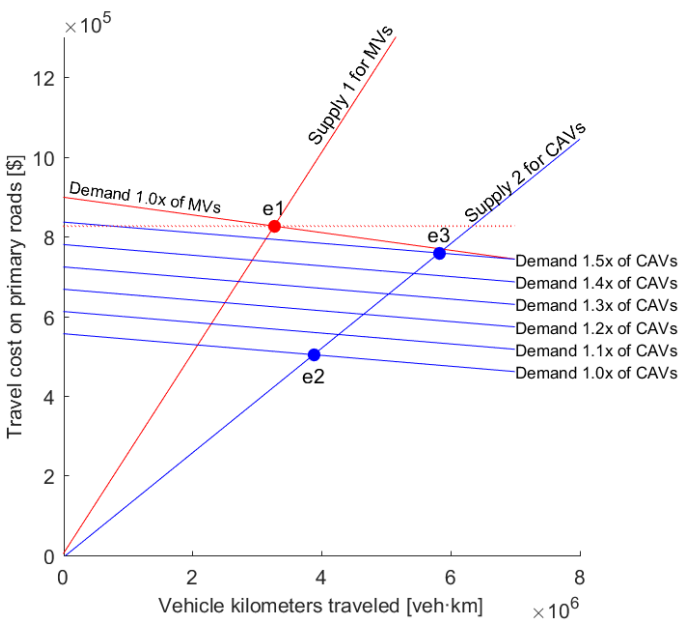

(b) Effect of the induced demand by CAVs on the travel cost

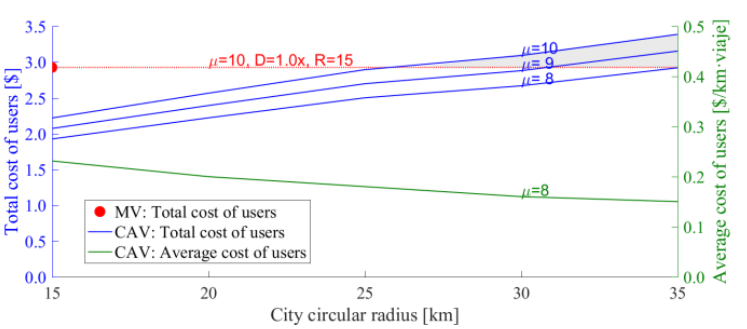

(c) Effect of the urban radius on the cost of users

Figure H.5. Influence of indirect effects of CAVs for the CAV policy.

AV indirect effects

On the other hand, the consequences of AV and CAV indirect effects will offset the savings by direct effects (Medina-Tapia & Robusté, 2018a, 2018b).

- *Reduction of the value of travel time*: Figure H.5(a) shows blue lines that represent the reduction of the total cost if the value of travel time decreases and a red point that represents the total cost in the current scenario (only MVs). Kohli and Willumsen (2016) asserted that the value of travel time could decrease by 20% in the scenario with only AVs. Therefore, if $\mu = 8$ in our model (blue point), then the total cost will decrease by 35%: This is the gap of difference between the red point and the blue point.
- *Induced demand*: Figure H.5(b) shows the economic model of this system: the price axis represents the travel cost, and the VKT indicator represents the quantity in the horizontal axis. Red lines represent the supply and demand curves for MVs in which the red point (e1) is the current equilibrium. With the operation of only CAVs, the transportation supply should increase (blue line). Therefore, the system will have a new equilibrium point (point e2) that will have less congestion than the current scenario, but new users will enter the system. Blue demand lines represent this consequence. If the demand increases 50% (Demand 1.5x), the total cost in the new equilibrium (point e3) will be a little smaller than (or similar to) the current scenario (point e1). Figure H.5(a) shows that if $\mu = 8.2$, the total costs of the current scenario and the scenario with 1.5x demand are equivalent.
- *The increment of the VKT*: This indicator could increase if AVs started to look for a parking spot only once the user gets out of the car at the destination. The results show an increment of over 5,104 km by CAVs compared to the current scenario (Medina-Tapia & Robusté, 2018a, 2018b), although this result is relative because CAVs will look for a vacant parking space using V2I technology in a Smart City.
- *Changes in trip distribution and urban structure*: If the trips are more extended than nowadays, the city size will increase, and the vicious cycle will be encouraged. Blue lines in Figure H.5(c) represent the variation of the value of travel time between the city radius and the total cost with only AVs. The exhibit shows that the total cost will increase if the city grows; hence, this cost could be equivalent to the present scenario (MVs) around a radius of 35 km with $\mu = 8$ [$/h]. Therefore, the city size is as considerable as the induced demand. The green curve in Figure H.5(c) shows that if the urban radius increases, the average user cost per kilometer will slightly decrease. Therefore, if the generalized cost, including the value of time, will be smaller than now, the trips will aim to be longer, and the users will modify the destination. This reduction of costs will cause dispersion along with long-term changes in the activity system and the urban structure. Fortunately, these cars are in the early implementation phases, but urban problems such

as spatial segregation or urban sprawl are profound in some cities, and AVs and CAVs could deepen them even more (Medina-Tapia & Robusté, 2018a, 2018b).

4.6. Progressive implementation analysis

The research analyzes the evolution of the CAV implementation through two factors: the total cost (Figure H.6(a)) and the congestion level (Figure H.6(b)) by the penetration of CAVs from 0% to 100%. Both charts exhibit that the cost and congestion will decrease with this new technology if the demand is constant over time (Medina-Tapia & Robusté, 2018c). The curve fluctuates when it decreases because the model assigns the infrastructure (number of lanes) progressively according to the type of car, which will generate congestion. In Figure H.6(a), the user costs tend to decrease while the agency costs rise when the system has the infrastructure dedicated to CAVs, reaching almost the convergence when all vehicles are driverless cars. Additionally, the total cost fluctuates, decreasing by the implementation of CAV-dedicated roads. Therefore, agencies have to invest in mitigating imbalances between supply and demand. Figure H.6(b) shows that the gradual implementation could generate scenarios that are worse than the initial stage. In the early years of the implementation, the users' perception will be averse to incorporating this new automation.

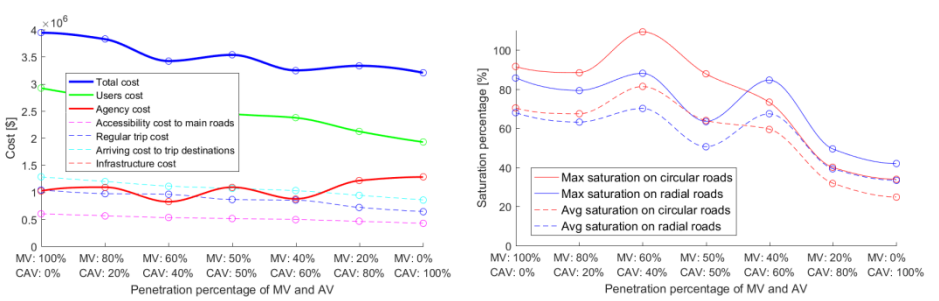

(a) Cost variation by CAV penetration (b) Saturation variation by CAV penetration

Figure H.6. Progressive implementation effects for the CAV policy.

5. Conclusions

Transportation policies should reduce the possible impacts and enhance the potential benefits of AVs. Agencies have to prepare and adapt cities for this change of paradigm in urban mobility. This research seeks to provide some initial ideas on the implementation of new technologies, in which planning

agencies should consider them in long-term plans under sustainable development. Consequently, this paper analyzed three topics related to the implementation of CAVs.

First, the direct effects of CAVs will positively influence cities. According to our model, CAVs could influence the optimal structure of a city in two aspects. Firstly, the city will require less road supply. These savings are more significant with circular road supply than in radial roads. This reduction will allow agencies to manage this infrastructure better. Secondly, traffic congestion with CAVs decreases even with less road infrastructure. Despite this, not all of the expected effects are positive.

Second, indirect effects will mitigate the direct effects because the reduction of road capacity is not the only factor of importance. Several significant conclusions come from the results of this work. Firstly, the value of travel time is another crucial factor. On the one hand, it can reduce a third of the total cost; on the other hand, it might cause other significant externalities explained in the following points. Secondly, the induced demand is another element that might limit the benefits obtained through CAVs. Thirdly, the increment of vehicle-kilometers traveled is a difficult factor to measure, but the consequences can be substantial over the city. Finally, the dispersion of cities is a factor that has not received as much attention, and they have been less researched than other impacts of AVs. Thus, urban growth could be more significant than other factors, such as induced demand. All factors as a whole will tend to encourage the vicious cycle of public transportation and to promote unsustainable cities in the long-term.

Third, the analysis done on the progressive implementation of CAVs shows that the operation of these cars will be a complicated process, as reaching the optimal equilibrium requires additional resources for reducing possible scenarios as bad as the current scheme.

The three aspects previously analyzed expose the advantages and limitations of the implementation of CAVs, considering a point of view of travel costs. Therefore, a city with only CAVs will not be sustainable; urban sustainability should complement modes such as public and shared transportation. Moreover, these changes will boost the operation of new technologies such as shared autonomous vehicles (SAV), mobility as a service (MaaS), personal mobility devices (electric scooters, segways, hoverboards, unicycles), and others.

In future works, the model will permit the proposal of different solutions in a city with heterogeneous demand spatially. Moreover, the research will analyze the influence of changes in user behavior in each stage of the trip, considering aspects such as modal choice, trip distribution, and assignment. Finally, in future analysis, the modeling will also consider extending the studies in the case of a real city.